NOVEL APPROACH FOR SELECTIVE REMOVAL OF RADIONUCLIDES BY STIMULI-RESPONSIVE GEL BEADS CARRYING AZA-CROWN ETHERS

A thesis submitted to The University of Manchester for the degree of Doctor of Philosophy in the faculty of Engineering and Physical Science

DARIO DELI

School of Chemistry

2010

TABLE OF CONTENTS

Glossary

AEMA	2-amino-ethyl methacrylate
APS	ammonium persulfate
ATR	attenuated total reflection
AR	analytical reagent
ATRP	atom transfer radical polymerization
AAc	acrylic acid
BIS	bis acryl amide
Bq	Becquerel
CER	cohesive energy ratio
CE	crown ether
$^{30}D_m$	mean diameter of 30 beads
$^{200}D_m$	mean diameter of 200 beads
DMF	di methyl formamide
Da	Dalton
D	distribution ratio
DMSO	di methyl sulfoxide
DCM	dichloromethane
Et	ethyl
EO	ethylene oxide
ΔE	difference in potential
ΔG	difference in Gibbs free energy
ΔH	difference in enthalpy
ΔS	difference in entropy
ES±	positive/negative ion electrospray
eq	equivalent
E	potential
EGDMA	ethylene glycol di methacrylate
FT-IR	Fourier transform infrared spectroscopy
FIPA	flow Injection Polymer Analysis

ε	molar absorptivity
GPC	gel permeation chromatography
I	polydispersity
HLB	hydrophilic lipophilic balance
HEMA	2-hydroxyethyl methacrylate
HSAB	hard-soft acid-base theory
HEC	hydroxyethyl cellulose
Hex	hexane
HESH	2-hydroxy ethane thiol
IPA	isopropanol
ISE	ion selective electrode
ICD	induced circular dichroism
IR	infrared
LCST	lower critical solution temperature
l	length
m/z	mass of the ion
MAS	magic angle spinning
MeV	mille electron volt
MMA	methyl methacrylate
Me	methyl
M^+	metal cation
M	metal
MALDI-TOF	Matrix-assisted laser desorption/ionization (time-of-flight mass spectrometer)
MAA	methacrylic acid
mmol	mille mole
mol	mole
Mn	number average molecular weight
Mw	weight average molecular weight
ῡ	antineutrino
N	number of neutrons

NA	not achieved
NABS	3-nitro-4-acetoxybenzene sulfonate
NMR	nuclear magnetic resonance
NIPAM	N-isopropyl acryl amide
PEG	poly-ethylene glycol
PMMA	poly-methyl methacrylate
PMEMA	poly-methyl ethyl methacrylate
$PMEO_2MA$	poly-di-ethylene glycol methyl ether methacrylate
$PMEO_3MA$	poly-tri-ethylene glycol methyl ether methacrylate
$POEGMA_{300}$	poly-oligo-(ethylene glycol) methacrylate (average molecular weight=300)
$POEGMA_{475}$	poly-oligo-(ethylene glycol) methacrylate (average molecular weight=475)
PSL	photo stimulated luminescence
PMT	photomultiplier tube
PDI	polydispersity index
PEGMA	poly-(MEO_2MA-co-$OEGMA_{475}$) hydrogel (85:15 mol % feed ratio)
PEGMAf	PEGMA functionalized with chloroacetyl chloride
PGMAf1	PEGMAf functionalized with 1-Aza-12-crown-4
PEGMAf2	PEGMAf functionalized with 1-Aza-15-crown-5
PEGMAf3	PEGMAf functionalized with 1-Aza-18-crown-6
ppm	parts per million
PN	poly-NIPAM hydrogel
PNA	poly-(NIPAM-co-AAc) hydrogel (80:20 mol % feed ratio)
PNA1	PNA functionalized with 1-Aza-12-crown 4
PNA2	PNA functionalized with 1-Aza-15-crown 5
PNA3	PNA functionalized with 1-Aza-18-crown 6
PVA	poly vinyl alcohol
R	side arm
R_h	hydrodynamic radius
rpm	revolutions per minute

RT	room temperature
SPAN40	sorbitan monopalmitate
SPAN80	sorbitan monooleate
SPAN83	sorbitan sesquioleate
SDS	sodium dodecyl benzene sulfonate
TEA	triethylamine
T_c	critical temperature
Tos	tosylate
THF	tetrahydrofuran
TEMED	N,N,N',N'-Tetramethylethylenediamine
T_g	glass transition temperature
$t_{1/2}$	half life time
TGA	thermogravimetric analysis
TEGD	tetraethylene glycol diacrylate
UV	ultraviolet
UCST	upper critical solution temperature
Z	number of protons

Abstract

The synthesis and properties of two novel gel beads incorporating N-Aza crown ethers is reported: the first based on N-isopropyl acryl amide/acrylic acid and the second based on oligo-ethylene glycol methacrylate copolymers. Both hydrogels show rapid response to environmental stimuli and their size can be tuned by both pH and temperature. Swollen states lead to high adsorption of water and high contact surface area with ions whereas in the collapsed state the material releases water and the ions not selectively retained by the polymer (Figure 1)

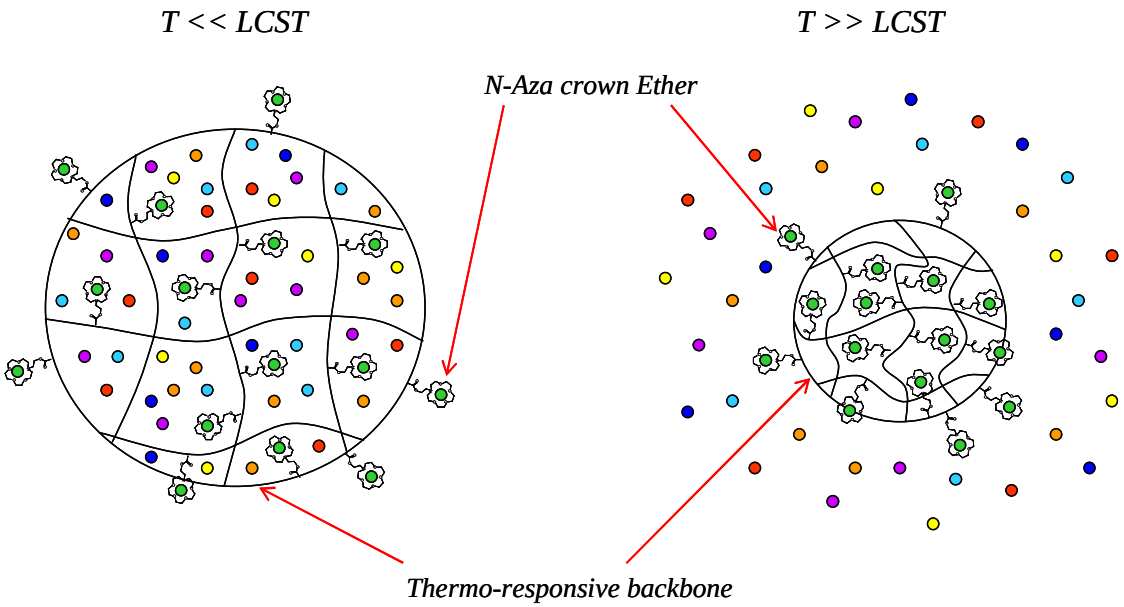

Figure 1: Scheme of selective adsorption and release of metals using a thermo-reversible gel.

Autoradiography tests show that these materials can strongly bind Sr 90 and Co 60 and both pH and temperature can fine tune binding selectivity. Scintillation tests also show that some of the materials prepared exhibit high selectivity toward the targeted radionuclide in presence of high concentrations of other non-hazardous cations. This results in such materials being very promising for use as smart scavenging agents for radioactive decontamination.

Declaration & Copyright

The experiments in this project constitute work carried out by the candidate and no portion of the work referred to in this thesis has been submitted in support of an application for another degree or qualification at this or any other university or institute of learning unless otherwise stated.

Certain aspects of this study were delegated to passing students and colleagues: part of the work involving the swelling experiments was done by Victoria Gibbons whereas the autoradiography experiments and the decontamination tests were carried out by Kathleen Law.

Reproductions described in it may take place is available from the Head of School of Chemistry (or the Vice-president).

Chapter 1

Introduction

1.1. Context.

Over the past few years, radioactive decontamination of aqueous solutions has received increasing interest due to concerns over human health and environment. Many studies have focused on developing new scavenging materials which strongly and selectively bind radionuclide ions.[1-4] Intermediate level fusion products such as Cs 137, Sr 90 and Co 60, which have relatively long half-lives and high beta and gamma emission energies, are considered the most environmentally hazardous radiotoxic elements.[4-6]

A key issue in radionuclide contamination is that it also presents a significant hazard in very low concentration and other elements with similar chemical and physical properties are often present in large excess. Sequestering materials should, therefore, display a high selectivity for the targeted radionuclide and a much lower affinity for the other elements (Ca^{2+}, Na^{+}, K^{+}); lack of selectivity would, in fact, lead to the generation of large amounts of excess waste, which requires expensive and special disposal procedures.

N-Aza-crown ethers have been widely proved to bind strongly to various heavy and radioactive ions on the basis of their ring sizes.[7] Their amino groups can also allow easy incorporation into a wide range of materials. However, *N*-Aza-crown ether recovery after complexation is often difficult due to their good solubility in different solvents and the stability of the complex is sometime quite low;[8] incorporation of these compounds in well-designed polymer supports opens the way to novel scavenging agents for radiological decontamination.

Hydrogels in the form of beads are very attractive polymer supports as they are easy to handle and recover after complexation and can absorb large quantities of water allowing high concentration of contaminants to be removed rapidly. Some of these materials have attracted particular attention due to their ability to undergo large geometrical changes in response to environmental stimuli. Temperature and pH responsive materials have

received most of the interest as they can be easily controlled. So far, poly-*N*-isopropyl acryl amide (poly-NIPAM) has been the most studied thermo-responsive polymer and exhibits a lower critical solution temperature (LCST) of ~ 32 °C in water solution.[9] This thermo-responsive polymer can be cross-linked in order to prepare an insoluble but swellable hydrogel in form of droplets by inverse suspension polymerization technique.[10] This three-dimensional polymer network can rapidly and reversibly swell or shrink in water by environmental temperature stimulus. At temperatures below the LCST the material absorbs water exhibiting a swollen "sponge-like" structure. As the temperature is increased above the LCST, the material displays a reduction in volume due to dehydration of the polymer network. However, the major problem on using poly-NIPAM in selective radioactive remediation is its ability in binding metal ions and in particular heavy metals.[11] Hydrogel beads which are also responsive to pH can be prepared by copolymerizing NIPAM with acid[10] or basic[12] monomers. Variations in pH can change the ionization sphere of the hydrogel, and thus, a change of the volume occurs due to electrostatic forces. Poly-acrylic acid (poly-AAc) is a common pH-responsive polymer and does not only provide the pH responsive property to the material but also the functionality for further post-reaction. In addition, the deprotonated AAc (at pH > pKa) enhances the affinity of the materials towards cations by electrostatic attraction increasing the contact area of the resulting hydrogel towards metals ions; at low pH (< pKa) the completely protonated acrylic acid reduces the interactions with heavy metals.[9]

Although a polymer support based on NIPAM and AAc may interfere on the binding activity of *N*-Aza-crown ethers, their incorporation into such fascinating and complex material may lead to interesting sequestering agents.

On the other hand, a well-designed polymer support for incorporation of selective N-Aza-crown ethers should not display significant interaction towards metal ions. Recently, Lutz *at al.* reported the copolymerization of two oligo-(ethylene glycol) macromonomers of different chain lengths.[13] These copolymers also exhibit thermo-responsive behaviour and their LCST was found to be tuneable by varying the comonomers compositions and they were comparable to, and in some cases, superior to that of poly-NIPAM. An aspect which makes these copolymers very interesting in selective removal of metal ions is the total

absence of strong electron donors. Poly-(ethylene glycol) hydrogels incorporating *N*-Aza-crown ethers are, therefore, selective towards metal ions only on the base of the crown ether ring sizes with reduced interference by the polymer support.

In order to address the radiological contamination of waters, radionuclide absorbents are used and subsequently safely disposed after sequestration. Materials currently used are ion exchanger compounds. Natural inorganic cation exchangers such as clays[14] and zeolites[15] have been widely studied and used in the removal of radioactive ions from aqueous solutions. Clays are hydrated aluminosilicates and are composed of a mixture of fine grained clay minerals and clay-sized crystals of other minerals such as quartz, carbonate and metal oxides. They are natural scavengers as they can uptake cations and anions through both ion exchange and normal adsorption. Clays contain exchangeable cations and anions (such as Ca^{2+}, Mg^{2+}, H^{+}, K^{+}, NH_4^{+}, Na^{+}, and SO_4^{2-}, Cl^{-}, PO_4^{3-}, NO_3^{-}) into their structure and these can be exchanged with other ions relatively easily without affecting the clay mineral structure.[16] Zeolites have similar compositions to clays (hydrated alumina silicate minerals) and absorb cations and anions in the same way. However, clays have a layered crystalline structure and most importantly are subject to shrinking and swelling as water is absorbed and removed between the layers. In contrast, zeolites have a rigid and three-dimensional crystalline structure composed of an arrangement of interconnected tunnels and cages. Although the water can freely move in and out of these pores, the zeolites organization remains rigid. Another aspect which make the zeolites special is that their pores and channel sizes are nearly uniform, allowing the crystal to act as a more selective scavenger: only the cations of appropriate molecular size that fit into the pores are admitted into the mineral creating the "sieving" property.[17] However, this natural materials have numerous disadvantages such as low exchange capacity, low abrasion resistance and mechanical durability, non-controllable pore-size, tendency to peptize (i.e. convert to the colloidal form) and low chemical stability (they easily decompose in acids or alkalis).[18]

Synthetic inorganic cation exchange materials have also been studied and currently are far better than the natural materials in terms of both stability[19] and, more importantly, selectivity in the removal of radionuclides from aqueous solutions.[3] Examples are

synthetic micas,[4, 20, 21] γ-zirconium phosphate,[19] niobate molecular sieves,[22,23] and titanate.[3] The main limitations are, however, the high costs compared with natural compounds, limited chemical stability at extreme pH ranges (high or low), interference in selectivity with ions of similar size and limited mechanical stability.[18]

Natural and synthetic organic ion exchange resins are an alternative to inorganic ion exchangers. A large number of natural organic materials (polysaccharides, proteins and carbonaceous materials) exhibit ion exchange properties; however, such ability is much smaller compared with the synthetics. Furthermore, the organic natural materials exhibit weak physical structure, non-uniform physical properties, non-selectivity, instability outside a moderate neutral pH and very limited radiation stability.[18] Synthetic ion exchange resins are commonly composed of styrene and divinylbenzene copolymers. They are typically in a powdered or bead form and their three dimensional structure is a flexible random network of hydrocarbon chains which carries fixed ionic charges. These resins are insoluble as they are cross-linked. The degree of cross-linking confers to the material a particular mesh size of the matrix, swell ability, mobility of the ions, hardness and mechanical durability. Highly cross-linked resins are rigid, more resistant to mechanical degradation but less porous and swellable in solvent. The most important advantages of synthetic ion exchange resins are their high capacity, wide applicability, wide versatility and low cost relative to the synthetic inorganic media. However, restrictions in their use are given by their limited radiation and thermal stabilities.[18]

1.2. Crown Ethers.

1.2.1. General description.

Crown ethers are heterocyclic chemical compounds that consist of a ring containing several groups. The most common crown ethers are oligomers of ethylene oxide, the repeating unit being ethylene-oxy, i.e., $-CH_2CH_2O-$. Important members of this series are the tetramer, pentamer, and hexamer although macro-cyclic compounds are well known (Figure 2).

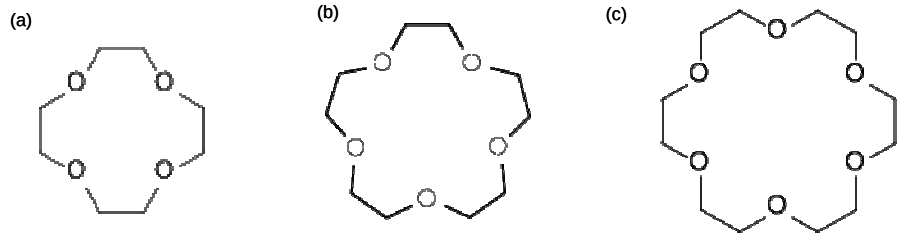

Figure 2: Generalised structure of the crown ethers: (a) 12-crown-4, (b) 15-crown-5 and (c) 18-crown-6.

Regarding crown ethers, the first number refers to the number of atoms in the cycle, and the second refers to the number of those atoms that are oxygen.

The first synthesis of crowns was achieved by Pederson in 1967[24, 25] in an attempt to prepare an alkyl phenolic ether. The partially protected catechol he was using was partially contaminated with about 10 % of catechol but an unexpected product was obtained instead, due to the presence of catechol in the reaction mixture.[26] The product was isolated to be dibenzo-18-Crown-6 (Figure 3). Many other crowns were subsequently prepared in Pederson's Laboratory.[27-36]

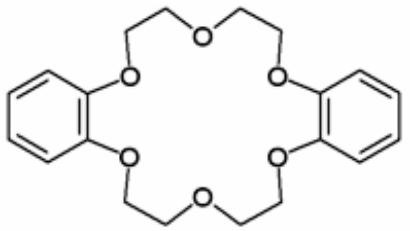

Figure 3: First crown ether isolated in 1967 in Pederson's Laboratory, dibenzo-18-Crown-6.

Since their accidental discovery by Pedersen the crown ethers have proved to be very accepted and useful ligands (hosts) for a wide range of metal ions and neutral or ionic organic species. Indeed, it seems to bind to the majority of the elements of the periodic table.

In fact the term "crown" was applied to this class of macro-cyclic poly-ethers by Pederson because of the similarity between the computer-simulating space-filling-model

of the crown ether bound to a cation with a crown sitting on the head. A more current model of the potassium complex of 18-crown-6 is shown in Figure 4 where the hydrophilic oxygen atoms surround the cation while the lipophilic ethylenic groups dispose themselves around the complex as a shell.

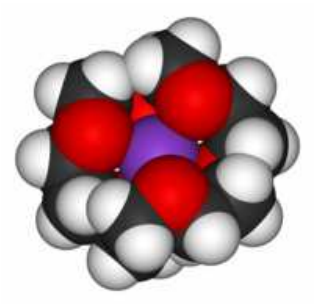

Figure 4: Computer-simulating space filling model of the potassium complex of 18-crown-6.

The chemistry of the crown ethers was first review in 1974 by Izatt[37] and he (along with a growing group of other scientists[38]) has been kept busy by the productivity of the field ever since.[39, 40] The chemistry of crown ether has become so popular by the notion that these ligands may bind to the metal cations on the basis of their size and geometry within the cavity of the macro-cycle. Indeed it was suggested as early as 1971 that ratios of cation radius to crown ether internal Van Der Waals diameter of 0.75 - 0.90 : 1 were suitable for metal ion inclusion within the macrocycle.[41] The ionic radii of some alkali metal cations and the approximate diameter of crown ethers in idealised binding conformation is shown in Figure 5.

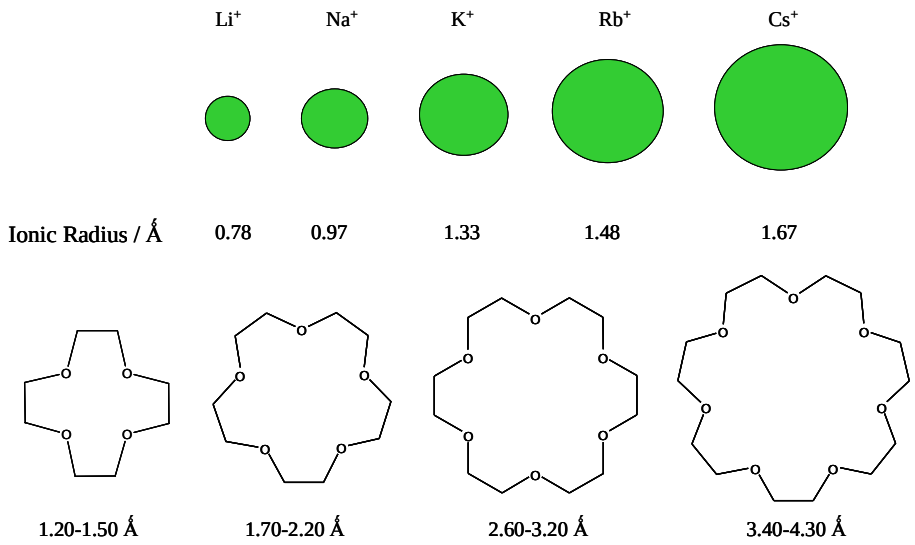

Figure 5: ionic radii of alkali metal cations and idealised crown ether diameter.

When the cation size is comparable with the crown ether cavity, the binding will be with a “key” and “lock” type combination, although for flexible and large crown ethers such as 18-crown-6, this is not often encountered as the adoption of symmetrical conformations will result in an unfavourable empty cavity. Therefore, the crown ether will adjust its conformation to surround it and the cation will be centro-symmetrically fitted within the cavity (Figure 4).

The ionic radii of the most important metals are reported in the following Table 1.

Table 1: Metal ionic radius of interest.

Element	Charge	Ionic Radius (Å)	Element	Charge	Ionic Radius (Å)
Na	+1	0.97	Cu	+1	0.77
K	+1	1.33		+2	0.73
Ca	+2	1.00		+3	0.54
Fe	+2 (low spin)	0.61	Se	-2	1.98
	+2 (high spin)	0.78		+4	0.50
	+3 (low spin)	0.55		+6	0.42
	+3 (high spin)	0.65	Sr	+2	1.18
	+4	0.59	Pb	+2	1.19
	+6	0.25		+4	0.78
Co	+2 (low spin)	0.65	Po	+4	0.94
	+2 (high spin)	0.75		+6	0.67
	+3 (low spin)	0.55	U	+3	1.03
	+3 (high spin)	0.61		+4	0.89
	+4	0.53		+5	0.78
Ni	+2	0.69		+6	0.73
	+3 (low spin)	0.56	Pu	+3	1.00
	+3 (high spin)	0.60		+4	0.86
	+4	0.48		+5	0.74
				+6	0.71

It is important to emphasise that the simple crown ether is only a two dimensional ligand and leaves the “North and South poles” of the metal cation exposed to other interactions, while it wraps the “equator and tropics”. When the difference between the size of the cation and the size of the crown ether cavity is particularly high, the cation is too large or too small to fit comfortably and centro-symmetrically, the complex will adopt a much more likely “sandwich” conformation where a single cation is held between two crown ether ligands. The stability of this kind of conformation is relatively low, however, these complexes have been observed. Other different conformations such as 2 : 2 complex have been observed[42], however they are rarely encountered.

Crown ethers which carry simply a crown ether function may preclude wider applications because of their limited mode of complexation. In addition, the rather low stability of the complexes may not meet various practical needs. Functionalization reactions of crown ethers eliminate these restrictions and provide ample applications in many areas.

While the first crown ether that was characterized contained only oxygen donor atoms, sulphur and nitrogen-containing crown ethers were subsequently prepared. Following Pederson's discovery, many other different organic macro-cyclic molecules were synthesized including thio-crown ethers[32], Aza-crown ethers[43], lariat ethers[44], chiral crown ethers[45, 46], cryptands[47] etc. These materials (Figure 6) have the ability to bind to both cations and anions.

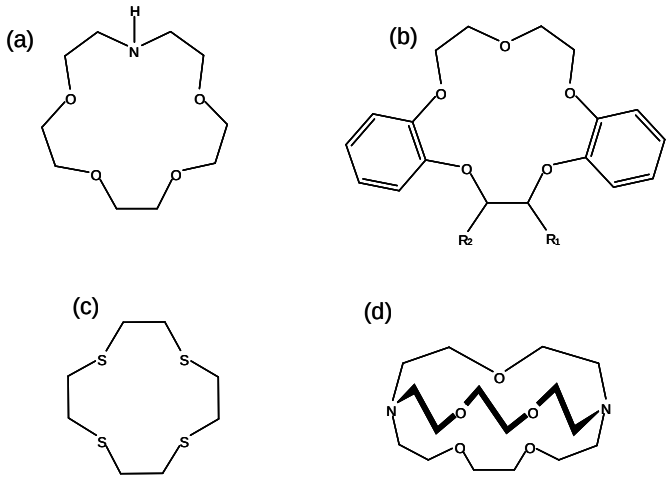

Figure 6: (a) Aza-crown ether, (b) lariat crown ether, (c) thio-crown ether, (d) cryptand.

Due to their high flexibility they have proved to be capable of adapting themselves to a wide variety of coordination requirements and media. Their flexibility imparts some very interesting properties such as solubility in both aqueous and lipophilic solvents and rapid, reversible ion binding characteristics. On the Hansch lipophilicity scale (based on measurement of the octanol water partition coefficient), 18-crown-6 has a value of exactly zero, indicating a perfect balance between hydrophilicity and lipophilicity, a feature that is a result of ligand flexibility enabling it to expose either hydrophilic ether oxygen atoms or lipophilic ethylenic groups to the surrounding medium. The versatile solubility and transport capabilities of the crown ethers make them highly suited to

applications as ionophores (phase transport catalysis)[48, 49], in sensing and signalling applications[50], to stabilize unstable molecules or act as a host for chemical reactions.

All of these works led to the 1987 Nobel Prize in chemistry being awarded to Charles Pedersen[26], Jean Marie Lehn[51] and Donald Cram[52] for their pioneering work in the field.

Recently much interest was focused on the use of crown ethers in the extraction of radioisotopes, i.e. ^{90}Sr is well known to be one of the most important nucleotides present in nuclear wastes, separation of such radioisotope by solvent extraction using crown ethers was described.[53] Another example is the extraction of ^{22}Na, ^{45}Ca, ^{85}Sr and ^{133}Ba isotopes from aqueous solutions by crown ethers and di-carbollyl-cobaltate in nitrobenzene.[54]

1.2.2. Aza-crown ethers.

Due to differences in polarizability, nitrogen-containing crown ethers (Aza-crowns) and sulphur-containing crown ethers (thio-crowns) display different ionic selectivities than oxygen-containing crown ethers. These differences in behaviour can be explained by hard-soft acid-base theory, also known as HSAB.[55, 56] This approach was developed by Pearson in the nineteen sixties and it has been widely used in chemistry to explain stability of compounds, reaction mechanisms and pathways. It assigns “hard or “soft” and “acid” of “base” to chemical species. “Hard” is applied to species which are small, have high charge states (the charge principle is mainly applied to acids than bases), and are weakly polarisable. “Soft” is applied to species which are big, have low charge density and are strongly polarisable. “Soft” acids react faster and form stronger bonds with “Soft” bases, whereas “Hard” acids react faster and form stronger bonds with “Hard” bases. Thus, soft ligands, such as those that contain only sulphur or nitrogen, provide polarisable sites that have increased affinities for soft metal ions such as heavy metals (including precious metals). In contrast, hard ligands, such as those which contain oxygen, have sites of low polarizability and increased affinities for hard metal ions such as the alkali and alkaline earth metals.[57, 58] An Aza-crown ether nitrogen-oxygen-containing has complexation properties that are intermediate between those of the oxygen only crowns, which strongly complex alkali and alkaline earth metal ions, and those of the nitrogen

only cyclams, which strongly complex heavy metal cations.[59] These mixed complexation properties make the Aza-crown ether interesting to research in many areas.

One of the most popular Aza-crown ethers is the mono-Aza-crown where a heteroatom of oxygen is substituted with nitrogen. This kind of material can be purchased or synthesised. They are usually expensive to purchase and the most common route in literature is the reaction of an alkyl amine, usually a benzyl amine, with an ethylene glycol di-tosylate followed by the reduction of the benzyl Aza-crown ether obtained (Figure 7).[60]

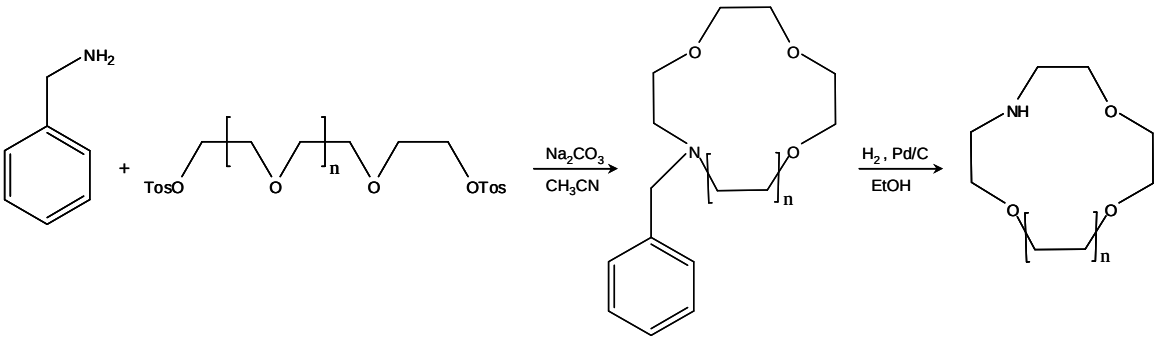

Figure 7: Synthesis of mono-Aza-crown ether.

In general, the Aza-crowns are more suitable than crown ethers themselves because it is possible to introduce a variety of side chains onto nitrogen; therefore modification of the nature of the cavity is more feasible. In fact macro-cyclic poly-ethers with a side group containing other donor atoms (lariat crown ethers) can form complexes with a three dimensional coordination sphere, similar to cryptands, since the donor atoms of both the macro-ring and the side chain can be involved in the coordination. Flexible and long side chains ease this coordination process and the result is an unusual improvement of the complex-forming properties, which are not directly related to the concept of size compatibility of cation and macro-ring cavity but are strongly dependent upon the nature of the side chains. The single-armed nitrogen pivot lariat ethers are shown as example in the following Table 2.

Table 2: Logarithm of the equilibrium constants (log K) of single-armed nitrogen-pivot lariat ethers assuming 1:1 complexes.[61]

R (side arm)	*Cation Binding, log K*			
	Na^+	K^+	NH_4^+	Ca^{2+}
-H	1.70	1.60	2.99	ND
-CH2COOH	2.31	2.02	ND	ND
-CH2COOCH3	3.88	3.95	3.14	3.75
-(CH2CH2O)2CH3	4.54	4.68	3.19	4.06

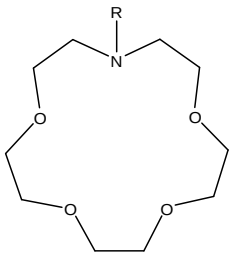

An interesting example is the lariat crown ether which has been studied from Gokel *et al.* where the cation was trapped in a "sandwich" conformation between the interaction of the mono-Aza-crown ether and the non-covalent interaction of the cation with the π-system (Figure 8).[62]

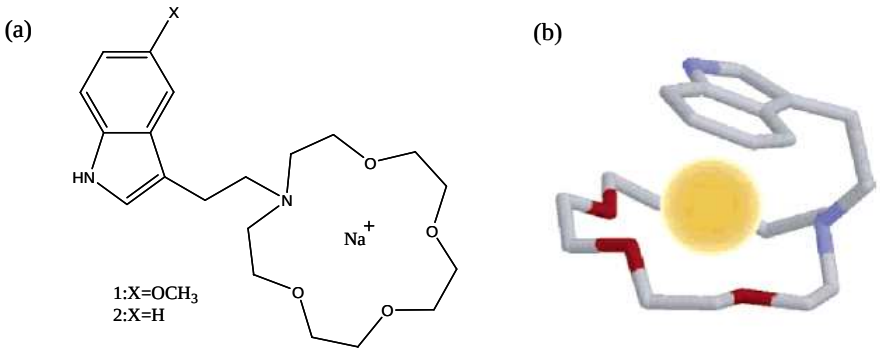

Figure 8: Structures of the lariat ether studied from Gokel *et al.* (a) two-dimensional structural representation. (b) 3-dimensional representation. Hydrogen atoms are not shown for clarity; the sodium cation is shown in orange.[62]

In this respect, N-hydroxyl-ethyl Aza-crown ethers are interesting representatives of lariat ethers. These compounds are easy to synthesise and the terminal hydroxyl groups (or alkoxy groups in the case of N-alkoxy-ethyl derivatives) usually participate in the coordination with a cation.[63-66] In addition, the N-hydroxy-ethyl mono-Aza-crown ether has a hydroxyl functional group which can be used to add other functional groups to the

Aza-crown ether, obtaining more complex compounds. R. Suzuki *at al*. used N-hydroxy-ethyl mono-Aza-crown to synthesise an interesting material where the cation capturing/transporting property of the Aza-crown ether and the anion capturing/transporting property of organo-germanium compounds were combined to form the compound shown in Figure 9. The cation capturing/transporting property of the Aza-crown ether was enhanced by the presence of the germanium[67] in the lariat ether as it binds the counter ions (anions) stabilising the whole complex.

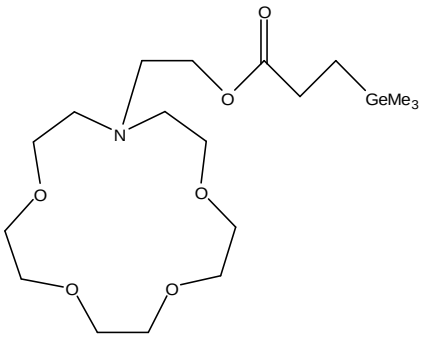

Figure 9: Mono-Aza-crown with germanium-containing side-chain.

There are a few different possible routes to obtain the N-hydroxy-ethyl Aza-crown ether and the most common is the reaction of the popular mono-Aza crown ether with oxirane. This process has strict optimal conditions; if the optimal reaction time is exceeded, the products of further addition of oxirane (to the hydroxyl-ethyl group) start to accumulate in large amount, decreasing the yield and complicating the purification of the target product. Under the optimal conditions, the yields of the target products do not exceed 60 %.[68]

Another interesting route which does not require the expensive mono Aza crown ether is shown in Figure 10. This method, which is a modification of the one reported by Newkombe and Marsden[69], has been developed by R. Suzuki et al.[67]

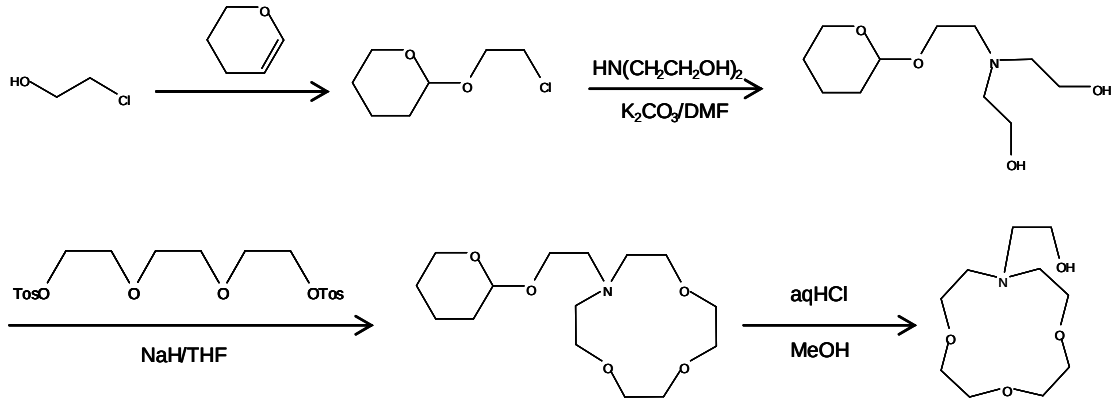

Figure 10: Synthesis of N-hydroxy-ethyl Aza-crown ether.[67]

The process appears to be a little complicated because the NH function of the di-ethanolamine must be protected during the ring closure. The protecting procedure is selected such that the protecting group will eventually be the side chain of the nitrogen with the terminal hydroxyl group. Thus, the 2-chloro ethanol is treated with 1, 2-di-hydropyran in order to protect its hydroxyl group and avoid auto polymerization. The pyranyl ether is made to react with di-ethanolamine to form the N-(2-pyranyloxyethyl)-di-ethanolamine which is the substrate for the cyclization of the Aza-crown ether. The cyclization proceeds between this intermediate and tri-ethylene-glycol di-tosylate to give pyranyl-oxyethyl Aza-crown ether. In the last step the hydroxyl group is de-protected through simple hydrolysis.

The Aza-crowns also have important uses as synthetic receptors in molecular recognition processes[70] and in some cases, anion complexation properties that are similar to those in certain biological systems.[71-73] They have enhanced complexing ability for ammonium salts[74, 75] and for transition metal ions[75, 76] over the oxygen only crown compounds. In addition, the Aza-crown ethers are important intermediates for the synthesis of cryptands (from di-Aza-crowns)[47, 77], nitrogen pivot lariat crown ethers[63] and other species requiring one or two nitrogen in the macroring.[78] There are a number of interesting uses of Aza-crowns as a catalyst in nucleophilic substitution and oxidation reactions[79], in the design of chromogenic reagents that are sensitive to alkali and alkaline earth metal cations[80] and for analytical applications[81] such as chromatographic separation of metal cations, ion-selective electrodes, colorimetry.

The ability of Aza-crown ethers to form stable complexes with metals have also been used for radioisotope extractions i.e. ^{85}Sr was extracted using Aza-crown ethers in a liquid/liquid extraction[82] and in 2002 an open-chain Aza-crown ether was used as a decontaminant of radioactive caesium from natural NaCl.[83] A few works in literature also involve isotope separations using Aza-crown i.e. ^{6}Li-^{7}Li [84]; ^{24}Mg-^{25}Mg, ^{25}Mg -^{26}Mg and ^{24}Mg-^{25}Mg.[85]

1.2.3. Determination of metal-ion distribution ratio.

The complexation phenomenon, in the case of 1:1 crown ether-cation complex, can be defined by:

$$M^+ + CE \rightleftharpoons M(CE)^+$$

where M^+ is the metal cation and *CE* is the crown ether. The thermodynamic stability constant of the complex, K_1, is given by the equation 1:

$$K_1 = \frac{[M(CE)^+]}{[M^+]_{free}[CE]} \qquad (1)$$

Assuming all activity coefficients are 1. The concentration of free $[M^+]$ may be obtained using a variety of techniques including calorimetry[86], spectroscopic methods[87] and ion selective electrode (ISE) techniques.[61] The most popular method to detect Aza-crown ethers (and more in general for crown ethers) is the ISE technique which was described for the first time in 1971 by Frensdorff.[88] A simple method using the Frensdorff approach was described in 1986 by Gokel *et al.*[89] and measures potential at 25°C by a voltmeter equipped with ion selective electrodes. The free concentration of $[M^+]$ is calculated by the Nerst Equation:

$$\Delta E = E_{ref} - E_{crown} \qquad (2)$$

$$[M^+] = e^{-\Delta EnF/RT}[M^+]_{ref} = 10^{-\Delta E/0.0591}[M^+]_{ref} \qquad (3)$$

where E_{ref} is the potential of the solution containing only the metal, and E_{crown} is the potential of the solution containing the metal and the crown ether.

The complex concentration is calculated by subtracting the $[M^+]_{free}$ from the total salt concentration added to the sample before adding the crown ether.

$$[M(CE)^+] = [M^+]_{total} - [M^+]_{free} \qquad (4)$$

From the total crown concentration and the complex concentration, $[CE]_{free}$ can be calculated:

$$[CE]_{free} = [CE]_{total} - [M(CE)^+] \qquad (5)$$

At this point the equilibrium constant, K_1, is calculated from the values of $[M^+]_{free}$, $[CE]_{free}$ and $[M(CE)^+]$ using equation 1. The *log* K_1 values of the same sample are then averaged and if the standard deviation is too high (i.e. Gokel *et al*. did not accept standard deviation >0.04) the situation is complicated by the presence of second order or higher equilibrium because the crown ether is forms 1 : 1 and 2 : 1 complexes. In this case the original approach of Frensdorff has to be applied. This method consists in ΔE measurements of the salt solution while the crown ether is added. A second equilibrium and a second equilibrium constant have to be considered:

$$CE + M(CE)^+ \rightleftharpoons M(CE)_2^+$$

$$K_2 = \frac{[M(CE)_2^+]}{[M(CE)^+][CE]} \qquad (6)$$

assuming activity coefficients of 1 and where $[M(CE)_2^+]$ is the concentration of the 2 : 1 complex. If the crown ether is added by titration and *m* is the ml of $[M^+]_{total}$ and *c* the ml of $[CE]_{total}$ added the equation 1 and 6 will become:

$$K_1 = (1-u-y)/\{uD[cC_0/m - M_0(1-u+y)]\} \qquad (7)$$

$$K_2 = y/\{D(1-u-y)[cC_0/m - M_0(1-u+y)]\} \qquad (8)$$

Where the dilution factor D= m/(m+c), *u* is the fraction of cation left un-complexed and *y* is the fraction of cation in the 2:1 complex. If equation 7 and 8 are combined equation 9 can be obtained:

$$y = 1 - uR - [(1 - uR)^2 - (1 - u)^2]^{1/2} \qquad (9)$$

where $R = 1 - K_1 / 2K_2$. Thus if *u* is known and *R* is assumed K_1 and K_2 can be calculated. The R value assumed by Frensdorff was one that when substituted into equation 9 gave a theoretical curve that fitted with the experimental values.

Another method to evaluate the complexation properties of crown ether is the extraction of a coloured salt monitored by spectroscopic techniques. The salt of a coloured organic acid, i.e. picric acid, is dissolved in water and an immiscible organic solvent, i.e. CH_2Cl_2, is added. If the two phases are shaken, no extraction occurs because the salt is insoluble in the organic phase. When the crown ether is added, the cation and its coloured anion are complexed and conducted into the organic layer. Values of metal ion extraction are obtained by measurements of absorbance before and after the crown ether is added. Most of the papers simply calculate a percentage of salt extracted from the aqueous solution by the crown ether using the following equation

$$\%\ extracted = \frac{A_0 - A}{A_0} \times 100 \qquad (10)$$

Where A_0 and A are the absorbance of the picrate ion (350nm) for the aqueous phase before and after the extraction, respectively. The concentration of $[M+]_{free}$ can also be calculated using the Beer-Lambert Law ($A = \varepsilon \cdot C \cdot l$).

Shono[90] *et al.* also measured a distribution ratio of the cation between the two phases (*D)* and consequently the equilibrium constants. The extraction equilibrium between the aqueous solution of metal cation (M^+), picrate anion (A^-) and a CH_2Cl_2 solution of the crown ether can be defined for the 1:1 crown ether-cation complex by the equations

$$M^2_{aq} + A^-_{aq} + CE_{org} \rightleftharpoons M(CE)A_{org}$$

$$K_e = \frac{[M(CE)A]_{org}}{[M^+]_{aq}[A^-]_{aq}[CE]_{org}} \quad (11)$$

Since CH_2Cl_2 is used as the organic solvent the concentration of un-complexed cation in the organic phase is extremely low compared with that of the complex. The concentration of the crown ether in aqueous phase should also be quite low but experiments have to be carried out to confirm this assumption. Consequently other assumptions can be made:

$$\frac{[M(CE)A]_{org}}{[M^+]_{aq}} = D \quad (12)$$

$$[M^+]_{aq} = [A^-]_{aq} = M^0 - A \quad (13)$$

$$[CE]_{org} = (CE)^0 - A \quad (14)$$

Where M^0 and $(CE)^0$ are the initial concentration of metal and crown ether, respectively, and A is the concentration of the picrate transferred to the organic phase which can be determined spectrophotometrically. Equation 11 can now be rewritten to form equation 15:

$$D = K_e(M^0 - A)[(CE)^0 - A] \quad (15)$$

If these assumptions are reasonable, the plot of $-\log D$ *vs.* $-\log (M^0-A)[(CE)^0-A]$ should give a straight line with a slope of 1 and $\log K_e$ as the intercept of the straight line. If the straight line is not obtained it suggests that the material also forms 2 : 1 complexes and the following equation can be applied:

$$D = K_e(M^0 - A)[(CE)^0 2A]^2 \quad (16)$$

This equation considers that a “sandwich” complex is formed by two different units of crown ether. When it is formed intra-molecularly, the two singular units can be considered as a single entity and equation 17 can be used:

$$D = K_e(M^0 - A)[(CE)^0 - 2A) \quad (17)$$

1.3. Linear Polymers containing Crown ether groups.

1.3.1. General description.

Incorporation of crown ethers into linear polymers or immobilized polymer supports provides attractive aspects:

1) Modification of their complexation properties.

2) Facility in their recovery.

3) Improvement of their physical and chemical properties.

At this point, it should be pointed out that the dipolar interaction between a cation and its partner (crown ether) is often inefficient especially when the cation diameter exceeds that of the crown ether cavity or vice versa. Subsequently many studies were aimed to functionalise crown ethers and obtain more efficient lariat ethers. In fact the stability of the complex is tightly dependent on the number and type of the ether-atom donors and the size/shape of the cavity relative to the cation size. When the crown ethers are incorporated in a polymer matrix, they tend to form their most stable 1:1 complex either by “key “ and “lock” combination or crown ether adjustments with ions having diameters comparable to that of their opened cavity as if they would be single units. However, they can also form stable “sandwich” complexes with ions of larger size. In fact two adjacent crown ethers in the same chain, can cooperate to hold a cation between each other more efficiently than two independent units, the result is an improvement of the 2 : 1 complexes stability. Moreover the entire structure of the polymer can cooperate to raise the complexation properties of the material, i.e. two non-adjacent crown ethers of the same chain or two crown ethers of different chains.

Polymer supports also offer the advantage of easy handling and recoverability of the material, an aspect especially useful when the polymer is used in the removal of toxic compounds. Crown ethers are in fact soluble in most solvents therefore their separation, after extraction is often difficult. This aspect limits their technological use. In addition they have low thermal and chemical stability and need a physical support for most of

their applications; a polymer matrix provides an excellent means of immobilization and improves their properties.

The crown ethers can be part of the main chain, pendant groups anchored to a polymer backbone or the end groups of a macromolecular chain (Figure 11).

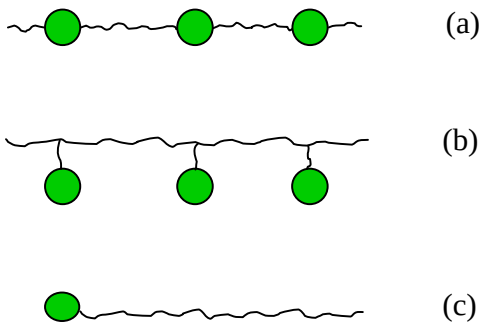

Figure 11: Linear polymers containing crown ether as (a) part of the main chain, (b) as side groups and (c) as terminal group. The crown ethers are represented by green circles for clarity.

Crown ether polymers of type (b) in which the crown ether moieties are bound through a flexible, long side chain can interact more effectively with cations and form both 1: 1 and 2: 1 complexes depending on the size of the cavities and the ions. This results in a high metal selectivity and complex formation ability. 1: 1 complexes are favoured when the crown ether groups are spaced sporadically even if 2: 1 complexes are also formed from intermolecular cooperation leading to physical cross-linking. Moreover if the side chain that connects the crown moieties to the main polymer chain has additional donor atoms, they can also participate in complexation, further raising their stability.

Linear polymers of type (a) may also form “sandwich” complexes but the decreased mobility of the crown ethers results in a more difficult arrangement of the chains in a suitable disposition for the 2: 1 complexes. Complexes 1: 1 are instead possible depending on the size of both cavities and ions.

Finally, the polymer type (c) is obviously not suitable as a scavenger material because of the low presence of the crown ether in the chains.

1.3.2. Side chain crown ether polymers.

In general, two methods (Figure 12) are applied to prepare linear polymers with crown ethers as side groups:

1. Radical polymerization of a vinyl derivative of the crown ether.

2. Reaction of functional groups on crown ethers with functional polymers.

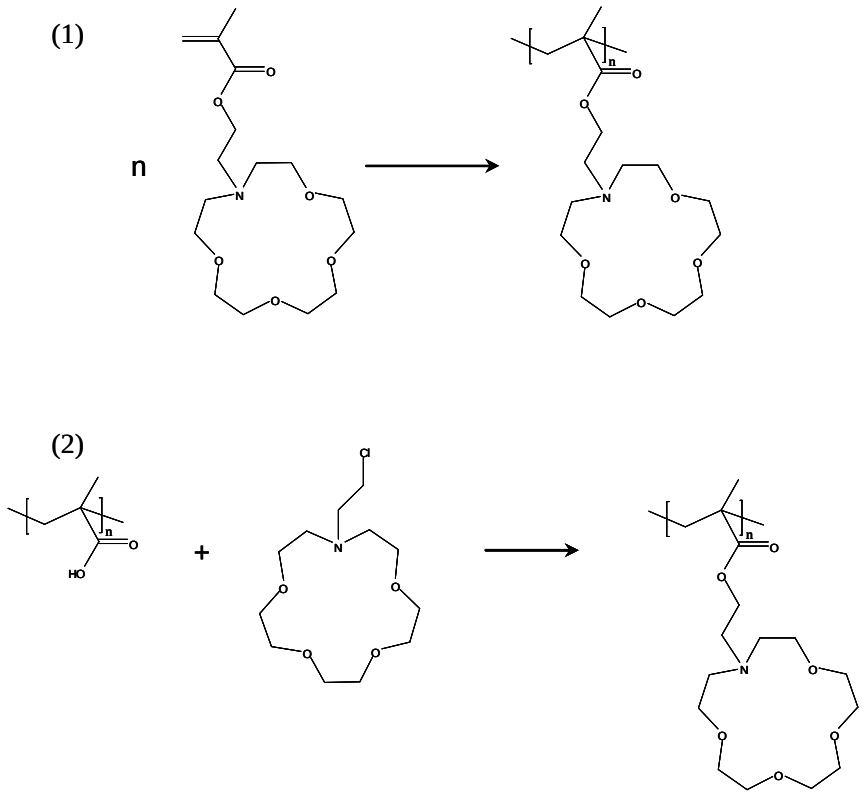

Figure 12: Synthetic routes for the synthesis of side chain Aza-crown ether polymers: 1) direct polymerization of a vinyl derivative; 2) post-functionalization of a preformed polymer.

The first method involves the polymerization of crown ether-containing monomers. With this approach the crown ether content can be controlled by the insertion of comonomers and it is the most favourable route for the preparation of polymers especially regarding specific control of monomer contents.

The second method is the reaction between functionalised crown ethers and the reactive functional groups, randomly attached to the backbone of a pre-formed linear polymer. This synthetic route offers limited and less controllable crown ether content along the polymer backbone and it may be difficult to achieve reaction completion but in some cases it is the only method for obtaining functionalised polymers. In fact due to the steric hindrance of the large ring structure in crown ethers the polymerization of its monomer derivatives is a very difficult synthesis and thus these monomers often do not polymerise efficiently to give high molecular weight polymers but instead give short oligomers.

As already mentioned, polymers containing crown ethers as pendant groups exhibit a cooperative effect of adjacent crown ether moieties which results in the formation of 2 : 1 complexes. Such complexes are generally more lipophilic and stable than those of the corresponding monocyclic crown ethers and these compounds are therefore effective extracting reagents for various cations. The complexation properties of poly-, bis- and mono-crown ether, shown in Figure 13, were compared by Shono *et al.*[90]

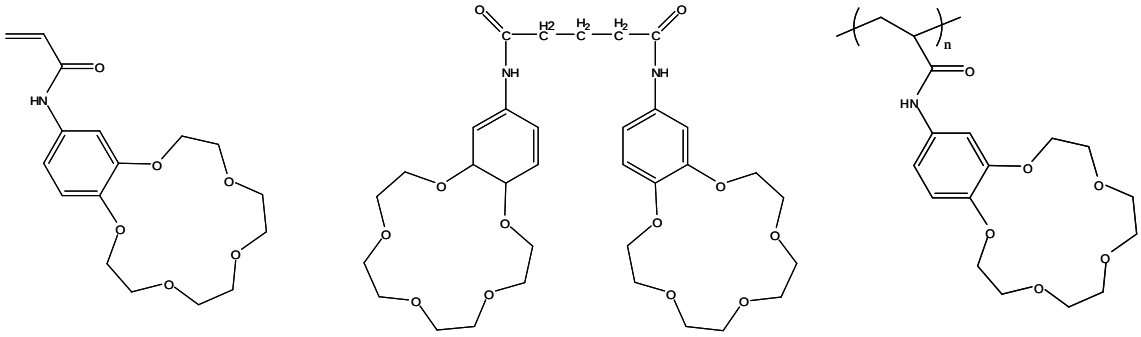

(a) (b) (c)

Figure 13: Crown ethers derivatives used in Shono's studies.[90]

Results are shown in Table 3 and they are expressed as D, the distribution ratio of a picrate salt of a metal ion between two phases (aqueous and organic) monitored by spectrophotometric techniques.

It is particularly noteworthy that the logD values of the poly- and bis-crown ether are higher than those of its monomeric analogous because of the cooperative action of two adjacent crowns. Moreover the values of the poly-crown ether are higher than those of

the dimeric analogous and this can only be explained by a cooperative action of the entire polymer chain.

Table 3: Extraction of compounds shown in Figure 13 (a, b and c) expressed as distribution ratio (D).[90]

Crown Ether	*logD*			
	Na^+	K^+	Rb^+	Cs^+
(a)	-2.28	-1.94	-2.28	-3.15
(b)	-2.21	-0.565	-0.747	-1.51
(c)	-1.66	0.097	-0.284	-1.05

The vinyl-benzo derivatives (Figure 14) of the poly-acrilamide-benzo-15-crown-5 (Figure 13) were first synthesised and polymerised by Smid and Hogen Esch[91]. These omo-polymers (Figure 13) are both able to extract salt from an aqueous solution to an organic solution more efficiently than the corresponding monomers but they exhibit lower extraction equilibrium constants than that of the poly-acryl amide benzo-crown-ether. This difference can be explained by the effect of the hydrogen bonding between the NH and the CO groups in the poly-acryl amide-benzo-15-crown-5 which help to establish 2 : 1 complexes.

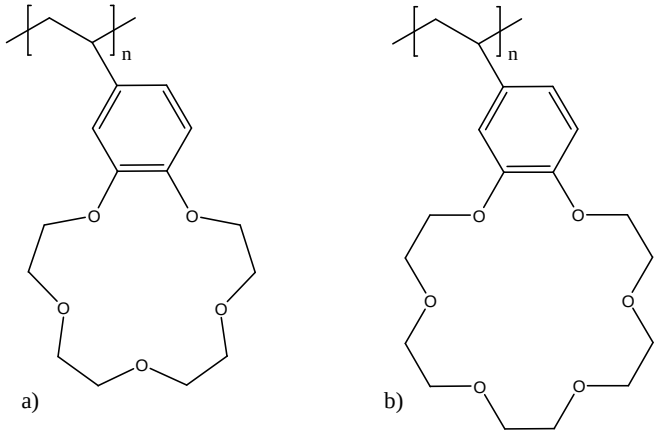

Figure 14: (a) poly-4'-vinylbenzo-15-crown-5; (b) poly-4'-vinylbenzo-18-crown-6.

Yagi's group[8] copolymerized methacrylamide and methyl methacrylamide of benzo-15-crown-5 and benzo-18-crown-6 with methyl-methacrylate. The insertion of the methacrylate units resulted in a rapid decrease in the extraction properties of the material.

Thus careful consideration of comonomer and side chain (used to attach the crown ether to the polymer matrix) is very important as these groups play a critical role in maximising the access of the metal ions into the polymer matrix by increasing the polymer's hydrophilicity. Low levels of complexation by immobilized crown ethers may not reflect the thermodynamic properties of the ligand-ion interaction but rather, the inaccessibility of the ions into the matrix.

In this aspect the counter-ions also play an important role; a study of membrane-supported benzo-18-crown-6 was carried out to examine the transport affinities for alkali metals (Figure 15).[92] Vinylbenzo-18-crown-6 was copolymerized with di-ethylene glycol ethyl ether acrylate in varying amounts and 2-5 mol % of hexa-methylene diacrylate as cross-linking agent on a support matrix of micro-porous polyethylene membrane. The membranes obtained were studied for the transport of K^+. High flux rates were observed and assigned to the high ligand density within the membrane. Additionally, transport increased with increasing hydrophilicity of the accompanying anion. The flux rate observed was greater when the ions were present as chloride rather than perchlorate salts due to the hydrophilicity of the membrane, allowing good access to the more hydrated chloride ions and hindering access to the less hydrated perchlorate ion.

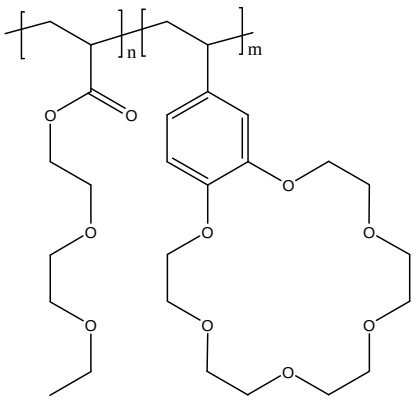

Figure 15: Benzo-18-crown-6/di ethylene glycol ethyl ether copolymer.

Another application of these polymers is their use as catalysts in organic reactions. For example, poly-4'-vinylbenzo-18-crown-6 and poly-4-vinyl pyridine were used[93] to catalyse the hydrolysis of negatively charged 3-nitro-4-acetoxybenzene sulphonate (NABS) in aqueous ethanol. With the crown ether units in the copolymer positively charged by potassium ions, the material attracts the negatively charged NABS, catalysing its hydrolysis at neutral pH. Poly-methyl methacrylamide benzo-16-crown-6, synthesised by Yagi's group, was instead used[94] as a catalyst for the conversion of C1-C6 fatty acid salts to their bromophenacyl- or penta fluoro-benzyl esters.

Recycling and reusing these materials, allowing a more cost-effective treatment process and waste remediation, is very important, so careful consideration is necessary. Baumann *et al.*[95] synthesised polymer pendant crown thio-ethers (Figure 16) for the removal of Hg^{2+} from an acidic mixed-waste, containing a wide variety of metals, such as Al^{3+}, Fe^{3+}, Cd^{2+} and Pb^{2+}.

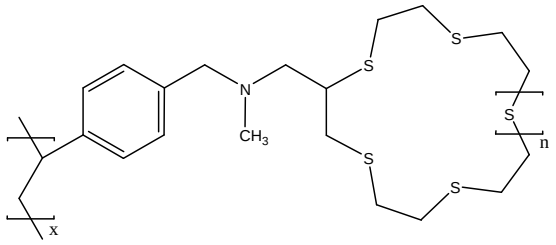

Figure 16: Polymer pendant crown thio-ether with n = 0 and n = 1.

Crown thio-ethers are well-known to be suited for this task due to their high affinity for Hg^{2+} ion. Interesting in this work is the regeneration of the polymer which requires a stripping of the metals from the binding sites of the polymer. This can be achieved using a ligand which competes with the crown ethers immobilised on the polymer. Baumann *et al.* found a convenient method which utilises the dithizone ligand and apparently the recovery of the Hg^{2+} from the polymer was determined to be quantitative. The crown ether was then reused to treat another aliquot of the acidic metal waste without significant loss of loading capacity.

Crown ether polymers have been studied intensively as solid electrolytes[96, 97]. Their applicability for such task is based fundamentally on their ability to solvate metal ions,

thereby isolating them from their anions and thus avoiding the formation of immobile ion pairs. Two prerequisites for such kind of materials is that the polymer has to be flexible, as indicated by a low T_g (glass transition temperature), so that the chains can be spatially reorganized during the complexation to form the best local geometry and the crown ether moieties has not to have too high complexation properties. In fact this would be associated to a lower mobility of the ions and therefore lower conductivity. This is another example where the polymer plays an important role for the material's properties.

All these examples just shown, prove that the polymer matrix is able to change and improve the properties of the material not only as a better handling but as better chemistry behaviour thus the choice of the comonomers of the crown ether is one of the most important aspect to consider.

Synthetic polymers bearing stimuli-responsive groups in their main chains or in their pendants can change their physical and chemical properties in response to stimuli. Incorporating crown ethers in a polymer matrix with stimuli responsive groups can give materials where the binding properties of the crown ether moieties can be controlled by selective stimuli (temperature, pH, light etc.). For example polymers with photo-functional groups such as azo-benzene or spiropyran change their physical and chemical properties in response to photo-irradiation. Shinkai *et al* .[98] synthesised a polymer where a photo-functional azo-benzene was incorporated between a crown ether moiety and a styrene monomer and demonstrated that its binding properties can be controlled by light. This control is related to configurational and polarity transitions of the photo-functional groups once irradiated by a particular wave length; in fact the *cis*-isomers, which exhibit a great affinity for large metal ions can be photo-isomerised to their *trans*-isomers which exhibit high affinity for smaller metal ions. This isomerisation can be achieved by irradiating the *cis*-isomers with Hg-lamp with $330 < \lambda < 380$ nm. The different complexation properties of the two isomers are attributed to the formation of intra-molecular sandwich complexes between the *cis*-isomers and metals (Figure 17).

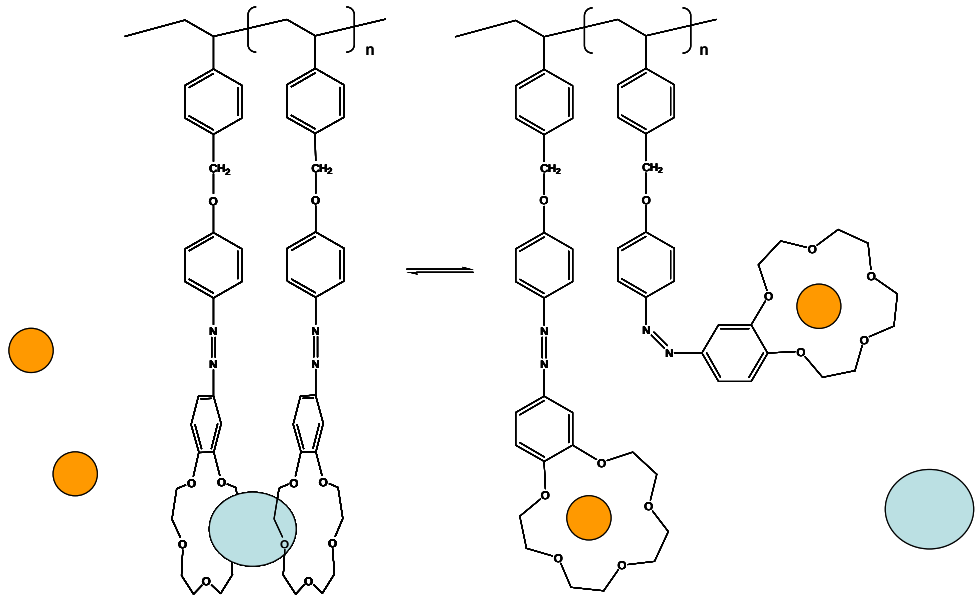

Figure 17: Photo-responsive sandwich complexes formed between pendant crown ether rings.[98]

Crown ethers have also been copolymerized with N-isopropyl-acryl amide in the presence of a cross-link agent to give an intelligent hydrogel.[99] Poly-(N-isopropyl-acryl amide) is a typical thermo-responsive material which exhibits a transition temperature (lower critical solution temperature, LCST) at ~ 32 °C in aqueous solution, above this temperature the polymer is hydrophobic while below the same temperature it becomes hydrophilic (an explanation of the phenomenon is given in section 1.5.2.). The cross-linked polymer is an insoluble but swellable hydrogel that adsorbs a large amount of water in its network below the LCST of the material, and thus exhibits a swollen state. But its swollen state collapses and displays a reduction in volume as the temperature is increased above the LCST. This process of phase separation is thermo-reversible. The incorporation of crown ethers in such polymer matrices can give this material the ability to extract metals during the thermo-reversible transition. However, no work has been carried out regarding this preparation and therefore there are not evidences of the complexation properties of these materials.

1.3.3. Side chain Aza-crown ether polymers.

The literature is limited regarding Aza-crown ether polymers although more can be found for the simple crown ether polymers.

One of the most interesting works involving Aza-crown ethers is the novel compound synthesised in Yashimi's Laboratory. They designed the stereo-regular poly-(phenyl-acetylene) bearing Aza-crown ethers as pendant groups (Poly-1 in Figure 18) for the amino acid binding sites.[100] In fact Aza-crown ethers are well known to form stable complexes with amino acids[51], a property that has been exploited by Yashimi et al. for synthesising a material able to detect free L-amino acids. This polymer proved to be highly sensitive to amino acid chirality and was able to detect an extremely small imbalance of the L-amino acid (less than 0.005% enantiomeric excess of alanine). In fact the amino acid transmits its chiral information to the polymer backbone leading to an excess of the one-handed helical sense, which is a source of optical activity (Figure 18). The crown ether pendants, represented in green and blue rings, arrange themselves in a helical array with a predominant screw-sense along the polymer back-bone; this arrangement determines an induced circular dichroism (ICD) which is used for the detection of the amino acid.

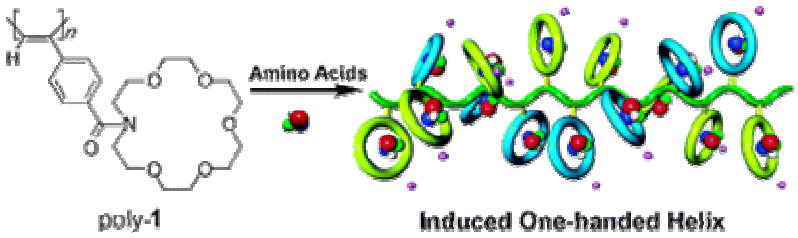

Figure 18: Schematic representation of the macromolecular helicity induction on Poly-1 upon complexation with L-alanine.[100]

Kimura *et al.* reported the synthesis of a polymer with pendant groups containing two Aza-crown ether moieties.[101] They designed a polymer where two moieties are incorporated to each tri-phenyl-methyl dye monomer derivative, more precisely Malachite Green leuconitrile (Figure 19). Many tri-phenyl-methyl dyes undergo photo-ionization to tri phenyl methyl cations and their counter ions, which thermally revert to the electrically neutral species, in particular Malachite Green leuconitrile is well known for this purpose.[102, 103] In this material the metal ion complexation can be controlled photo-chemically, based on electrostatic repulsion between the tri phenyl methyl cation

and a metal ion complexed by its crown moiety. The electrically neutral form binds strongly to a metal ion by cooperation of two adjacent Aza-crown ether rings. However, the cationic form ejects the metal ion by efficient electrostatic repulsion between the ion and the positive charge delocalized on the crown ring nitrogen atoms (Figure 19).

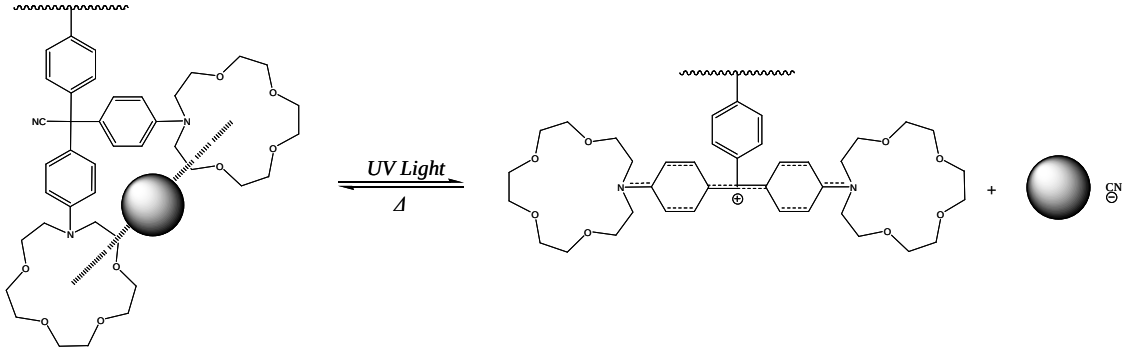

Figure 19: Representation of the photo-chemically transition of the polymer carrying bis-crowned malachite green leuconitrile moiety at the side chain.

In a previous work Kimura et al. also synthesised the bis-crowned malachite green leuconitrile[104] (Figure 20) which has the same properties as the previously mentioned polymer. Yet the polymer is generally better than the monomeric model in the metal ion concentration ability, especially for Cs^+. Moreover the metal ion complexing ability for the polymer is in the order $Cs^+ > K^+ > Na^+ > Li^+$ and that for the monomeric model is in the order $K^+ > Na^+ > Cs^+, Li^+$. The monomeric model likely form sandwich complexes with K^+ by a cooperative action of the two crown ether rings contained in the molecule because the K^+ is slightly greater in size than the crown ether cavity. The higher affinity of the polymer for Cs^+ rather than K^+ is attributed to the polymer effect which is a more sophisticated cooperative action of two or more crown ether rings in the polymer on the metal ion complexation.

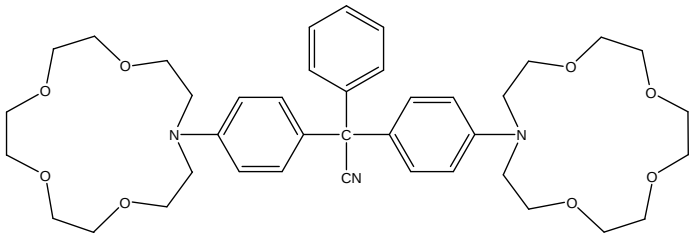

Figure 20: Monomeric model bis-crowned malachite green leuconitrile.

In the meantime Kimura *et al.*[105] synthesised other photo-chromic compounds containing Aza-crown ethers and spirobenzo-pyran derivatives and studying their complexation properties. Spirobenzo-pyran derivatives are useful compounds for the photo control of physical properties since they isomerise photo-chemically from their electrically neutral spiropyran form to the zwitterionic merocyanine form (Figure 21). These derivatives, when isomerised to their zwitterionic form, are likely to aggregate to form merocyanine pairs by electrostatic attraction. Moreover the negative charge on the oxygen can interact with the metal ion within the cavity of the Aza-crown ether increasing its complexation properties giving a more stable complex.

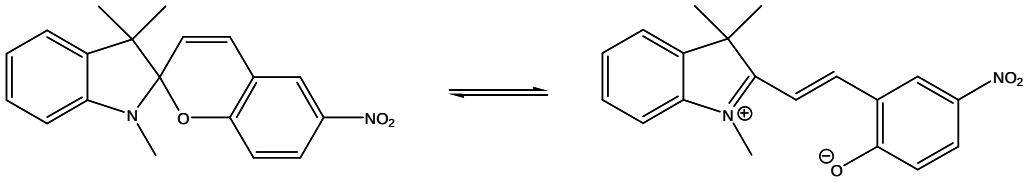

Figure 21: Photochromism of spyrobenzo-pyran.

Firstly a spirobenzo-pyran derivative was designed incorporating a crown ether moiety into the 8-position and subsequently a copolymer of methacrylate monomers possessing crown ethers and spirobenzo-pyran moieties and both are shown in Figure 22.

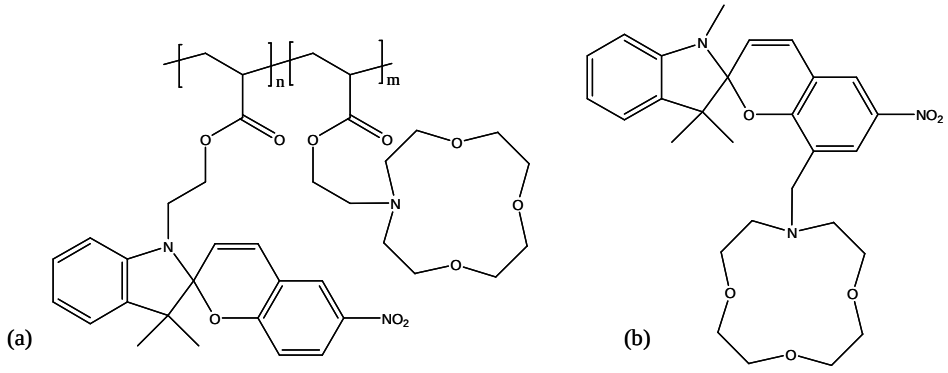

Figure 22: (a) Aza-crown ether- spirobenzo-pyran copolymer; (b) spirobenzo-pyran with Aza-crown ether in 8-position.

The merocyanine aggregation seems to be enhanced in polymers carrying the spirobenzo moiety in the side chain, which also enhances the complexation properties. On the other

hand, the metal ion-complexation by the Aza-crown ether moieties in the polymer brings rheology and photo chromic changes due to expansion of the chains for the intra-molecular electrostatic repulsion between the cationic charges. The effect is an enhancement of the merocyanine aggregation which allows the formation of a photo-induced precipitate; in fact prolonged UV irradiation led to marked precipitation of the polymer complexed to the metal ions. Notably, the polymer precipitate induced by UV irradiation in the presence of a metal ion was again dissolved in solution by a subsequent visible-light irradiation, in other words the precipitation process was reversible.

Aza-crown ethers have also been incorporated to Merrifield peptide resin[85] and used as a chromatographic stationary phase for the separation of $^{24}Mg^{2+}$ and $^{26}Mg^{2+}$. The production of ^{24}Mg is an important task because this isotope is the precursor of the ^{22}Na, a rare β^+ emitter. These isotopes are used in various scientific fields[106]. The heavier isotopes of magnesium were enriched in the resin phase, while the lightest isotopes were enriched in the solution phase. The capacity of the Aza-crown ether exchanger was 0.89 meq/g dried resin although total separation was not carried out.

This ability of the Aza-crown ethers to selectively complex different isotopes can be used to design new materials for the decontamination of radioactive isotopes. Incorporating Aza-crown ether moieties to a well designed matrix polymer can lead to the development of great materials for decontaminating solid surfaces or solutions.

1.4 Hydrogels.

Hydrogel materials are a class of polymer materials having a three dimensional structure. Such materials can absorb large amounts of water without dissolving and maintaining their distinct structure. Traditional methods of synthesis include cross-linking polymerization, cross-linking of reactive small polymer precursors and cross-linking via polymer-polymer reaction.

Copolymerization of hydrophilic monomers with low amounts of poly-functional comonomers leads to the formation of a hydrophilic three dimensional network. Poly-functional comonomers, such as methylene bis-acryl amide (BIS), carry two double bond

functionalities and during radical polymerization they can both react producing a junction (cross-link) in the material as shown in Figure 23.

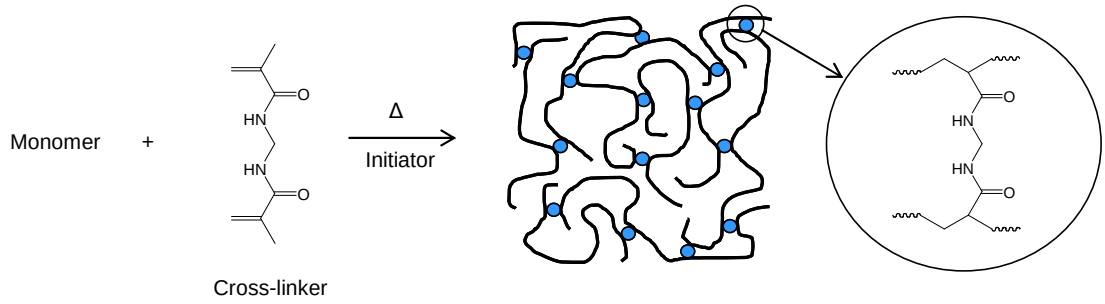

Figure 23: Schematic representation of a three-dimensional structure of a hydrogel.

Hydrophilic methacrylates and methacrylamides are the most commonly used monomers.[107, 108] One of the first example reported in the literature has been a copolymer of 2-hydroxyethyl methacrylate (HEMA) with ethylene glycol bis methacrylate (EGDMA) as cross-linker agent.[107] These materials have been used to produce soft contact lenses. These polymerizations are common radical polymerization and can be initiated via radical initiators (peroxides or Aza compounds). The radical can be generated by heating, by using redox initiators (ammonium persulphate + N,N`-tetramethyl ethylene diamine, TEMED) or photo-initiator.

In the second method, hydrogels can be prepared by reaction of low molecular weight hydrophilic polymers or oligomers. An example is the reaction schematically shown in Figure 24.

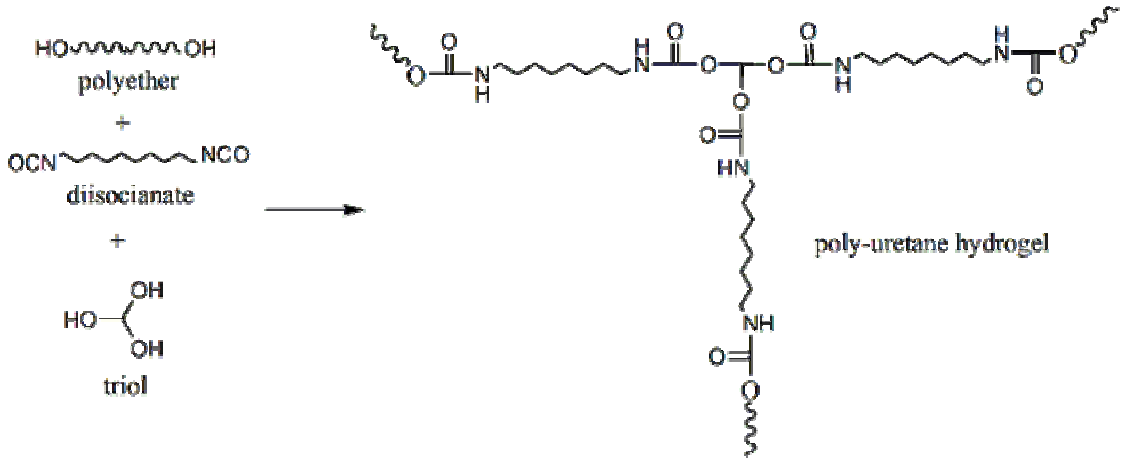

Figure 24: An example of hydrogel prepared from prepolymers.

The oligomers carry two functionalities which enable them to react with each other. A triol, carrying three functionalities, acts as a cross-linker leading to the formation of three armed junctions, thus, to cross-linked hydrophilic poly-uretanes.[109] An alternative approach can be the conversion of hydroxyl groups of poly-(ethylene glycol) into methacrylate and then crosslinking of these via normal radical polymerization.[110]

Chemical cross-linking of hydrophilic polymers leads to the formation of a hydrogel. Ionic polymers can be cross-linked by adding di- or trivalent counter ions and an example is the gelation of sodium alginate by addition of Ca^{2+}. The cross-linking of the alginate molecules occurs according to the egg box model as shown in Figure 25.[111]

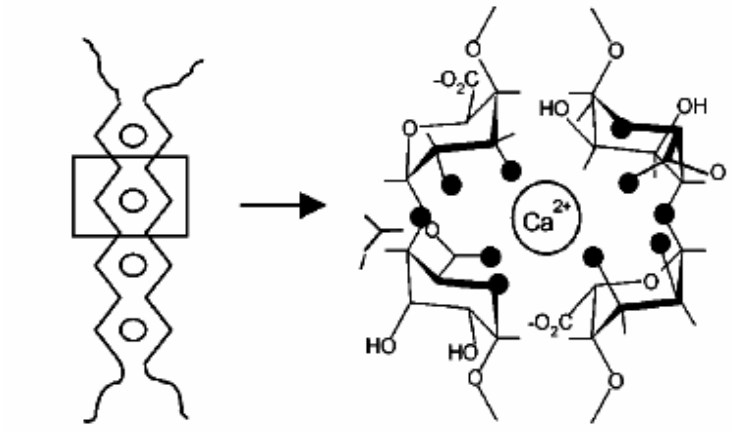

Figure 25: Egg box gelation of calcium alginate.[111]

Other examples are the cross-linking of proteins with formaldehyde, gluteraldehyde or a poly-aldehyde.[112, 113]

1.4.1. Hydrogel beads and Suspension Polymerization technique.

Hydrogels can also be prepared in form of small droplets in order to produce a material easy handle and with enhanced adsorption properties. At equal volume and type of hydrogel, a material in form a small beads have higher surface area than one normally prepared in bulk. Being the material in contact with higher amount of water this can speed up the adsorption and improve its efficiency. In addition, smaller beads require the water to diffuse through a thinner portion of material and this can further enhance the speed and efficiency of the water intake.

It appears clear now that the size of material plays an important role in the water adsorption of a hydrogel and that small beads result in a more efficient material. But how small these beads have to be? A material easy to be handled should possibly be filterable by a common filter paper (particles of diameter in the range of 50-100 μm).

Several methods for the production of polymer particles by heterogeneous polymerization processes exist. These include emulsion, emulsifier-free emulsion, dispersion, precipitation and suspension polymerization. Suspension polymerization is particularly suited to the production of large polymer beads, typically in the range 5-1000 μm. The other processes referred, in general, to produce much smaller particles.[114, 115] Suspension Polymerization was first developed by Hoffman and Delbruch in 1909.[116]

The first suspension polymerization, based on acrylic monomers, lead to the formation of beads and was performed by Bauer and Lauth in 1931.[117] In a typical suspension polymerization (Figure 26) the initiator is soluble in the water-insoluble monomer phase, which is dispersed either pure, or as an organic solution by combination of efficient stirring and the use of a small amount of suspending agent (stabilisers) into the dispersion medium (usually water) to form droplets (i.e. an emulsion is formed). The solubilities of the dispersed monomer (droplet) phase and also the resultant polymer in the dispersion medium are usually low. The volume fraction of the monomer phase is usually within the

range 0.1-0.5. However, polymerization reactions are sometimes performed at a lower monomer volume fraction but are not usually economically viable on a large scale. At higher volume fractions, the concentration of continuous phase may be insufficient to fill the space between droplets.[118]

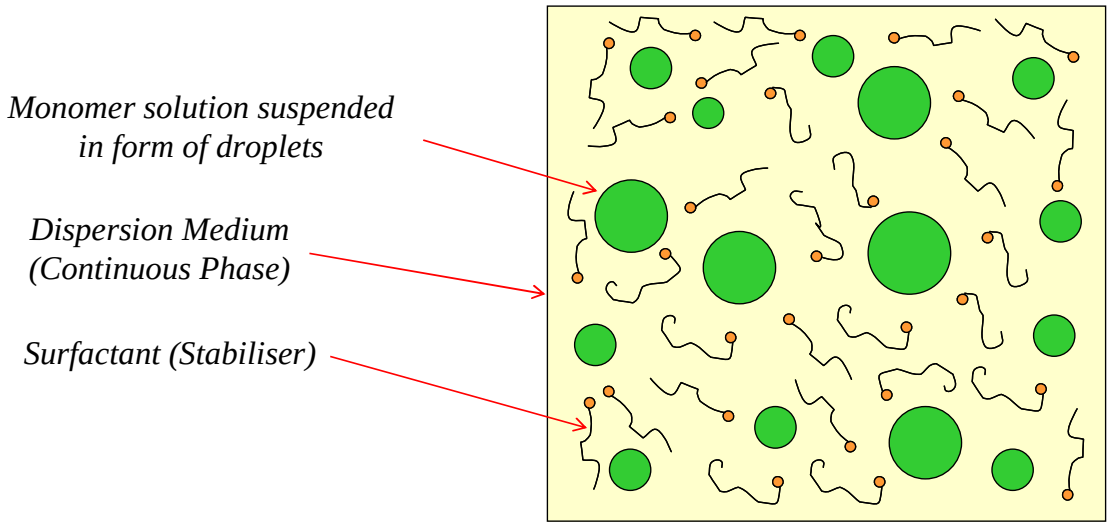

Figure 26: Scheme of a typical Suspension Polymerization.

The polymerization proceeds in the droplet phase and, in the most cases, occur by free radical mechanism. In order to prevent settling or creaming, efficient conditions of mechanical agitation is normally continued throughout the course of the reaction while the monomer droplets are slowly converted from a highly mobile liquid state, through a sticky syrup-like dispersion (conversion 20-60 %), to hard solid polymer particles (conversion > 70 %).[119] Suspension Polymerization usually requires the addition of small amounts of stabiliser to hinder coalescence and initially break-up of monomer droplets. Then when the polymerization has advanced to the point where the polymer beads become sticky it provides stability to the polymer beads whose tendency to agglomerate may become critical. The size distribution of the initial emulsion droplets and hence the polymer beads that are formed, is dependent upon the balance between droplet break-up and droplet coalescence. This, in turn, is controlled by the type and speed of agitator used, the volume fraction of the monomer phase, the shape of the vessel and the type and concentration of stabiliser used. Numerous publications and patents have focused in this subject. However, despite the efforts to understand the droplet formation mechanism and

more importantly the relationship between the particle properties and the operating parameters they have had limited success.[120]

If the polymer is soluble in the monomer phase, a gel is formed within the droplets at low conversion. If the monomer is insoluble in the monomer phase, precipitation will occur within the droplets, which will result in the formation of opaque and often irregularly shaped particles. If the polymer is partially soluble in the monomer mixture, the composition of the final product can be difficult to predict.

Polymers produced by inverse suspension polymerization are generally those where the monomers are relatively water-soluble. The monomers are dispersed either pure, or as an aqueous solution, into an immiscible organic solvent. The polymerization reaction is usually initiated thermally, with a water soluble initiator such as ammonium persulphate.

In the case of a water-in-oil system, the HLB (hydrophile lipophile balance) values of the surfactants are mostly used to control the stability of the dispersions. Recently, some attempts were made to predict quantitatively the optimal HLB value corresponding to the most stable dispersions.[121, 122] The treatment was based on the so-called cohesive energy ratio (CER) concept developed by Beerbower and Hill for the stability of conventional emulsion.[123] The approach relies on a perfect chemical match between the partial solubility parameters of oil (δ_O^2) and the lipophile tail of the surfactant (δ_L^2) as well as those of water and hydrophile head. When these conditions are met, the following relationship is obtained:

$$HLB_0 = 20\delta_L^{\,2} / \left(K + \delta_L^{\,2}\right)$$

where HLB_0 is the optimum HLB when $\delta_O^2 = \delta_L^2$ and K is a constant estimated at 230 for a water-in-oil system.[124] It is, therefore, possible to calculate the required HLB for a given oil. Pichot at al. analysed the concentration dependence on surface tension of acryl amide from the CER concept and predicted the optimum HLB value, HLB_0, with the concentration up to 40 % (w/w). The optimal HLB_0 value for the water-in-oil system containing acryl amide was found to be within the range of 4 and 6.5.[122] For example, a decrease of HLB values will enhance the gel bead diameters because of an increasing

surface tension influencing the droplet break-up/coalescence mechanism. On the other hand, if the HLB values are too low this will cause a coagulum of the droplets.

Examples of inverse suspension polymerization include the polymerization of poly-(ethylene oxide) methacrylate monomers[125] and the production of acrylic-based polymers.[126-128] Copolymer of acrylics have also been produced with methyl methacrylate [129] and N,N'-methylene bis acryl amide[130, 131] and temperature/pH sensitive poly(N-isopropyl acryl amide) variants.[10] Poly-(N-isopropyl acryl amide) mini-gel particles (cross linked using N, N'-methylene bis acryl amide) have been synthesised by Suspension polymerization.[124] These mini-gel particles have a porous gel-like structure, resulting from a relatively low concentration of cross-linker (typically up to ~ 10% of the total monomer concentration) and can undergo reversible changes in particle size with temperature. Upon heating above their lower critical solution temperature (LCST) a decrease of solvation in water occurs, which result in a collapse of the particles. If an acidic comonomer is added (e.g. acrylic acid) swelling and de-swelling may be induced by changes in pH. The study of such particle is an area of growing interest in a number of applications, in particular for selective uptake of heavy metal ions.[9, 11]

In general, time-conversion curve, heat of polymerization and the dependence of initial polymerization rate upon initiator concentration in suspension polymerization are in good agreement with bulk polymerization kinetics. In addition, particle size, type and concentration of stabiliser and agitation conditions seem to have no influence on the polymerization rate in batch suspension homopolymerization processes and also the mass transfer phenomena between the two phases do not particularly effect the process.[120] This leads to the meaning that the process taking place inside a suspended droplet can be simply considered to be a bulk polymerization in a small scale. This conclusion has been also confirmed and for example the polymerization kinetic of vinyl chloride in bulk polymerization and in suspension polymerization are very similar.[132]

1.5 Stimuli-responsive materials.

Stimuli responsive polymers are defined as polymers that undergo a rapid physical or chemical change in response to a small external change in the environmental conditions

(i.e. pH, temperature, ionic strength etc.). These materials have been given many names: stimuli sensitive, intelligent, smart or environmentally sensitive polymers but they are all able to recognize and magnitude a signal changing their conformation in response to the stimulus. Because of this unique volume phase-transition property, stimuli-sensitive materials have attracted much attention in the last 20 years based on their potential for applications in numerous fields, including drug delivery, chemical separation, chemical sensors, enzyme, and cell immobilization.

Moreover, some works recently reported the synthesis of materials where two or more different stimuli-responsive mechanism were combined into one polymer system; these novel materials were coined as dual-stimuli responsive polymer systems.[133]

There are many either physical or chemical stimuli to modulate the response of polymer systems. Chemical stimuli, such as pH, ionic factors and chemical agents, will affect the interactions between the polymer chains or polymer chains and solvent on a molecular level. On the other hand, the physical stimuli, such as temperature and electric or magnetic fields will act on the level of various energy sources subsequently changing the molecular structure. In particular, this work is focused on dual-responsive materials that are pH and temperature sensitive.

A very interesting form of stimuli-responsive polymers are cross-linked (permanently) hydrogels which are essentially hydrophilic polymers chemically cross-linked. Due to their hydrophilic three dimensional polymer network, these gels have the ability to be solvated by water without dissolution. As a result of water absorption these gels can swell and change their dimension considerably. If a thermo-responsive component is present into the material this could cause reversible swelling/de-swelling according to a little change in stimuli.

1.4.1. pH-responsive polymers of acrylic acid.

The pH-responsive polymers are composed of a polymer backbone with ionisable pendants that can accept and donate protons in response to an environmental change in pH. As the environmental pH changes, the degree of ionization for a polymer bearing

weakly ionisable groups is altered and at pH = pK_a the polymer will form its poly-electrolyte analogue. The corresponding rapid change of net charge will subsequently result in a change of hydrodynamic volume of the chains, with a transition from a collapsed state to an expanded state. There are two different types of pH-responsive poly-electrolytes: weak poly-acids and weak poly-bases. Poly-acrylic acid (poly-AAc) has been most frequently reported as pH-responsive poly-acid;[134] its carboxylic pendant groups accept protons at low pH and release protons at neutral and high pH. Therefore, they are transformed in poly-electrolyte at high pH with a resulting electrostatic repulsion between the polymer chains.

Weak pH-responsive poly-acids are usually hydrophobically combined in order to have a sensitive balance between charged repulsion and hydrophobic interactions. When ionisable groups are protonated and the electrostatic repulsion forces disappear within the polymer network, hydrophobic properties dominate, introducing hydrophobic effects that cause aggregation of the polymer chains from the aqueous environment.

If the monomer is incorporated in a cross-linked three dimensional polymer network, this will provide pH-sensitivity in the gel, with the ability to swell and shrink in response of environmental pH changes. Above its pK_a (4.25 at 25 ºC) the polymer chains will form their poly-electrolyte analogue and the repulsion forces caused by the increase of the net charge will induce their expansion and therefore swelling of the hydrogel occurs. This transition is totally reversible and therefore below the pK_a (~5) the weakly ionisable groups will be protonated and the repulsion forces will disappear with a consequent de-swelling of the material.[10] This phenomenon is further enhanced by the increasing of solubility of AAc in water in its deprotonated form.

1.4.2. Thermo-responsive polymers of N-isopropyl acryl amide.

Miscibility of a polymer in a given solvent is well explained in the mean-field theory.[135] In general, when a polymer is dissolved into a solvent the free energy of the polymer-solvent system ($\Delta G = \Delta H - T \cdot \Delta S$) decreases when the enthalpy (ΔH) decreases by dissolution or when the product of the temperature and the entropy of mixing ($T \cdot \Delta S$) is greater than the enthalpy of mixing. Polymer-solvent system miscibility is much lower

than that of a low molecular solute as the entropy of mixing of the polymer does not substantially increase by adding solvent molecules.[136] Phase separation of a binary mixture composed of a polymer and a solvent is a phase transition. This phase transition relies on the difference of Gibbs free energy between the mixed and the unmixed state (ΔG_{mix}). There are different types of phase diagram and Figure 27a shows the most commonly observed.

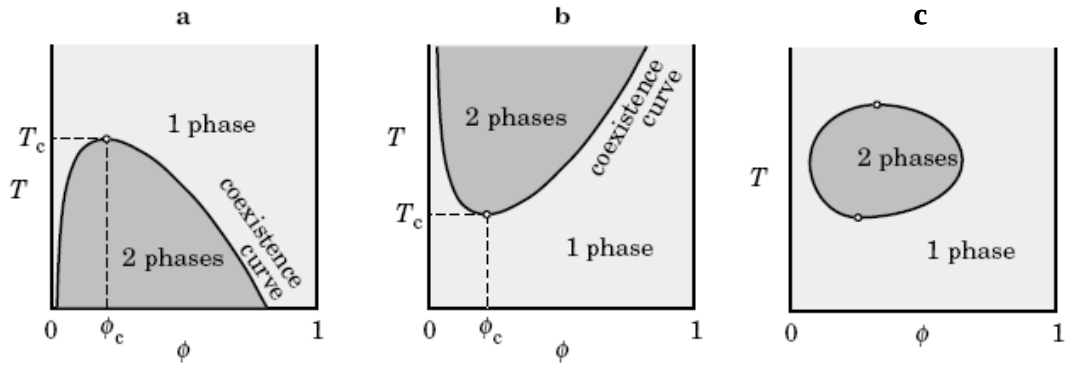

Figure 27: Phase diagram of polymer solution on temperature-composition (θ) plot: a) UCST-type phase diagram; b) LCST-type phase diagram; c) Loop-type phase diagram.[136]

The phase diagram has the critical temperature (T_c) at the highest point of the coexistence curve. Therefore, this critical temperature is referred to upper critical solution temperature (UCST) and the diagram is called UCST-type phase diagram. At high temperature the solution is clear and uniform, hence, transparent. At temperature below the coexistence curve ($T < T_c$), the system has a miscibility gap and the solution separates in two phases. Each of these two phases is uniform but they have different compositions. An inverted phase diagram shown in Figure 27b is observed in some polymer-solvent systems. As the T_c is at the lowest point in the coexistence curve, it is referred as lower critical solution temperature (LCST) and the diagram is called LCST-type phase diagram. A polymer soluble in water due to hydrogen bonding usually has an LCST-type phase diagram as the hydrogen bonding disrupts at higher temperatures.

In some rare cases a polymer-solvent system can show a closed coexistence curve and both UCST and LCST as shown in Figure 27c. The solution is in a single phase outside the loop but in two phases inside the loop.

N-isopropyl-acryl amide is a hydrophilic monomer and its polymer is a typical and well known thermo-sensitive polymer which exhibit a lower critical solution temperature (LCST) around 32 °C in water.[137] Below the LCST the amidic function interacts with the water molecules forming H-bonds ensuring the solubility of the polymer. Above the LCST these H-bonds break with expulsion of water molecules and subsequently reverse conformational change "coil-globule" (Figure 28).

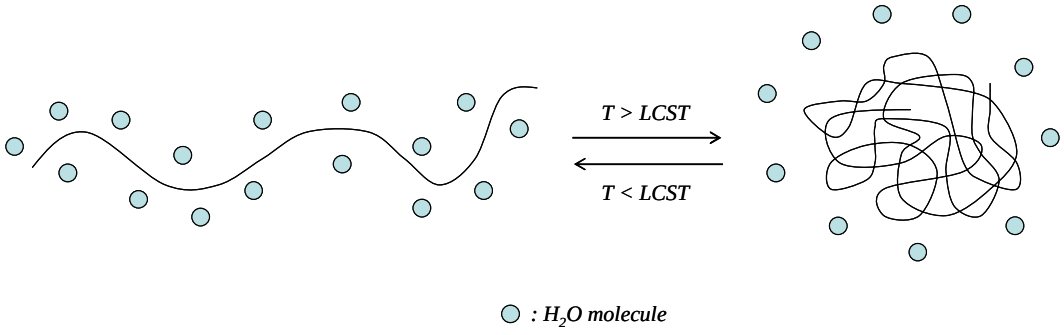

Figure 28: Conformational changes of a poly-NIPAM chain in aqueous solution for a temperature change.

Because of this property of inverse solubility at almost physiological temperature, NIPAM has been used to synthesise gels, homopolymers and copolymers which have been used for a wide range of applications.

Furthermore, the LCST of poly-NIPAM can be adjusted by copolymerization with hydrophilic (increase of LCST) or hydrophobic (decrease of LCST)[138, 139] monomers depending on the macromolecule application.

Thermo-sensitive gels based on poly-NIPAM can be used to absorb and release various substances. This action can be regulated by small changes in temperature, an example of which is schematically shown in Figure 29.

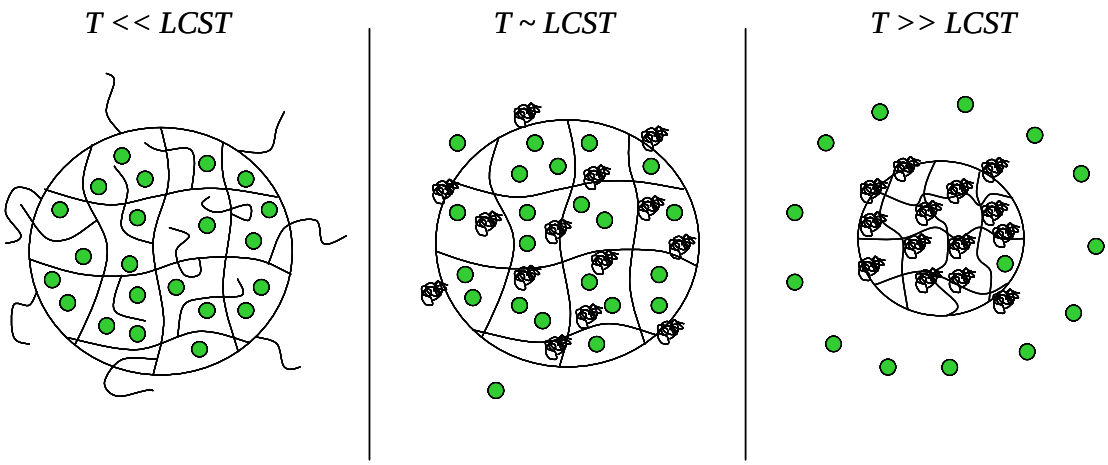

Figure 29: Scheme of adsorption and release of substances using a thermo-reversible gel based on poly-NIPAM.

Below the LCST the gel is swollen and expanded and in this state the material is able to incorporate the molecules (the green circle in Figure 29) dissolved in the aqueous solution. Above the LCST, the gel will shrink with subsequent release of the molecules previously adsorbed. On the basis of this mechanism, this kind of gel can be employed for the controlled release of drugs[103, 124] or for immobilising biomolecules as enzymes or antibodies.[140, 141] The functionalization of these intelligent hydrogels with materials capable to selectively bind metal ions (in particular heavy metals), such as Aza-crown ethers, is a very attractive route in order to prepare novel compounds for selective decontamination of aqueous solutions. Theoretically, when the hydrogel is in the swollen state the ions dissolved in the water solution may be absorbed in the polymer network. By raising the temperature above the LCST, the gel will shrink and only the metal ions trapped in the Aza-crown will be retained in the polymer network whereas the others will be released in the water solution (Figure 30).

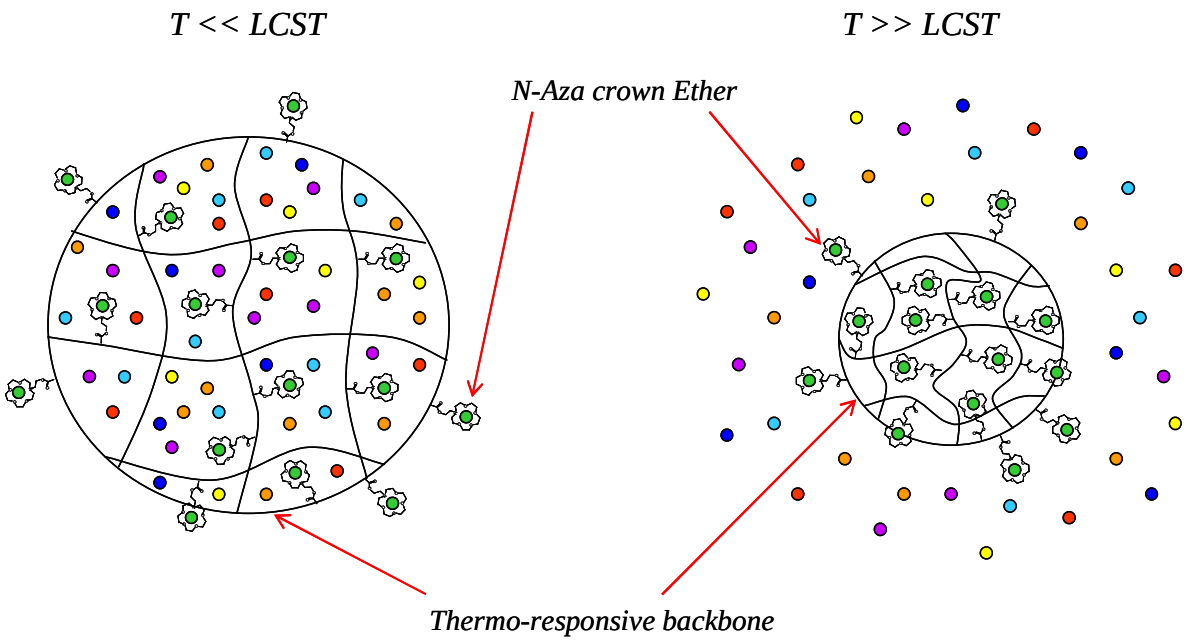

Figure 30: Scheme of selective adsorption and release of metals using a thermo-reversible gel.

Hydrogels in the form of polymer beads are of interest due to their high surface area and hydrogel beads based on poly-NIPAM have already been synthesised. Okano at al. first reported the synthesis of a novel architecture gel network based on poly-NIPAM[142, 143] and lately the synthesis of a series of comb-type (graft-type) and normal-type N-isopropyl-acryl amide hydrogel beads by inverse suspension polymerization techniques (Figure 31).[124]

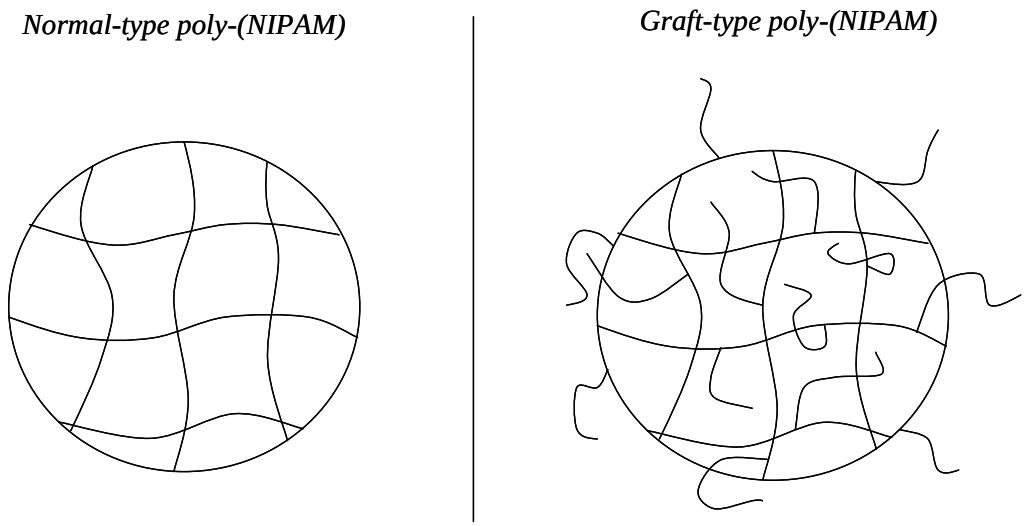

Figure 31: Schematic representation of comb-type (graft-type) and normal-type poly-(N-isopropyl-acryl amide).

Comb-type hydrogel beads are gel particles where poly-N-isopropyl-acryl amide chains are grafted onto the polymer network by inverse suspension copolymerization of NIPAM and a poly-NIPAM methacrylate macro monomer. Okano also reported that the comb-type gel beads exhibited a larger volume change and faster response to temperature in comparison to the normal-type gel beads and additionally the incorporation of grafted chains made the effective mesh size smaller and with a narrower size distribution. The latter phenomenon was certainly caused by the presence of the macro monomer which acted as an internal stabiliser into the droplets during inverse suspension polymerization.

Other hydrogel beads based on N-isopropyl-acryl amide copolymerized with other monomers were also synthesised. For example Zhu et al., in 2004, published the synthesis of poly-(N-isopropyl-acryl amide)-co-2-hydroxythyl methacrylate (NIPAM-co-HEMA) macro porous resins in the form of beads by inverse suspension polymerization technique.[144] The HEMA comonomer can, in theory, be subsequently functionalised due to its reactive hydroxyl group and thus, other functionalities can be incorporated into the polymer network.

Recently, Ju and coworkers reported the preparation of dual-stimuli responsive gel beads based on graft-type and normal-type poly-(N-isopropyl acryl amide-co-acrylic acid) and

their properties in response of temperature and pH.[10] These hydrogels showed synchronously rapid thermo- and pH- response property in ultrapure water and confirmed that the performances of the graft-type hydrogels are, in general, higher than normal-type gels. As already mentioned, the introduction of hydrophilic comonomers (i.e. the ionic groups of acrylic acid) into poly-(N-isopropyl acryl amide) will result in an adverse effect for the thermo-sensitivity of the copolymer inducing an increase of LCST. If the amount of hydrophilic comonomers is above a certain level, this can cause a permanent loss in the thermo-responsive properties. Ju and coworkers maintained, for this reason, the total molar ratio of NIPAM/AAc at about 9 : 1.

1.4.3. Thermo-responsive polymers of Oligo-(ethylene glycol) methacrylates.

Oligo-(ethylene glycol) methacrylates polymers structurally differ from the standard linear poly-(ethylene oxides) since they are composed of a carbon-carbon backbone and multiple oligo ethylene glycol side chains (Figure 32).

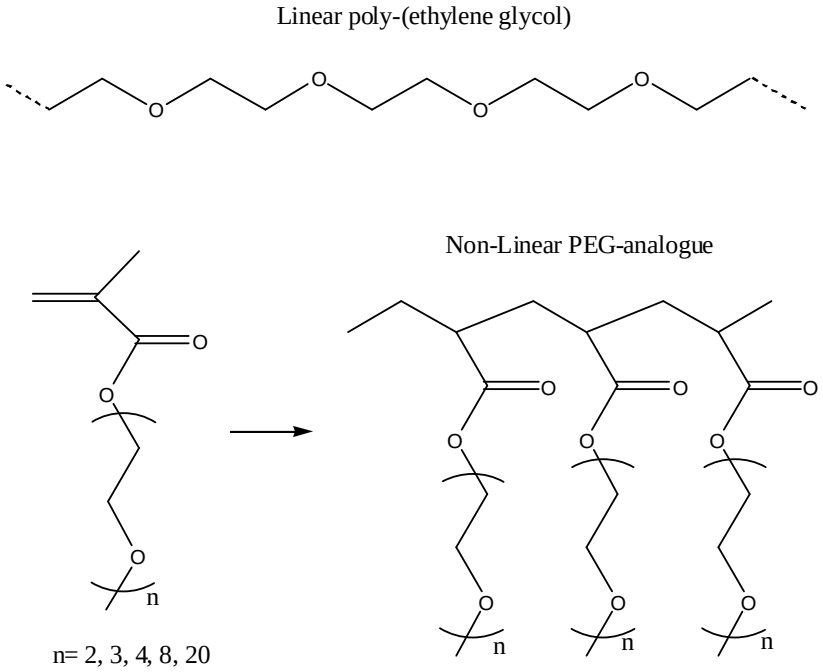

Figure 32: Structure of linear PEG and non-linear PEG produced by polymerising oligo-(ethylene glycol) methacrylates.

These polymers are generally, or at least in the most of the cases, water soluble and biocompatible being mainly composed (up to 85% in weight) of oligo-(ethylene glycol) segments. Their monomers, also known as PEG macromonomers (molecule composed of a polymerizable moiety connected to a short oligo-ethylene glycol chain), are generally cheap and commercially available (most of them) and can be polymerised via a variety of mechanisms and mild synthetic conditions. However they are not all water soluble. These monomers first appeared in literature in the early 1980's [145, 146] with the initial motivation of new macromolecular architectures. Later Lutz[13] and others[147, 148] demonstrated that these graft polymers generally display a lower critical solution temperature (LCST) in pure water or in physiological mediums which are not typically attainable with linear-PEG. In other words, these polymers are soluble in water below the LCST but precipitate at temperatures above it. However, not all oligo-(ethylene glycol) methacrylate polymers exhibit this property. In fact, polymers with short PEG side chains are not water soluble at all or are just slightly hydroscopic (Figure 33) while polymers with very long side chains are soluble in water even at high temperatures. This different behaviour is due to the amphiphilic nature of the macromolecule. In fact, while the ether oxygens of PEG form stabilising H-bonds with water, the apolar carbon-carbon backbone leads to a competitive hydrophobic effect. Therefore, long side chains mean many stabilising H-bonds with the same hydrophobic carbon-carbon backbone and so solubility in water.

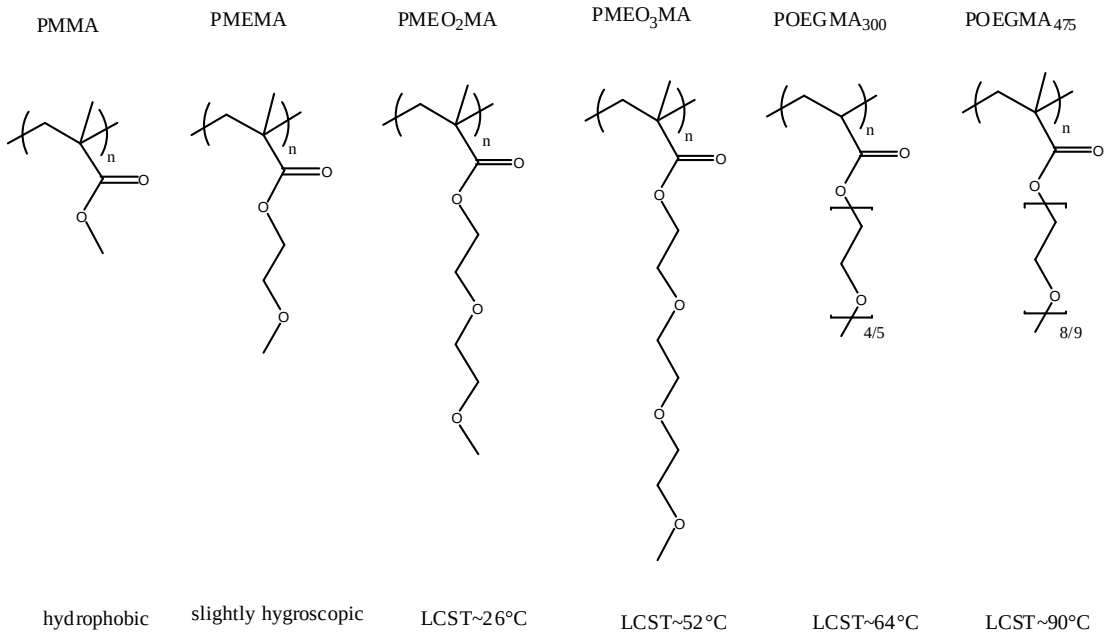

Figure 33: Properties of polymers prepared from oligo-(ethylene glycol) methacrylates. The LCST values actually depend on the polymer concentration and the molecular weight.[149]

In between the two extremes, the non-linear PEG with intermediate side chain lengths (2 ≤ EO unites ≤ 10) display the stimuli-responsive behaviour. For example, poly-MEO_2MA (2 EO units) and poly-MEO_3MA (3 EO units) are water soluble thermo-responsive polymers with a LCST of 26 and 52 °C respectively (Figure 33). Non-linear PEG polymers with slightly higher EO units (4/5 and 8/9) are very hydrophilic materials with high LCST (60-90 °C).

Lutz explained this thermo-responsive behaviour as a consequence of the amphiphilicity of the PEG macromonomers[149]; below the LCST the balance between the ether oxygens-water interaction (stabilising H-bonds) and the carbon-carbon backbone hydrophobic competitive effect is sufficient to allow the solubilization. Above the LCST, the polymer-polymer interaction became more favourable and this causes the precipitation of the material. The mechanism is very similar to that of poly-NIPAM.

So why use oligo-(ethylene glycol) methacrylate polymers as thermo-responsive materials rather than poly-NIPAM? Lutz explains the advantages of non-linear PEG polymer over poly-NIPAM.[149] He recalls that the phase transition for the non-linear PEG

polymers is generally reversible (heating and cooling behaviour is very similar), whereas poly-NIPAM usually shows a significant hysteresis[13] with the tendency to slowly decrease its thermo-responsive behaviour after many heating/cooling cycles. Above the LCST, poly-NIPAM chains collapse forming very strong intermolecular and intramolecular H-bonds and releasing water outside the globules. In the cooling process, because of these very strong interactions, the re-hydration of the globules is hindered and this leads to hysteresis. Non-linear PEG does not have a strong H-bond donor and thus the re-hydration from the collapsed state is not as hindered as for poly-NIPAM.

Furthermore, the thermo-responsivity of poly-NIPAM is generally highly affected by external physical conditions and in particular by the presence of other comonomers. For example, the introduction of ionic groups will result in an adverse effect, reducing or even eliminating the thermo-sensitivity due to the increase of hydrophilicity of the resulting material.[10] Instead, as Lutz observed[149], the phase transitions of non-linear PEG are relatively insensitive to external physical conditions but depend to some degree on molecular weight, concentration, and ionic strength. These variations are, however, generally quite small.

As for poly-NIPAM, the LCST of non-linear PEG polymers can be adjusted by a simple random copolymerization of non-linear PEG monomers with different side chain length. In this case the comonomers are of the same kind and so, the copolymer can be considered a homopolymer, whereas poly-NIPAM requires copolymerization with different comonomers.[150] For example, Lutz reported the synthesis of poly-(MEO_2MA-co-$OEGMA_{475}$) with LCST of either: 32 °C (5 % of $OEGMA_{475}$ units per chain), 37 °C (8 % of $OEGMA_{475}$ units per chain) or 40 °C (10% of $OEGMA_{475}$ units per chain) in distilled water proving that the LCST can be precisely adjusted.[13] This pair of monomers is not the only ones that can be exploited, virtually all the monomers in Figure 33 can be combined to give copolymers with different LCST values.

The major problem with using poly-NIPAM in selective radioactive remediation is its ability to strongly bind metal ions and in particular heavy metals due to the presence of a strong electron-donor group.[9, 11] A well-designed polymer support for incorporation of

selective N-Aza-crown ethers should not display significant interaction toward metal ions. This would lead to an unselective material due to the overlapping of the different sequestering properties. An aspect which renders non-linear PEG copolymers very attracting materials in selective removal of metal ions is the total absence of strong electron donors. Poly-(ethylene glycol) hydrogels incorporating *N*-Aza-crown ethers would, therefore, be selective towards metal ions only on the base of the crown ether ring sizes with reduced interference by the polymer support. However, the combination of these two different materials has not been published yet.

Lutz *et. al.* also prepared an hydrogel based on 2-(2-methoxyethoxy)-ethyl methacrylate and oligo-(ethylene glycol) methacrylate by atom transfer radical polymerization in the presence of small amounts of the di-functional cross-linker ethylene glycol di-methacrylate.[151] Such cross-linked copolymer networks not only maintained the characteristic thermo-responsive behaviour of the linear copolymer but the LCST values was found to be roughly comparable to those observed for their single chains analogues. Lutz explained the thermo-responsive behaviour of the hydrogel caused by a subtle balance between favourable and unfavourable interactions in water where the hydrogen bonding between the ether oxygens of poly-(ethylene glycol) with the surrounding water molecules is the driving-force, which promotes the aqueous solubilization of poly-(MEO_2MA-co-OEGMA) at room temperature. However for poly-(MEO_2MA-co-OEGMA) copolymers, this favourable effect is counterbalanced by the hydrophobicity of the apolar backbone. The phase transition mechanism of the hydrogel proposed by Lutz is reported in Figure 34.

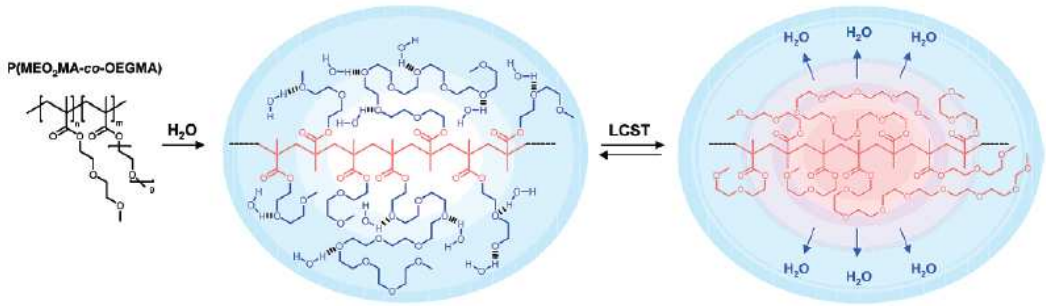

Figure 34: Proposed mechanism by Lutz *at Al.* for the temperature-induced phase transition of copolymers poly-(MEO_2MA-co-OEGMA) in aqueous solutions.[151]

MEO_2MA and $OEGMA_{475}$ were also copolymerized via Atom Transfer Radical Polymerization (ATRP) in the presence of star shaped poly-ethylene glycol (PEG) macro-initiator. The formed copolymers possess permanently hydrophilic PEG inner blocks and thermo-responsive poly-(MEO_2MA-co-$OEGMA_{475}$) outer blocks. Below the LCST, the material is fully soluble in aqueous solution as result of the double hydrophilic contribution of the outer and inner blocks. Above the LCST, the chains precipitate as a result of the formation of a defined hydrogel network (Figure 35).[152]

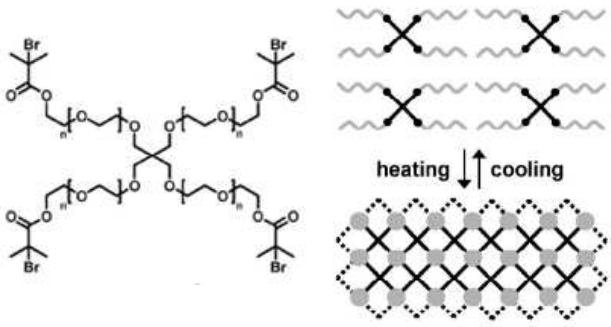

Figure 35: Molecular structure of the 4-arm star PEG macro initiator and schematic representation of the thermogelation of the material.[152]

In general, literature about non-linear PEG copolymers is quite limited and in particular only one study has been published regarding the synthesis of a thermo-responsive hydrogel in form of small particles based on these monomers.[153] Different microgels having different ratios of MEO_2MA and $OEGMA_{475}$ were prepared by emulsion polymerization technique and their sizes were in the range of 80-400 nm. These materials

exhibited thermo-responsive behaviour and their LCST was tuneable and increased with the $OEGMA_{475}$ to the MEO_2MA molar ration. They also compared their material with a similar hydrogel base on poly-NIPAM and both its transition and volume change at the LCST were sharper and larger than those of the poly-(MEO_2MA-co-$OEGMA_{475}$) microgels (Figure 36).

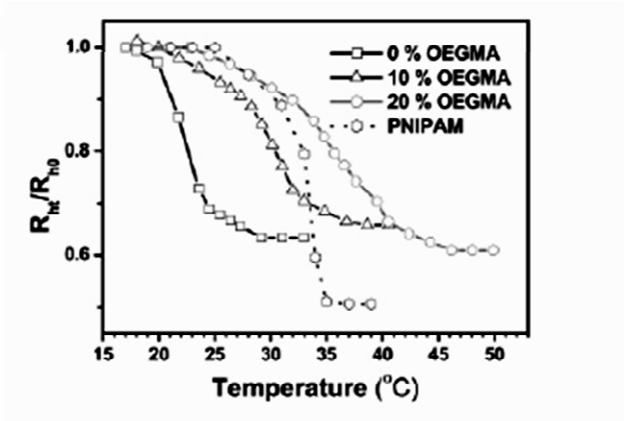

Figure 36: Temperature-dependent normalized hydrodynamic radius (Rh (T) / Rh at18 °C) of poly-(MEO_2MA-co-$OEGMA_{475}$) microgels with different molar ratios of $OEGMA_{475}$ to MEO_2MA: 0%, 10% and 20%. Hexagons are for PNIPAM microgels.[153]

1.5. Aims of the Project.

The aim of the group is to study and develop new scavenging materials to remedy radioactive contamination and selectively remove radionuclides from contaminated solutions and surfaces. In particular this project is focused on radioactive decontamination of aqueous solutions by materials where the well-known sequestering properties of *N*-Aza-crowns ether are combined with the properties of stimuli-responsive hydrogel supports in form of polymer beads.

Two different supporting materials were selected: the first a dual-stimuli (temperature and pH) responsive hydrogel based on poly-NIPAM and poly-AAc (in order to confer also pH-responsive behaviour) and the second a thermo-responsive hydrogel based on poly-oligo-(ethylene glycol). The primary interest is to develop a material capable to trap radionuclides such as ^{137}Cs, ^{90}Sr and ^{60}Co in the presence of large quantities of Ca^{2+}, Na^+, K^+ which are the elements usually present in larger quantities in common water. Thus,

both polymer supports were functionalized with different *N*-Aza-crown ethers in order to observe whether the selectivity of the material varies with the change of the ring size towards such ions. Moreover, we are also very interested in studying whether the environmentally induced geometrical changes of the polymer supports have an effect in the complexation properties of the material.

Chapter 2

Experimental Methods

2.1. Nuclear magnetic resonance spectroscopy (NMR).

^{1}H-NMR spectra were recorded on Varian Inova 300, Varian Inova 400 or Brucker AMX 500 spectrometers. Chemical shifts are quoted on the δ-scale in units of parts per million (ppm). Di methyl sulfoxide (DMSO) and Chloroform ($CDCl_3$) were used as solvents.

Solid ^{13}C-NMR spectra were performed by Durham University (Solid State NMR Service) using a Varian VNMRS spectrometer operating at 100.56 MHz for 13C, spectra referencing is with respect to tetramethylsilane and cross-polarisation with magic-angle spinning (MAS) was used to record the spectra.

2.2. Elemental Analysis.

Elemental analyses were performed by the University of Manchester micro-analytical laboratory using a Carlo Erba instruments EA1108 Elemental Analyser. The error associated to the measurement is ~ ± 0.04 %.

2.3. Thermo gravimetric Analysis (TGA).

TGA analysis was performed in a Q5000IR Thermo gravimetric Analyzer; the samples were heated from 25 to 600 °C at 10 °C / min rate.

2.4. Fourier Transform Infrared Spectroscopy (FT-IR).

Infrared spectra were recorded on a Specac single reflectance ATR instrument (4000 – 400 cm^{-1}; resolution 4 cm^{-1}).

2.5. Mass Spectroscopy (MS).

Mass Spectra were recorded using a Fision VG Trio 2000 EI/CI spectrometer, equipped with a standard ES source. ES (±) spectra were recorded using a Micromass Platform II

ES spectrometer, equipped with a standard ES source. Units are mass to charge (m/z) with relative peak intensities given as percentages.

2.6. MALDI-TOF.

MALDI-TOF mass spectra were measured on Micromass Tof Spec 2E Spectrometer. Samples were prepared by dissolving the polymers in THF at a concentration of 10mg/ml. The matrix used for all experiments was dithranol. This matrix was dissolved in THF (10mg/ml). A volume of 50 µl of the matrix solution was then mixed with 5 µl of the polymer solution. An aliquot of 1 µl of the resulting mixture was spotted on the MALDI sample plate and air-dried. The spot was treated with an aliquot of 1 µl of a solution of sodium trifluoroacetate in THF (10mg/ml) and air-dried before analysis.

2.7. Gel Permeation Chromatography (GPC).

GPC analyses were carried out on a Viscotek GPC Max VE2001 equipped with a column set of two Polystyrene PL 2MB and one 500A. The system was attached to a Viscotek VE 3240 UV/Vis Multichannel detector. All samples (1 mg/ml in THF) were analysed using dodecane as a marker with THF at 1 ml/min flow rate. The standards used were standard of Polystyrene. The results have been rounded to the nearest hundreds $g \cdot mol^{-1}$ value.

2.8. Flow Injection Polymer Analysis (FIPA).

FIPA was carried out on a Viscotek GPC Max VE2001 equipped with a polystyrene pre-column. The system was attached to a Viscotek TDA 302 Triple Detection Array. All samples (1mg/ml in THF) were run, using THF as eluent, at 1lm/min flow rate. The standard used was Polystyrene (Mn = 110000, I < 1.06).

2.9. Bead size analysis.

Beads sizes analysis was carried out on an optical microscope (Olympus BH-2). The hydrogel beads were allowed to swell in deionized water, pH 2 hydrochloric acid/potassium chloride and pH 7.2 phosphate buffer solutions at room temperature over 1 hour. The selected swollen hydrogel was placed in a sealed glass cell. The sample was,

then, transferred in a thermostatic stage system (Linkam THMSE600 connected to Linkam TMS94 controller) and the pictures were recorded using a digital camera (Olympus C-7070) connected to the microscope. By observing about 200 hydrogel beads at both 25 and 70 °C the distribution of diameters and a mean diameter ($^{200}D_m$) were obtained. Thermo-responsive behavior was evaluated by controlling the temperature in a range from 25 and 70 °C with 1°C/min heating rate. Diameters of about 30 hydrogel beads were analyzed at each temperature in order to calculate the mean diameter, $^{30}D_m$.

PNA1 and PEGMAf1 (25 mg of each one) were also allowed to swell in aqueous solutions (1ml) containing increasing amounts of KCl (4.4, 8.9, 13.3, 17.7 and 22.1 $g \cdot L^{-1}$) and a population of about 200 beads was observed in order to obtain $^{200}D_m$ values.

2.10. Decontamination Experiments: Autoradiography and Liquid Scintillation Counting.

2.10.1. Introduction to radioactivity.[154]

The Rutherford-Bohr model depicts the atom as made of heavy protons ($1.672079 \cdot 10^{-27}$ Kg, positive) and neutrons ($1.674385 \cdot 10^{-27}$ Kg, neutral) concentrated in a small volume called nucleus (diameter of approximately 10-15 m) localized in the centre of the atom, whereas the very light electrons ($0.000911 \cdot 10^{-27}$ Kg, negative) surround and neutralize the nucleus at distance up to 10^{-10} m. The forces at which these nuclear particles are subject (attraction of electrons and protons, repulsion between electrons and spin forces) result in the electron occupying certain quantized distances and energies from the nucleus known as orbitals. Despite there is a high repulsion among the positive protons in such small distances these are held together by stronger attractive nuclear forces which comes from the conversion of some of the masses of the nuclear particles into energy. As long as the nuclear attractive forces are higher than the electrostatic repulsion between the protons the nucleus is stable.

The atomic mass (A) of an atom is the sum of the number of protons (Z) and the number of neutrons (N), this is also known as mass number. This mass number describes the nucleus of an atom and it always written as superscript on the left side of the symbol (^1H,

^{12}C, ^{14}N and ^{16}O). The number of protons and electrons is equal and indicated by the atomic number. This value is accommodated as subscript on the left side; thus, $_{1}^{1}H$, $_{6}^{12}C$, $_{7}^{14}N$ and $_{8}^{16}O$. At last, the number of neutrons (N) can be obtained from $N = A - Z$.

An atom so accurately described is known as nuclide. The same element can have the same Z but different N and A. Therefore, in nature some elements exist in form of different isotopes. An element can contain only one stable isotope, for instance ^{27}Al, or many stable isotopes, for instance ^{24}Mg, ^{25}Mg and ^{26}Mg.

The most of the stable isotopes contains an even number of neutrons and/or protons and thus, this evenness is a property for nuclear stability. Another requirement for this stability is given by the number of neutrons. In fact up to mass number of 50, approximately equal amounts of protons and neutrons are enough for nuclear stability. Above mass number of 50, to guarantee nuclear stability the number of neutrons becomes progressively larger than the number of protons.

In conclusion, the nuclear stability of an element depends upon:

- The strong attractive nuclear force; mass is converted into energy of attraction which bind the nucleus together.
- Even numbers of proton and/or neutrons in the nucleus to complete spin pairing.
- An equal number of protons and neutrons or at least a larger number of neutrons than the repulsive protons in the nucleus.

Any deviation from the requirements for nuclear stability results in instability and thus, radioactivity.

Ionising radiations are radiations able to ionise atoms and molecules. Materials capable to emit such kind of radiations are radioactive and can be found in nature or produced. The source of these emissions resides inside the atoms of the material where unstable nuclei emit radiations to gain stability. The elements of these materials (isotopes or nuclides) are

also called radioactive isotopes or radionuclide. The causes of this nuclear instability are, as said, any deviation from the stability requirements given above and are:

- The number of nuclear particles in the nucleus increases with the result that the nuclear electrostatic repulsion becomes higher than the attractive nuclear force.
- Unevenness of the nuclear particles in the nucleus.
- Excess or deficiency of neutrons inside the nucleus.

The last two points can be artificially made by introducing one or more nuclear particles inside a stable nucleus. This would activate the weak nuclear forces and cause the neutrons changing into protons and vice versa depending on which are in excess.

Three are the important properties for a radionuclide:

- The type of ionising radiation emitted: α^{2+} or $\beta^{\pm}$ particles or γ-rays or a combination of these.
- The radioactive decay calculated as a half-life ($t_{1/2}$). The half-life is the time during which the radioactive isotope loses half of its radioactivity. This can be less than a second and up to $> 10^8$ years.
- The radioactive decay energy: the kinetic energy of the particles (α^{2+} or $\beta^{\pm}$) emitted or the wavelength for the γ-rays. The radioactive decay energy is expressed in million electron volts (MeV).

In nature, all the elements with an atomic number higher than 83 contain only radioactive isotopes. These are naturally radioactive and still exist now days as their radioactive isotope sources have very long half-lives. The natural radioactive series starts from ^{232}Th (Thorium), ^{238}U (Uranium) and ^{235}Ac (Actinium) and finish with Lead (Z = 82). There are really few natural radioactive isotopes with atomic number below 82 and relatively high half-life, an example is ^{40}K although its abundance is very small. Natural short half-life radioactive isotopes are often formed by cosmic radiation (^{3}H, ^{10}Be and ^{14}C).

Radionuclides which emit β and γ radiations present the least radiation hazard, for this reason they are often employed as markers in biological science and medicine.[155] All β decay processes result in a change of the element and a little change in mass. They are essentially due to the weak nuclear forces present in the nucleus which allow neutrons changing into protons and vice versa.

Radioactive isotopes with an excess in number of neutrons show a β^- (negatron) emission which can be represented, for example, by:

$$^{14}_{6}C \rightarrow {}^{14}_{7}N + \beta^- + \tilde{\nu} + energy\ (E_{\beta\max}).$$

$$n \rightarrow p^+ + \beta^- + \tilde{\nu} + energy\ (E_{\beta\max})$$

The β-particle and antineutrino ($\tilde{\nu}$) are produced with the radioactive decay and expelled from the nucleus with energy. The β^- particle has the same properties as an electron and is emitted with a whole range of energies up to a maximum value ($E_{\beta max}$) which is carried just by a few particles, the average E_β is approximately a third of $E_{\beta max}$. The antineutrino, instead, carries no charge and no rest mass but more important it carries some radioactive decay energy so its associated electron carries less energy.

Radioactive isotopes with neutron deficiency and nuclear instability with enough energy to produce two electrons (> 1.032 MeV) shows positron emission which is essentially the reverse of the previous process. This transformation can be represented, for example, by:

$$^{18}_{9}F \rightarrow {}^{18}_{8}N + \beta^+ + \tilde{\nu} + energy\ (E_{\beta\max}).$$

$$p^+ \rightarrow n^+ + \beta^+ + \tilde{\nu} + energy\ (E_{\beta\max}).$$

As the previous case, the β^+ particles (positrons) are emitted with a whole range of energies up to $E_{\beta max}$. All the energy which is not removed by the positrons is carried by the associated antineutrinos. Positrons are positively charged particles which once outside the nucleus cannot exist in earth and are annihilated.

When the nucleus energy is not sufficient to form two electrons, an extra nuclear electron can be captured inside the nucleus; the process is called the electron capture (EC) and produce energy and X-rays.

Many unstable nuclei are left excited after emission of $\beta^{\pm}$ or also α^{2+} particles, this excess of energy is lost with an emission of electromagnetic γ-rays. These γ-rays are emitted instantaneously and with defined energies, confirming the shell structure of the nucleus. Once formed inside the nucleus the γ-ray is not always emitted outside atom. In fact, sometimes the radiation emerges from the nucleus and transfers its energy to an electron which is emitted from the atom. This electron is mono-energetic and causes an empty electron shell in the atom and a characteristic X-ray emission.

The most hazardous decay is the alpha which is caused by the presence of too many nuclear particles in the nucleus. This causes an increase of the electrostatic repulsion upon the attractive nuclear force with the result that some nuclear particles will leave the nucleus, in particular protons. Protons cannot escape alone and so two are combined with two neutrons to form a stable α^{2+} particle. This particle arises from the nucleus and "tunnel" its way through the electrostatic repulsion surrounding the nucleus. Finally the α^{2+} particles are emitted with a specific kinetic energy and according to the Geiger-Nuttal rule, greater is this energy and shorter is the half-life of the radionuclide. The result of this decay is that the atom is transformed into one with a decrease of 4 in mass number and 2 in atomic number and α^{2+} particle equivalent of helium- 4 nucleus is emitted; for example:

$$^{238}_{92}U \rightarrow {}^{234}_{90}Th + {}^{4}_{2}He^{2+}$$

The alpha-decay is the main form of radioactivity for natural radionuclide whose the atomic number is above 82 (above lead in the periodic table).

The Becquerel (Bq) is the S.I. unit for radioactivity, named for Henri Becquerel who shared a Nobel Prize with Pierre and Marie Curie for their work in discovering radioactivity.[156] One Bq is defined as the activity of a quantity of radioactive material in which one nucleus decays per second (1 Bq = 1 disintegration per second = 1 d.p.s. = 60

d.p.m.; 1 kBq = 1 kilobecquerel = 103 d.p.s. = 60 x 103 d.p.m.; 1 MBq = 1 megabecquerel = 106 d.p.s. = 60 x 106 d.p.m.; 1 GBq = 1 gigabecquerel = 109 d.p.s. = 60 x 109 d.p.m.). Radioactivity is usually expressed in unit per weight or volume, for example, Bq/g, Bq/ml, Bq/mmol, etc.

Ionising radiations with energy < 8 MeV can ionise and chemically excite atoms and molecules. Thus, all biological damage effects begin with the consequence of radiation interactions with the atoms forming the cells. As a result, radiation effects on humans proceed from the lowest to the highest levels. Initially, ionising radiations affect a little portion of the absorber and the particles lose their energy mainly by inelastic collisions. The loss of energy from the absorption of these radiations is much higher than the first ionisation potential of the most substances (the electron pulled out from its orbit is not necessarily from the outer shell of the atom) and the difference in energies is translated in atomic or molecular excitation.

Alpha-particles (α^{2+}) are heavy and have a charge and they react strongly with matter, producing large numbers of ions per unit length of their path (1 Bq source gives 5 MeV/sec and form 1.43 x 105 ions/sec). However, they are not very penetrating and, for example, 5 MeV alpha particles will only travel about 3.6 cm in air and will not penetrate an ordinary piece of paper. Thus, the alpha-emitters are not an external hazard as they cannot penetrate the dead part of the skin. However, once incorporated into the body they are a great internal hazard as the alpha particles are often more damaging than most other types of particles due to the comparatively large amounts of energy deposited within a very small volume of tissue. Whenever the alpha particle is sufficiently close to an electron, it pulls it out from its orbit although the coulomb attraction. Each time this occurs, the alpha loses kinetic energy slowing its speed. The particle also loses kinetic energy by exciting orbital electrons with interactions that are insufficient to cause ionization. Once the α^{2+} particles have lost all their kinetic energy, they pick up two electrons and become helium.

Beta particles can also excite and ionise atoms and molecules of materials they are passing through, interacting with electrons as well as nuclei. They are emitted with a

whole range of energies up to $E_{\beta max}$ which result in the particles producing a small number of ionisation per unit track. Beta particles passing near nucleus will be deflected by the coulomb forces and may lose some of its kinetic energy (Rutherford scattering). More likely the beta particles will interact with the orbital electrons of the absorbent and the coulomb repulsion between the particles and electrons frequently results in ionization. In each ionization process, the beta particles lose some of their energy (kinetic energy of the electron plus the energy to free it) and each particle may produce from 50 to 150 ion's pairs per centimetre of air before its energy is completely dissipated. At this stage the vacant internal electron orbits get refilled with other electrons and the characteristic X-rays are emitted. These particles can also cause excitation of external orbital electrons leading to the emission of ultraviolet photons. However, these particles are very light in weight, travel much faster and further than alpha particles. For example, beta particle with energy about 2 MeV will travel up to 9 m in air and about 10 mm in water. The ultimate fate of a beta particle after its kinetic energy has been dissipated depends upon its charge: β^--particles (negatron) will either add to the first electrophilic atom or molecule or become a "free electron" whereas β^+-particles (positrons and anti-particle) will be annihilated by the nearest electron and the collision will produce two protons each carrying 0.512 MeV of energy. In conclusion, β emitters are both an internal and an external hazard.

Gamma-rays are electromagnetic radiations with wavelength smaller than the atom radius and larger than the nucleus radius. The interaction of the photons with the absorber atoms depends upon the γ-ray energy. Low energy photons are usually only deflected after interaction with no energy transferred to the atoms (Rayleigh scattering). A photon with energy slightly higher than the binding energy of an atomic electron, instead, strikes an orbital electron which is ejected with the same energy of the γ-ray. The radiation is completely absorbed by the absorber and the ejection of the electron results in an ion pair formation (Photoelectric transfer). A medium-energy photon (0.3 to 3 MeV) interacts with an atomic electron sufficiently to eject it from its orbital. Some of the energy of the incident γ-ray is transferred to the electron resulting in an ion pair formation where as the secondary γ-ray of lower energy is emitted from the electron with different direction (Compton scatter). The scattered photon can interact again, but as its energy has

decreased it has more likely a Rayleigh interaction with another atom. The free electron produced can be quite energetic and behave like a β-particle of similar energy. Finally, γ-ray of high energy (> 1.02 MeV) can interact with the nucleus of the absorber atoms. The reverse of the annihilation reaction occurs and a negatron and a positron are formed (pair formation). The ejected positron is annihilated at the end of its track emitting 2 γ-rays (each of 0.51 MeV).

To summarise, external hazards can be caused by natural and/or artificial β- and γ-emitting radionuclides whereas internal hazards by any radioactive isotopes (α-, β-, γ-emitting). The degree of the hazard directly depends on the type, amount of radionuclide and the physical and chemical form of the material. Three are the aspects which have to be considered for protection by external hazard: time of the exposure, the distance from the source and the shielding. Clearly, the less the time of exposure and the lower is the radio-contamination. Regarding the distance, instead, it is easy to calculate the dose-equivalent rate of a γ-source for a specific distance whereas it is not for a β-source which is a more complicated system due to the scattering phenomena in air of the β-radiation. However, while both α- and β-radiation are easily shielded using a tin box, γ-radiation is difficult to shield against (the best result is achieved by interlacing lead bricks). On the other hand, internal hazard clearly arise when the radionuclide is incorporated into the body by ingestion, inhalation or through wounds.

2.10.2. Autoradiography.

The autoradiography is the localization of a radiolabel inside a specimen by placing the sample against a detector material (Figure 37).

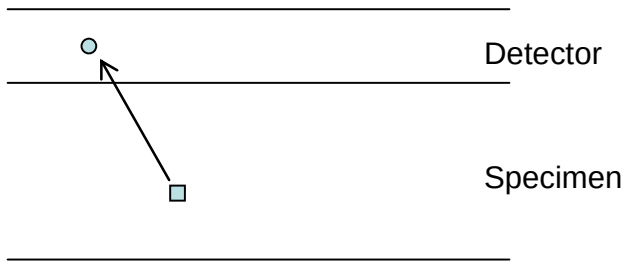

Figure 37: Schematic representation of autoradiography (□: radioactive label; ○: Image).

The principle of this technique is that radioactive decay taking place inside the specimen emits particles of radiation which, after a sufficient exposure time, produce certain changes in the detector layer. These alterations, sometimes, need to be amplified in order to become visible to the naked eye and the image produced gives information about both distribution and quantity of the radiolabel.

The detect ability of a radionuclide radiation depends upon three characteristics: mass, energy and direction. Charge has only a little effect on interaction with the detector.

There are at least two different kinds of detectors: non-photographic and photographic detectors and the most common used are the second type. However, in certain application where the emitter (for example uranium-243) produce alpha particles layer of plastic are used. These particles (equivalent to helium nuclei) are heavy and have high energy and so can penetrate thin plastic layers producing very short tracks. These tracks result invisible but can be made visible in a light microscope by etching in a mixture of NaOH and EtOH.

Photographic detectors can, instead, be used for β- and γ-radiations and are generally made up of salt emulsions. Many salts can be sensitized by light or other radiations and in particular the most exploited in photographic processes are the silver halides (AgI, AgBr and AgCl). In photographic emulsions the detector is generally made of crystalline halides mixtures dispersed in gelatine, whereas the nuclear emulsions used in autoradiography are usually mainly made of silver bromide relatively pure. When these emulsions are exposed to a radiation, metallic silver is formed in those crystals in which the energy is deposited by irradiation producing a “latent image”. If the emulsion is composed of prefect halide crystals these latent images will not formed. Therefore, faults, as silver sulphide, are commonly introduced in the material by the manufacturer. These latent images are sub-microscopic and therefore no visible to the naked eye and need to be converted in visible images by specific processes of development.[157]

Autoradiography employing non-photographic detector are also called “track autoradiography”. This technique is mainly used with alpha-emitters as the particles have sufficient energy to travel in straight line and produce many silver grains along their track. In this case the thickness of the emulsion needs to be at least equal to the path length of

the emitted particles (α and/or β). On the other hand, light particles rapidly lose their energy and are deflected while passing through emulsion. This makes the position of their origin much less clear. In order to obtain good resolution, the most of autoradiography are of the "grain density" kind where each particle gives one or few silver grains. Most of the silver grains are kept as close as possible to the decay source by minimizing the thickness of the emulsion layer and the specimen.

Storage phosphor screens are more current systems used in autoradiography for quantitative image analysis. These screens are approximately 0.5 mm in thickness and composed of photo stimulable phosphor's crystal lattice (BaFBr: Eu^{2+}) combined with an organic binder. This system can capture latent images produced by ionizing radiation (X-rays, β-, and γ-emissions from isotopes such as ^{14}C, ^{3}H, ^{125}I, ^{131}I, ^{32}P, ^{33}P, ^{35}S, etc.) and respect to the more qualitative methods in film autoradiography, they have a number of advantages in capturing the radioactivity of the radiolabels (i.e. improved response to isotopes for shorter exposure times, possibility to be erased and used many times). The photo stimulable phosphor's crystal lattice can store energy imparted from energetic particles or ionising radiation within an excited state. Essentially the energy of the radioisotope ionizes the Eu^{2+} to Eu^{3+} liberating electrons to the conduction band of the phosphor crystals. The electrons are trapped in the bromine vacancies, introduced during the manufacturing process, to form temporary colour centres also called "F centres". Upon laser-induced stimulation, light is emitted in form of photo-stimulated luminescence (PSL) from the storage phosphor screen. The PSL signal released from the phosphor screen is proportional to the amount and energy of the incident ionising radiation. The wavelength of the PSL ($\lambda \sim 390$ nm) and the stimulation light ($\lambda \sim 633$ nm) are sufficiently separated and the resulting digital image can be collected by a conventional high quantum efficiency photo-multiplier-tube (PMT). The schematic representation of the storage phosphor process is reported in Figure 38.[158]

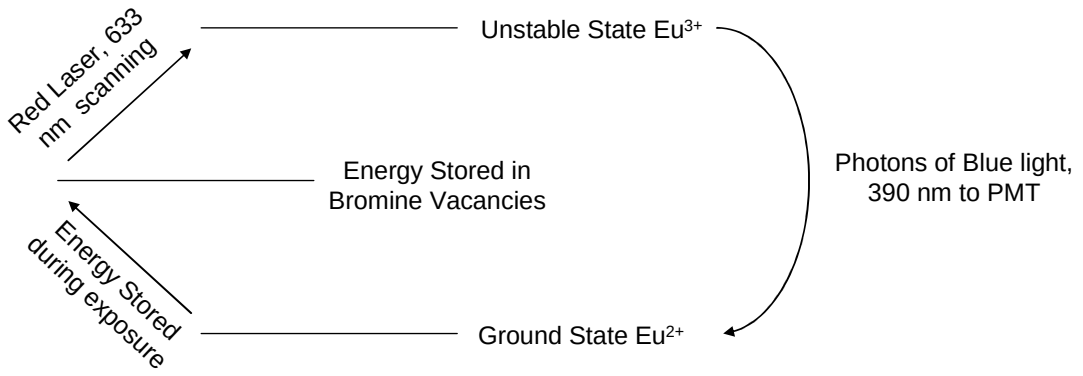

Figure 38: Schematic representation of the phosphorous process.[158]

2.10.3. Autoradiography Method.

The autoradiography experiment for the Sr-90 and Co-60 tests was carried out in a 96 well-plates with filters on the bottom of each well in order to screen a relatively large number of compounds simultaneously. Each result was carried out in quadruplet on 20mg of sample under each of four different conditions (pH 2 and 7, 25 and 70 °C). ^{90}Sr solutions (200 Bq) in HCl previously prepared were taken to the selected temperature using a water bath and pH was adjusted by adding NaOH. The appropriate volume for the selected activity was added, vacuum then applied and the beads left in contact with the solution for 2 minutes before being left to dry under vacuum. The plate was then "read" using a HeNe laser (λ =633 nm) in a Typhoon™ phosphor imager (GE Healthcare, Amersham). The degree of darkening associated with each well is quantitatively related to the activity bound and the average pixel intensities were determined using ImageQuant™ software.

2.10.4. Principles of Liquid Scintillation Counting.

Occasionally some atoms are not completely ionised after collisions with emitted particles but instead have electrons promoted to excited states. Alternatively also some ionised ions can recombine with other ions of opposite charge leading to similar excited states. Such excited ions can then release this excess of energy as a photon of light which can be detected by an appropriate radiation detection system. In a solid scintillation system, the scintillator is a crystal of an organic or inorganic material which is irradiated

by the sample and the emitted light is proportional to the amount of radioactivity of the sample. Such technique is excellent for γ radiations as they can highly penetrate and generate scintillation throughout the crystal while it is not suitable for α and β particles as they are not capable to cross the barrier prior the scintillator essential to protect the crystal by contamination of the sample (Figure 39).

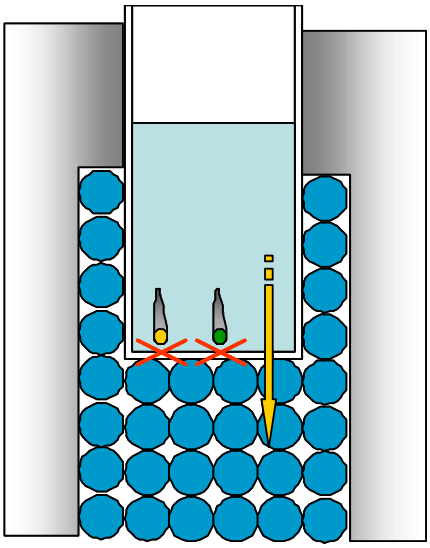

Figure 39: In a solid scintillator only the gamma rays (yellow arrow) can cross the barrier between the sample well and the crystal whereas alpha (●) and beta (●) particles are stopped.

Liquid scintillation (LSC) was evolved in order to analyse organic isotopic compounds and in general water soluble β emitter materials. LSC is based on the same principles of the solid scintillation but the key difference is that the light emission takes place in a solution containing at least the radioisotope, the scintillator (phosphor) and solvent. In this way the short path length of the weak β emissions is not an impediment as there is close contact between the isotope and scintillator. Essentially in LCS the liquid scintillation cocktails absorb the energy emitted by the radionuclides and re-emit it as flashes of light. When a radioisotope undergoes an emission event, it is highly probable that the particle emitted will only encounter solvent molecules as the solvent is from 60 to 99 % of the total solution. For this reason, the solvent plays a very important role as it has to collect the energy, conduct it to the scintillator and avoid quenching of the

phosphor energy. In addition, the solvent also need to dissolve the scintillator and produce a stable and countable solution.

Aromatic organic compounds, such as toluene, are the best solvents for LSC as the π electrons provide a perfect substrate which captures the energy of the incident particle. This energy is generally then transferred to other solvent molecules until it reaches a phosphor which will convert this energy in emission of light. PPO (2, 5-diphenyloxazole) is the most commonly used phosphor but other examples are showed in Figure 40.

Butyl PBD
2-[4-biphenylyl]-5-[4-*tert*-butylphenyl]-1,3,4-oxadiazole)

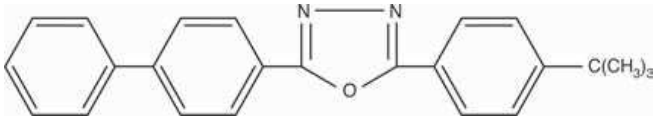

Naphthalene

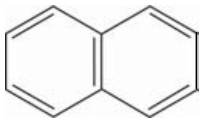

PPO
2,5-diphenyloxazole

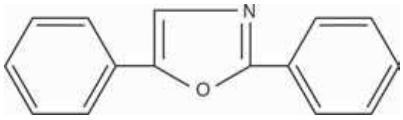

p-Terphenyl

Figure 40: Example of scintillators.

When a β particle passes through a scintillation cocktail leaves a short track (0.1 cm) of excited solvent molecules. These energized molecules, then, transfer their energy to multiple phosphors and each of these will emit one photon on activation. As both the path of the β particle and the half life are short, the photon emission take place in a small space and reaches the PMT (photomultiplier tube) in one pulse of light. The number of photons generated is proportional to the path length of the β particle, which in turn depends upon its emission energy. The intensity of each light pulse depends to this emission energy and the number of pulses per second corresponds to the number of

radioactive emissions. A scintillation counter categorizes the light pulses according to the number of photons and collects them into channels. Each channel corresponds to a specific range of β energy and most commonly there are three channels at low, medium and high energy. In case of a theoretical cocktail where all the β energy is converted into light, the max energy of the sample is compared with the maximum energy of a known radioisotope to confirm the isotope identity. For real cocktails, where the conversion is never 100%, the data interpretation is much more complex.

2.10.5. Liquid Scintillation Counting Method.

The compounds were tested against Cesium-137, Strontium-90 and Cobalt-60 on their own and in competition with Ca^{2+} (for Caesium), K^{+} (for Strontium) and tap water (for Cobalt). Four different conditions were investigated: 20 °C pH 2 and pH 7, 70 °C at pH 2 and pH 7. Initial testing was carried out with contact times of 1, 6 and 24 hours. Samples and solutions were heated using a water bath with thermostat and lid (sample tube are good quality and able to withstand temperature). A contact time of 1 hour was used as they appeared to have no discernable difference between time points. Ten milligrams of each material was weighed into the appropriate number of micro centrifuge tubes and labelled accordingly. A solution of the selected radioisotope (Caesium, Strontium or Cobalt) was prepared to a concentration of 200 Bq/ml, this was then pH adjusted using NaOH (1 M) to either pH 2 or 7. A solution of the selected radioisotope (Caesium or Strontium) was prepared to a concentration of 200 Bq/ml, plus enough $CaCl_2 \cdot 6(H_2O)$ or K_2CO_3 to make a 10 mM solution. This was then pH adjusted using NaOH (1M) or HCl (1M). A solution of Cobalt was prepared to a concentration of 200 Bq/ml in tap water, this was then pH adjusted using NaOH (1 M) to either pH 2 or 7.

One millilitre of solution (200 Bq) was added to each sample. Samples were then vortexed and either left at room temperature (~20 ºC) or placed in a water bath (in a floating tube holder) at a constant temperature of 70 ºC. Samples were vortexed at 5-10 minute intervals over the contact time of 1 hour. They were then placed into to an ice bath for 15 minutes, vortexed again before centrifuging for 15 minutes at 14000 rps. An aliquot of 600 µl was removed to a prepared liquid scintillation vial. Each vial

contained 5mls of Scintisafe 3 (Fisher Scientific). Samples were vortexed again and counted for 10 minutes on a Perkin Elmer Tricarb 1900TC Liquid scintillation counter. Samples were calibrated using a standard of the solution added to the experiments (i.e. 100 % of sample) a blank for background as well as an efficiency standard of know activity in the same geometry.

Chapter 3

Synthesis

This chapter details the synthetic methods used in chapter 4, 5 and 6.

3.1. Materials.

All reagents and solvents were purchased in the highest purity available from Sigma-Aldrich, Fisher Scientific and Alfa Aesar and used without further purification unless stated otherwise.

THF (Fisher Scientific, AR) was distilled over sodium diphenylketone just before use. Anhydrous pyridine was obtained by drying in KOH pellets over 48 hours. Methacryloyl Chloride (Fluka, ≥ 97%) was purchase by Sigma-Aldrich and stored at ~ -20 °C. Di-(ethylene glycol) methyl ether methacrylate (MEO_2MA, 95 %), poly-(ethylene glycol) methyl ether methacrylate ($POEGMA_{475}$, Mn ~ 475), 2-Hydroxyethyl methacrylate (HEMA, ≥ 99%), tetra(ethylene glycol) diacrylate (TEGD, technical grade), Vazo 67 (≥ 98%), Magnesium Oxide (MgO, ≥ 99%), Sodium dodecyl benzene sulfonate (SDS, technical grade), Poly vinyl alcohol (PVA, Mw ~ 67000), hydroxyl ethyl cellulose (HEC, Mw ~ 90000), acetone (99 %), triethylamine (TEA, ≥ 99%), chloroacetyl chloride (98 %), 1-aza-12-crown-4 (≥ 97 %),1-aza-15-crown-5 (≥ 98 %), 1-aza-18-crown-6 (≥ 98 %), N,N'-Methylene-bis-acryl amide (BIS, ≥ 99 %), N,N,N',N'-Tetra-methyl ethylene-diamine (TEMED, ≥ 99 %), ammonium persulfate (APS, ≥ 98 %), cyclohexane (≥ 99 %), sorbitan monooleate (SPAN 80), acetone (99 %), 1-aza-12-crown-4 (≥ 97 %),1-aza-15-crown-5 (≥ 98 %),1-aza-18-crown-6 (≥ 98 %), dichloromethane (DCM, 99.8 %) were used as received. Fresh deionized water from a "pure1TE Select" purification system (Ondeo) was used throughout this work. N-isopropyl acryl amide (NIPAM, 97 %) was recrystallized from hexane. Acrylic Acid (AAc, ≥ 99 %) was purified just before use by vacuum distillation at 40 °C.

3.2. Synthesis of statistical MMA-HEMA copolymers incorporating *N*-Aza-crown ethers.

The methods of synthesis discussed in chapter 4 are provided in this section. All experiments were carried out in a fume cupboard and under N_2 in a round bottom flask equipped with a condenser and a thermometer unless stated otherwise. All the polymerizations were carefully degassed over a period of at least half an hour.

3.2.1. Preparation of N-(hydroxyethyl)-1-aza-15-crown-5.

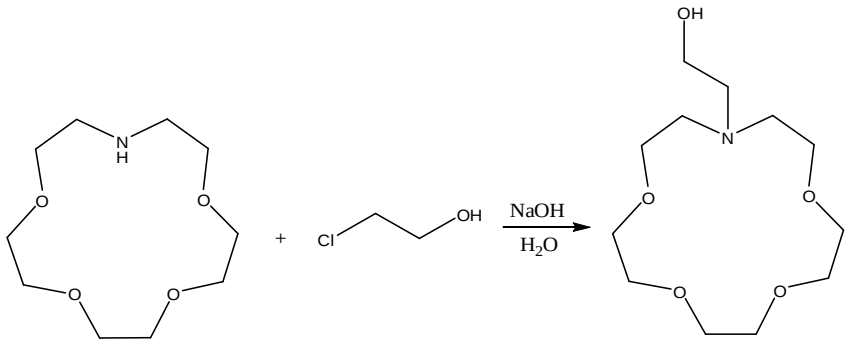

Figure 41: reaction scheme.

A solution of NaOH (256 mg, 6.39 mmol, 1.4 eq)) in water (12.4 ml) was added drop-wise over a period of half an hour at RT to a stirred solution of 1-Aza-15-crown-5 (1 g, 4.56 mmol, 1.0 eq) and 2-chloroethanol (0.43 ml, 514 mg, 6.39 mmol, 1.4 eq). The mixture was then gradually heated to 50-60 ºC over one hour, cooled, dilute with water (2ml) and extracted with DCM (3 x 5 ml). The organic layer was dried with $MgSO_4$ and evaporated to yield 15 % of oily crude product. To increase the yield, other experiments were carried out with longer reaction times at 60 °C, with the best conditions found to be 2 hour. This reaction yielded 50 % of crude product which was directly used for the next step.

^{1}H-NMR ($CDCl_3$): δ 3.2-3.8 (m, 18H, 8 Aza-crown-CH_2 and CH_2-OH), (m, 6H, 3 N-CH_2).

Mass Spectra (ES+): m/z 286.2 (100 %), 264.2 (45 %).

3.2.2. Preparation of 1-Aza-15-crown-5 methacrylate monomer.

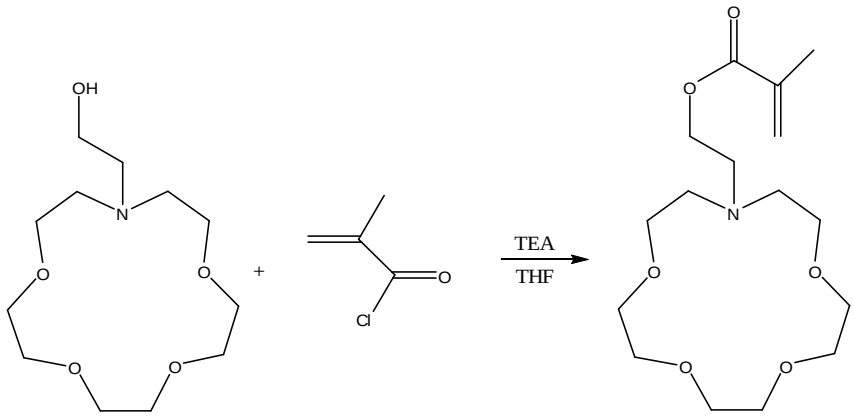

Figure 42: Reaction scheme.

A solution of methacryloyl chloride (0.28 ml, 298 mg, 2.85 mmol, 1.5 eq) and 5 ml of anhydrous THF was added drop-wise at 4-5 ºC over a period of 45 minutes to a stirred solution of N-(hydroxyethyl)-1-aza-15-crown-5 (500 mg, 1.9 mmol, 1.0 eq), dry triethylamine (0.4 ml, 288 mg, 2.85 mmol, 1.5 eq), hydroquinone (1-2 mg) and anhydrous THF (15 ml). The suspension was stirred vigorously over 3 hours and 30 minutes at 5 ºC and then the temperature was gradually increased to RT. The suspension was left to stir for 24 hours, filtered and concentrated. The yellow oil obtained was dissolved in a solution of K_2CO_3 (~10 ml, 0.72 M) and the aqueous solution was extracted with DCM (3 x 5 ml).The organic layer was dried by $MgSO_4$ and concentrated to obtain the crude product as an oil. The reaction yielded 93 % of clean crude product which was directly used for further polymerizations.

^{1}H-NMR ($CDCl_3$): δ 1.93 (s, 3H, -CH_3 of methyl methacrylate), 2.95 (m, 6H, 3 N-CH_2), 3.65 (s, 16H, 9-CH_2- on the Aza-crown ether ring), 4.2 (s, 2H, -CH_2-O-), 5.6 (S, 1H, double bond), 6.2 (s, 1H, double bond).

Mass Spectra (ES+): m/z 354 (100 %), 332 (20 %).

3.2.3. Preparation of 2-chloroethylpyranil ether.

This reaction was part of the alternative synthesis in order to prepare N-(hydroxyethyl)-1-aza-15-crown-5. In particular the reaction in this paragraph is the first step of the full reaction scheme shown in Figure 43.

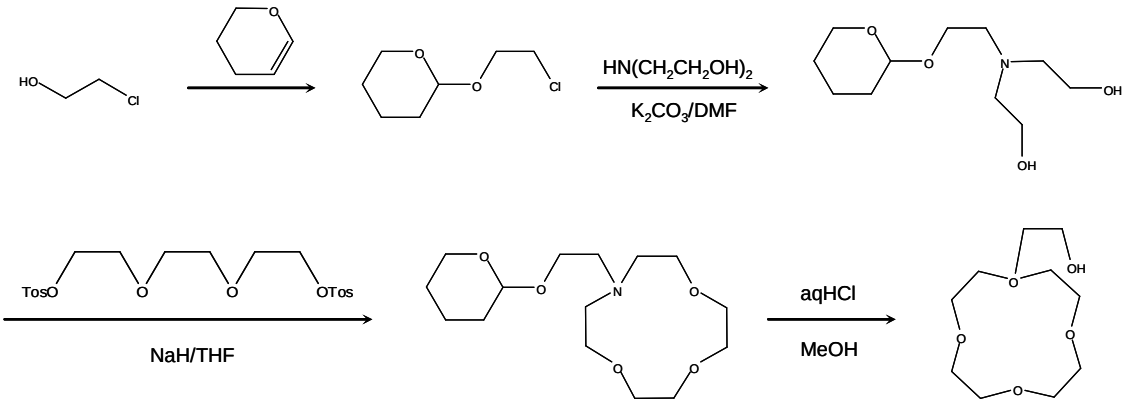

Figure 43: Reaction scheme.

A mixture of 2-chloroethanol (28.68 ml, 34.44 g, 428 mmol, 1.0 eq) and p-toluensulfonic acid monohydrated (9.75 g, 51 mmol, 0.12 eq) was added drop-wise at 0 ºC over a period of 5 hours to a stirred dihydropyran (80 ml, 73.76 g, 877 mmol, 2.04 eq). The mixture was left to stir overnight at 0 ºC, dilute with 800 ml of aqueous solution of $NaHCO_3$ (10 weight %) and extracted with DCM (600 ml). The organic layer was then dried over $MgSO_4$ and the solvent was removed under reduced pressure. The residue was distilled in vacuum (80 ºC oil bath and distillation temperature of 40 ºC) to yield 38 % of colourless oil.

^{1}H-NMR ($CDCl_3$): δ 1.2-1.8 (m, 6H, -CH_2- on the pyranyl ring), 3.3-3.9 (m, 6H, -O-CH_2-CH_2-Cl, -CH_2-O- on the pyranyl ring), 4.5 (s, 1H, -O-CH- on the pyranyl ring).

Mass Spectra (ES+): 209 (100 %), 187 (20 %).

3.2.4. Preparation of N-2-(pyranyl oxyethyl)-di ethanol ammine.

This paragraph reports the method for the synthesis of the second step of the full reaction reported in Figure 43.

2-chloroethylpyranil ether (10 gr, 60.97 mmol, 1.0 eq) was added drop-wise at RT to a stirred mixture of di ethanol ammine (6.64 g, 63.12 mmol, 1.04 eq), K_2CO_3 (10.09 g, 72.88 mmol, 1.2 eq) and DMF (98 ml). The mixture was stirred vigorously at RT over a period of 48 hours. DMF was then removed under reduced pressure and the sticky solid obtained was re-suspended with DCM. The organic layer was dried with $MgSO_4$ and evaporated. The residue was distilled (100-120 ºC oil bath and distillation temperature of 80 ºC) to yield 57 % of colourless viscous oil.

^{1}H-NMR ($CDCl_3$): δ 1.4-1.8 (m, 6H, -CH_2- on the pyranyl ring), 2.6-2.8 (m, 6H, -CH_2-N), 3.4-3.9 (m, 8H, -CH_2-O-), 4.3 (s, 1H, -O-CH- on the pyranyl ring), 4.5 (s, 2H, 2 –OH).

Mass Spectra (ES+): 256 (100 %), 234 (20 %).

3.2.5. Homopolymerization of the mono Aza-crown ether monomer.

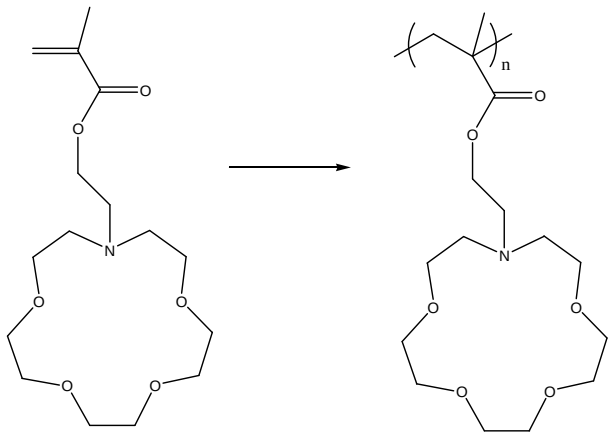

Figure 44: Reaction scheme.

The Free Radical Polymerization was carried out in a Schlenk tube where 1-Aza-15-crown-5 methacrylate monomer (0.5 g) and 2-propanol (2 ml) was stirred and degassed at RT for half an hour. Initiator Vazo 67 (10 mg) was added and the mixture was allowed to

reflux. The mixture was left to react over 48 hours and monitored by ^{1}H-NMR. All samples were cooled down, precipitated with hexane, filtered and washed.

GPC analyses and MALDI-TOF spectra were recorded and are discussed in chapter 4.

3.2.6. Copolymerizations of the mono Aza-crown ether monomer (DD65, DD66).

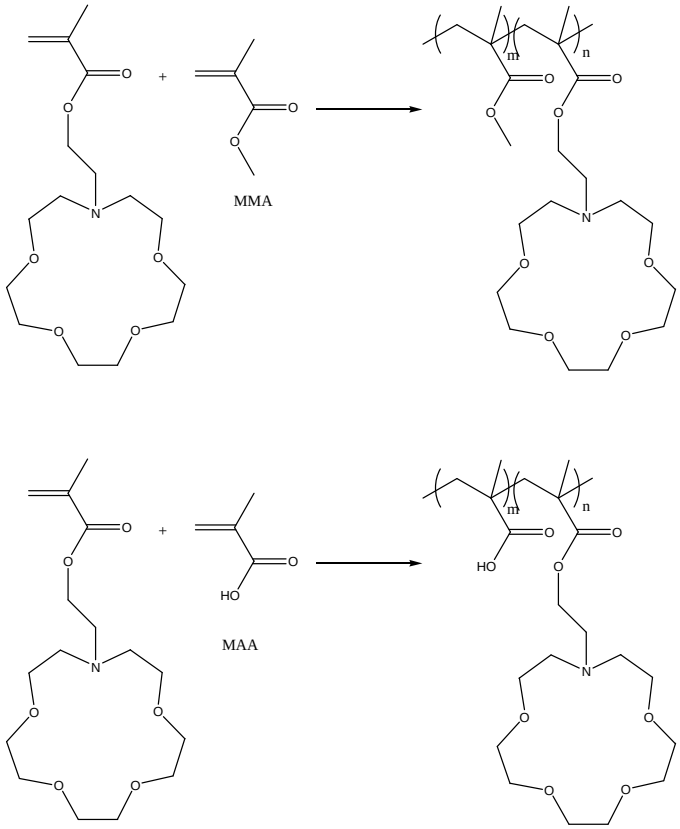

Figure 45: Reaction schemes.

The Free radical copolymerizations were carried out in a Schlenk tube where the monomers and 2-propanol was stirred and degassed at RT over half an hour. Initiator Vazo 67 was added and the mixture was allowed to reflux. Two copolymerizations were carried out and they are summarized in Table 4.

Table 4: Free Radical copolymerizations of the Aza-crown ether monomer with common monomers.

Sample	*1-Aza-15-crown-5 methacrylate*	*MMA*	*MAA*	*Vazo 67*	*2-propanol*
DD65	200 mg	1.8 g	----	20 mg	20 ml
DD66	185 mg	832 mg	832 mg	18.5 mg	7.4 ml

In both copolymerizations the mixture was left to react for at least 48 hours and monitored by ^{1}H-NMR. All samples were cooled down, precipitated with hexane, filtered off and washed.

GPC analyses: DD65: Mn ≈ 4500, Mw ≈ 7200, I = 1.589; DD66: Mn ≈ 5100, Mw ≈ 7400, I = 1.558.

Elemental analyses DD65: expected C (59.46 %), H (8.20 %), N (1.14 %); found C (59.58 %), H (8.39 %), N (0.39 %).

The ^{1}H-NMR spectrum of DD65 was recorded and it is discussed in section 4.1.2.

3.2.7. Preparation of MMA-HEMA Copolymers via Free Radical Polymerization (DD5, DD6, DD7 and DD30).

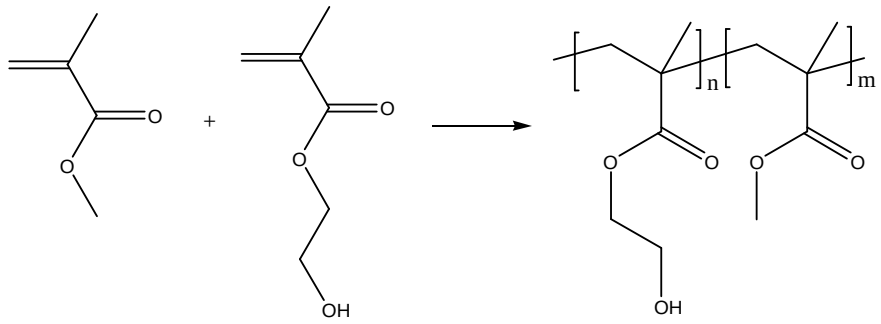

Figure 46: Reaction scheme.

Three different copolymers were prepared using masses that depend on target mass ratios (90/10, 75/25 and 50/50). Free Radical Polymerization's example for 5000 g mol^{-1} of a copolymer 50/50 MMA/HEMA (DD5): MMA (10 g), HEMA (10 g), 1-dodecanethiol

(0.6 g) and 2-propanol (80 g) was stirred and degassed at RT over half an hour. Initiator Vazo 67 (0.4 g) was added and the mixture was allowed to reflux over 4 hours. The mixture was cooled by an ice bath and precipitated with a large excess of hexane. The product was filtered, washed and dried in vacuum oven at 50 ºC overnight. All the experiments carried out are shown in the Table 5 and yielded the final products with conversions around 100 %.

Table 5: Free Radical Copolymerizations of MMA and HEMA.

Sample	MMA (g)	HEMA (g)	IPA (g)	1-dodecanethiol (g)	Vazo 67 (g)
DD5	10	10	80	0.6	0.4
DD6	15	5	80	0.6	0.4
DD7, DD30	18	2	80	0.6	0.4

GPC analyses: DD5 (MMA/HEMA 50/50): Mn ≈ 6400, Mw ≈ 10600, I = 1.719; DD6 (MMA/HEMA 75/25): Mn ≈ 6800, Mw ≈ 11400, I = 1.650; DD7 (MMA/HEMA 90/10): Mn ≈ 6000, Mw ≈ 10000, I = 1.664.

FIPA analyses: DD5 (MMA/HEMA 50/50): Mw ≈ 10400, IV = 0.0012, Rh = 0.59; DD6 (MMA/HEMA 75/25): Mw ≈ 6700, IV = 0.0011, Rh = 0.49; DD7 (MMA/HEMA 90/10): Mw ≈ 12500, IV = 0.0014, Rh = 0.65.

^{1}H-NMR (DMSO) DD5 (MMA/HEMA 50/50): δ 0.4-1.3 (m, -CH_3 on the backbone), 1.4-1.8 (m, -CH_2- on the backbone), 3.5-3.7 (m, 5H, 1 pendant -CH_3 on the methacrylic acid and -O-CH_2- on the HEMA), 3.9 (s, 2H, –CH_2-OH), 4.8 (s, 1H, -CH_2-OH).

^{1}H-NMR (DMSO) DD6 (MMA/HEMA 75/25): δ 0.4-1.3 (m, -CH_3 on the backbone), 1.4-1.8 (m, -CH_2- on the backbone), 3.5-3.7 (m, 11H, 3 pendant -CH_3 on the methacrylic acid and -O-CH_2- on the HEMA), 3.9 (s, 2H, –CH_2-OH), 4.8 (s, 1H, -CH_2-OH).

^{1}H-NMR (DMSO) DD7 (MMA/HEMA 90/10): δ 0.4-1.3 (m, -CH_3 on the backbone), 1.4-1.8 (m, -CH_2- on the backbone), 3.2-3.4 (m, 29H, 9 pendant -CH_3 on the methacrylic acid and -O-CH_2- on the HEMA), 3.7 (s, 2H, -CH_2-OH), 4.6 (s, 1H, -CH_2-OH).

MALDI-TOF spectra were recorded for DD5, DD6 and DD7 and the data for DD7 is reported in the appendix. These data did not show useful information.

Elemental analyses is reported in Table 6

Table 6: Elemental analyses.

Sample	*Expected (%)*			*Found (%)*		
	C	H	N	C	H	N
DD5	57.39	7.83	0	56.67	7.79	Trace
DD6	58.60	7.91	0	57.42	8.35	Trace
DD7	59.42	7.96	0	59.32	7.92	Trace

3.2.8. Preparation of chloroacetyl copolymers of MMA-HEMA by grafting to preformed copolymers (DD8-11, 13, 14, 21, 22, 26, 27, 29, 40, 45, 55, and 73).

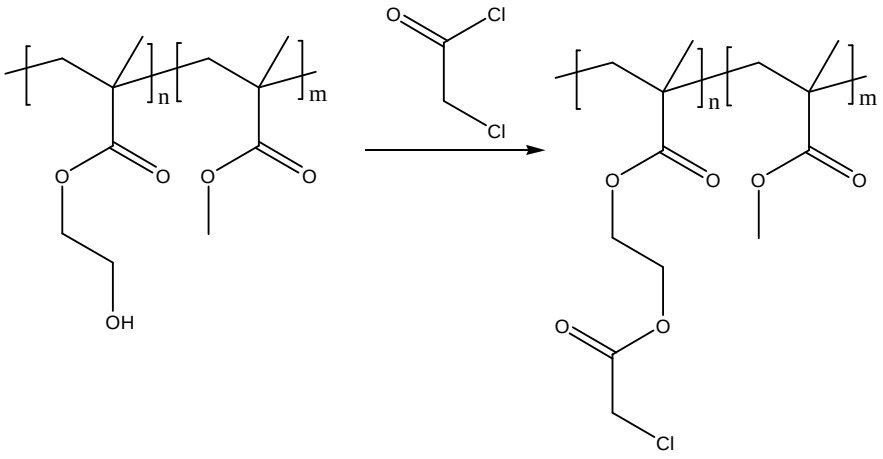

Figure 47: Reaction scheme.

Many reactions were carried out in different conditions, all of which are summarized in Table 7, Table 8 and Table 9. Masses depend on the mass ratios of the MMA/HEMA copolymer used, but molar ratios were generally the same although different molar ratios were also tested. Esterification example for a 5000 g mol^{-1} of 50/50 MMA/HEMA (DD40) copolymer: chloroacetyl chloride (5.25 ml, 7.45 g, 66 mmol, 3.0 eq) was added drop-wise

at 25-30 ºC to a stirring solution of the 50/50 MMA/HEMA copolymer (5 g, 22 mmol and 1.0 eq of HEMA), triethylamine (9.2 ml, 6.68 g, 66 mmol, 3.0 eq) and THF (50 ml) (in some experiments base and solvent were different but the procedure remained the same). The reaction was left to stir at RT over a period of 24 hours. The suspension was filtered and the filtrate was precipitated in a 9: 1 solution of 2-propanol/HCl (hexane was the best solvent for the 90/10 and 75/25 copolymers) and filtered off. The product was washed and dried in vacuum oven at 50 ºC overnight. All the experiments carried out yielded final products with conversions of around 100 %.

DD73 was the only exception to this procedure as in this experiment, after the chloroacetyl chloride was added drop-wise, the mixture was allowed to reflux for 24 hours.

Table 7: MMA/HEMA copolymer 50/50 esterification reactions.

Sample	*Copolymer MMA/HEMA 50/50*	*Base*	*Chloroacetyl chloride*	*Solv.*	*Notes*
DD8	DD5 copolymer (1.0g ; 4.4mmol ; 1.0eq)	TEA (1.85ml ; 13.2mmol ; 3.0eq)	(1.05ml ; 13.2mmol ; 3.00eq)	THF 15ml	ppt in IPA/HCl
DD9	DD5 copolymer (1.0g ; 4.4mmol ; 1.0eq)	$NaHCO_3$ (1.11gr ; 13.2mmol ; 3.0eq)	(1.05ml ; 13.2mmol ; 3.00eq)	THF 15ml	Ppt in H_2O; *NA*
DD10	DD5 copolymer (1.0g ; 4.4mmol ; 1.0eq)	$NaHCO_3$ (1.11gr ; 13.2mmol ; 3.0eq)	(1.05ml ; 13.2mmol ; 3.00eq)	IPA 15ml	Ppt in H_2O/HCl
DD11	DD5 copolymer (1.0g ; 4.4mmol ; 1.0eq)	TEA (2.47ml ; 17.6mmol ; 4.0eq)	(1.4ml ; 17.6mmol ; 4.00eq)	Acet. 10ml	Ppt in IPA
DD13	DD5 copolymer (1.0g ; 4.4mmol ; 1.0eq)	Pyridine (1.07ml ; 13.2mmol ; 3.0eq)	(1.05ml ; 13.2mmol ; 3.00eq)	THF 15ml	Ppt in IPA
DD14	DD5 copolymer (1.0g ; 4.4mmol ; 1.0eq)	Pyridine (1.07ml ; 13.2mmol ; 3.0eq)	(1.05ml ; 13.2mmol ; 3.00eq)	THF 15ml	Ppt in IPA; *NA*
DD40	DD5 copolymer (5.0g ; 22mmol ; 1.0eq)	TEA (9.2ml ; 66mmol ; 3.0eq)	(5.25ml ; 66mmol ; 3.00eq)	THF 50ml	Ppt in IPA/HCl
DD45	DD5 copolymer (5.0g ; 22mmol ; 1.0eq)	Pyridine (12.27ml ; 88mmol ; 4.0eq)	(7.0ml ; 88mmol ; 4.00eq)	THF 60ml	Ppt in IPA/HCl
DD73	DD5 copolymer (1.0g ; 4.4mmol ; 1.0eq)	$NaHCO_3$ (1.48g ; 17.6mmol ; 4.0eq)	(1.40ml ; 17.6mmol ; 4.00eq)	THF 15ml	Ppt in IPA/HCl

Table 8: MMA/HEMA copolymer 75/25 esterification reactions.

Sample	*Copolymer MMA/HEMA 75/25*	*Base*	*Chloroacetyl chloride*	*Solv.*	*Notes*
DD55	DD6 copolymer 3.0gr ; 7mmol ; 1.0eq)	TEA (2.93ml ; 21mmol ; 3.00eq)	(1.67ml ; 21mmol ; 3.0eq)	THF 40ml	ppt in Hex.

Table 9: MMA/HEMA copolymers 90/10 esterification reactions.

Sample	*Copolymer MMA/HEMA 90/10*	*Base*	*Chloroacetyl chloride*	*Solv.*	*Notes*
DD21	DD7 copolymer 2.0gr ; 1.9mmol ; 1.0eq)	TEA (1.08ml ; 7.8mmol ; 4.00eq)	(0.62ml ; 7.76mmol ; 4.0eq)	THF 15ml	ppt in IPA
DD22	DD7 copolymer 2.0gr ; 1.9mmol ; 1.0eq)	TEA (1.08ml ; 7.8mmol ; 4.00eq)	(0.62ml ; 7.76mmol ; 4.0eq)	THF 15ml	ppt in Hex.
DD26	DD7 copolymer 2.0gr ; 1.9mmol ; 1.0eq)	Pyridine (0.3ml ; 3.76mmol ; 1.93eq)	(0.3ml ; 3.76mmol ; 1.93eq)	THF 30ml	ppt in Hex.
DD27	DD7 copolymer 5.0gr ; 4.8mmol ; 1.0eq)	Pyridine (1.6ml ; 19.4mmol ; 4.0eq)	(1.55ml ; 19.4mmol ; 4.00eq)	THF 35ml	ppt in Hex.
DD29	DD7 copolymer 5.0gr ; 4.8mmol ; 1.0eq)	TEA (2.03ml ; 14.6mmol ; 3.0eq)	(1.16ml ; 14.55mmol ; 3.0eq)	THF 35ml	ppt in Hex.

The characterization of the key experiments is reported:

GPC analyses: DD40 (MMA/Chloroacetyl 50/50): Mn ≈ 7600, Mw ≈ 14400, I = 1.888; DD55 (MMA/Chloroacetyl 75/25): Mn ≈ 6700, Mw ≈ 11400, I = 1.698; DD29 (MMA/Chloroacetyl 90/10): Mn ≈ 6100; Mw ≈ 10100; I = 1.661.

FIPA analyses: DD40 (MMA/Chloroacetyl 50/50): Mw ≈ 45000, IV = 0.0010, Rh = 0.88; DD55 (MMA/Chloroacetyl 75/25): Mw ≈ 11900, IV = 0.0011, Rh = 0.59; DD29 (MMA/Chloroacetyl 90/10): Mw ≈ 14000, IV = 0.0010, Rh = 0.61.

^{1}H-NMR (DMSO) DD40 (MMA/HEMA 50/50): δ 0.4-1.3 (m, -CH_3 on the backbone), 1.4-1.8 (m, -CH_2- on the backbone), 3.3 (s, 3H, 1 pendant -CH_3 on the methacrylic acid), 3.9 (s, 2H, –CH_2-Cl), 4.1-4.3 (m, 4H, -O-CH_2-CH_2-O- on the HEMA).

^{1}H-NMR (DMSO) DD55 (MMA/HEMA 75/25): δ 0.4-1.3 (m, -CH_3 on the backbone), 1.4-1.8 (m, -CH_2- on the backbone), 3.6 (s, 9H, 3 pendant -CH_3 on the methacrylic acid), 4.0-4.5 (m, 6H, –CH_2-OH and -O-CH_2-CH_2-O- on the HEMA).

^{1}H-NMR (DMSO) DD29 (MMA/HEMA 90/10): δ 0.4-1.3 (m, -CH_3 on the backbone), 1.4-1.8 (m, -CH_2- on the backbone), 3.5 (s, 27H, 9 pendant -CH_3 on the methacrylic acid), 4.1 (s, 2H, –CH_2-Cl), 4.3-4.5 (m, 4H, -O-CH_2-CH_2-O- on the HEMA).

MALDI-TOF spectra for DD40, DD55 and DD29 were recorded and discussed in Chapter 4.

Elemental analyses were recorded for all copolymers synthesised and they are shown in the following Table 10.

Table 10: Elemental analyses for MMA/Chloroacetyl copolymers.

Sample	*Expected (%)*				*Found (%)*			
	C	H	Cl	N	C	H	Cl	N
DD8	50.90	6.20	11.58	0	50.73	6.35	11.36	Trace
DD11	50.90	6.20	11.58	0	51.04	6.35	12.11	0
DD13	50.90	6.20	11.58	0	51.49	6.54	11.28	Trace
DD21	57.47	7.56	3.20	0	57.17	8.08	3.94	Trace
DD22	57.47	7.56	3.20	0	57.05	7.79	4.35	0.36
DD26	57.47	7.56	3.20	0	57.47	7.82	2.87	0.26
DD27	57.47	7.56	3.20	0	56.27	5.67	5.59	0.40
DD29	57.47	7.56	3.20	0	57.02	7.86	3.90	0.22
DD40	50.90	6.20	11.58	0	51.12	6.26	11.59	Trace
DD45	50.90	6.20	11.58	0	50.33	6.12	12.71	Trace
DD55	54.49	6.91	7.0	0	54.04	6.87	8.06	0.34
DD73	50.9	6.20	11.58	0	51.51	6.46	10.75	0

3.2.9. Synthesis of MMA/Aza-crown ether copolymers by grafting to chloroacetyl functionalized copolymer (DD15, 24, 28, 31, 32, 34, 42, 46, 47, 49, 50, 52, and 56).

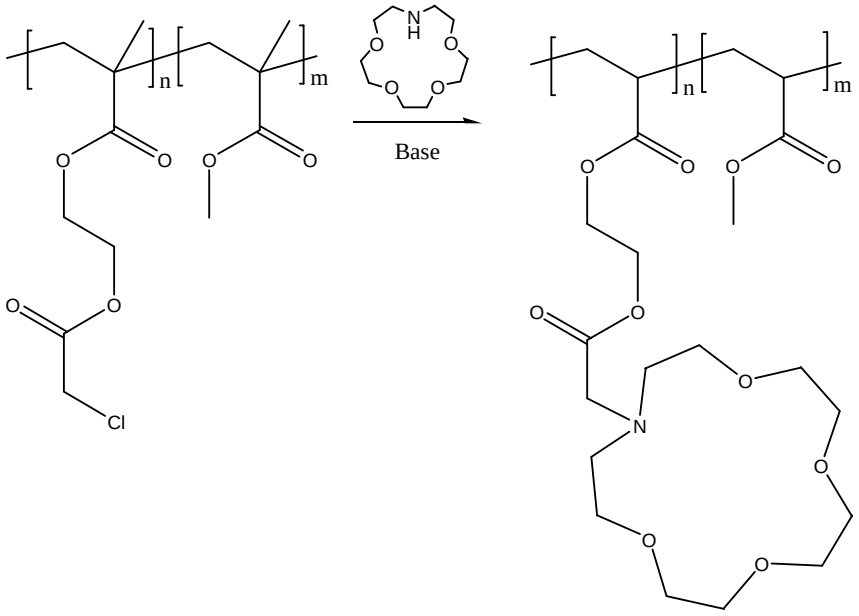

Figure 48: Reaction scheme.

All reactions carried out are listed below in Table 13, Table 12 and Table 13. Masses depend on the copolymer used, the molar ratios were the same for 90/10 and 75/25 copolymers, with the exception of triethylamine used for the 50/50 copolymer (2.0 eq instead that 1.2 eq). Aza-crown ether incorporation example for a 5000 g mol-1 of 90/10 chloroacetyl MMA/HEMA copolymer: a solution of 1-Aza-15-crown-5 (250 mg, 1.14 mmol, 1.2 eq) in THF (1 ml) was added drop-wise at RT to a stirring solution of chloroacetyl copolymer (1.02 g, 0.95 mmol and 1.0 eq of chloroacetyl HEMA), triethylamine (0.16 ml, 1.14 mmol, 1.2 eq) and THF (11 ml). The suspension was allowed to reflux over a period of 24 hours. The suspension was filtered and the filtrate was precipitated in a large excess of water (50/50 and 75/25 copolymers were precipitated in a large excess of hexane) and filtered. The product was washed and dried in a vacuum oven at 50 ºC overnight. All the experiments successfully carried out yielded final products with conversions around 100 %.

Table 11: MMA/Aza-crown ether copolymer 50/50 syntheses.

Sample	MMA/Chloroacetyl copolymer 50/50	Base	Aza-crown ether	Solv.	Notes
DD15	DD8 copolymer (80mg ; 0.07mmol ; 1.0eq)	TEA (0.12ml ; 0.83mmol ; 9.0eq)	1-Aza-12-crown-4 (48mg ; 0.28mmol ; 3.0eq)	THF 2.5ml	NA
DD42	DD8 copolymer (0.3g ; 0.95mmol ; 1.0eq)	TEA (0.16ml ; 1.14mmol ; 1.2eq)	1-Aza-15-crown-5 (250mg ; 1.14mmol ; 1.2eq)	THF 4ml	ppt in Hex.
DD46	DD45 copolymer (0.3g ; 0.95mmol ; 1.0eq)	TEA (0.16ml ; 1.14mmol ; 1.2eq)	1-Aza-15-crown-5 (250mg ; 1.14mmol ; 1.2eq)	THF 4ml	NA
DD47	DD40 copolymer (0.3g ; 0.95mmol ; 1.0eq)	TEA (0.27ml ; 1.9mmol ; 2.0eq)	1-Aza-15-crown-5 (250mg ; 1.14mmol ; 1.2eq)	THF 4ml	NA
DD49	DD45 copolymer (0.3g ; 0.95mmol ; 1.0eq)	TEA (0.16ml ; 1.14mmol ; 1.2eq)	1-Aza-15-crown-5 (250mg ; 1.14mmol ; 1.2eq)	THF 4ml	ppt in Hex.
DD50	DD40 copolymer (0.3g ; 0.95mmol ; 1.0eq)	TEA (0.27ml ; 1.9mmol ; 2.0eq)	1-Aza-15-crown-5 (250mg ; 1.14mmol ; 1.2eq)	THF 4ml	ppt in Hex.
DD52	DD40 copolymer (0.3g ; 0.95mmol ; 1.0eq)	TEA (0.27ml ; 1.9mmol ; 2.0eq)	1-Aza-15-crown-5 (250mg ; 1.14mmol ; 1.2eq)	THF 4ml	ppt in Hex.

Table 12: MMA/Aza-crown ether copolymer 75/25 syntheses.

Sample	MMA/Chloroacetyl copolymer 75/25	Base	Aza-crown ether	Solv.	Notes
DD56	DD55 copolymer (481mg ; 0.95mmol ; 1.0eq)	TEA (0.16ml ; 1.14mmol ; 1.2eq)	1-Aza-15-crown-5 (250mg ; 1.14mmol ; 1.2eq)	THF 6ml	ppt in Hex.

Table 13: MMA/Aza-crown ether 90/10 copolymers syntheses.

Sample	MMA/Chloroacetyl copolymer 90/10	Base	Aza-crown ether	Solv.	Notes
DD24	DD22 copolymer (1.02g ; 0.95mmol ; 1.0eq)	TEA (0.16ml ; 1.14mmol ; 1.2eq)	1-Aza-15-crown-5 (250mg ; 1.14mmol ; 1.2eq)	THF 6ml	ppt in Water
DD28	DD26 copolymer (1.02g ; 0.95mmol ; 1.0eq)	Pyridine (0.1ml ; 1.14mmol ; 1.2eq)	1-Aza-15-crown-5 (250mg ; 1.14mmol ; 1.2eq)	THF 13ml	ppt in Water
DD31	DD27 copolymer (1.02g ; 0.95mmol ; 1.0eq)	Pyridine (0.1ml ; 1.14mmol ; 1.2eq)	1-Aza-15-crown-5 (250mg ; 1.14mmol ; 1.2eq)	CH_3CN 11ml	ppt in Water NA
DD32	DD29 copolymer (1.02g ; 0.95mmol ; 1.0eq)	TEA (0.16ml ; 1.14mmol ; 1.2eq)	1-Aza-15-crown-5 (250mg ; 1.14mmol ; 1.2eq)	CH_3CN 11ml	ppt in Water NA
DD34	DD29 copolymer (1.02g ; 0.95mmol ; 1.0eq)	TEA (0.16ml ; 1.14mmol ; 1.2eq)	1-Aza-15-crown-5 (250mg ; 1.14mmol ; 1.2eq)	THF 12ml	ppt with Water

The characterization of the key experiments is reported:

FIPA analyses: DD52 (MMA/Aza-crown ether 50/50): Mw ≈ 287000, IV = 0.0003, Rh = 1.0.8; DD56 (MMA/Aza-crown ether 75/25): Mw ≈ 376000, IV = 0.0007, Rh = 1.64; DD29 (MMA/Aza-crown ether 90/10): Mw ≈ 218000, IV = 0.0011, Rh = 1.57.

^{1}H-NMR (DMSO) DD52 (MMA/Aza-crown ether 50/50): δ 0.4-1.3 (m, -CH_3 on the backbone), 1.4-1.8 (m, -CH_2- on the backbone), 2.8 (s, 4H, 2 -CH_2-N- on Aza-crown ring), 3.3-3.7 (m, 21H, 8-CH_2- on the Aza-crown ring, 1 -CO-CH_2-N-, 1 pendant -CH_3 on the methacrylic acid), 4.-4.3 (m, 4H, -O-CH_2-CH_2-O- on the HEMA).

^{1}H-NMR (DMSO) DD56 (MMA/Aza-crown ether 75/25): δ 0.4-1.3 (m, -CH_3 on the backbone), 1.4-1.8 (m, -CH_2- on the backbone), 2.8 (s, 4H, 2 -CH_2-N- on Aza-crown ring), 3.4-3.7 (m, 27H, 8-CH_2- on the Aza-crown ring, 1 -CO-CH_2-N-, 3 pendant -CH_3 on the methacrylic acid), 4.-4.3 (m, 4H, -O-CH_2-CH_2-O- on the HEMA).

^{1}H-NMR (DMSO) DD34 (MMA/Aza-crown ether 90/10): δ 0.4-1.3 (m, -CH_3 on the backbone), 1.4-1.8 (m, -CH_2- on the backbone), 2.8 (s, 4H, 2 -CH_2-N- on Aza-crown ring), 3.4-3.6 (m, 45H, 8-CH_2- on the Aza-crown ring, 1 -CO-CH_2-N-, 9 pendant -CH_3 on the methacrylic acid), 4.-4.3 (m, 4H, -O-CH_2-CH_2-O- on the HEMA).

MALDI-TOF spectra for DD52, DD56 and DD34 were recorded and the DD52 spectrum is reported in the appendix (Figure 3). The other spectra are not reported as they did not provide any useful information as they appeared very similar to the DD52 spectrum.

Elemental analyses were recorded for all copolymers synthesised and they are shown in the following Table 14.

Table 14: Elemental analyses for MMA/Aza-crown ether copolymers.

Sample	*Expected (%)*				*Found (%)*			
	C	H	Cl	N	C	H	Cl	N
DD24	58.34	7.98	0	1.10	57.73	7.99	1.59	1.53
DD28	58.34	7.98	0	1.10	58.78	8.42	5.84	0.68
DD34	58.34	7.98	0	1.10	59.02	8.49	0	0.94
DD42	56.44	7.98	0	2.86	57.01	8.35	0	2.31
DD49	56.44	7.98	0	2.86	55.12	7.95	1.30	2.74
DD50	56.44	7.98	0	2.86	55.77	8.27	Trace	2.54
DD52	56.44	7.98	0	2.86	55.76	8.25	0	2.62
DD56	57.47	7.98	0	2.03	56.61	8.30	0.93	1.98

3.2.10. Synthesis of amino-ethyl methyl methacrylate (AEMA).

This was part of an alternative method to incorporate crown ether into polymers. This monomer was prepared following the reaction shown in Figure 49.

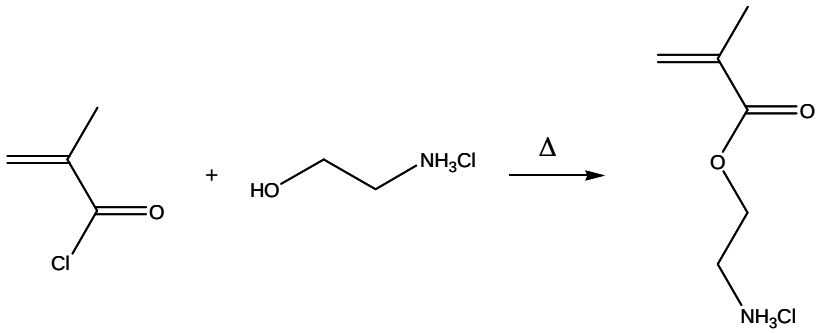

Figure 49: Reaction scheme.

Methacryloyl chloride (14.9 ml, 16.1 g, 154 mmol, 3 eq) was added drop-wise at 100 ºC over a period of 2 hours to a molten mixture of ethanolamine hydrochloride (5 g, 51.3 mmol, 1.0 eq) and hydroquinone (40 mg). The round bottom flask was equipped with a coil jacketed condenser because of the high volatility of the methacryloyl chloride. The mixture was stirred vigorously for further 2 hours and cooled down to 60 ºC. The HCl gas evolved during this esterification was neutralised using an aqueous NaOH solution connected to the reaction vessel. Ethyl acetate (20 ml) was added to the viscous oil and white solid was obtained. The crude product was filtered off, washed and dried in vacuum at 50 ºC overnight. A yield of 45 % was obtained.

^{1}H-NMR (DMSO): δ 1.9 (s, 3H, -CH_3 on the double bond), 3.1 (s, 2H, -CH_2-NH_3^+), 4.3 (s, 2H, -CH_2-O-), 5.7 (s, 1H on the double bond), 6.3 (s, 1H on the double bond).

3.2.11. Homopolymerization of AEMA.

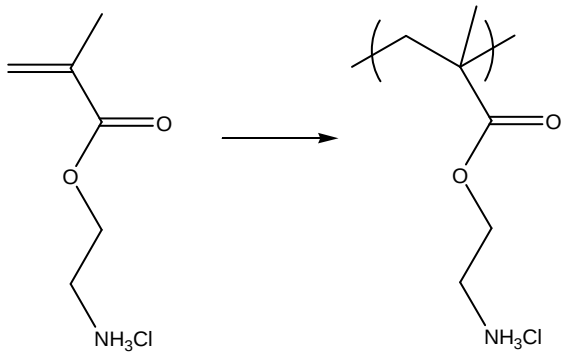

Figure 50: Reaction scheme.

A mixture of AEMA (2 g) and water (8 ml) was stirred and degassed at RT over half an hour (pH = 2.28 at T=23 °C). Initiator Ammonium Per-sulphate (40 mg) was added and the mixture was allowed to reflux over 4 hours. The mixture was cooled down by an ice bath and precipitated with a large excess of 2-propanol. The sticky white solid was filtered off, washed and dried in vacuum oven at 50 ºC overnight. The reaction yielded about 100 % of white product.

^{1}H-NMR (D_2O): δ 0.7-1.1 (m, 3H, -CH_3 on the polymer backbone), 1.8-2.2 (m, 2H, -CH_2- on the polymer backbone), 3.3 (s, 2H, -CH_2-NH_3^+), 4.2 (s, 2H, -O-CH_2-).

3.2.12. Aza-crown ether polymer synthesis by grafting to poly AEMA.

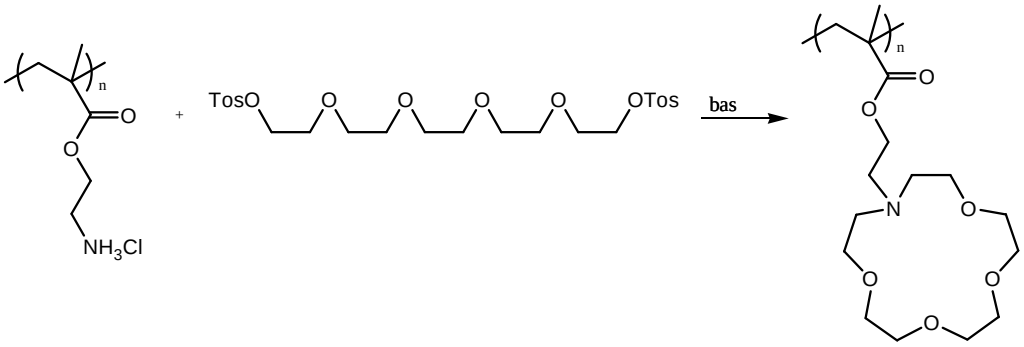

Figure 51: Reaction scheme.

A solution of penta ethylene glycol di-(p-toluene sulfonate) (90 mg, 0.1646 mmol, 0.14 eq) in CH_3CN (0.5 ml) was added drop-wise to a stirred mixture of poly AEMA (200 mg, 1.21 mmol, 1.00), CH_3CN (2 ml) and K_2CO_3 (0.26 gr, 2.42 mmol, 2.00) at RT. The mixture was then stirred vigorously for further 2 hours and filtered. The product exhibited insolubility in all most common solvents. High cross-linking was probably obtained.

3.2.13. Synthesis of Hexa-ethylene glycol di tosylate (hexa penta ethylene glycol di-(p-toluene sulfonate).

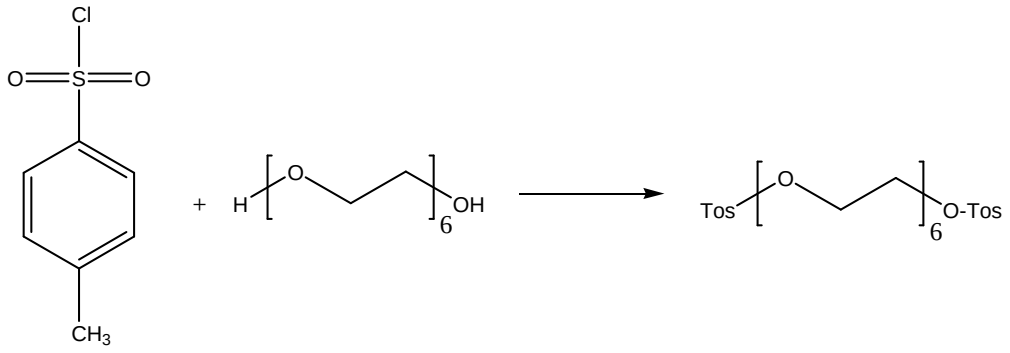

Cl-Tos

Figure 52: Reaction scheme.

A solution of p-toluene-sulphonyl chloride (9.964 g, 52.26 mmol, 2.95 eq) and pyridine (44 ml) was added drop-wise over a period of an hour and half to a stirred solution of hexa-ethylene glycol (5 gr, 17.71 mmol, 1.00 eq) and pyridine (44 ml) at -4 °C. The mixture was stirred for further 3 hours at -4 °C and placed in the fridge over night. The solution was poured in water/ice (120 ml) and subsequently extracted with DCM (3 x 60 ml). The combined organic layer was then washed with cold 6 N aqueous HCl (3 x 60 ml) and saturated aqueous ammonium chloride solution (60 ml) and dried with anhydrous magnesium sulphate. The solvent was removed under reduced pressure yielded 89 % of a product as viscous yellow oil.

^{1}H-NMR ($CDCl_3$): δ 2.5 (s, 6H, 2 -CH_3 on the aromatics), 3.6 (m, 20H, 10 -CH_2- on the hexa-ethylene glycol group), 4.2 (s, 4H, 2 -CH_2-O-S-), 7.4 (s, 4H, 4 -CH- on the aromatics), 7.8 (s, 4H, 4 -C-CH- on the aromatics).

3.3. Synthesis of Dual-Stimuli responsive NIPAM-AAc hydrogel beads incorporating *N*-Aza-crown ethers.

The methods of synthesis discussed in this chapter 5 are provided in this section.

3.3.1. Preparation of poly-NIPAM gel beads by Inverse Suspension Polymerization Method (PN).

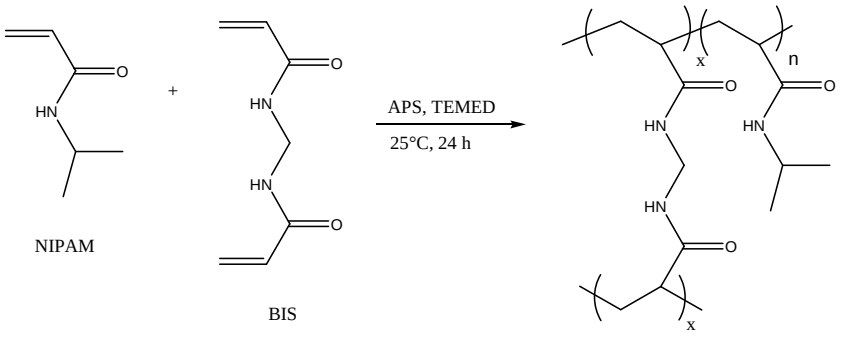

Figure 53: Reaction scheme.

Inverse suspension Polymerization and in general suspension polymerization is a procedure which depends upon different variables. Many experiments were carried out testing different size of flask, type of blade, size of blade, stirring speed, ratio between continuous phase and aqueous monomer solution etc. in order to find the suitable conditions for our process. The following procedure produces beaded microgels using a 700 ml round bottom quick-fit flask equipped with a steel propeller of 5 cm blade and 350 rpm (*) stirring speed.

Poly-NIPAM gel beads were prepared by Inverse Suspension Polymerization technique using cyclohexane as the continuous phase and SPAN 80 (Sorbitan monooleate) as oil-soluble surfactant. Different surfactants were tested (**) but SPAN 80 resulted to have the more suitable HLB value (hydrophile-lipophile balance, 4.3) to control the stability of the dispersion. NIPAM (1 gr, 8.84 mmol, 9 eq) and the cross linker N, N′-Methylenebis acryl amide also known as BIS (25 mg, 0.164 mmol) were dissolved in 5ml distilled water. This mixture was purged with nitrogen over 30 min in order to remove dissolved oxygen.

The initiator APS (Ammonium Persulphate, 12.5 mg, 0.055 mmol) was added to the aqueous monomer solution. After its solubilization the mixture was promptly transferred with a syringe previously flushed with nitrogen into a 700 ml quickfit round bottom flask containing a solution of 0.1 ml (***) of SPAN 80 dissolved in 200 ml of cyclohexane

previously purged with nitrogen over a period of 2 hours. The mixture was stirred at 350 rpm under nitrogen atmosphere for further 30 min to allow the surfactant to form relatively uniform aqueous emulsion droplets in the continuous phase. The catalyst N,N,N′,N′-Tetramethylethylenediamine (TEMED, 37.5 μl, 0.25 mmol) was added to the mixture using a syringe previously flushed with nitrogen in order to initiate polymerization which was allowed to proceed until completion over a period of 24 hours. After completion, the beads were separated from the oil phase and washed several times with distilled water and acetone and dried in the vacuum oven at 50 °C overnight. IR Spectra: 3600-3200 cm^{-1} (NH stretching of poly-NIPAM), 1643 cm^{-1} (CO stretching of poly-NIPAM), 1534 cm^{-1} (NH vibration of poly-NIPAM).

Elemental Analysis was carried out and it is reported in Figure 15.

Table 15: Elemental analysis.

Expected (%)			*Found (%)*		
C	H	N	C	H	N
63.7	9.7	12.5	62.07	9.13	10.12

* Different stirring speeds were tested in the range 250-600 rpm but only 350 rpm gave a beaded product without evident amorphous polymer.

** SPAN40 and SPAN83 were also tested but produced amorphous polymer.

*** Different quantities of the selected surfactant (SPAN40, SPAN80 and SPAN83) were also tested (0.1, 0.2 ml, 1 ml, 2 ml, 100 ml) but 0.1 ml was the only quantity that allowed a beaded material without evident amorphous polymer.

3.3.2. Preparation of poly-(NIPAM-co-HEMA-co-AAc) gel beads (9:1:1) by Inverse Suspension Polymerization Method (PNHA).

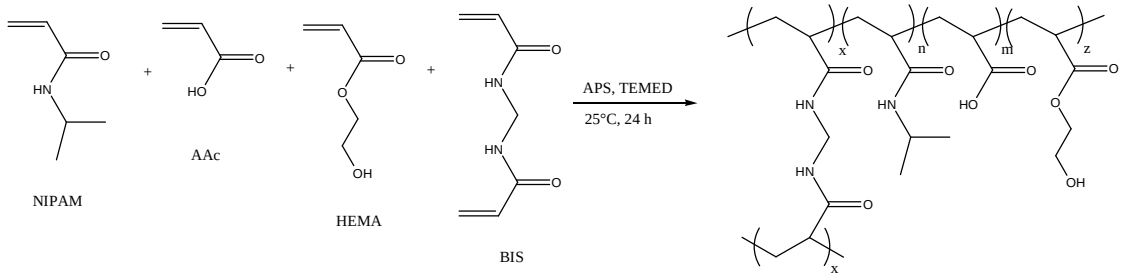

Figure 54: Reaction scheme.

Inverse suspension Polymerization and in general suspension polymerization is a procedure which depends upon different variables. Many experiments were carried out testing different size of flask, type of blade, size of blade, stirring speed, ratio between continuous phase and aqueous monomer solution etc. in order to find the suitable conditions for our process. The following method is the more suitable procedure that was found, however, some amorphous microgel was also obtained and fully characterization of the material was not carried out. A 700ml round bottom quick-fit flask equipped with a propeller with 5cm blade was used in this method. Inverse Suspension Polymerization of these three monomers resulted a more difficult system in order achieve the uniform beading of the microgel.

Poly-(NIPAM-co-HEMA-co-AAc) gel beads were prepared by Inverse Suspension Polymerization using cyclohexane as the continuous phase and SPAN 40 (Sorbitan monopalmitate) as oil-soluble surfactant. Different surfactants were tested (*) but SPAN 40 resulted to have the more suitable HLB value (hydrophile-lipophile balance, 6.7) to control the stability of the dispersion. NIPAM (1 gr, 8.84 mmol, 9 eq), HEMA (0.132 ml, 1.09 mmol, 1.11 eq), AAc (67.4 μl, 0.98 mmol, 1 eq) and the cross linker N, N′-Methylenebis acryl amide also known as BIS (25 mg, 0.164 mmol) were dissolved in 5 ml distilled water. This mixture was purged with nitrogen over 30 min in order to remove dissolved oxygen.

The initiator APS (Ammonium Persulphate, 12.5 mg, 0.055 mmol) was added to the aqueous monomer solution. After its solubilization the mixture was promptly transferred with a syringe previously flushed with nitrogen into a 700 ml quickfit round bottom flask containing a solution of 0.1 ml of SPAN 40 dissolved in 200 ml of cyclohexane previously purged with nitrogen over as period of 2 hours. The mixture was stirred at 350 rpm under nitrogen atmosphere for further 30 min to allow the surfactant to form relatively uniform aqueous emulsion droplets in the continuous phase. The catalyst N,N,N′,N′-Tetramethylethylenediamine (TEMED, 37.5 µl, 0.25 mmol) was added to the mixture using a syringe previously flushed with nitrogen to initiate the polymerization which was allowed to proceed until completion over a period of 24 hours. After completion, the beads were separated from the oil phase and washed several times with distilled water and acetone and dried in the vacuum oven at 50 °C overnight.

Elemental analysis was carried out and it is reported in Table 16.

Table 16: Elemental analysis.

Expected (%)			*Found (%)*		
C	H	N	C	H	N
61.7	11.0	10.2	48.61	8.54	8.25

* SPAN80 and SPAN83 were also tested but produced more visible amorphous polymer.

3.3.3. Preparation of poly-(NIPAM-co-HEMA) gel beads (9:1) by Inverse Suspension Polymerization Method (PNH).

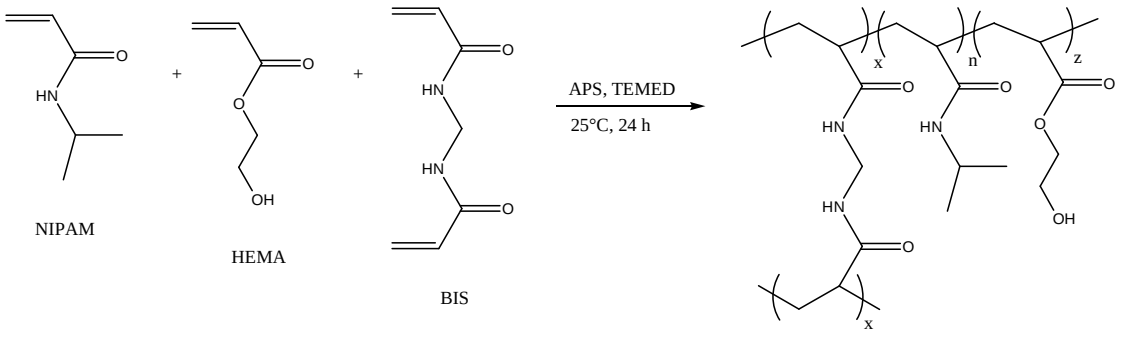

Figure 55: Reaction scheme.

The following procedure produce beaded microgels using a 700 ml round bottom quick-fit flask equipped with a steel propeller of 5 cm blade and 350 rpm stirring speed.

Poly-(NIPAM-co-HEMA) gel beads were prepared by Inverse Suspension Polymerization using cyclohexane as the continuous phase and SPAN 80 (Sorbitan monooleate) as oil-soluble surfactant. SPAN 80 resulted to have the more suitable HLB value (hydrophile-lipophile balance, 4.3) to control the stability of the dispersion. NIPAM (1 gr, 8.84 mmol, 9 eq), HEMA (0.132 ml, 1.09 mmol, 1.11 eq) and the cross linker N, N′-Methylenebis acryl amide also known as BIS (25 mg, 0.164 mmol) were dissolved in 5 ml distilled water. This mixture was purged with nitrogen over 30 min in order to remove dissolved oxygen.

The initiator APS (Ammonium Persulphate, 12.5 mg, 0.055 mmol) was added to the monomer aqueous solution. After its solubilization the mixture was promptly transferred with a syringe previously flushed with nitrogen into a 700 ml quickfit round bottom flask containing a solution of 0.1 ml of SPAN 80 dissolved in 200 ml of cyclohexane previously purged with nitrogen over as period of 2 hours. The mixture was stirred at 350 rpm under nitrogen atmosphere for further 30 min to allow the surfactant to form relatively uniform aqueous emulsion droplets in the continuous phase. The catalyst N,N,N′,N′-Tetramethylethylenediamine (TEMED, 37.5 µl, 0.25 mmol) was added to the mixture using a syringe previously flushed with nitrogen to initiate polymerization which

was allowed to proceed until completion over a period of 24 hours. After completion, the beads were separated from the oil phase and washed several times with distilled water and acetone and dried in the vacuum oven at 50 °C overnight.

Elemental analysis was carried out and it is reported in Table 17.

Table 17: Elemental analysis.

Expected (%)			*Found (%)*		
C	H	N	C	H	N
62.7	9.5	10.9	57.14	9.86	9.99

^{13}C-NMR (Solid State): δ 16-26 (methyl groups NIPAM and contribution the CH carbons in the backbone), 30-50 (contribution of the CH and CH_2 in the backbone and CH-N in the NIPAM), 58-70 (CH_2OH and CH_2O of HEMA), 170-180 (carbonyl groups of NIPAM and AAc).

IR Spectra: 3600-3200 cm^{-1} (NH stretching of poly-NIPAM), 1712 cm^{-1} (CO stretching of poly-HEMA), 1643 cm^{-1} (CO stretching of poly-NIPAM), 1534 cm^{-1} (NH vibration of poly-NIPAM).

3.3.4. Preparation of poly-(NIPAM-co-AAc) gel beads (8:2) by Inverse Suspension Polymerization Method (PNA).

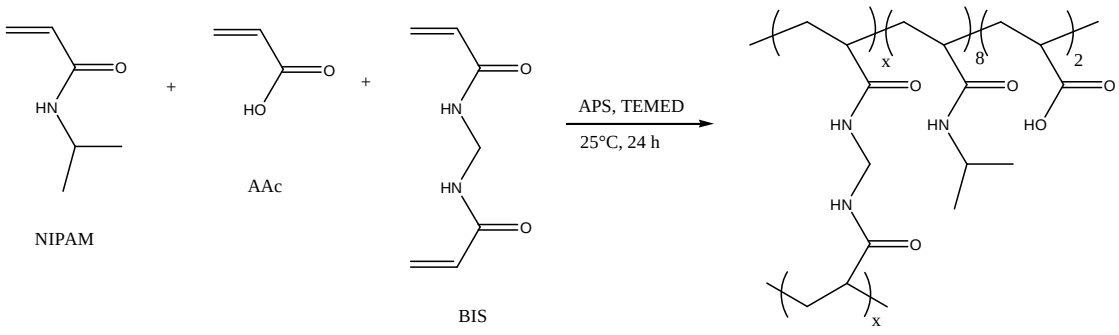

Figure 56: Reaction scheme.

Inverse suspension Polymerization and in general suspension polymerization is a procedure which depends upon different variables. Many experiments were carried out testing different size of flask, type of blade, size of blade, stirring speed (range 200-600 rpm), ratio between continuous phase and aqueous monomer solution etc. in order to find the best conditions for our process. The following procedure produce beaded microgels using a 2l round bottom quick-fit flask equipped with a steel propeller of 10 cm blade and 250 rpm stirring speed. The same procedure was scaled down to 1 g of NIPAM, 200 ml of Cyclohexane and was carried out in a 700 ml round bottom quick-fit flask equipped with a steel propeller of 5 cm blade stirred at 350 rpm resulting in a beaded microgel.

Poly-(NIPAM-co-AAc) gel beads were prepared by Inverse Suspension Polymerization using cyclohexane as the continuous phase and SPAN 80 (Sorbitan monooleate) as oil-soluble surfactant. Different surfactants were tested (*) but SPAN 80 resulted to have the more suitable HLB value (hydrophile-lipophile balance, 4.3) to control the stability of the dispersion. NIPAM (8 gr, 61.9 mmol, 8 eq), AAc (1.22 ml, 17.7 mmol, 2 eq) and the cross linker N, N′-Methylenebis acryl amide also known as BIS (204 mg, 1.33 mmol, 1.5 mol % on the total monomer) were dissolved in 40 ml distilled water. This mixture was purged with nitrogen over 30 min in order to remove dissolved oxygen. The catalyst N,N,N′,N′-Tetramethylethylenediamine (TEMED, 0.64 ml, 4.27 mmol) was added to the mixture using a syringe previously flushed with nitrogen. This solution was immediately poured into a 2 L quickfit round bottom flash equipped with a propeller with 10cm blades containing a solution of 4 ml of SPAN 80 dissolved in 1.6l of cyclohexane previously purged with nitrogen over as period of 2 hours. The mixture was stirred at 250 rpm under nitrogen atmosphere for further 30 min to allow the surfactant to form relatively uniform aqueous emulsion droplets in the continuous phase. The initiator APS (Ammonium Persulphate, 100.8 mg, 0.5 mol % on the total monomer) was dissolved in 0.5ml of degassed distilled water and added to the mixture to initiate polymerization which was allowed to proceed until completion over a period of 24 hours. After completion, the beads were separated from the oil phase, washed several times with distilled water and acetone and dried in the vacuum oven at 50°C overnight.

The polymerization yielded 8.5 g of white beads (90 % yields).

Elemental analysis was carried out and it is reported in Table 18.

Table 18: Elemental analysis.

Expected (%)			*Found (%)*		
C	H	N	C	H	N
61.8	9.2	10.7	59.36	9.60	11.15

** SPAN40 and SPAN83 were also tested but produced amorphous polymer.

^{13}C-NMR (Solid State): δ 20-26 (methyl groups NIPAM and contribution the CH carbons in the backbone), 30-50 (contribution of the CH and CH_2 in the backbone and CH-N in the NIPAM), 170-180 (carbonyl groups of NIPAM and AAc).

IR Spectra: 3600-3200 cm^{-1} (NH stretching of poly-NIPAM), 1712 cm^{-1} (CO stretching of poly-AAc), 1643 cm^{-1} (CO stretching of poly-NIPAM), 1534 cm^{-1} (NH vibration of poly-NIPAM).

3.3.5. Synthesis of chloroacetyl Aza-crown ether.

Three different chloroacetyl Aza-crown ethers carrying different ring size were prepared (12, 15 and 18). Only the synthesis of chloroacetyl 1-Aza-15-crown-5 is reported (Figure 57).

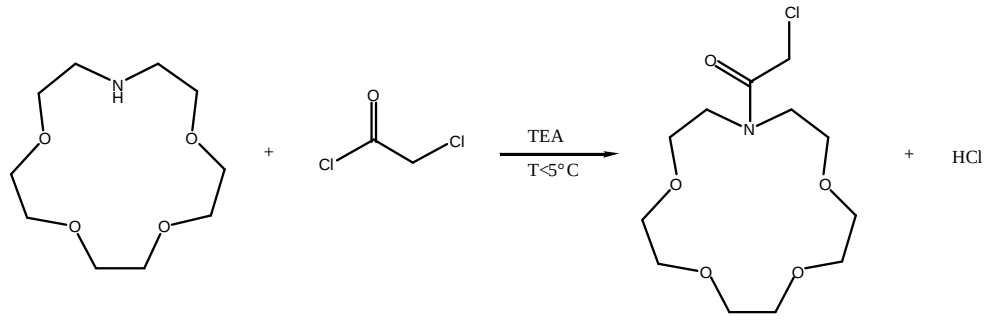

Figure 57: Reaction scheme.

A mixture of chloroacetyl chloride (1.2 ml, 15.04 mmol) and anhydrous THF (9 ml) was slowly added dropwise at 3-4 °C to a stirring solution containing 1-Aza-15-crown-5 (3 gr, 13.68 mmol), triethylamine (2.28 ml, 16.42 mmol) and anhydrous THF (36 ml) into a 100ml round bottom flask under nitrogen atmosphere. The reaction mixture was stirred for further 3 hours at 3-4 °C. The temperature was then increased to room temperature and the mixture stirred for further 24 hours. The resulting suspension was filtered and the filtrate rotaevaporated in order to remove the solvent. The resulting brown oil was dissolved in DCM and washed with H_2O (3 x 30 ml), $NaHCO_3$ saturated aqueous solution (1 x 30 ml) and NaCl saturated aqueous solution (1x30ml). The organic layer was dried over $MgSO_4$ and the solvent rotaevaporated. The product was dried under high vacuum at 60 °C overnight. 2.95 gr of brown oil was obtained (Yield = 73 %).

Chloroacetyl 1-Aza-12-crown-4 analysis:

Yield = 69.6 %

^{1}H-NMR ($CDCl_3$): δ 3.4-3.6 (m, 16H, -O-CH_2-CH_2-O- Aza-crown ether ring), 4.2 (s, 2H, -CO-CH_2-Cl the chloroacetyl function).

Mass Spectra (ES+): m/z 525.2 (80 %), 353.1 (100 %), 273.9 (80 %), 252.0 (20 %), 239.6 (30 %), 175.9 (30 %).

Chloroacetyl 1-Aza-15-crown-5 analysis:

^{1}H-NMR ($CDCl_3$): δ 3.4-3.6 (m, 20H, -O-CH_2-CH_2-O- Aza-crown ether ring), 4.2 (s, 2H, -CO-CH_2-Cl the chloroacetyl function).

Mass Spectra (ES+): m/z 318.0 (100 %), 296.0 (20 %).

Chloroacetyl 1-Aza-18-crown-6 analysis:

Yield=70%

^{1}H-NMR ($CDCl_3$): δ 3.4-3.6 (m, 24H, -O-CH_2-CH_2-O- Aza-crown ether ring), 4.2 (s, 2H, -CO-CH_2-Cl the chloroacetyl function).

Mass Spectra (ES+): m/z 362.1 (100%), 340 (10%).

3.3.6. Functionalization of poly-(NIPAM-co-HEMA) gel beads, PNH, with chloroacetyl Aza-crown ethers (PNH2).

Poly-(NIPAM-co-AAc) gel beads, PNH, (0.2 gr) were dispersed in anhydrous THF (5 ml) at room temperature in a 10 ml round bottom flask equipped with a condenser and purged with nitrogen. Triethylamine (0.04 ml, 0.287 mmol) and chloroacetyl 1-aza-15-crown-5 (0.0846 g, 0.287 mmol) were added to the mixture which was allowed to reflux over a period of 24 hours.

The hydrogel beads were filtered and washed several times with distilled water and acetone in order to remove un-reacted reagents. The microgel was dried in the vacuum oven at 50 °C overnight.

^{13}C-NMR (Solid State): δ 16-26 (methyl groups NIPAM and contribution the CH carbons in the backbone), 30-50 (contribution of the CH and CH_2 in the backbone and CH-N in the NIPAM), 58-70 (CH_2OH and CH_2O of HEMA), 170-180 (carbonyl groups of NIPAM and AAc).

IR Spectra: 3600-3200 cm^{-1} (NH stretching of poly-NIPAM), 1712 cm^{-1} (CO stretching of poly-HEMA), 1643 cm^{-1} (CO stretching of poly-NIPAM), 1534 cm^{-1} (NH vibration of poly-NIPAM).

3.3.7. Functionalization of poly-(NIPAM-co-AAc) gel beads with chloroacetyl Aza-crown ethers (PNA1, PNA2 and PNA3).

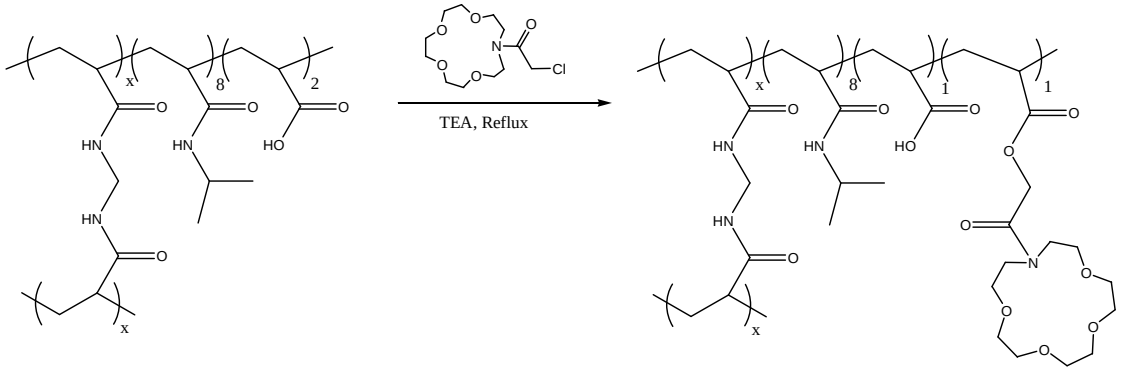

Figure 58: Reaction scheme for the functionalization with 1-aza-15-crown-5 (PNA2).

Three different compounds with different crown ether ring size (1-aza-12-crown-4, 1-aza-15-crown-5 and 1-aza-18-crown-6 for PNA1, PNA2 and PNA3, respectively) were prepared following the same procedure and the synthesis of Normal-type poly-(NIPAM-co-AAc) gel beads incorporating chloroacetyl 1-aza-15-crown-5 (PNA2) is reported as example.

Poly-(NIPAM-co-AAc) gel beads - PNA - (2 gr, ~ 3.82 mmol) were dispersed in anhydrous THF (50 ml) at room temperature in a 100 ml round bottom flask equipped with a condenser and purged with nitrogen. Triethylamine (0.4 ml, 2.87 mmol) and chloroacetyl 1-aza-15-crown-5 (0.846 g, 2.87 mmol) were added to the mixture which was allowed to reflux over a period of 24 hours.

The hydrogel beads were filtered and washed several times with distilled water and acetone in order to remove un-reacted reagents. The microgel was dried in the vacuum oven at 50 °C overnight.

IR Spectra (PNA2): 3600-3200 cm^{-1} (NH stretching of poly-NIPAM), 1712 cm^{-1} (CO stretching of poly-AAc), 1643 cm^{-1} (CO stretching of poly-NIPAM), 1534 cm^{-1} (NH vibration of poly-NIPAM), ~1212 cm^{-1} (C-O-C stretching of Aza-crown ether). Similar IR-spectra was obtained for PNA1, PNA2 and PNA3.

^{13}C-NMR (Solid State - PNA2): δ 20-26 (methyl groups NIPAM and contribution the CH carbons in the backbone), 30-50 (contribution of the CH and CH_2 in the backbone and CH-N in the NIPAM), 65-75 (CH_2O carbons of the Aza-crown ether), 170-180 (carbonyl groups of NIPAM and AAc). Similar NMR-spectra was obtained for PNA1, PNA2 and PNA3.

Elemental analysis was carried out and is reported in Table 19.

Table 19: Elemental analysis for PNA1, PNA2 and PNA3.

Sample	*Expected (%)*				*Found (%)*			
	C	H	N	Cl	C	H	N	Cl
PNA1	60.8	8.9	10.0	0	58.2	9.5	10.4	0
PNA3	60.4	9.0	9.3	0	57.8	9.5	10.2	0
PNA2	60.6	9.0	9.6	0	59.5	9.6	10.8	0

3.3.8. Controlling experiment to determine the quantity of crown ether incorporated during PNA2 preparation.

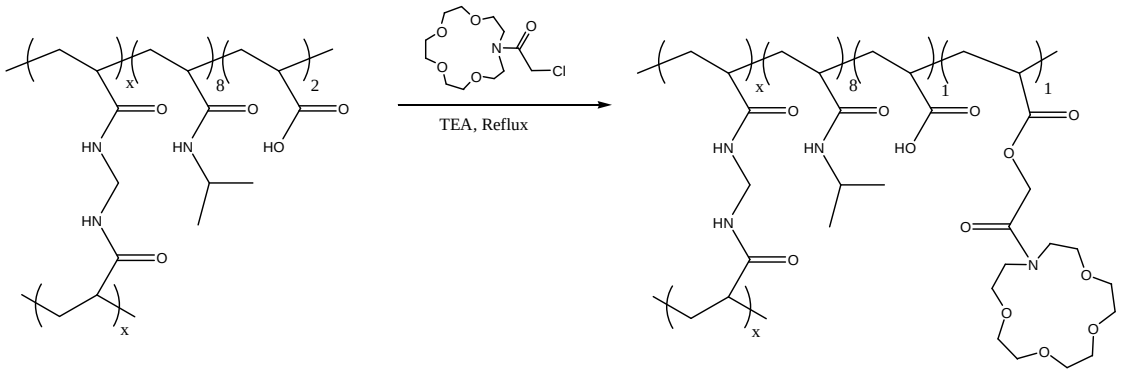

Figure 59: Reaction scheme.

This experiment is discussed in section 5.1 at page 158. Normal-type poly-(NIPAM-co-AAc) gel beads - PNA - (200 mg, ~0.382 mmol) were dispersed in anhydrous THF (5 ml) at room temperature in a 10ml round bottom flask equipped with a condenser and purged

with nitrogen. Triethylamine (0.04 ml, 0287 mmol) and chloroacetyl 1-aza-15-crown-5 (90 mg, 0.31mmole) were added to the mixture which was allowed to reflux over a period of 24 hours.

The hydrogel beads were filtered and washed with acetone (3 x 5 ml). The organic layers were collected and the solvent was evaporated. The brown oil was dried in the vacuum oven at 70 ºC for 48 hours.

The brown oil was weighed as 68 mg.

^{1}H-NMR ($CDCl_3$): δ 1.3 (t, 9H, -CH_3 of TEA), 2.1 (s, 2H H_2O), 3.1 (m, 6H -CH_2- of TEA), 3.5-3.9 (m, 20H crown ether ring), 4.2 (s, 2H -CO-CH_2-Cl).

3.3.9. Synthesis of Aza-crown ether methacrylate monomers.

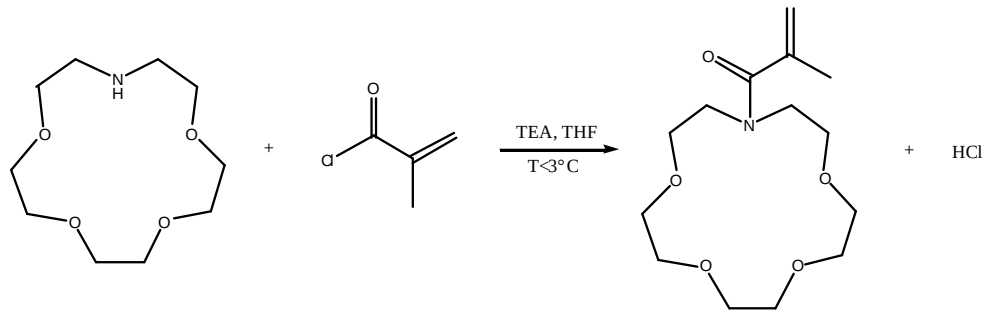

Figure 60: Synthesis of 1-aza-15-crown-5 methacrylate monomer.

Three different monomers with different Aza-crown ether ring size (12, 15 and 18) were prepared. The synthesis of 1-aza-15-crown-5 methacrylate monomer is reported as example (Figure 60); however, the synthesis of the other two monomers follows the same procedure.

1-aza-15-crown-5 (0.5 g, 2.28 mmol, 1.0 eq) was dissolved in anhydrous THF (15 ml) in a 50 ml round bottom flask. Triethylamine (0.477 ml, 3.42 mmol, 1.5 eq) was added to the mixture at room temperature. The temperature was decrease to 2-3 °C using an ice/water bath. Methacryloyl chloride (0.331 ml, 3.42 mmol, 1.5 eq) was dissolved in THF (5ml) and added dropwise to the mixture at 3 °C over a period of 45 minutes. The suspension obtained was stirred at 3 °C for further 3 hours and then the temperature was

slowly left to increase to room temperature. The reaction mixture was stirred overnight at room temperature.

The suspension was filtered and the solid discarded. The supernatant was rotaevaporated and the yellowish oil obtained was re-dissolved in 10 % aqueous K_2CO_3 (10 ml). This mixture was then extracted with DCM (3 x 5 ml). The organic fractions were combined and dried through $MgSO_4$. The solvent was removed by rota-evaporator and the product was dried in the vacuum oven at 50 °C overnight.

The procedure yielded 0.51 gr of yellowish oil (78 % Yield).

1-aza-15-crown-5 methacrylate monomer analysis:

^{1}H-NMR ($CDCl_3$): δ 1.9 (s, methyl group on the double bond), 3.4-3.7 (m, 20H, -O-CH_2-CH_2-O Aza-crown ether ring), 4.9 (s, 1H, proton on the double bond), 5.1 (s, proton on the double bond).

Mass Spectra (ES+): m/z 310 (100 %), 288 (30 %).

1-aza-18-crown-6 methacrylate monomer analysis:

^{1}H-NMR ($CDCl_3$): δ 1.9 (s, methyl group on the double bond), 3.4-3.7 (m, 24H, -O-CH_2-CH_2-O Aza-crown ether ring), 4.9 (s, 1H, proton on the double bond), 5.1 (s, proton on the double bond).

Mass Spectra (ES+): m/z 331 (100 %), 332 (10 %).

1-aza-12-crown-4 methacrylate monomer analysis:

^{1}H-NMR ($CDCl_3$): δ 1.9 (s, methyl group on the double bond), 3.4-3.7 (m, 16H, -O-CH_2-CH_2-O Aza-crown ether ring), 4.9 (s, 1H, proton on the double bond), 5.1 (s, proton on the double bond).

Mass Spectra (ES+): m/z 266 (100 %), 244 (20 %).

3.3.10. Synthesis of poly-(NIPAM-co-1-aza-15-crown-5 methacrylate) by Inverse Suspension Polymerization (PNCE).

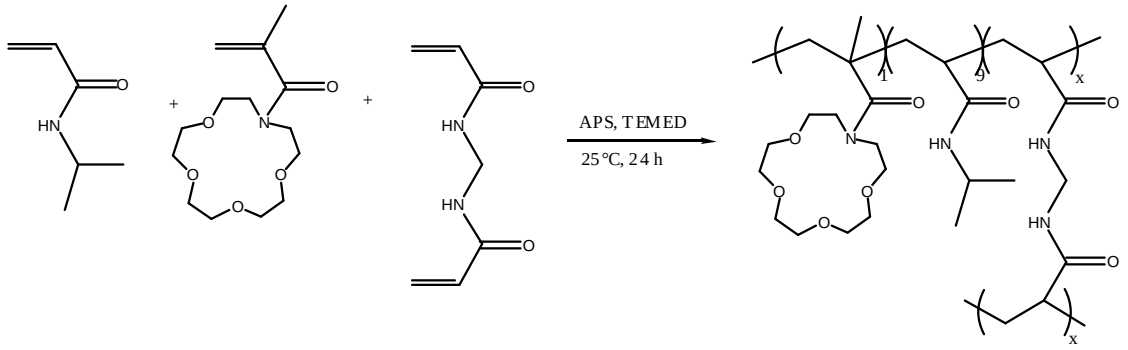

Figure 61: Reaction scheme.

Poly-(NIPAM-co-1-aza-15-crown-5 methacrylate) gel beads were prepared by Inverse Suspension Polymerization using cyclohexane as the continuous phase and SPAN 80 (Sorbitan monooleate) as oil-soluble surfactant.

NIPAM (0.9 g, 7.95 mmol, 9 eq), AAc (1.22 ml, 17.7 mmol, 2 eq), 1-aza-15-crown-5 methacrylate (254 mg, 0.88 mmol, 1 eq) and the cross linker N, N′-Methylenebis acryl amide also known as BIS (20.4 mg, 0.13 mmol, 1.5 mol % on the total monomer) were dissolved in 5 ml distilled water. This mixture was purged with nitrogen over 30 min in order to remove dissolved oxygen. The catalyst N,N,N′,N′-Tetramethylethylenediamine (TEMED, 80 µl) was added to the mixture using a syringe previously flushed with nitrogen. This solution was immediately poured into a 700 ml quick-fit round bottom flash equipped with a propeller with 5cm blades containing a solution of 4ml of SPAN 80 dissolved in 1.6l of cyclohexane previously purged with nitrogen over as period of 2 hours. The mixture was stirred at 300 rpm under nitrogen atmosphere for further 30 min to allow the surfactant to form relatively uniform aqueous emulsion droplets in the continuous phase. The initiator APS (Ammonium Persulphate, 10 mg, 0.5 mol % on the total monomer) was dissolved in 0.5 ml of degassed distilled water and added to the mixture to initiate polymerization which was allowed to proceed until completion over a period of 24 hours stirring at 300 rpm. After completion, the beads were separated from

the oil phase and washed several times with distilled water and acetone and dried in the vacuum oven at 50 °C overnight.

^{13}C-NMR (Solid State): δ 20-26 (methyl groups NIPAM and contribution the CH carbons in the backbone), 30-50 (contribution of the CH and CH_2 in the backbone and CH-N in the NIPAM), 65-75 (CH_2O carbons of the Aza-crown ether), 170-180 (carbonyl groups of NIPAM and AAc).

3.3.11. Copolymerization of NIPAM and 1-aza-15-crown-5 methacrylate monomer by Free Radical Polymerization (PNCEP).

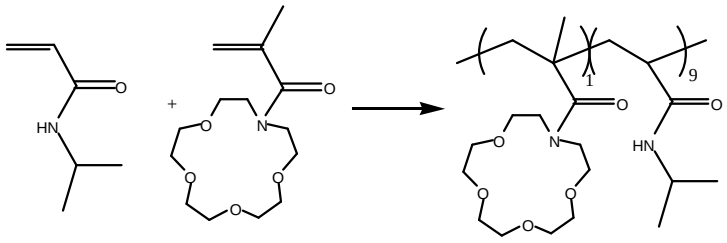

Figure 62: Reaction scheme.

NIPAM (257 mg, 2.269 mmol, 8 eq), 1-aza-15-crown-5 methacrylate monomer (163 mg, 0.567 mmol, 2 eq) and the initiator Vazo 67 (5.5 mg, 0.028 mmol, 1% m/m) were dissolved in anhydrous THF (2 ml). The mixture was degassed with nitrogen over 30 minutes and allowed to reflux over a period of 24 hours.

The reaction mixture was poured into an excess of diethyl ether to precipitate the crude product. The poly-(NIPAM-co-1-aza-15-crown-5 methacrylate) was collected by filtration and was purified by repeated precipitation in diethyl ether from acetone.

The purified product was dried out in the vacuum oven at 50 °C overnight.

GPC analyses: Mn = 3177, Mw = 5284, I = 1.663.

^{1}H-NMR ($CDCl_3$): δ 0.8-1.2 (m, 6H, 2 -CH_3 on NIPAM), 1.4-2.2 (m, -CH_2- on the backbone), 3.2-3.9 (m, 1H for the CH_3-CH-CH_3 on NIPAM and - CH_2- on the Aza-crown ether ring).

The amount of 1-aza-15-crown-5 methacrylate incorporated in the copolymer measured by ^{1}H-NMR was 18 mol %.

3.3.12. Synthesis of a macromonomer incorporating NIPAM and Aza-crown ether methacrylate monomers (poly-(NIPAM-co-1aza-15-crown-5 methacrylate) macromonomer) by Radical Telomerization (PNCEM1, 2 and 3).

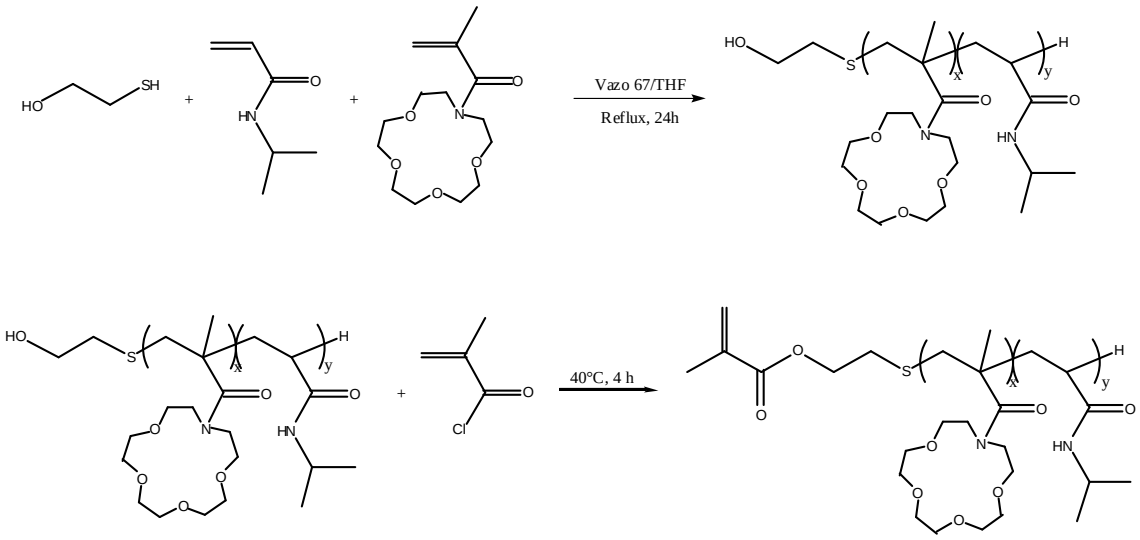

Figure 63: Reaction scheme for 1-aza-14-crown-5.

Three different macromonomers were prepared carrying different Aza-crown ethers with different ring sizes (12, 15 and 18) following the same procedure. The synthesis poly-(NIPAM-co-1aza-15-crown-5 methacrylate) macromonomer is reported as example.

A poly-(NIPAM-co-1-aza-15-crown-5 methacrylate) with a terminal hydroxyl group (poly-(NIPAM-co-1aza-15-crown-5 methacrylate)-OH) was prepared by radical telomerisation of NIPAM and 1aza-15-crown-5 methacrylate monomer using HESH (2-Hydroxyethanethiol) as a chain transfer agent. NIPAM (500 mg, 4.419 mmol, 8 eq), 1-aza-15-crown-5 methacrylate monomer (317 mg, 1.105 mmol, 2 eq), HESH (7.7 µl, 0.111 mmol, 2 mol % on the total monomer) * and Vazo 67 (5.3 mg, 0.0276 mmol, 0.5 mol % on the total monomer) were dissolved in anhydrous THF (3 ml). The yellow solution containing the monomers was degassed with nitrogen over 30 minutes. The polymerization was carried out under reflux for 24 hours. The reaction mixture was

poured into an excess of diethyl ether to precipitate poly-(NIPAM-co-1aza-15-crown-5 methacrylate)-OH. Poly-(NIPAM-co-1aza-15-crown-5 methacrylate)-OH was collected by filtration and was purified by repeated precipitation in diethyl ether from acetone. The sample was dried in the vacuum oven at 50 °C overnight. The reaction yielded 0.73 gr of poly-(NIPAM-co-1aza-15-crown-5 methacrylate)-OH.

^{1}H-NMR ($CDCl_3$): δ 0.8-1.2 (m, 6H, 2 -CH_3 on NIPAM), 1.4-2.2 (m, -CH_2- on the backbone), 3.2-3.9 (m, 1H for the CH_3-CH-CH_3 on NIPAM and - CH_2- on the Aza-crown ether ring).

The amount of 1-aza-15-crown-5 methacrylate incorporated in the copolymer measured by ^{1}H-NMR was 12 mol %. **

Poly-(NIPAM-co-1aza-15-crown-5 methacrylate)-OH (500 mg) was dissolved in chloroform (3ml) and a large excess of methacryloyl chloride (110 µl, 1.105 mmol) was added. The mixture was stirred at 40 °C for 4 hours under nitrogen atmosphere. The reactant was poured into an excess of diethyl ether to precipitate poly-(NIPAM-co-1aza-15-crown-5 methacrylate) macromonomer. Poly-(NIPAM-co-1aza-15-crown-5 methacrylate) macromonomer was collected by filtration and was purified by repeated precipitation in diethyl ether from acetone. The sample was dried in the vacuum oven at 50 °C overnight. The reaction yielded ~ 0.5 gr of poly-(NIPAM-co-1aza-15-crown-5 methacrylate) macromonomer.

^{1}H-NMR ($CDCl_3$) – PNCEM2: δ 0.8-1.2 (m, 6H, 2 -CH_3 on NIPAM), 1.4-2.2 (m, -CH_2- on the backbone), 3.2-3.9 (m, 1H for the CH_3-CH-CH_3 on NIPAM and - CH_2- on the Aza-crown ether ring), 5.6 (s, 1H on the double bond), 6.0 (s, 1H on the double bond).

GPC analysis of PNCEM2 - Poly-(NIPAM-co-1-aza-15-crown-5 methacrylate) macromonomer: Mn = 1769, Mw = 2878, I = 1.664.

GPC analysis of PNCEM3 - Poly-(NIPAM-co-1-aza-18-crown-6 methacrylate) macromonomer: Mn = 1762, Mw = 2574, I = 1.461.

GPC analysis of PNCEM1 - Poly-(NIPAM-co-1-aza-12-crown-4 methacrylate) macromonomer: Mn = 2242, Mw = 3473, I = 1.549.

* 1 mol % of HESH was also tested.

^{1}H-NMR ($CDCl_3$): δ 0.8-1.2 (m, 6H, 2 -CH_3 on NIPAM), 1.4-2.2 (m, -CH_2- on the backbone), 3.2-3.9 (m, 1H for the CH_3-CH-CH_3 on NIPAM and - CH_2- on the Aza-crown ether ring).

This material was then also reacted with methacryloyl chloride and the ^{1}H-NMR spectra obtained for the product was:

^{1}H-NMR ($CDCl_3$): δ 0.8-1.2 (m, 6H, 2 -CH_3 on NIPAM), 1.4-2.2 (m, -CH_2- on the backbone), 3.2-3.9 (m, 1H for the CH_3-CH-CH_3 on NIPAM and - CH_2- on the Aza-crown ether ring), 5.6-6.0 (small bounce of the 2H of the methacrylate double bond).

** In order to increase the percentage of crown ether copolymerized, a second experiment was carried out using the same procedure but changing the NIPAM : crown ether ratio from 4 : 1 of the previous experiments to 3 : 2 (discussion of the experiment in section 5.3).

3.3.13. Preparation of Graft-type poly-(NIPAM-co-AAc-co-Aza-crown methacrylate) by Inverse Suspension Polymerization (PGNACE).

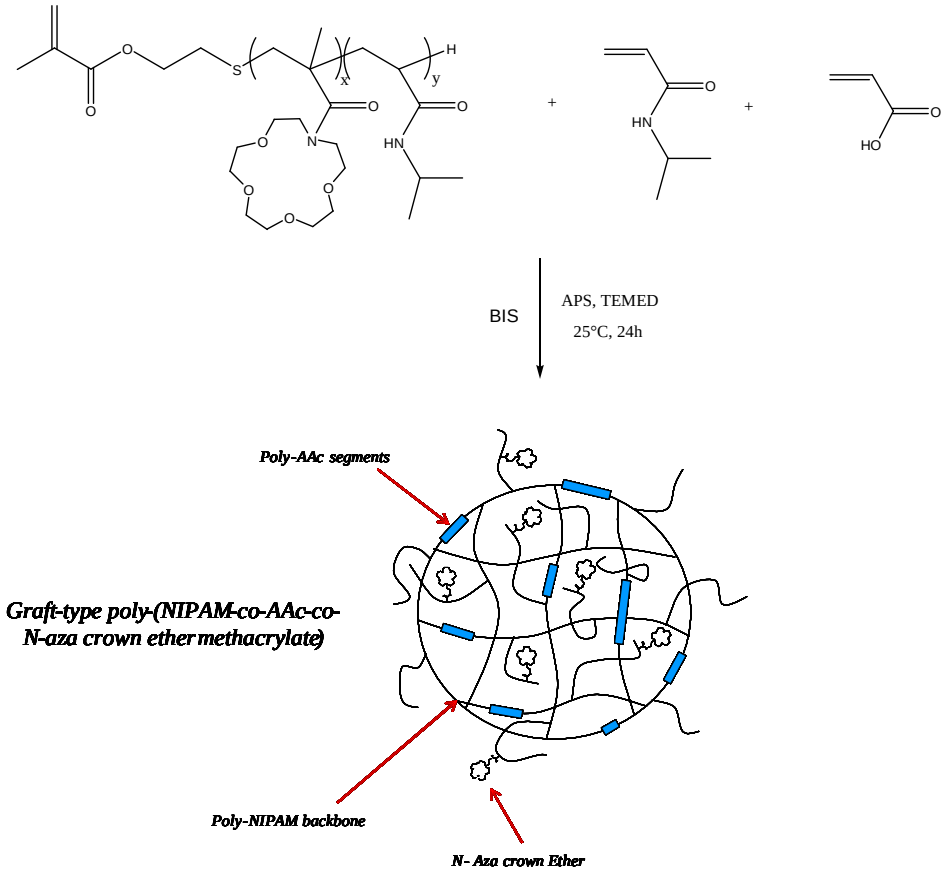

Graft-type poly-(NIPAM-co-AAc-co-Aza-crown methacrylate) gel beads were prepared by Inverse Suspension Polymerization using cyclohexane as the continuous phase and SPAN 80 (Sorbitan monooleate) as oil-soluble surfactant. The following method produces beaded microgels using a 700 ml round bottom quick-fit flask equipped with a steel propeller of 5 cm blade and 350 rpm stirring speed.

Different surfactants were tried but SPAN 80 proved to have the suitable HLB value (hydrophile-lipophile balance, 4.3) to control the stability of the dispersion.

NIPAM (657 mg, 5.817 mmol), AAc (53 µl, 0.77 mmol), poly-(NIPAM-co-1aza-15-crown-5 methacrylate) macromonomer (170 mg, ~ 0.1 mmol) and the cross linker N, N′-Methylenebis acryl amide also known as BIS (15.5 mg, 0. 1mmole, 1.5 mol % on the

total monomer) were dissolved in 5ml distilled water. This mixture was bubbled with nitrogen over 30 min in order to remove dissolved oxygen. The catalyst N,N,N′,N′-Tetramethylethylenediamine (TEMED, 80 µl) was added to the mixture using a syringe previously flushed with nitrogen. This solution was immediately poured into a 700ml quick-fit round bottom flash equipped with a propeller with 5cm blades containing a solution of 2ml of SPAN 80 dissolved in 200 ml of cyclohexane previously bubbled with nitrogen over as period of 2 hours. The mixture was stirred at 300 rpm under nitrogen atmosphere for further 30 min to allow the surfactant to form relatively uniform aqueous emulsion droplets in the continuous phase. The initiator APS (Ammonium Persulphate, 15.2 mg, 1 mol % on the total monomer) was dissolved in 0.5 ml of degassed distilled water and added to the mixture to initiate the polymerization which was allowed to proceed until completion over a period of 24 hours. After completion, the beads were separated from the oil phase and washed several times with distilled water and acetone and dried in the vacuum oven at 50 °C overnight.*

Elemental analysis was carried out and it is reported in Table 20.

Table 20: Elemental analyses.

Expected (%)			*Found (%)*		
C	H	N	C	H	N
62.55	9.3	11.2	60.76	9.95	11.61

^{13}C-NMR (Solid State): δ 20-26 (methyl groups NIPAM and contribution the CH carbons in the backbone), 30-50 (contribution of the CH and CH_2 in the backbone and CH-N in the NIPAM), 65-75 (a bump is located in the baseline at this shift, CH_2O carbons of the Aza-crown ether), 170-180 (carbonyl groups of NIPAM and AAc).

* The same procedure was also successful using different amounts of reagents, PGNACEX, (NIPAM: 1 g, 8.838 mmol; AAc: 106 µl, 1.54 mmol; Macromonomer; 680 mg, ~0.4 mmol; BIS: 31.0 mg, 0.2 mmol, 1.9 mol % on the total monomer moles; H_2O:

10 ml; TEMED: 160 µl; Cyclohexane: 400 ml; SPAN 80: 2 ml; APS: 24 mg, 1 mol % on the total monomer moles). The quantity of macromonomer was increased in order to incorporate a larger amount of crown ether into the resulting microgel.

^{13}C-NMR (Solid State): δ 20-26 (methyl groups NIPAM and contribution the CH carbons in the backbone), 30-50 (contribution of the CH and CH_2 in the backbone and CH-N in the NIPAM), 65-75 (a bump is located in the baseline at this shift, CH_2O carbons of the Aza-crown ether), 170-180 (carbonyl groups of NIPAM and AAc).

3.4. Synthesis of Thermo-responsive hydrogel beads based on non-linear poly-ethylene glycols monomers and incorporating *N*-Aza-crown ethers.

The methods of synthesis discussed in chapter 6 are provided in this section.

3.4.1. Synthesis of poly-(MeO_2MA) gel beads, PEGN, by Suspension Polymerization (DD151, 52, 166, 170).

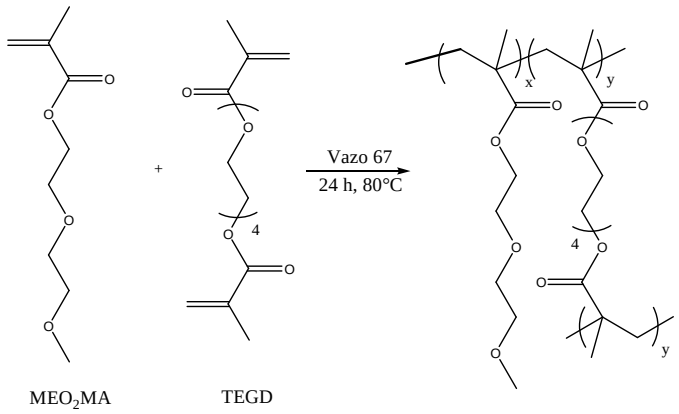

Figure 64: Reaction scheme.

Suspension polymerization is a procedure which depends upon different variables. Many experiments were carried out testing different stirring speed, ratio between continuous phase and aqueous monomer solution and type of surfactant in order to find the suitable conditions for our process. The experiments carried out are listed in Table 21.

Table 21: Experiments carried out for the synthesis of poly-(MEO_2MA) gel beads. Sodium Dodecyl Benzene sulfonate (SDS), Na2SO4 saturated aqueous solution (sat. Na2SO4), Poly acrylic Acid (PAA).

Exp.	MeO_2MA	TEGD	Vazo 67	$CHCl_3$	Cont. Phase	Surfactant	Hydrogel Stirrer Speed
DD151	(1.845ml, 10mmole)	(41μl, 0.15mmole)	(9.6mg, 0.05mmole)	2ml	H_2O (200ml)	SDS (0.5g)	Amorphous 300 rpm
DD152	(1.845ml, 10mmole)	(41μl, 0.15mmole)	(9.6mg, 0.05mmole)	2ml	Sat. Na_2SO_4 (200ml)	SDS (0.5g)	Beads + amorphous 350 rpm
DD166	(5.535ml, 20mmole)	(123μl, 0.45mmole)	(28.8mg, 0.15mmole)	6ml	H_2O (180ml)	PAA (0.4g)	Amorphous 300 rpm
DD170	(10ml, 54.19mmole)	(221μl, 0.81mmole)	(52.1mg, 0.27mmole)	5ml	H_2O (200ml)	SDS (0.5g)	Beads 350 rpm

The following procedure produces beaded microgels using a 700 ml round bottom quick-fit flask equipped with a steel propeller of 5 cm blade and 350 rpm stirring speed.

Poly-(MEO_2MA) gel beads were prepared by Suspension Polymerization technique using H_2O as the continuous phase and SDS (Sodium Dodecyl Benzene sulfonate) as water-soluble surfactant. MEO_2MA (10 ml, 54.19 mmol), the cross linker tetra-(ethylene glycol) diacrylate also known as TEGD (221 μl, 0.81 mmol) and the initiator Vazo 67 (52.1 mg, 0.27 mmol) were dissolved in 5 ml $CHCl_3$. This mixture was purged with nitrogen over 30 min in order to remove dissolved oxygen.

The degassed mixture was then carefully transferred using a syringe previously flushed with nitrogen into a 700 ml quick-fit round bottom flask containing a solution of 0.5 gr of SDS dissolved in 200 ml of H_2O previously purged with nitrogen over a period of 2 hours. The resulting dispersion was stirred at 350 rpm under nitrogen atmosphere for further 30 min to allow the surfactant to form relatively uniform aqueous emulsion droplets in the continuous phase. The temperature was increased to 90 °C in order to initiate polymerization which was allowed to proceed until reaction completion over a period of 24 hours. After reaction completion, the beads were separated from the aqueous phase

and washed several times with distilled water and acetone and dried in the vacuum oven at 50°C overnight.

Elemental analyses (DD170): C (57.0 %), H (8.59 %).

IR Spectra (DD170): 2900 cm^{-1} (CH stretching), 1720 cm^{-1} (CO stretching).

^{13}C-NMR (Solid State – DD170): δ 18 (methyl groups), 45.4 (CH and CH_2 in the polymer backbone), 59.1 (O−CH_3), 60-80 (CH_2−O), 178 (−O−C═O).

3.4.2. Synthesis of poly-(MeO_2MA-co-$OEGMA_{475}$) gel beads by Suspension Polymerization (PEG).

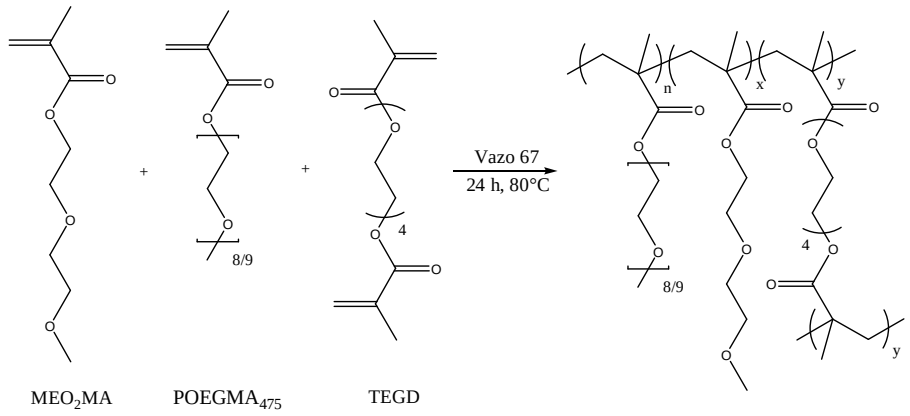

Figure 65: Reaction scheme.

Poly-(MeO_2MA-co-$OEGMA_{475}$) was synthesised by suspension polymerization technique using H_2O as the continuous phase and SDS (Sodium Dodecyl Benzene sulfonate) as water-soluble surfactant. MEO_2MA (8.5 ml, 46.06 mmol), $OEGMA_{475}$ (3.58 ml, 8.13 mmol), the cross linker tetra-(ethylene glycol) diacrylate also known as TEGD (221 µl, 0.81 mmol) and the initiator Vazo 67 (52.1 mg, 0.27 mmol) were dissolved in 5 ml $CHCl_3$. This mixture was purged with nitrogen over 30 min in order to remove dissolved oxygen.

The degassed mixture was then carefully transferred using a syringe previously flushed with nitrogen into a 700 ml quickfit round bottom flask equipped with a steel propeller of 5 cm and containing a solution of 0.5 gr of SDS dissolved in 200 ml of H_2O previously

purged with nitrogen over a period of 2 hours. The resulting dispersion was stirred at 350 rpm under nitrogen atmosphere for further 30 min to allow the surfactant to form relatively uniform aqueous emulsion droplets in the continuous phase. The temperature was increased to 90 °C in order to initiate polymerization which was allowed to proceed until reaction completion over a period of 24 hours. After reaction completion, the beads were separated from the aqueous phase and washed several times with distilled water and acetone and dried in the vacuum oven at 50 °C overnight.

Elemental analyses: C (56.68 %), H (8.75 %).

IR Spectra: 2900 cm^{-1} (CH stretching), 1720 cm^{-1} (CO stretching).

^{13}C-NMR (Solid State): δ 18 (methyl groups), 45.4 (CH and CH_2 in the polymer backbone), 59.1 ($O-CH_3$), 60-80 (CH_2-O), 178 ($-O-C=O$).

3.4.3. Synthesis of poly-(MeO_2MA-co-$OEGMA_{475}$-co-1-Aza-crown ether methacrylate) gel beads, PEGCE, by Suspension Polymerization (DD185, DD201).

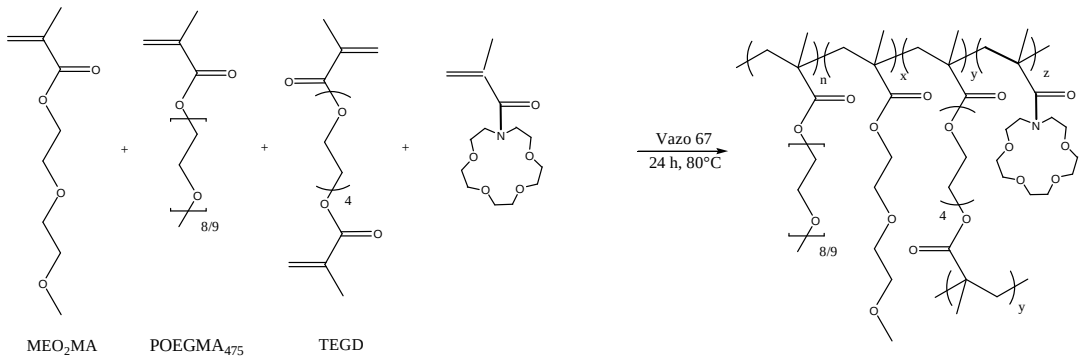

Figure 66: Reaction scheme.

The synthesis of hydrogel in form of beads based on MeO_2MA and $OEGMA_{475}$ with Aza-crown ether methacrylate was attempted by suspension polymerization technique. Two different experiments were attempted and they are listed in Table 22.

Table 22: Experiments carried out for the synthesis of gel beads based on MeO_2MA and $OEGMA_{475}$ with Aza-crown ether methacrylate.

Experiment	Monomer Phase	Continuous Phase
DD185	MEO_2MA (9.0ml, 48.77mmole) OEGMA (2.38ml, 5.419mmol) 1-Aza-18-crown-6 met. (1.46gr, 4.41mmole) TEGD (239µl, 0.88mmol) Vazo 67 (56mg, 0.29mmol) $CHCl_3$ (5ml)	H_2O (200ml) + SDS (0.5gr)
DD201	MEO_2MA (10.0ml, 54.19mmole) 1-Aza-15-crown-5 met. (1.73gr, 6.02mmole) TEGD (246µl, 0.90mmol) Vazo 67 (58mg, 0.30mmol) $CHCl_3$ (5ml)	10% aq. NaCl (200ml) + PVA (Mw=67000, 0.02gr) + HEC (Mw~90000, 1gr)

The monomers, the cross linker (tetra-(ethylene glycol) diacrylate) and the initiator Vazo 67 were dissolved in 5 ml $CHCl_3$. This mixture was purged with nitrogen over 30 min in order to remove dissolved oxygen.

The degassed mixture was then carefully transferred using a syringe previously flushed with nitrogen into a 700 ml quickfit round bottom flask equipped with a steel propeller of 5 cm and containing the continuous phase previously purged with nitrogen over a period of 2 hours. The resulting dispersion was stirred at 350 rpm under nitrogen atmosphere for further 30 min to allow the surfactant to form relatively uniform aqueous emulsion droplets in the continuous phase. The temperature was increased to 90 °C in order to initiate polymerization which was allowed to proceed until reaction completion over a period of 24 hours. After reaction completion, the beads were separated from the aqueous phase and washed several times with distilled water and acetone and dried in the vacuum oven at 50 °C overnight.

Elemental analyses DD185: C (56.82 %), H (8.78 %), N (none found).

Elemental analyses DD201: C (56.08 %), H (8.43 %), N (none found).

^{13}C-NMR (Solid State) for DD185 and DD201: δ 18 (methyl groups), 45.4 (CH and CH_2 in the polymer backbone), 59.1 ($O-CH_3$), 60-80 (CH_2-O), 178 ($-O-C=O$).

3.4.4. Synthesis of poly-(MeO_2MA-co-HEMA) gel beads, PEGNH, by Suspension Polymerization (DD191-93, 97 and 199).

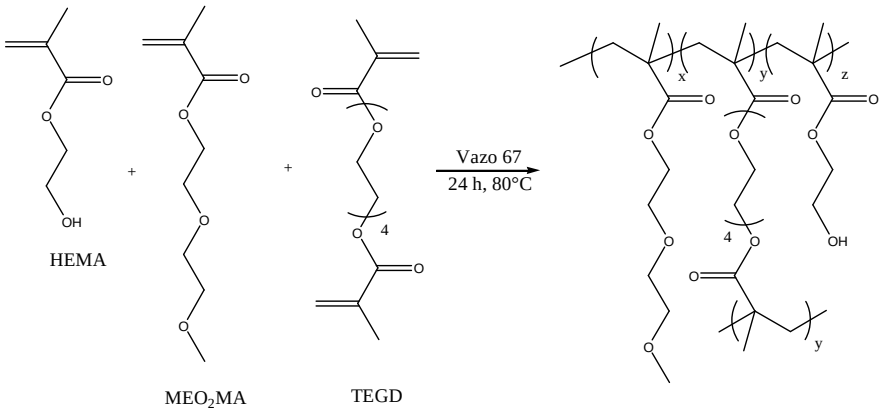

Figure 67: Reaction scheme.

Three experiments were carried out testing different stirring speeds and types of surfactant in order to find the suitable conditions for this synthesis. The experiments carried out are listed in Table 23.

Table 23: Experiments carried out for the synthesis of poly-(MEO_2MA-co-HEMA) gel beads.

Experiment	Monomer Phase	Continuous Phase	Product/Stirring Speed
*DD191	MEO_2MA (15.9ml, 86.17mmole) HEMA (2.6ml, 21.40mmol) TEGD (1.5ml, 5.51mmol) Vazo 67 (103mg, 0.54mmol)	MgO (3gr) + H_2O (200ml)	Beads + amorphous 350 rpm
**DD192	MEO_2MA (15.9ml, 86.17mmole) HEMA (2.6ml, 21.40mmol) TEGD (1.5ml, 5.51mmol) Vazo 67 (103mg, 0.54mmol)	20% aq. NaCl (180ml) + $MgCl_2 \cdot 6H_2O$ (11.5gr)	Beads + amorphous 350 rpm
DD193	MEO_2MA (15.9ml, 86.17mmole) HEMA (2.6ml, 21.40mmol) TEGD (1.5ml, 5.51mmol) Vazo 67 (103mg, 0.54mmol) Hexanol (30ml)	SDS (1.6gr) + H_2O (200ml)	Non spherical material 400 rpm
DD197	MEO_2MA (15.9ml, 86.17mmole) HEMA (2.6ml, 21.40mmol) TEGD (1.5ml, 5.51mmol) Vazo 67 (103mg, 0.54mmol)	SDS (1.0gr) + H_2O (200ml)	Amorphous 350 rpm
DD199	MEO_2MA (15.9ml, 86.17mmole) HEMA (2.6ml, 21.40mmol) TEGD (1.5ml, 5.51mmol) Vazo 67 (103mg, 0.54mmol)	20% aq. NaCl (180ml) + PVA (Mw~67000, 0.02gr) + HEC (Mw~90000, 1gr)	Beads 350 rpm

*The hydrogel product was washed with 0.1 M HCl in order to remove MgO

**1 N NaOH (61.5 ml) was added to the suspension before initiating the polymerization

Poly-(MEO_2MA-co-HEMA) synthesis was attempted by Suspension Polymerization technique. A mixture of MEO_2MA, HEMA, the cross linker tetra-(ethylene glycol) diacrylate (TEGD) and the initiator Vazo 67 was purged with nitrogen over 30 min in order to remove dissolved oxygen. DD194 experiment also contained Hexanol in order to increase the solubility of HEMA in the organic layer.

The degassed mixture was then carefully transferred using a syringe previously flushed with nitrogen into a 700 ml quickfit round bottom flask equipped with a steel propeller of 5 cm blade and containing the continuous phase previously purged with nitrogen over a period of 2 hours. The resulting dispersion was stirred under nitrogen atmosphere for further 30 min to allow the surfactant to form relatively uniform aqueous emulsion droplets in the continuous phase. The temperature was increased to 90 °C in order to initiate polymerization which was allowed to proceed until reaction completion over a period of 24 hours. The beads were separated from the aqueous phase and washed several times with distilled water and acetone and dried in the vacuum oven at 50 °C overnight.

Elemental Analysis (DD191): C (56.36 %), H (8.47 %).

IR Spectra (DD191): 3400-3600 cm^{-1} (-OH stretching), 2900 cm^{-1} (CH stretching), 1720 cm^{-1} (CO stretching).

^{13}C-NMR (Solid State – DD191): δ 18 (methyl groups), 45.4 (CH and CH_2 in the polymer backbone), 55.4 (CH_2−OH), 59.1 (O−CH_3), 60-80 (CH_2−O), 178 (−O−C═O).

3.4.5. Functionalization of poly-(MeO_2MA-co-HEMA) gel beads by chloroacetyl 1-Aza-12-crown-4 (PEGNHfCE).

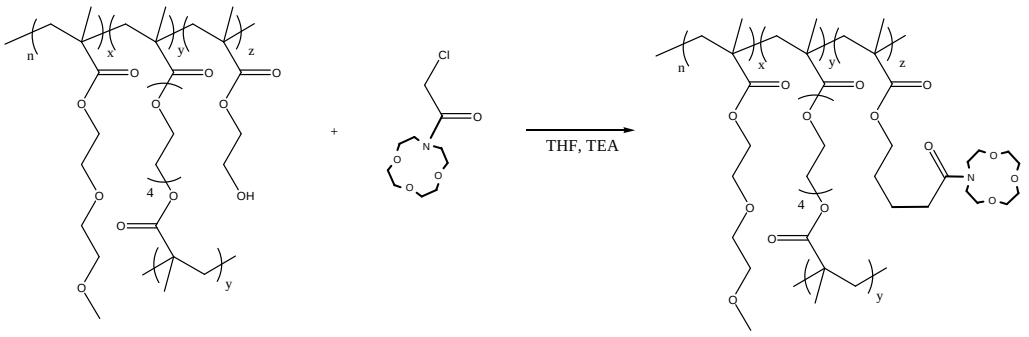

Figure 68: Reaction scheme.

A mixture containing chloroacetyl 1-Aza-12-crown-4 (216 mg, 0.86 mmol), poly-(MEO_2MA-co-HEMA) hydrogel beads (500 mg, HEMA content ~ 0.56 mmol), TEA (120 µl, 0.86 mmol) and anhydrous THF (12.5 ml) was refluxed for 48 hours under nitrogen atmosphere into a 100 ml round bottom. The mixture was then cooled to room

temperature, filtered and washed several time with deionized water and acetone. The hydrogel was dried in a vacuum oven at 50°C overnight.

Elemental Analysis: C (56.36 %), H (8.43 %), N (trace), Cl (< 0.3 %).

3.4.6. Functionalization of poly-(MeO_2MA-co-HEMA) gel beads by chloroacetyl chloride (PEGNHf).

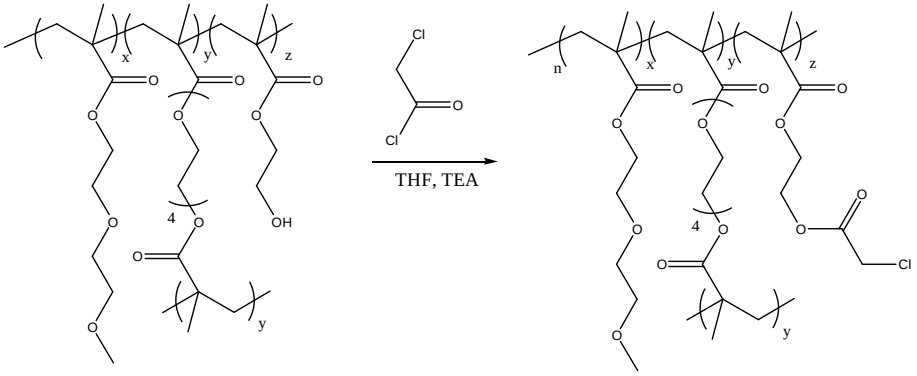

Figure 69: Reaction scheme.

Poly-(MeO_2MA-co-HEMA) hydrogel beads (500 mg, HEMA content ~ 0.56 mmol) were added to a mixture of anhydrous THF (3.5 ml) and triethylamine (234 µl, 1.68 mmol) in a round bottom flask purged in nitrogen. Chloroacetyl chloride (134 µl, 1.68 mmol) was added dropwise to the suspension which was stirred 24 hours at room temperature. The beads were then filtered and washed several times with deionized water and acetone. The product was dried in a vacuum oven at 50 °C overnight.

Elemental analysis: C (55.15%), H (8.13 %), N (none found) and Cl (2.21 %).

^{13}C-NMR (Solid State): δ 18 (methyl groups), 45.4 (CH and CH_2 in the polymer backbone), 55.4 (CH_2−OH), 59.1 (O−CH_3), 60-80 (CH_2−O), 178 (−O−C═O).

IR Spectra: bounce at 3400-3600 cm^{-1} (−OH stretching), 2900 cm^{-1} (CH stretching), 1720 cm^{-1} (O═C−O stretching), 1750 (O═C−CH_2Cl stretching).

3.4.7. Functionalization of chloro acetylated poly-(MeO_2MA-co-HEMA) gel beads by 1-Aza-15-crown-5 (PEGNHf2).

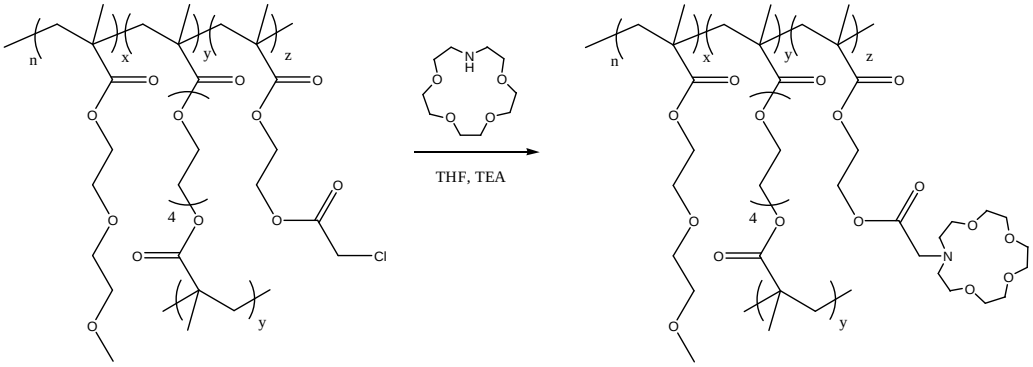

Figure 70: Reaction scheme.

Chloro acetyl functionalized poly-(MeO_2MA-co-HEMA) hydrogel beads (300 mg) were added to a mixture of anhydrous THF (3 ml), triethylamine (70 µl, 0.50 mmol) and 1-Aza-15-crown-5 (111 mg, 0.50 mmol) in a round bottom flask purged in nitrogen. The reaction mixture was allowed to reflux and stirred for 24 hours. The suspension was cooled, filtered and the beads were washed several times with deionized water and acetone. The product was dried in a vacuum oven at 50 °C overnight.

Elemental analysis: C (55.71 %), H (8.33 %), N (0.68 %) and Cl (none found).

IR Spectra: bounce at 3400-3600 cm^{-1} (−OH stretching), 2900 cm^{-1} (CH stretching), 1720 cm^{-1} (O═C−O stretching).

3.4.8. Synthesis of poly-(MeO_2MA-co-AAc) gel beads (PEGA).

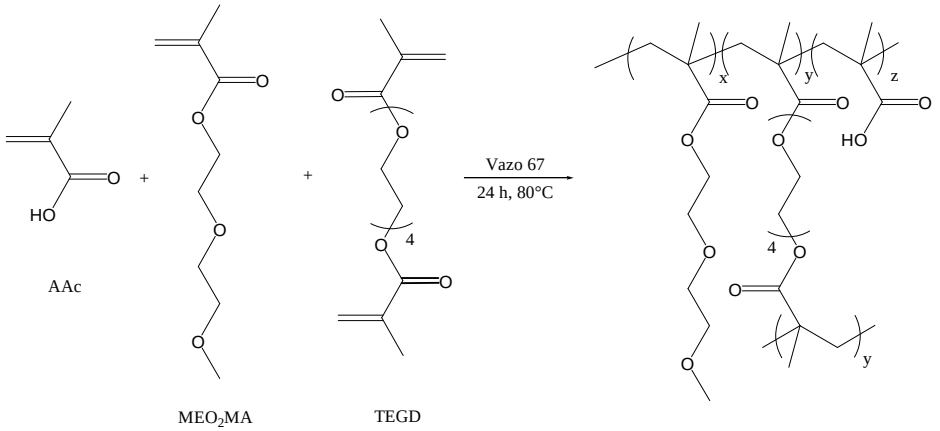

Figure 71: Reaction scheme.

The synthesis of hydrogel in form of beads based on MeO_2MA and AAc was attempted by suspension polymerization technique using 10 % NaCl aqueous solution as continuous phase and PVA and HEC as surfactant and stabilizer.

MEO_2MA (10.0 ml, 54.19 mmol), AAc (0.93 ml, 13.55 mmol), the cross linker tetra-(ethylene glycol) diacrylate also known as TEGD (277 µl, 1.02 mmol) and the initiator Vazo 67 (65 mg, 0.34 mmol) were dissolved in $CHCl_3$ (5 ml). This mixture was purged with nitrogen over 30 min in order to remove dissolved oxygen.

The degassed mixture was then carefully transferred using a syringe previously flushed with nitrogen into a 700 ml quickfit round bottom flask equipped with a steel propeller of 5 cm and containing a solution of 10% NaCl (200ml) containing PVA (Mw ~ 67000, 0.02 gr) and HEC (Mw ~ 90000, 1 gr) previously purged with nitrogen over a period of 2 hours. The resulting dispersion was stirred at 350 rpm under nitrogen atmosphere for further 30 min to allow the surfactant and the stabilizer to form relatively uniform aqueous emulsion droplets in the continuous phase. The temperature was increased to 90 °C in order to initiate polymerization which was allowed to proceed until reaction completion over a period of 24 hours. After reaction completion, the beads were separated from the aqueous phase and washed several times with distilled water and acetone and dried in the vacuum oven at 50 °C overnight.

IR Spectra: 2900 cm^{-1} (CH stretching), 1720 cm^{-1} (CO stretching).

3.4.9. Synthesis of poly-(MeO_2MA-co-$OEGMA_{475}$-co-HEMA) gel beads (PEGMA).

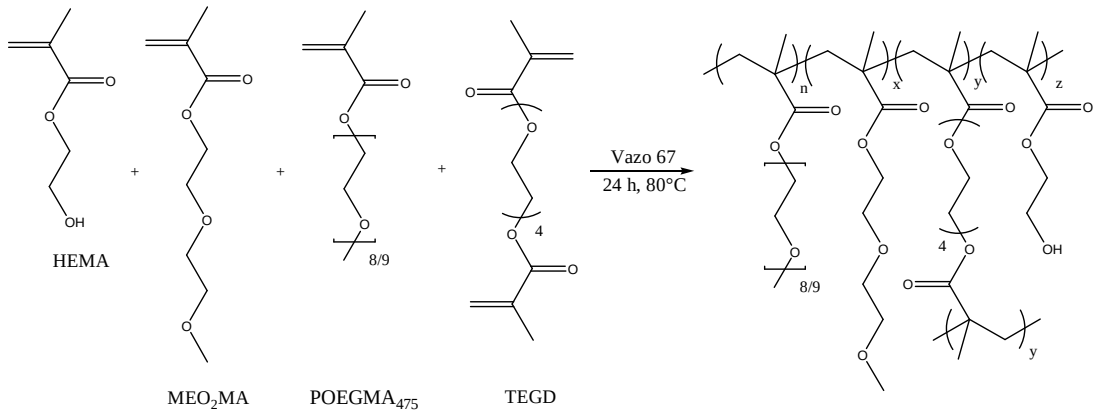

Figure 72: Reaction scheme.

Poly-(MEO_2MA-co-$POEGMA_{475}$-co-HEMA) hydrogel beads were prepared by suspension polymerization technique using deionized water as continuous phase and MgO as stabilizing and salting-out agent. A five-necked quick-fit flask (700 ml) with a propeller type stirrer (5 cm blade) was used as polymerization reactor. A mixture containing MEO_2MA (13.51 ml, 73.24 mmol), $POEGMA_{475}$ (5.68 ml, 12.93 mmol), HEMA (2.6 ml, 21.40 mmol), the cross linker TEGD (1.5 ml, 5.51 mmol, 5 mol %) and the initiator Vazo 67 (103 mg, 0.54 mmol, 0.5 mol %) was purged with nitrogen over 30 minutes. The mixture was then transferred into the polymerization reactor, containing a solution of MgO (3 gr) dissolved in deionized water (200 ml) previously purged with nitrogen for 2 hours, using a degassed syringe. The resulting dispersion was stirred at 350 rpm under nitrogen atmosphere over 45 minutes to allow the stabilizer to form relatively uniform aqueous emulsion droplets in the continuous phase. The temperature was increased to 80°C and maintained for 24 hours. After cooling the polymer beads were filtered and transferred into a beaker containing dilute HCl solution (0.1 M) in order to dissolve the residual MgO. The hydrogel beads were filtered, washed several times with deionized water and acetone and dried in a vacuum oven at 50 °C overnight.

Elemental Analysis: C (56.03 %), H (8.73 %).

IR Spectra: 3400-3600 cm^{-1} (-OH stretching), 2900 cm^{-1} (CH stretching), 1720 cm^{-1} (CO stretching).

^{13}C-NMR (Solid State): δ 18 (methyl groups), 45.4 (CH and CH_2 in the polymer backbone), 55.4 (CH_2−OH), 59.1 (O−CH_3), 60-80 (CH_2−O), 178 (−O−C═O).

3.4.10. Esterification of poly-(MeO_2MA-co-$OEGMA_{475}$-co-HEMA) gel beads (PEGMAf).

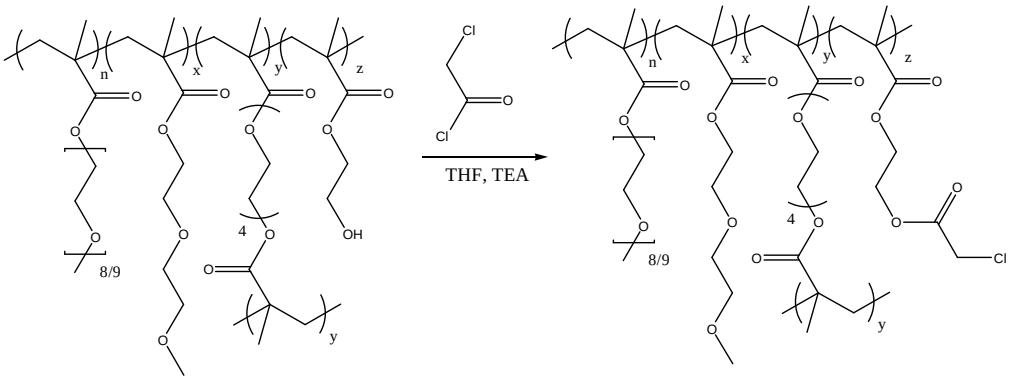

Figure 73: Reaction scheme.

Poly-(MeO_2MA-co-$OEGMA_{475}$-co-HEMA) hydrogel beads, PEGMA, (6 gr) were added to a mixture of anhydrous THF (42 ml) and triethylamine (2.73 ml, 19.62 mmol) in a round bottom flask purged in nitrogen. Chloroacetyl chloride (1.56 ml, 19.62 mmol) was added dropwise to the stirred suspension at 25 °C. The reaction was stirred for 24 hours at room temperature. The beads were then filtered and washed several times with deionized water and acetone. The product was dried in a vacuum oven at 50 °C overnight.

Elemental analysis: C (54.72%), H (8.18 %), N (none found) and Cl (3.05 %).

IR Spectra: 2900 cm^{-1} (CH stretching), 1720 cm^{-1} (O═C−O stretching), 1750 (O═C−CH_2Cl stretching).

^{13}C-NMR (Solid State): δ 18 (methyl groups), 42.43 (CO−CH_2−Cl), 45.4 (CH and CH_2 in the polymer backbone), 55.4 (CH_2−OH), 59.1 (O−CH_3), 60-80 (CH_2−O), 178 (−O−C═O).

3.4.11. Functionalization of chloro acetylated poly-(MeO_2MA-co-$OEGMA_{475}$-co-HEMA) gel beads by Aza-crown ethers (PEGMAf1, PEGMAf2 and PEGMAf3).

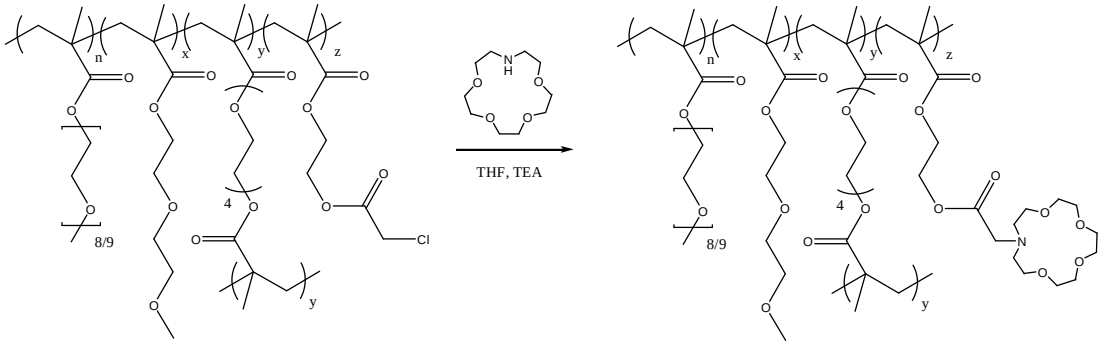

Figure 74: Reaction scheme.

The preparation of poly-(MEO_2MA-co-$POEGMA_{475}$-co-HEMA) hydrogel beads carrying 1-aza-15-crown-5 (PEGMAf2) is reported although other two compounds carrying 1-aza-12-crown-4 (PEGMAf1) and 1-aza-18-crown-6 (PEGMAf3) were synthesized following the same procedure.

Chloro acetylated poly-(MeO_2MA-co-$OEGMA_{475}$-co-HEMA) hydrogel beads (2 gr) were added to a mixture of anhydrous THF (20ml), triethylamine (456 μl, 3.27 mmol) and 1-Aza-15-crown-5 (717 mg, 3.27 mmol) in a round bottom flask purged in nitrogen. The reaction mixture was allowed to reflux and stirred for 24 hours. The suspension was cooled, filtered and the beads were washed several times with deionized water and acetone. The product was dried in a vacuum oven at 50 °C overnight.

PEGMAf2 characterization:

Elemental analysis: C (55.93 %), H (8.77 %), N (0.90 %) and Cl (none found).

IR Spectra: bounce at 3400-3600 cm^{-1} (−OH stretching), 2900 cm^{-1} (CH stretching), 1720 cm^{-1} (O═C−O stretching).

^{13}C-NMR (Solid State): δ 18 (methyl groups), 45.4 (CH and CH_2 in the polymer backbone), 55.8 (CH_2−OH), 59.1 (O−CH_3), 60-80 (CH_2−O), 178 (−O−C═O).

PEGMAf1 characterization:

Elemental analysis: C (56.13 %), H (8.56 %), N (0.97 %) and Cl (none found).

IR Spectra: bounce at 3400-3600 cm^{-1} (−OH stretching), 2900 cm^{-1} (CH stretching), 1720 cm^{-1} (O═C−O stretching).

^{13}C-NMR (Solid State): δ 18 (methyl groups), 45.4 (CH and CH_2 in the polymer backbone), 55.3 (CH_2−OH), 59.1 (O−CH_3), 60-80 (CH_2−O), 178 (−O−C═O).

PEGMAf3 characterization:

Elemental analysis: C (55.78 %), H (8.75 %), N (0.78 %) and Cl (0.45 %).

IR Spectra: bounce at 3400-3600 cm^{-1} (−OH stretching), 2900 cm^{-1} (CH stretching), 1720 cm^{-1} (O═C−O stretching).

^{13}C-NMR (Solid State): δ 18 (methyl groups), 45.4 (CH and CH_2 in the polymer backbone), 55.1 (CH_2−OH), 59.1 (O−CH_3), 60-80 (CH_2−O), 178 (−O−C═O).

3.4.12. Controlling experiment for the functionalization of chloro acetylated poly-(MeO_2MA-co-OEGMA$_{475}$-co-HEMA) gel beads by Aza-crown ethers.

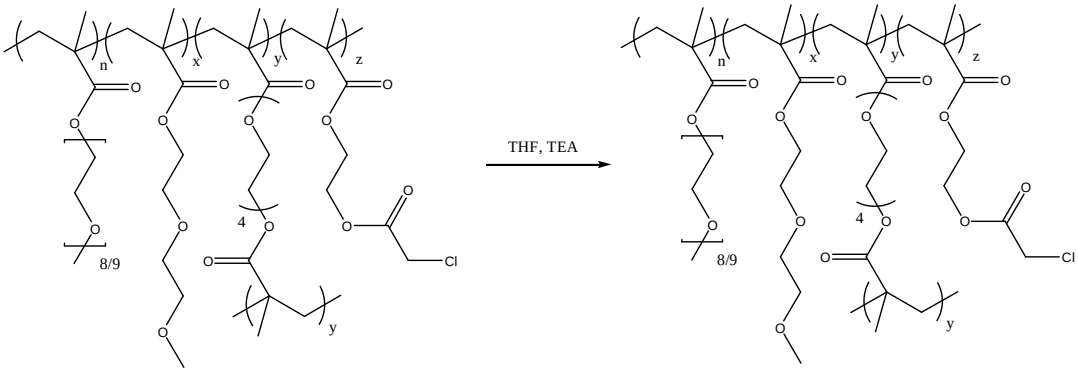

Figure 75: Reaction scheme.

Chloro acetylated poly-(MeO_2MA-co-OEGMA$_{475}$-co-HEMA) hydrogel beads (200 mg) were added to a mixture of anhydrous THF (2 ml) and triethylamine (45.6 µl, 0.33 mmol) in a round bottom flask purged in nitrogen. The reaction mixture was allowed to reflux

and stirred for 24 hours. The suspension was cooled, filtered and the beads were washed several times with deionized water and acetone. The product was dried in a vacuum oven at 50 °C overnight.

Elemental analysis: C (54.26 %), H (8.37 %), N (none found) and Cl (2.89 %).

Chapter 4

Statistical Methacrylate Copolymers incorporating *N*-Aza-crown ethers

Two approaches were considered in the early stage of the thesis and are reported here:

1. Copolymerization of an *N*-Aza-crown methacrylate with MMA.

2. Post functionalization of a MMA - HEMA copolymer with *N*-Aza-crown.

This chapter discusses their respective synthesis and where appropriate preliminary metal scavenge results.

4.1. Synthesis of Aza-crown ether polymers by polymerization of an Aza-crown ether methacrylate monomer.

4.1.1. Synthesis of O-(*N*-hydroxythyl-1-aza-15-crown-5)-methyl methacrylate (3.2.1 and 3.2.2).

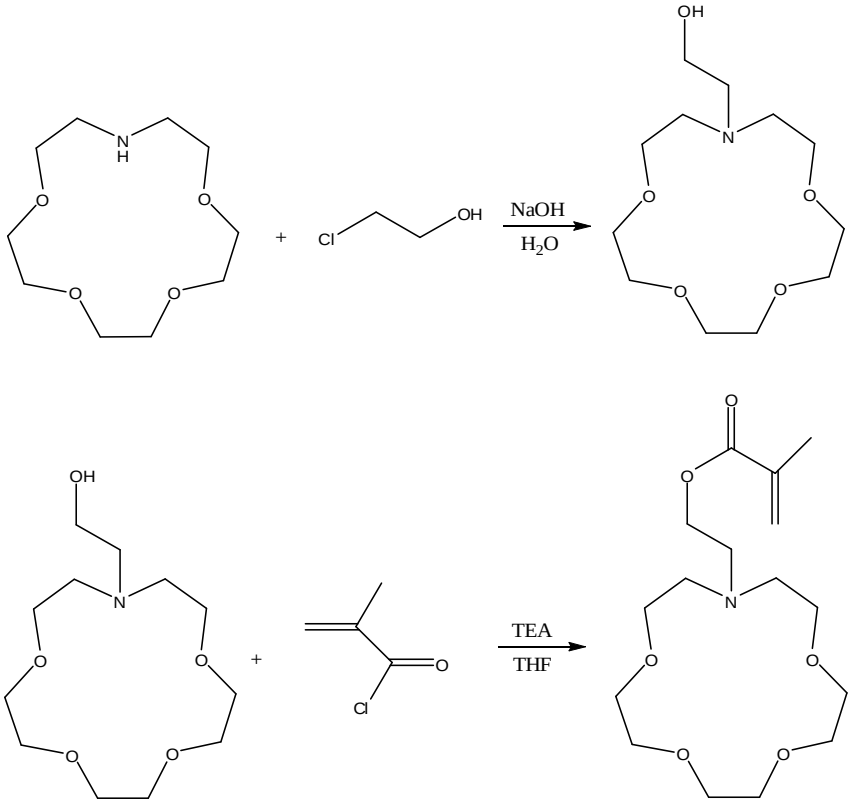

Figure 76: Synthesis of O-(N-hydroxyethyl-1-aza-15-crown-5)-methacrylate.

1-aza-15-crown-5 was reacted with chloro ethanol, in water, in presence of sodium hydroxide according to the scheme shown in Figure 76. The reaction proceeded smoothly to give the aimed product with acceptable yield (≈50%) and product purity which was verified by ^{1}H-NMR and mass spectra. Short reaction times were required in order to prevent the unwanted reactions between two molecules of 2-chloroethanol or between 2-chloro ethanol and the hydroxyl groups of the product.

N-(hydroxyl-ethyl)-1-aza-15-crown-5 was then reacted with methacryloyl chloride according to the scheme shown in Figure 76.

The reaction proceeded easily with high yields (≈ 95 %) to yield the crude product which was directly used for further polymerization.

4.1.2. Copolymerization of O-(*N*-hydroxythyl-1-aza-15-crown-5)-methyl methacrylate with MMA (3.2.6, DD65, 66).

O-(N-hydroxyethyl-1-aza-15-crown-5)-methyl methacrylate was first copolymerized with MMA by Free Radical Polymerization using Vazo67 as initiator, DD65. From a feed ratio of MMA/Aza-crown ether methacrylate 9/1, only 2 % of Aza-crown ether monomer was copolymerized (calculated by the ^{1}H-NMR reported in Figure 77), therefore only 20 % of the monomer successfully reacted. This result was also confirmed by elemental analysis (experimental section) as a low percentage of N was detected.

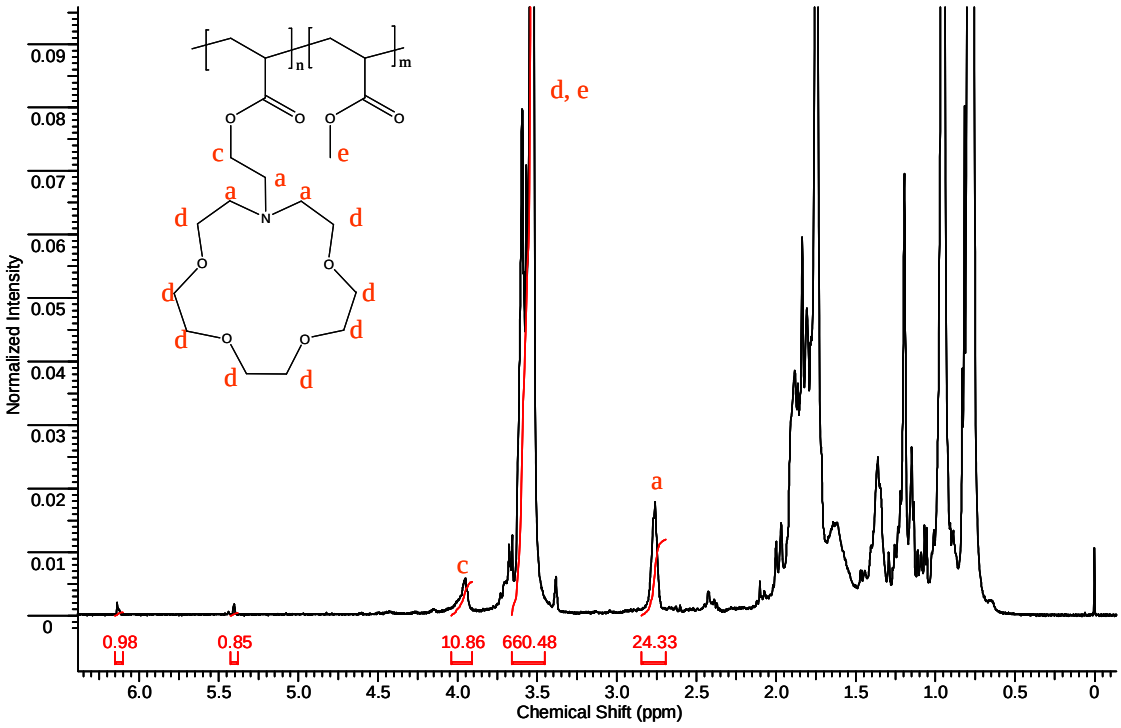

Figure 77: ^{1}H-NMR for the copolymerization of MMA and O-(N-hydroxyethyl-1-aza-15-crwon-5)-methyl methacrylate after 19 hours, DD65.

O-(N-hydroxyethyl-1-aza-15-crown-5)-methyl methacrylate was also copolymerized with MMA and MAA, with the aim of a polymer with 45 % of MMA, 45 % of MAA and 10 % of Aza-crown ether monomer, DD66. The same conditions were used and the

results obtained were similar to the previous reaction. In fact only 3% of the Aza-crown ether was incorporated into the polymer which was also confirmed by elemental analysis.

The O-(N-hydroxyethyl-1-aza-15-crown-5)-methyl methacrylate proved to have a very slow reactivity compared with those of MMA and MAA and thus their copolymerization was difficult. The Aza-crown ether monomer more likely reacts after the majority of the MMA and MAA due to the lower mobility of the larger monomer. A homopolymerization of the Aza-crown ether monomer was also attempted in order to verify whether the homopolymerization would result in a reasonably high molecular weight, section 3.2.5. However, MALDI TOF data of O-(N-hydroxyethyl-1-aza-15-crwon-5)-methyl methacrylate homopolymer, Figure 78, showed oligomers of maximum 7 units with separation of 331 Dalton, which is the Aza-crown ether monomer molecular weight.

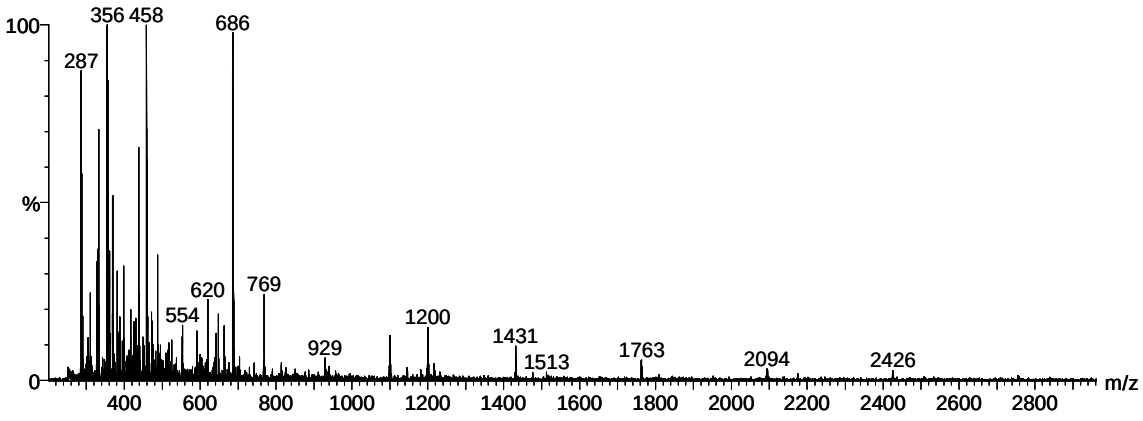

Figure 78: MALDI TOF data of poly-(N-hydroxyethyl-1-aza-15-crwon-5)-methyl methacrylate.

The precipitation of the material was not obtained as the oligomer was soluble in various solvents and mixtures of solvents; therefore the product was never isolated. The GPC analyses of the mixture was carried out, however, the graph obtained confirmed the result given by MALDI as the polymer peak was overlapped with the peak of the marker.

The steric hindrance of the large ring structure is likely the cause of the low and slow reactivity of the Aza-crown ether methacrylate monomer. In addition, the crown ether

ring also changes conformation partially surrounding the double bond implying that the double bond is not totally available for the radical polymerization thus, yielding a slower reactivity. A monomer with a shorter arm between the double bond and crown ether ring may result in higher reactivity.

4.2. Synthesis and characterisation of linear copolymers based on HEMA and MMA carrying Aza-crown as pendant groups for selective extraction of heavy metals from an aqueous solution to an organic solvent.

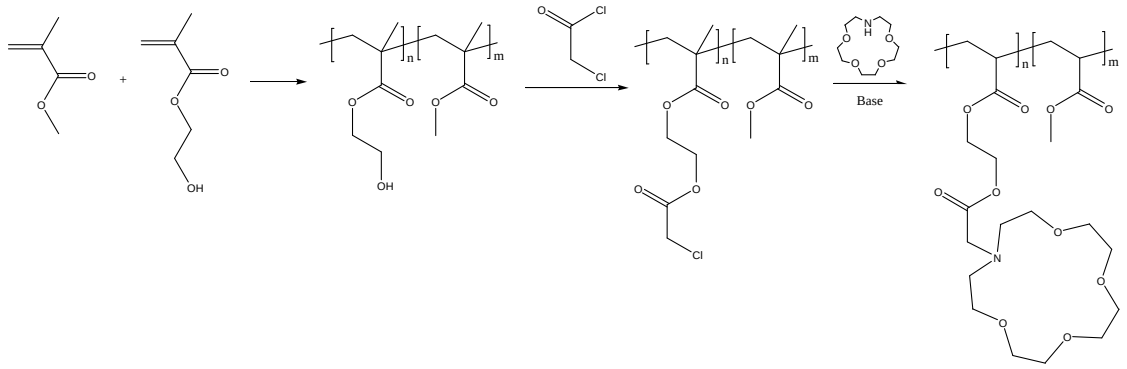

Figure 79: Full reaction scheme.

4.2.1. Synthesis of MMA/HEMA copolymers (section 3.2.7).

HEMA and MMA were initially randomly copolymerized by Free radical polymerization using 1-dodecanthiol as a chain transfer agent and Vazo 67 as an initiator to give the polymer shown in Figure 80. HEMA (2-hydroxyethyl methacrylate) was selected because of its hydroxyl group, useful substrate for subsequent post-functionalization reactions, whereas MMA was mainly selected in order to obtain a hydrophobic polymer insoluble in aqueous solutions.

These polymers are statistical copolymers as the sequential distribution of the monomeric units obeys to the following Mayo-Lewis equation.

$$\frac{d[M_1]}{d[M_2]} = \frac{[M_1]\cdot(r_1\cdot[M_1]+[M_2])}{[M_2]\cdot(r_2\cdot[M_2]+[M_1])}$$

Where r_1 and r_2 are the reactivity ratios of the monomer 1 and 2 whereas M_1 and M_2 are their molar concentrations. The reactivity ratios of HEMA and MMA are well known and are 0.63 and 0.824, respectively (polymer handbook, 4th edition).

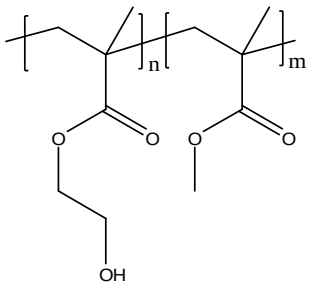

Figure 80: Random-poly-MMA-co-HEMA.

Copolymers with different HEMA ratios (10, 25, and 50 %) were synthesised and although free radical polymerization was employed, good control of the molecular weight with low polydispersity was achieved as a chain transfer agent was introduced in the copolymerization (the GPC results are listed in the experimental section). Chain transfer agents have at least one weak chemical bond which allows them to terminate one chain ($P^{\cdot}$) initiating another ($C_{12}H_{25}S^{\cdot}$) according to the mechanism shown in Figure 81. The use of a chain transfer agent reduces the average molecular weight (Mn) and polydispersity (I) of the polymer and for this purpose it was used.

$$P^{\bullet} + C_{12}H_{25}SH \longrightarrow PH + C_{12}H_{25}S^{\bullet}$$

Figure 81: Mechanism of action of the chain transfer agent.

The following Table 24 reports a summary of the samples prepared, compositions and molecular weights.

Table 24: Summary table of samples, compositions and molecular weights.

Sample	MMA	HEMA	Mn
DD5	50	50	6400
DD6	75	25	6800
DD7	90	10	6000

DD7 was also characterized by MALDI-TOF and the data are reported in the appendix section.

4.2.2. Preparation of chloroacetyl copolymers of MMA/HEMA by grafting to preformed copolymers (section 3.2.8).

Subsequently the pre-formed copolymers of MMA/HEMA were successively functionalised with chloroacetyl chloride by etherification of the HEMA hydroxyl groups (Figure 82). The aim was to incorporate an electrophilic group into the polymer backbone, useful for the incorporation of 1-aza-15-crown-5.

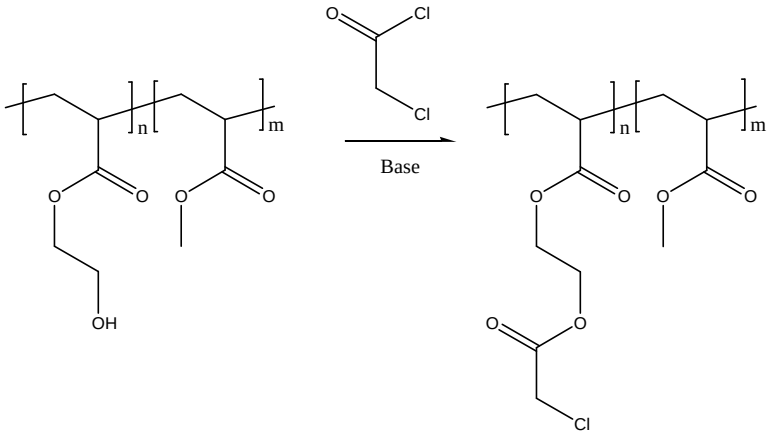

Figure 82: Etherification of hydroxyl groups of HEMA.

The majority of experiments yielded a product with approximately 100 % of chloroacetyl functionalization, in fact no significant amount of hydroxyl groups was observed in the product by ^{1}H-NMR (Figure 83).

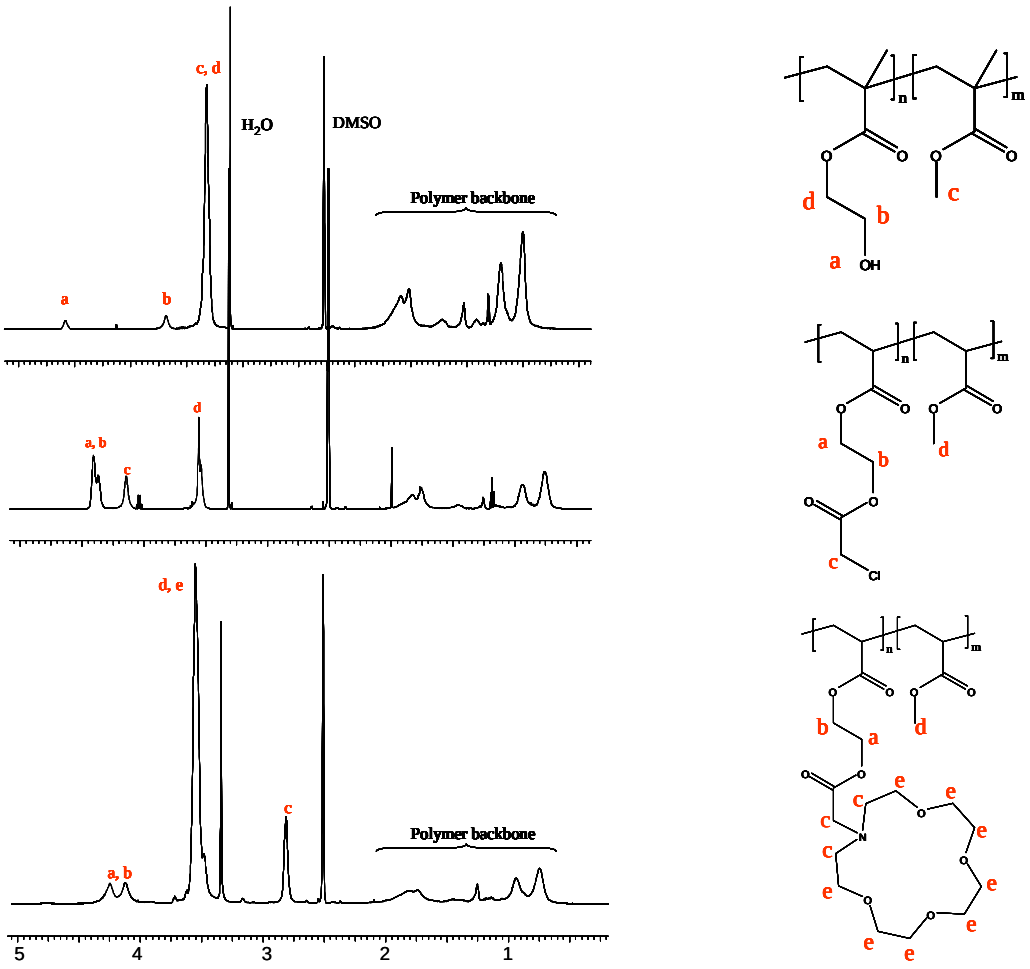

Figure 83: ^{1}H-NMR poly-(HEMA-co-MMA) 50/50, DD5, and the post-functionalised analogues copolymers (DD40, DD52).

A sample (DD55) was also characterised by MALDI-TOF and the data is reported in the appendix section.

4.2.3. Synthesis of MMA/Aza-crown ether copolymers by grafting chloroacetyl functionalised copolymers (section 3.2.9).

The random MMA/chloroacetyl copolymers were grafted with 1-aza-15-crown-5 to give the required product according to the scheme reported in Figure 84.

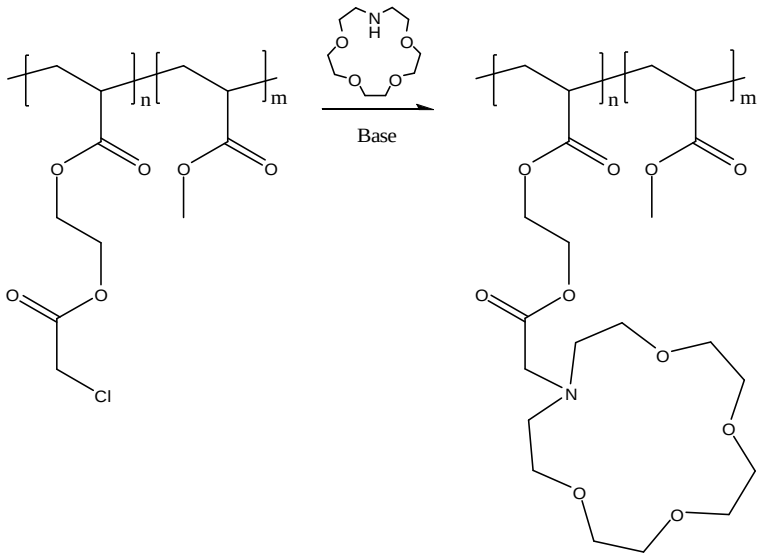

Figure 84: Synthesis of random MMA/Aza-crown ether copolymers by the grafting to method.

In this reaction, the use of inorganic bases should be avoided since the metal ions may be complexed by the Aza-crown ether rings, potentially deactivating their complexation ability, therefore triethylamine was employed.

The incorporation of the Aza-crown ether in the polymer was confirmed by ^{1}H-NMR (Figure 83), elemental analysis (experimental section) and TGA (Figure 85).

Post-functionalization was successful but tiny amounts of chlorine were observed in their elemental analysis for either 10, 25 and 50 % samples. Therefore, post-functionalization reactions with Aza-crown ethers were not carried out until reaction completion as un-reacted chloroacetyl groups were still present in the polymer chains.

Uncompleted functionalization was also confirmed by TGA. The first weight % derivative of the TGA analyses before and after functionalization for the poly-(HEMA-co-MMA) 50/50 is reported in Figure 85. After the chloroacetyl chloride was incorporated onto the polymer, a peak appeared at about 230 °C (green trace); after the second functionalization with Aza-crown ether, a little bounce in the same area was still observed confirming the un-completed functionalization.

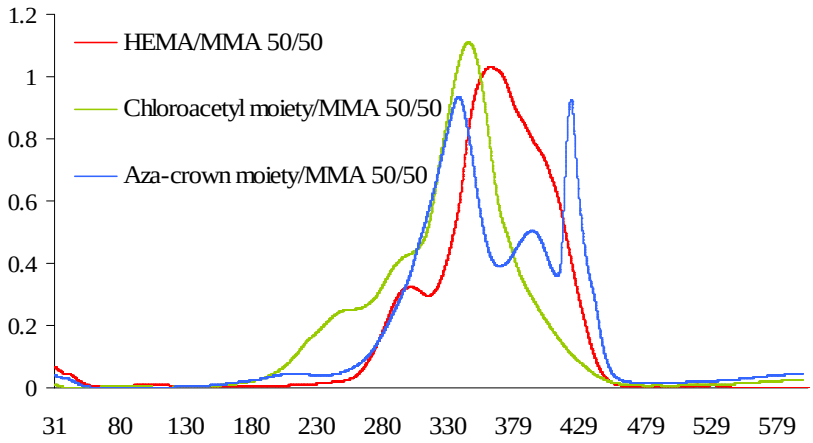

Figure 85: Weight % derivative of the TGA graphs for poly-(HEMA-co-MMA) 50/50 and the post-functionalised analogue copolymers.

GPC analysis was executed with different solvents tested, however a suitable system to detect the materials containing *N*-Aza-crown ethers was not found.

The materials prepared were also characterized by MALDI-TOF and the data are reported in the appendix section.

4.3. Solution studies on MMA/Aza-crown ether copolymers.

As previously mentioned in the Chapter 1, the high flexibility of the crown ether (probably enhanced by the presence of the long side arm), can impart some very interesting properties such as solubility in both aqueous and lipophilic solvents. In the case of a polymer, the situation is more complicated, especially considering that the polymer consists of two different monomers with completely different solubilities. Poly-MMA is well known to be a hydrophobic polymer shown by samples with high MMA ratio (90 % MMA and 10 % Aza-crown ether moiety) being insoluble in water, even though Aza-crown was incorporated. On the other hand, samples containing higher amounts of *N*-Aza-crown ethers (25 and 50 %) were partially soluble in water, although only small amounts were dissolved. However, more importantly these materials showed the capability to form emulsion on the interface between the two layers. A material for metal extraction should not have this capability as for these materials separation of the

layers after extraction should result in a simple operation. A reasonable explanation of this behaviour is the coexistence of two different effects: the high flexibility of the crown ether (probably enhanced by the long and polar side arm) favours its solubility in hydrophilic and lipophilic solvents. This flexible moiety is then incorporated into a long linear polymer which also retains flexibility and can achieve structures where the Aza-crown ethers are exposed to the solvent assuring solubility and surrounding the lipophilic MMA moieties disposed inside the structure as a hydrophobic core. This aggregation in water was confirmed by Dynamic Light Scattering; 1% aqueous solution of sample DD52 (50 % Aza-crown ether moiety, 50 % MMA) was analysed and one single peak at 176nm (width = 72.5 nm and PDI = 0.163) was observed (Figure 86).

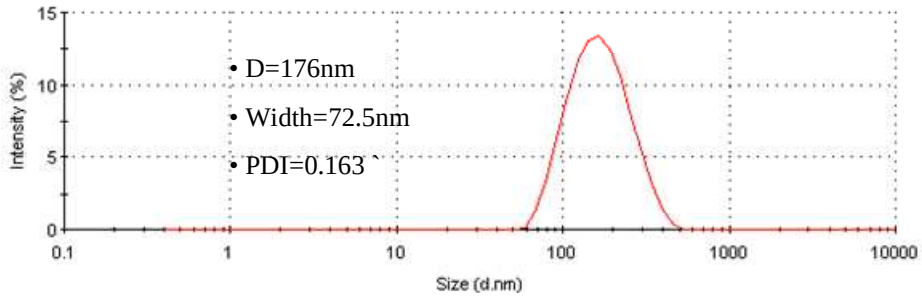

Figure 86: Dynamic Light Scattering of 1% aqueous solution of sample DD52 (50% Aza-crown ether moiety, 50% MMA)

Potential measurements using a Voltmeter and ion selective electrodes were carried out in order to investigate whether these materials were able to extract metal ions from an aqueous to an organic solution. K^+, Na^+, and Ca^{++} extractions were carried out but none of the materials synthesised appeared to be capable of extracting metal ions from aqueous solution to the organic layer. Experiments were carried out, solubilising the polymer in DCM in a concentration where the Aza-crown ether moiety was 2 eq of the metals solubilised in an aqueous solution (0.001 % w/v). The two phases were then mixed and stirred over a 24 hours and then separated. The potential of the aqueous layer was measured before and after extraction using an ion selective electrode previously calibrated and connected to a voltmeter. Unfortunately, no changes in potential were

observed although solutions containing an increase in concentration of polymer were tested.

4.4. Conclusions.

On the first year the present study was focused on the synthesis of materials for selective extraction of metals from an aqueous to an organic phase. For this purpose a copolymer based on MMA-HEMA subsequently functionalised with *N*-Aza-crown ether moiety was synthesised and its scavenging properties tested. The materials were successfully prepared, however measurements of potential showed that the copolymers were not able to extract Na^{+}, K^{+}, and Ca^{++} from an aqueous to an organic solvent. Extraction of metals ions in an organic solvent is, in fact, a very difficult task and the success of the extraction depends upon many different variables but most importantly upon the type of counter-ion. The well-known properties of crown ethers to complex cations on the base of the ring size were already intensively discussed in the chapter 1 but most of the studies found in the literature report extractions of salts of relatively hydrophobic anions whereas more common salts usually contain more hydrophilic counter-ions (i.e. Cl^{-}).[159, 160]

In fact, although the crown ether was successfully incorporated into the polymer matrix the stability of the complex formed with the metals in the organic layer was not sufficient to guarantee stability also for the counter-ion. Furthermore, the materials also formed emulsions on the interface between the organic and aqueous layer although those containing smaller amounts of the more hydrophilic functionalised HEMA showed a better behaviour on respect to this matter. Since such complications were encountered and because the primary interest was preparing a material easy to handle and to be recovered after complexation, this way was left behind. In the development of remediation technology, hydrogel supports in form of beads are more attractive materials as they can absorb large quantities of water and contaminants and are particularly easy to handle and removed after complexation.

Chapter 5

Dual-Stimuli Responsive NIPAM-AAc Hydrogel beads incorporating *N*-Aza-crown ethers

5.1. Synthesis of dual-stimuli responsive Aza-crown ether beads by post-functionalization of pre-formed copolymer beads (PNA1, 2 and 3, section 3.3.).

5.1.1. Synthesis of beads (section 3.3.1, 2, 3, 4.).

These hydrogel beads were synthesised by inverse suspension polymerization. Their backbone network is made of N-isopropyl acryl amide (NIPAM) and acrylic acid (AAc). NIPAM was selected in order to confer thermo-sensitivity (LCST around 32˚C) to the hydrogel and AAc (pKa = 4.25) for pH sensitivity (Figure 87).

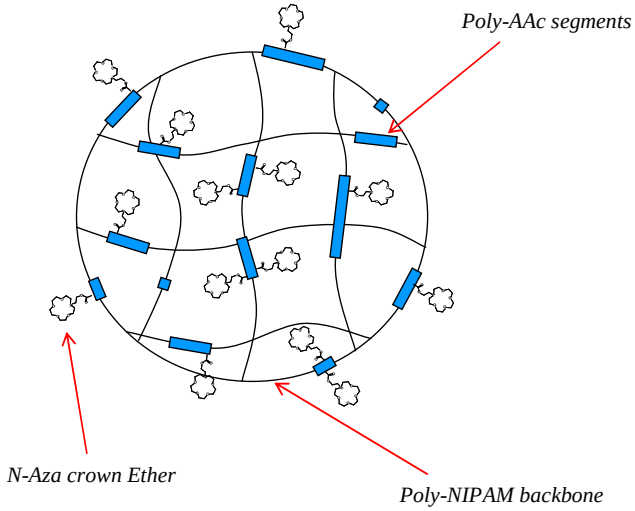

Figure 87: Poly-(NIPAM-co-AAc) incorporating N-Aza crown ethers.

In general, the quantity of AAc was maintained below 10 % as the thermo- responsivity of poly-NIPAM is affected by the presence of hydrophilic comonomers (section 1.4.2.). As the monomer solution used in the polymerization is mainly composed of NIPAM, initially experiments using inverse suspension homopolymerizations of NIPAM were carried out in order to find suitable conditions for the inverse suspension polymerization

(stirring speed, shape and size of the vessel, type and amount of surfactant etc.) in order to produce a material in the form of droplets in the range of 100-200 microns. Cyclohexane was used as continuous phase as monomers, cross linker and initiator system are all insoluble in such solvent. Three different surfactants (SPAN40, sorbitan monopalmitate, SPAN80, sorbitan monooleate and SPAN83, sorbitan sesquioleate) with different HLB values (6.7, 4.3 and 3.0, respectively) were tested. However, only SPAN80 gave an effective dispersion of the monomer solution and a beaded product. The quantity of surfactant used is also a decisive parameter for an effective dispersion and uniform beading; 100 μl of SPAN80 in 200ml of continuous phase was a suitable quantity. Different stirrers were tested (different types and sizes of blades, different types and sizes of propellers) but generally propellers resulted in more efficient stirring. It was also found that using a particular propeller of a certain size, size and shape of the vessel, vessel/mixture volume ratio and the stirring speed used were fundamental parameters in order to succeed in the beading of the product. A little change in these can result in either a complete polymer precipitation, coagulum, or a mixture of beads and coagulum.

In preliminary experiments, the initiator (APS, ammonium persulfate) was directly added into the monomer aqueous solution. The resulting mixture was carefully degassed and transferred into a previously degassed continuous phase. Subsequently, the polymerization was initiated by adding TEMED (catalyst, N,N,N',N'-tetrametilendiammina) into the suspension after the clear formation of suspended liquid droplets was observed. The formation of radicals is operated by the redox APS/TEMED system. The redox mechanism is reported in Figure 88. TEMED accelerates a homolytic scission of APS moieties in aqueous media. The radical formed initiates the polymerization through a normal free radical mechanism into the aqueous droplets as discussed in the section one.

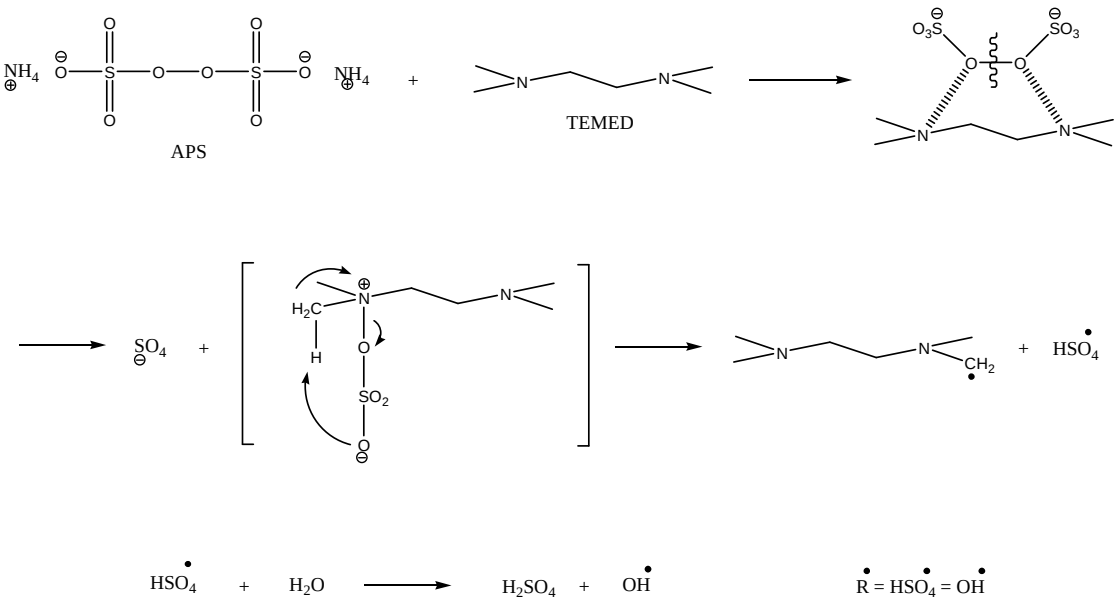

Figure 88: Mechanism of initiation of the couple redox initiator APS/TEMED.

Using this preliminary method, beads based on poly-NIPAM (PN) were successfully prepared. An IR spectrum was recorded and it is reported in Figure 89.

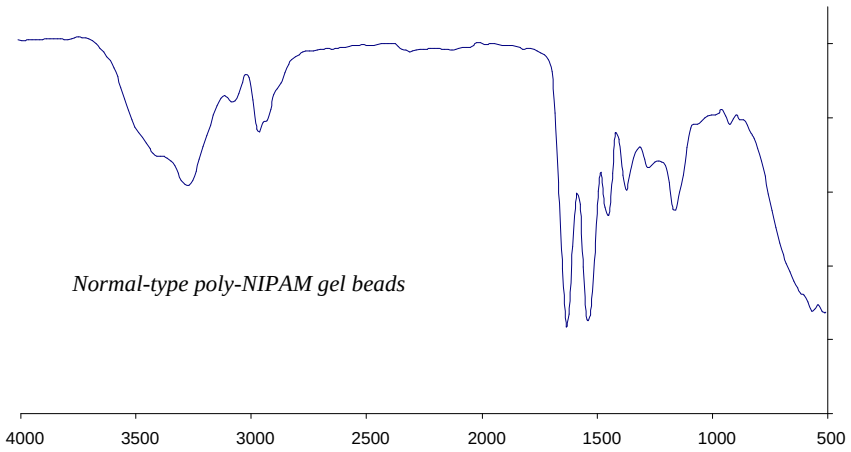

Figure 89: IR-Spectra of poly-NIPAM gel beads (PN).

The same conditions found suitable for homopolymerization of NIPAM were used for the copolymerization of NIPAM and HEMA (PNH) as successful post-functionalization with *N*-Aza-crown ethers was previously achieved employing this comonomer (chapter 4).

Thus, HEMA was copolymerized with NIPAM (NIPAM : HEMA 9 : 1 ratio) following the scheme reported in Figure 90.

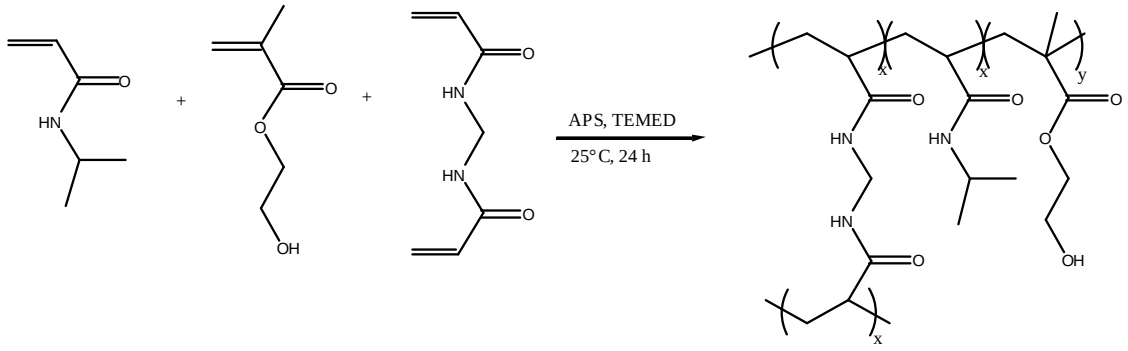

Figure 90: Synthesis of poly-(NIPAM-co-HEMA) gel beads (9:1) , PNH.

The same conditions found for the homo inverse suspension polymerization of NIPAM worked effectively in the copolymerization of NIPAM and HEMA and successful beads (100 micron range) were synthesised without a substantial amount of coagulum. Solid state ^{13}C-NMR (Figure 93), elemental analysis (experimental section) and IR (Figure 92) were recorded and confirmed successful copolymerization.

The same system was used to copolymerize NIPAM, HEMA and AAc in an 8 : 1 : 1 ratio respectively (PNHA). However, in this case copolymerization did not occur at the first attempt, possibly due to the high percentage of inhibitor in the AAc, used as received. Other experiments were carried out using fresh distilled AAc and over-reactivity of AAc was encountered. The monomer mixture in this case was too reactive and polymerization occurred during the degassing process. Therefore, the procedure was altered: distilled AAc was used. TEMED being oxygen sensitive was added to the monomer mixture after the degassing process and the initiator APS was added to the suspension (as an aqueous solution carefully degassed) after a clear formation of the droplets was observed. In these new conditions, beads were regularly obtained whether AAc was used or not.

5.1.2. Functionalization of the beads with Aza crown ether (section 3.3.5, 6, 7.).

A one step post-functionalization reaction on the hydrogel beads was selected. Firstly, chloroacetyl chloride was reacted with *N*-Aza-crown ether following the scheme reported

in Figure 91. Three different compounds were prepared with different ring sizes (12, 15 and 18) in order to synthesise 3 different materials with different *N*-Aza-crown ethers incorporated.

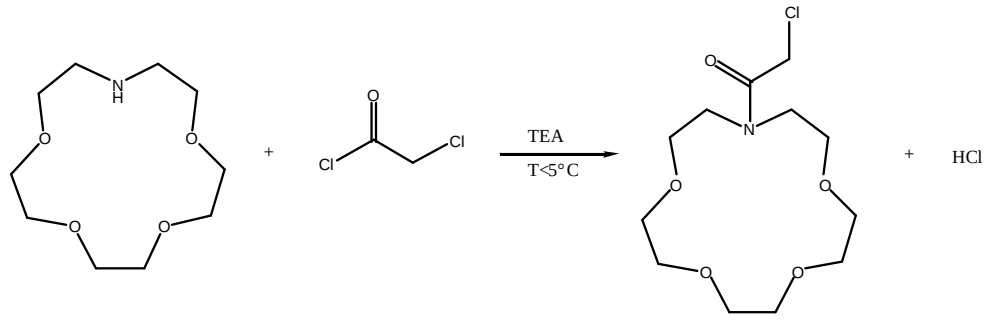

Figure 91: Preparation of chloroacetyl 1-aza-15-crown-5 (section 3.3.5.).

The reaction proceeded smoothly with high yields and good purity of the product: ^{1}H-NMR (Figure 6, 7 and 8 in the appendix section) and Mass Spectra (section 3.3.5.) were recorded.

Chloroacetyl 1-aza-15-crown-5 was then reacted with poly-(NIPAM-co-HEMA) beads (PNH) under reflux, in THF, over a period of 24 hours using TEA as base. The problem with these materials is their total insolubility which render characterisation much more complicated and undefined. The beads were analysed before and after functionalization by IR, elemental analysis and solid state ^{13}C-NMR. Elemental analysis was carried out but the results were not consistent with successful post-functionalization (the percentages of the elements were not supposed to change substantially with the reaction). IR before and after functionalization is reported in Figure 92; the peak at 1712 cm^{-1} confirmed that HEMA was copolymerized with NIPAM during inverse suspension polymerization. However, the IR of the functionalised product showed no difference. A new peak in the region of 1200cm^{-1} was expected due to the C-O-C stretching of the Aza-crown ether rings.

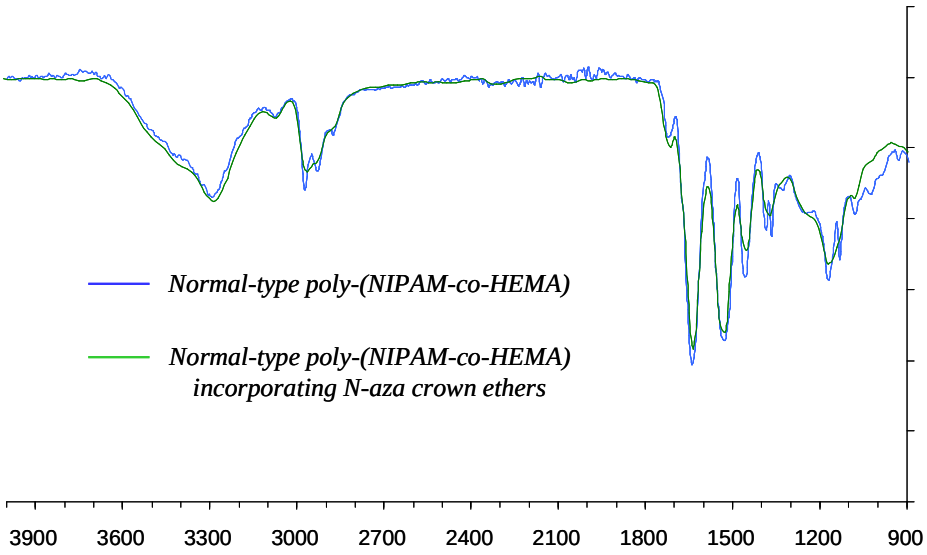

Figure 92: IR-Spectra of poly-(NIPAM-co-HEMA), PNH, and poly-(NIPAM-co-HEMA) gel beads (8:2) functionalised with chloroacetyl 1-aza-15-crown-5, PNH2.

Confirmation of the unsuccessful functionalization was given by solid state ^{13}C-NMR where no changes were observed in both the spectra before and after functionalization. An increase of the peaks in the region about 60-70, ppm should be observed for a successful functionalization. Additionally, the ^{13}C-NMR spectra of the poly-(NIPAM-co-HEMA), reported in Figure 93, shows that the copolymerization of NIPAM and HEMA occurred, although the HEMA component is quite low. Only the CH_2OH/CH_2O of HEMA should be distinct in the region of 60-75 ppm, as it is shown, these two signals are between 2 and 4 % of the total signal in the spectrum. In general, solid state ^{13}C-NMR spectra are usually not sufficiently accurate for quantitative analysis and therefore the HEMA incorporated was not calculated from the ^{13}C-NMR spectra.

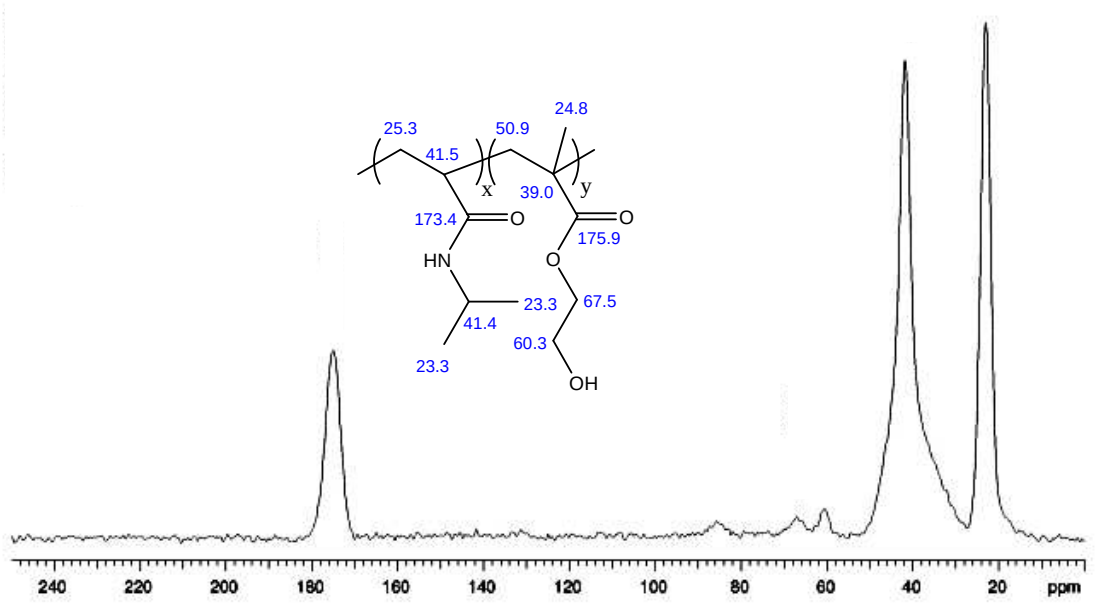

Figure 93: Solid State ^{13}C-NMR poly-(NIPAM-co-HEMA) gel beads (PNH).

As HEMA proved to be a relatively unsuitable substrate for post-functionalization using chloroacetyl Aza-crown ethers, a new hydrogel based on a poly-(NIPAM-co-AAc) (PNA) with a feed ratio 8 : 2 using similar conditions was synthesised (Scheme in Figure 94). The AAc was increased to 20 mol % aiming to post-functionalise about half of the acid sites in order to obtain hydrogel beads based on NIPAM: AAc: Aza-crown ether of about 8 : 1 : 1 ratio.

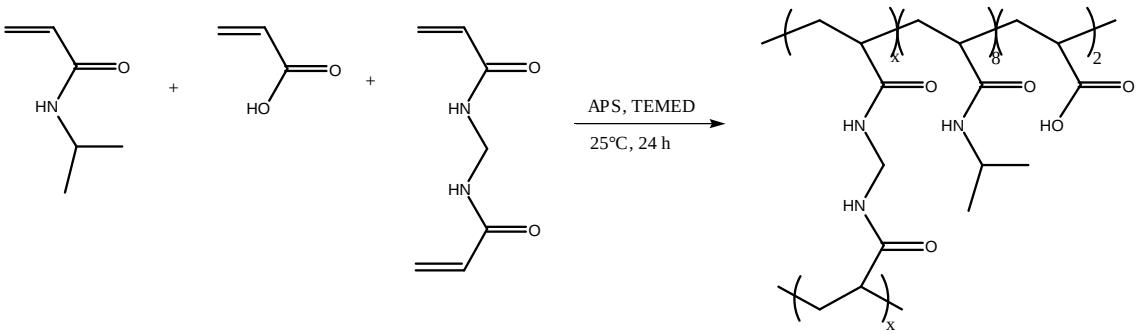

Figure 94: Synthesis of poly-(NIPAM-co-AAc) gel beads (8:2) , PNA.

The same conditions were effective with this new system and the product was obtained in form of beads. IR, solid state ^{13}C-NMR and elemental analysis were recorded. The IR

spectrum (Figure 97) shows a new peak around 1700 cm^{-1} which belongs to the carbonyl groups of the AAc copolymerized.

The ^{13}C-NMR spectrum of the poly-(NIPAM-co-AAc) (Figure 95) exhibited three broad peaks at 20-26 ppm (–CH_3 NIPAM and –CH– backbone), 30-50 ppm (–CH– and –CH_2– backbone and –CH–N– NIPAM) and 170-180 ppm (CO NIPAM and AAc).

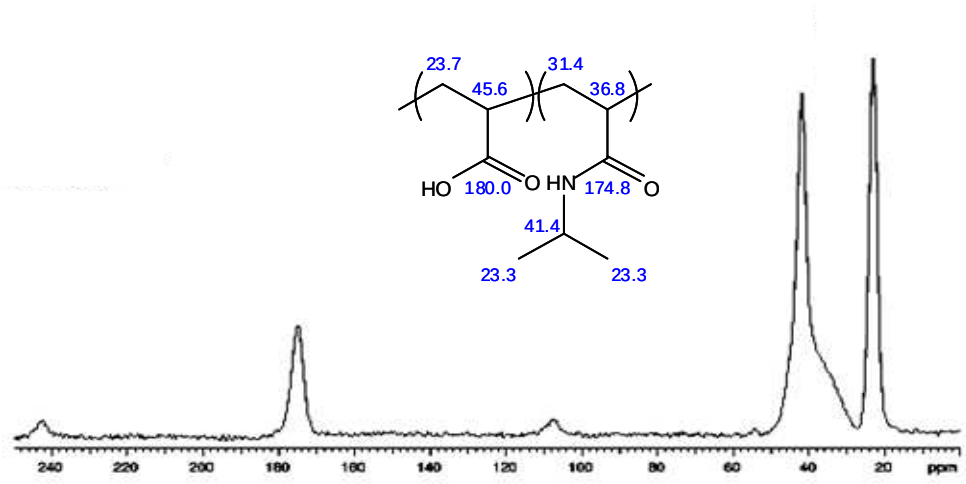

Figure 95: Solid State ^{13}C-NMR poly-(NIPAM-co-AAc) gel beads (8:2) - PNA.

In order to calculate the quantity of AAc effectively copolymerized with NIPAM, PNA was titrated with NaOH (0.005M). The ratio of NIPAM: AAc obtained is 7.6 : 2.4 whereas the theoretical value is 8 : 2. The difference is probably due to an error given by the titrating method, we have to take into account that AAc is functionalised in a solid swellable support and it is titrated in presence of large quantities of NIPAM. Certainly the complexity of the system cause an error on the measurement, however the result is near the expected value.

These hydrogel beads were subsequently functionalised using chloroacetyl 1-Aza-15 crown-5, previously synthesised following the scheme reported in Figure 96 in order to prepare the normal-type dual stimuli responsive gel beads incorporating Aza-crown ether

(PNA2). The reaction was carried out under nitrogen atmosphere, under reflux over a period of 24 hours using TEA as base.

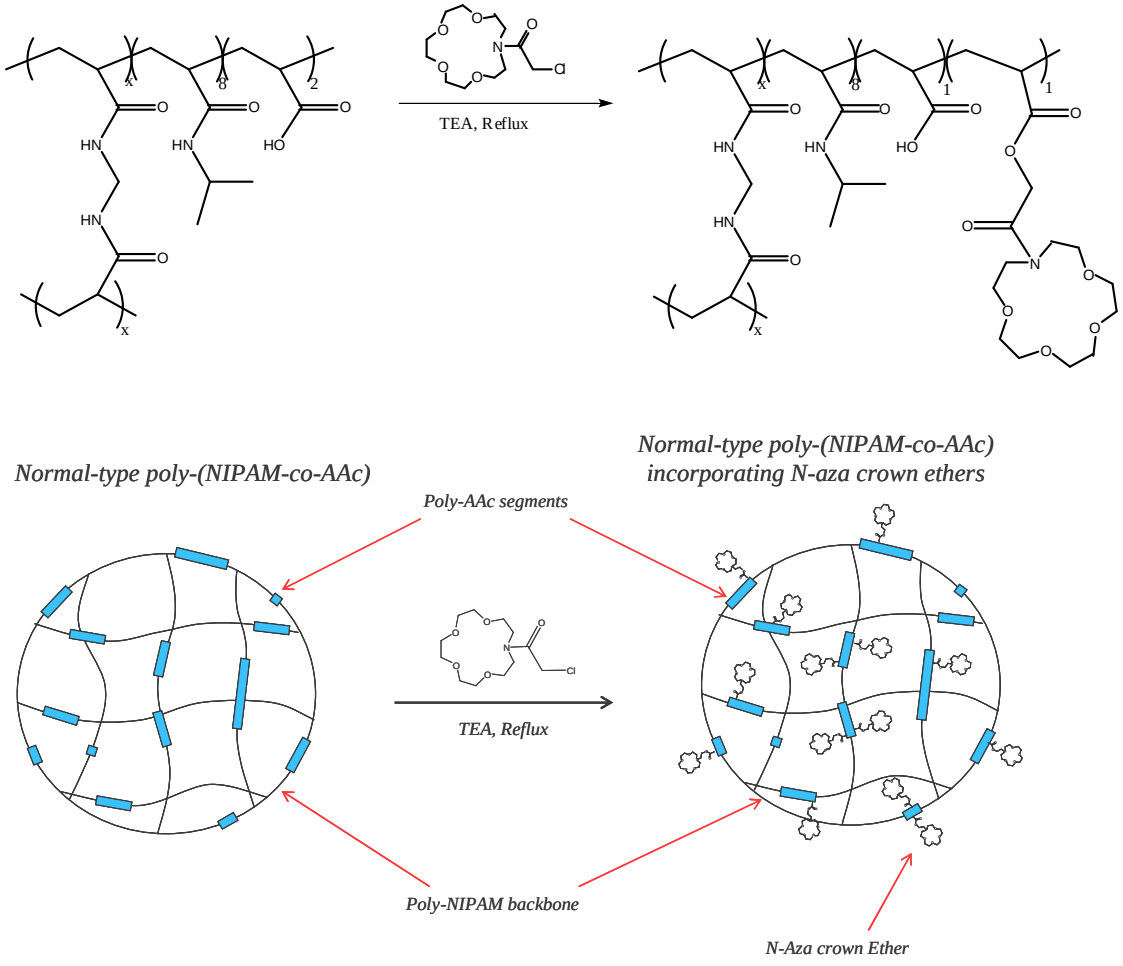

Figure 96: Synthesis of dual stimuli responsive gel beads incorporating Aza-crown ether (PNA2).

The post-functionalization was confirmed by IR and solid state ^{13}C-NMR. Elemental analysis was also recorded (section 3.3.7) and showed 0 % content of chlorine element. This result is consistent with the covalent bonding of chloroacetyl-*N*-Aza-crown ether to the beads. In case the molecules are only physically absorbed into the polymer matrix, small amounts of chlorine should be observed in the elemental analyses.

Figure 97 shows the IR spectra before and after functionalization. As expected, an increase in the region around 1200 cm^{-1} was observed, such signal belongs to the C-O-C stretching of Aza-crown ether rings.

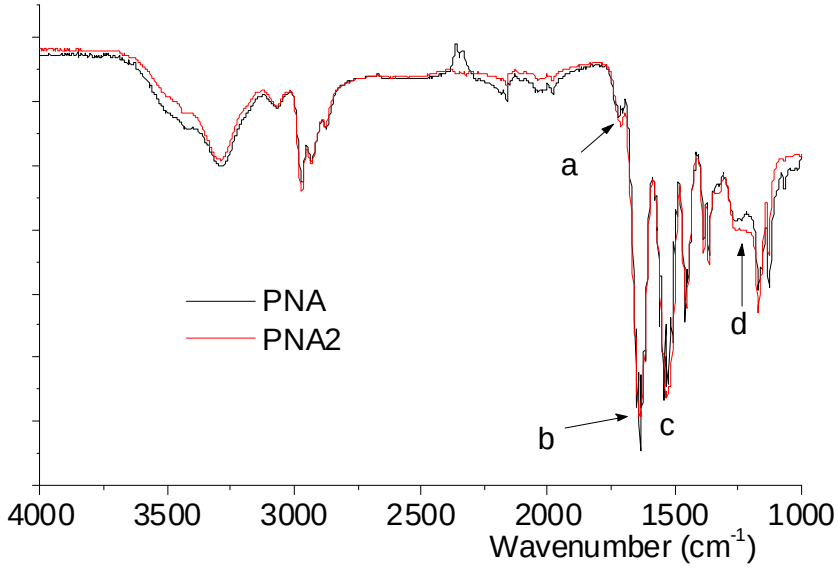

Figure 97: FT-IR spectra for PNA (poly-(NIPAM-co-AAc)) and PNA2 (poly-(NIPAM-co-AAc) functionalised with 1-Aza-15-crown-5). a ~1712 cm^{-1}, b ~1643 cm^{-1}, c ~1534 cm^{-1}, d ~1212 cm^{-1}.

Solid state ^{13}C-NMR also confirmed successful functionalization; the ^{13}C-NMR spectrum of the functionalised product (Figure 98) shows a new signal at 71 ppm which is consistent with the presence of crown ethers. However, both IR and solid state ^{13}C-NMR cannot be used to calculate the amount of crown ether incorporated.

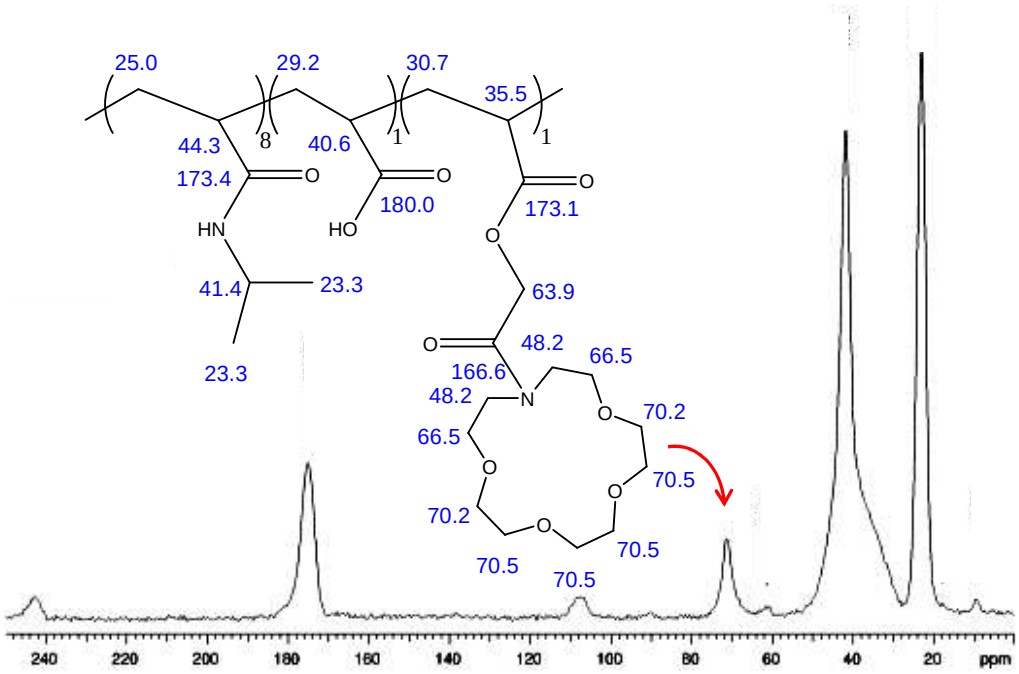

Figure 98: ^{13}C-NMR (Solid State) of poly-(NIPAM-co-AAc) gel beads with chloroacetyl Aza-crown ethers functionalised with chloroacetyl 1-aza-15-crown-5 (PNA2).

Three different hydrogel beads with different Aza-crown ethers were successfully synthesised carrying 1-aza-12-crown-4 (PNA1), 1-aza-15-crown-5 (PNA2), and 1-aza-16-crown-6 (PNA3), respectively.

In order to evaluate the quantity of *N*-Aza-crown ether post-functionalized into the materials, the remaining AAc was titrated with NaOH (0.005 M). The system was revealed to be much more complicated than the PNA hydrogel. The incorporation of crown ether adds, in fact, a very weak acidic group and an ester which is sensitive to hydrolysis as shown in Figure 99.

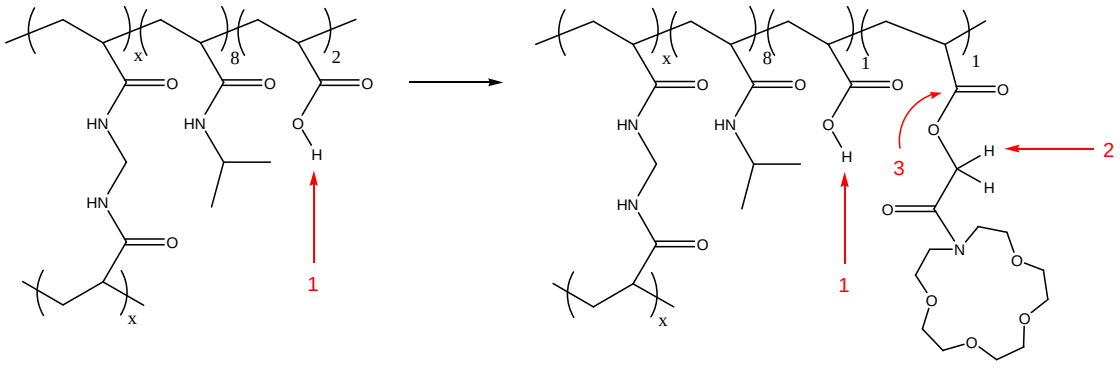

Figure 99: Possible routes during titration before and after functionalization: 1) deprotonation of AAc, 2) deprotonation of a weaker acid, 3) hydrolysis.

The evidence of this was given by the titration experiment. A larger NaOH quantity, compared with that required to titrate PNA, was necessary to complete titration of PNA1. However, in the case of PNA1 after the titration seemed completed the pH slowly decreased, caused by the slow hydrolysis of the ester.

A different method was employed (section 3.3.8.) for the PNA2 material. The experiment was repeated in exactly the same conditions and the un-reacted crown ether was separated from the beads by extraction with an organic solvent. The ^{1}H-NMR of the oil obtained after evaporation of the solvent is reported in Figure 100.

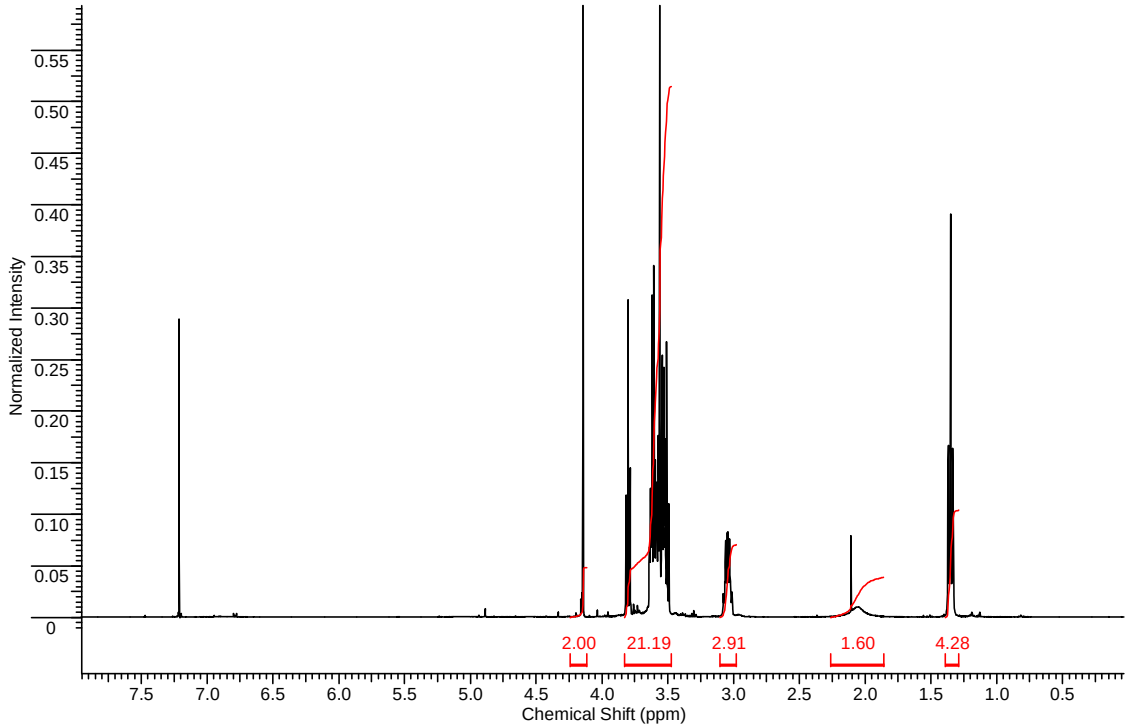

Figure 100: 1H-NMR of the residue obtained in the controlling experiment (section 3.3.8.).

The isolated residue contained crown ether but also a small quantity of water and TEA. The isolated residue weighed 68 mg from 90 mg starting material. The amount of water and TEA can be calculated from the NMR and result 12 mg which means that 34 mg – 90 – (68 – 12) = 34 – have been incorporated into PNA2. The amount of crown ether incorporated into PNA2 is 14.5 weight %.

5.2. Synthesis of poly-(NIPAM-co-*N*-Aza-crown methacrylate) thermo-responsive hydrogel beads by Inverse Suspension Polymerization (PNCE, PNCEP, section 3.3.9, 10, 11.).

During first year, an Aza-crown ether monomer was successively synthesised, however, attempts of its polymerizations failed (section 3.2.). In general, monomers carrying large groups, as in *N*-Aza-crown ether monomers, usually react slower than smaller monomers, due to the steric hindrance of the large ring structure. Additionally if the crown ether ring is attached to the double bond by a long arm, the molecule can achieve a conformation where the double bond is partially surrounded by the large ring and therefore it is not

totally available for radical polymerization. Therefore, the first monomer prepared, having a long polar arm connecting the double bond and *N*-Aza-crown ether ring, did not show efficient reactivity in homo- and copolymerizations. Subsequently, a new monomer with a short arm was synthesised following the scheme reported in Figure 101.

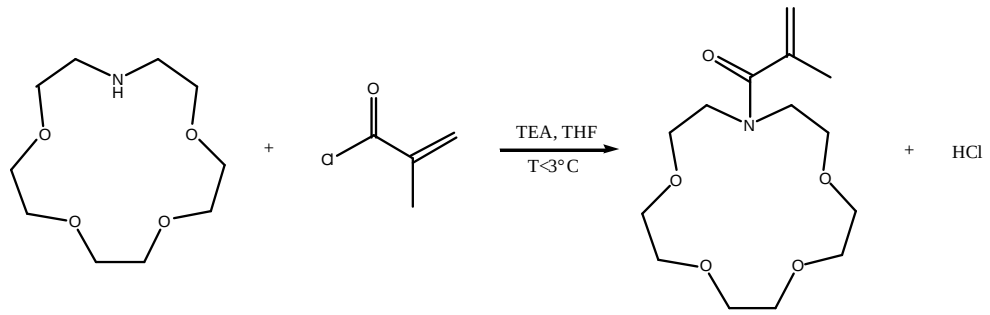

Figure 101: Synthesis of 1-aza-15-crown-5 methacrylate monomer.

This synthesis was carried out in THF at low temperature and dilute solution using an ice bath to cool the exothermic reaction. The reaction proceeded smoothly, giving good yields (~ 80 %) and three different monomers were prepared carrying 1-aza-12-crown-4, 1-aza-15-crown-5 and 1-aza-16-crown-6, respectively. ^{1}H-NMR and Mass Spectra were recorded for all the samples prepared and are reported in both the experimental section and the appendix.

Firstly, 1-Aza-15-crown-5 methacrylate was copolymerized with NIPAM with a feed ratio 8: 2 NIPAM: 1-Aza-15-crown-5 methacrylate by normal free radical polymerization in order to verify the reactivity of the new monomer (PNCEP). Vazo 67 (1 mol %) was used as initiator and the polymerization was carried out under reflux, over a period of 24 hours. The weight average and the number-average molecular weight of the polymer were determined to be 5284 Da and 3177 Da, respectively (I = 1.663), by gel permeation chromatography. In addition, a spectrum of the polymer obtained with ^{1}H-NMR spectroscopy measurements exhibited the peak of the NIPAM methyl groups (–CH_3) at 0.8-1.2 ppm and a broad peak at 3.2-3.9 ppm which is related to the –CH– of the NIPAM monomer and the –CH_2– of the Aza-crown ether ring; a broad peak at 1.4-2.2 of the –CH_2– and the –CH_3 of the polymer backbone was also observed. An estimation of crown-ether monomer copolymerized was also calculated by the peak intensities and 18 mol %

of monomer was obtained therefore the monomer in these conditions, reacted with 90% conversion.

Once the reactivity of the monomer was verified, the 1-aza-15-crown-5 methacrylate was directly copolymerized with NIPAM by inverse suspension polymerization (scheme in Figure 102) using the same conditions found for the previous experiments (PNCE).

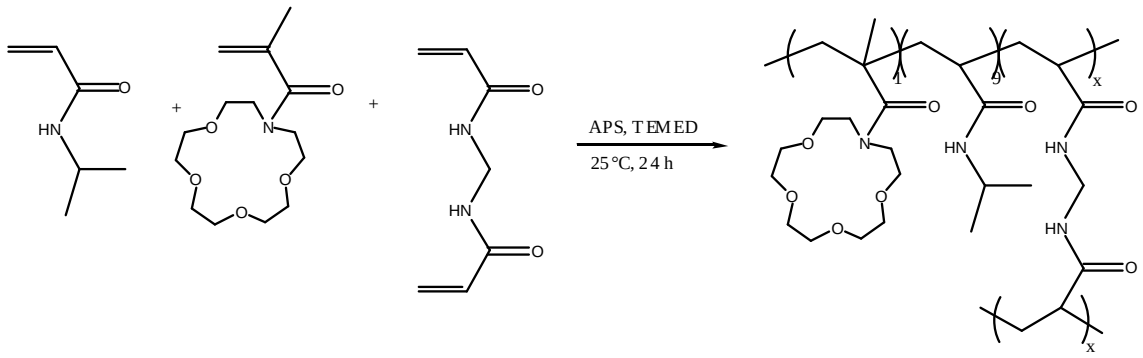

Figure 102: Synthesis of poly-(NIPAM-co-1-aza-15-crown-5 methacrylate) by Inverse Suspension Polymerization (PNCE).

Beaded hydrogels were obtained and solid state ^{13}C-NMR was used to confirm the incorporation of the Aza-crown ether monomer in the hydrogel. ^{13}C-NMR spectrum (Figure 103) shows a signal around 70 ppm which is consistent with the presence of the crown ether monomer, however the signal was small and therefore the incorporation did not achieve high yield. Unfortunately, as previously mentioned, solid state ^{13}C-NMR is not useful as a quantitative measurement and can only be used to detect the presence of chemical groups.

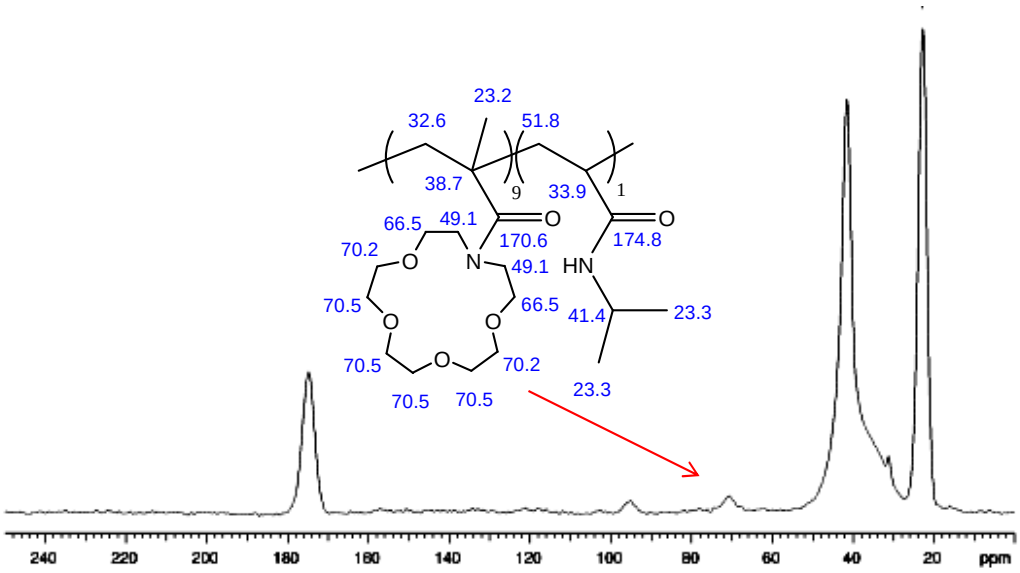

Figure 103: ^{13}C-NMR (Solid State) of poly-(NIPAM-co-1-aza-15-crown-5 methacrylate), PNCE.

For this reason the method of functionalizing pre-formed hydrogel poly-(NIPAM-co-AAc) beads discussed in paragraph 5.1 was preferred on this route.

5.3. Synthesis of graft-type dual-stimuli responsive hydrogel beads based on poly-(NIPAM-co-AAc-co-*N*-Aza-crown methacrylate) (PGNACE, section 3.3.12, 13.).

Since the new monomer synthesised proved to be reactive in the copolymerization with NIPAM, it was also employed for the synthesis of graft-type dual stimuli responsive hydrogel beads based on poly-(NIPAM-co-AAc-co-*N*-Aza-crown ether methacrylate) by Inverse Suspension Polymerization. The hydrogel beads are composed of a poly-(NIPAM-co-AAc) backbone with linear grafted poly-(NIPAM-co-*N*-Aza-crown ether methacrylate) side chains and a schematic representation is reported in Figure 104.

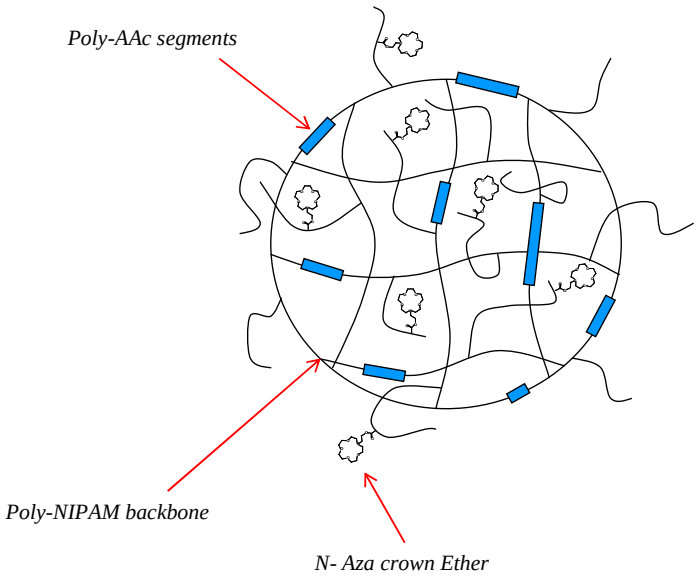

Figure 104: Graft-type poly-(NIPAM-co-AAc) incorporating N-Aza crown ethers (PGNACE).

A poly-(NIPAM-co-1-Aza-15-crown-5 methacrylate) macromonomer with a terminal hydroxyl group was first synthesised by radical telomerisation (telomerisation is a polymerization where a chain transfer agent, telomere, limits the molecular weight of the polymer product) of the NIPAM monomer and the 1-Aza-15-crown-5 methacrylate monomer, using HESH (2 mol %) as chain transfer reagent and Vazo 67 (0.5 mol %) as initiator (Figure 105). The weight average and the number-average molecular weights of the polymer were determined to be 2878 Da and 1729 Da, respectively (I = 1.664), by gel permeation chromatography. The presence of the chain transfer reagent, necessary in order to obtain the terminal –OH group, reduced the molecular weight even though the amount of the initiator was decreased to 0.5 mol % (in the first experiment, carried out without chain transfer agent, reported in the section 5.2, the initiator used was 1 mol % and the weight average and the number-average molecular weight were 5284 Da and 3177 Da, respectively). A spectrum of the polymer obtained by ^{1}H-NMR (reported in the appendix) confirmed the copolymerization of NIPAM and 1-Aza-15-crown-5 methacrylate. However, the amount of 1-Aza-15-crown-5 methacrylate copolymerized, calculated by ^{1}H-NMR, was 12 % and therefore, the monomer only reacted with 60 % conversion. Hence, the presence of the chain transfer reagent not only reduced the molecular weights of the copolymer but also the reactivity of the Aza-crown ether

monomer. Other experiments, following the same procedure described in section 3.3.11, were carried out increasing the ratio of Aza-crown ether monomer (NIPAM: 1-Aza-15-crown-5 methacrylate 3:1) in order to obtain a macromonomer with higher amounts of Aza-crown ether units but no substantial increase was detected by ^{1}H-NMR (13 mol % was obtained from a 3:1 feed against the 12 mol % obtained by a 4:1 feed).

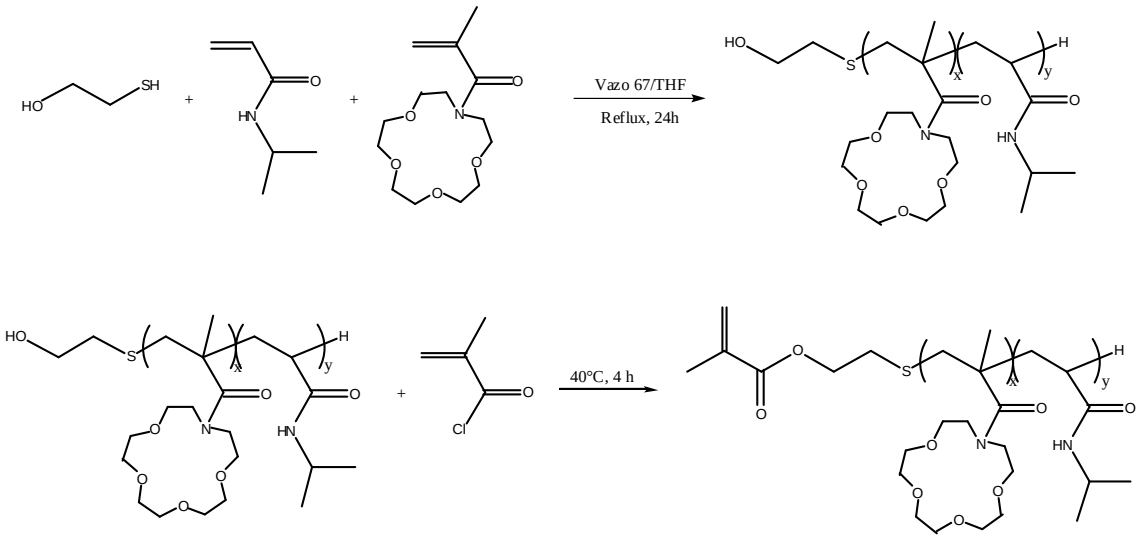

Figure 105: Synthesis of poly-(NIPAM-co-1-Aza-15-crown-5 methacrylate) macromonomer (PNCEM2) by Radical Telomerization.

The purified poly-(NIPAM-co-1-Aza-15-crown-5 methacrylate)-OH (section 3.3.12.) was subsequently reacted in mild conditions in a large excess of methacryloyl chloride at 40 °C (Figure 105).

^{1}H-NMR spectrum of the macromonomer was collected (Figure 106) and significantly, the peaks of the vinyl proton, at 5.2 and 6.0 ppm, were detected, indicating that a polymerizable end group was introduced into the hydroxyl poly-(NIPAM-co-1-Aza-15-crown-5 methacrylate).

Subsequently, three different macromonomers were successfully synthesised using the same procedure but changing the crown ether incorporated. Thus, poly-(NIPAM-co-1-Aza-12-crown-4 methacrylate) (PNCEM1), poly-(NIPAM-co-1-aza-15-crown-5

methacrylate) (PNCEM2), and poly-(NIPAM-co-1-aza-16-crown-6 methacrylate) macromonomers (PNCEM3) were synthesised.

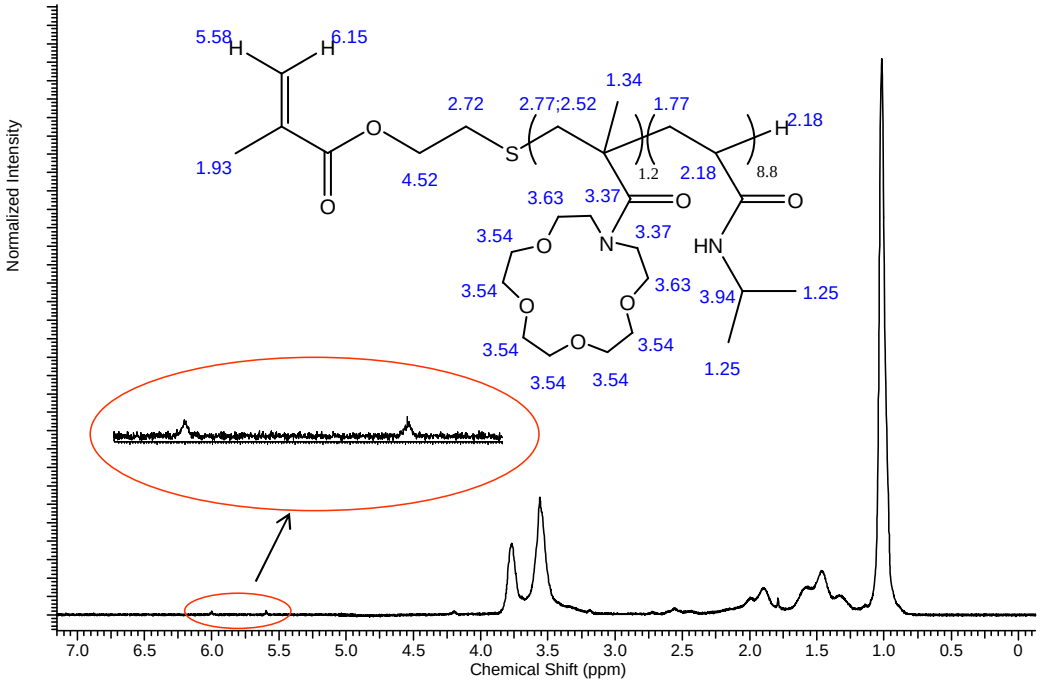

Figure 106: ^{1}H-NMR of poly-(NIPAM-co-1aza-15-crown-5 methacrylate) macromonomer (PNCEM2).

Graft-type poly-(NIPAM-co-AAc-co-1-Aza-15-crown-5 methacrylate) microgel was prepared by free radical inverse suspension copolymerization of poly-(NIPAM-co-1-Aza-15-crown-5 methacrylate) macromonomer (PGNACE) with NIPAM and AAc in the presence of BIS as a cross-linker (Figure 107). The backbone network was made of NIPAM and AAc monomers in order to confer to the material pH- and thermo-responsivity whereas, the linear poly-(NIPAM-co-1-Aza-15-crown-5 methacrylate) grafted served as free thermo-responsive chains able to catch and trap heavy metal ions in the Aza-crown ether cavity.

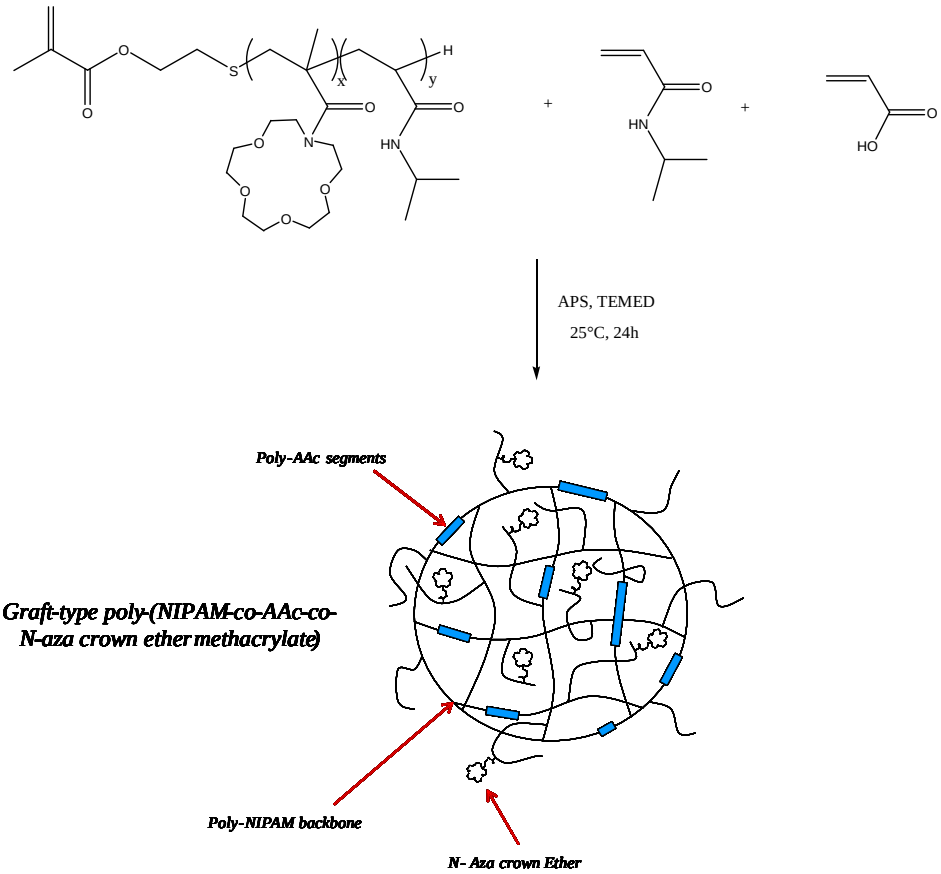

Figure 107: Synthesis of Graft-type poly-(NIPAM-co-AAc-co-Aza-crown methacrylate) by Inverse Suspension Polymerization (PGNACE).

The characterisation of these materials was complicated due to the low amount of crown ether incorporated in the macromonomer. In fact, assuming 100 % conversion of the macromonomer and the monomers, the total amount of Aza-crown ether incorporated is approximately 2 mol % which is not clearly detectable by solid state ^{13}H-NMR and IR.

Solid state ^{13}C-NMR did detect a bounce in the baseline at the correct place (70 ppm) but it is difficult to say for certain that it is due to the crown ether. The solid state ^{13}C-NMR spectrum is reported in Figure 108.

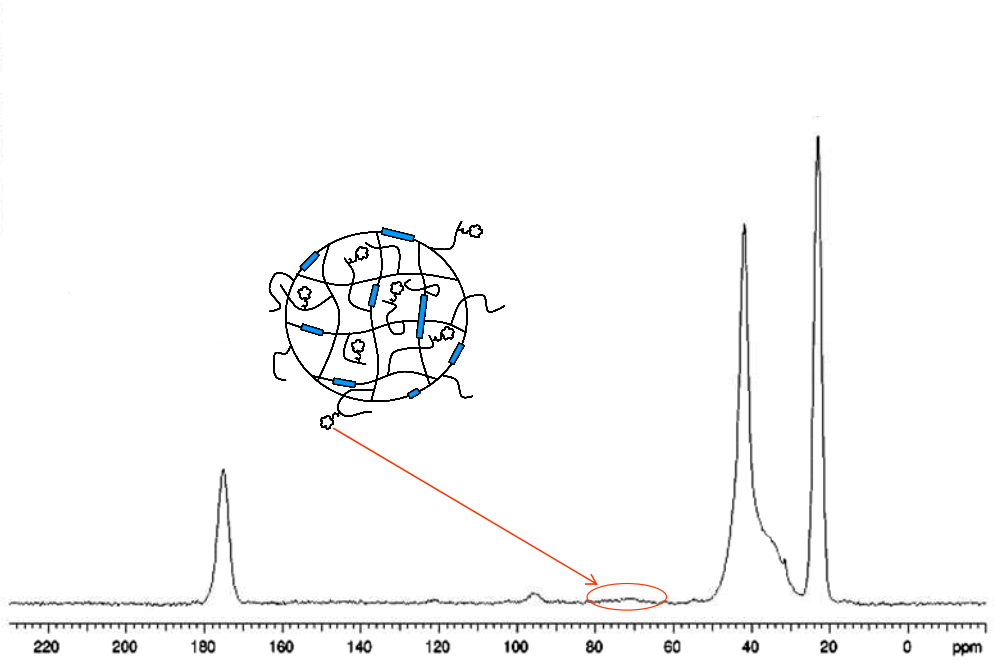

Figure 108: Solid state ^{13}C-NMR spectrum of Graft-type poly-(NIPAM-co-AAc-co-Aza-crown methacrylate) (PGNACE).

This issue was caused by the difficulty to introduce high amounts of Aza-crown ether monomers in the macromonomer. By decreasing the amount of chain transfer agent to 1 mol % in the synthesis of the poly-(NIPAM-co-1-Aza-15-crown-5 methacrylate)-OH, a small increase of incorporation was achieved (15 mol % with a 75 % conversion of the Aza-crown ether monomer). The ^{1}H-NMR of the final product (poly-(NIPAM-co-1-Aza-15-crown-5 methacrylate) macromonomer) showed that the methacryloyl chloride functionalised in the second step was dramatically reduced and therefore, a large part of the chains did not have a polymerizable end group. These macromonomers were also tested in the synthesis of graft-type hydrogel beads but more complications arose during the synthesis and beaded hydrogels were hardly obtained.

Other experiments were carried out increasing the macromonomer used, decreasing NIPAM and keeping AAc constant, in order to increase the amount of crown ether incorporated into the polymer network. This route has limitations since the macromonomer content cannot be too high as the hydrogel backbone has to be made mainly of linear polymers. In addition, high amounts of macromonomer can cause a

dramatic increase in viscosity of the monomer solution, and therefore a dramatic decrease of monomer reactivity due to the hindrance caused by the polymer chains. In an experiment carried out with twice amount of macromonomer (PGNACEX in section 3.3.12), significant increases in the Aza-crown ether was not detected by solid state ^{13}C-NMR.

5.4. Swelling measurements as function of temperature and pH of the dual-stimuli responsive poly-(NIPAM-co-AAc) hydrogel beads carrying *N*-Aza-crown ethers.

The materials studied in the following paragraph of this chapter are summarised in the following Table 25.

Table 25: Key materials discussed in this and in the following paragraphs of this chapter.

Sample	Composition	Section	Composition
PN	NIPAM	3.3.1.	----
PNA	NIPAM:AAc	3.3.4.	8 : 2
PNA1	NIPAM:AAc:1-aza-12-crown-4	3.3.7.	8 :1 :1
PNA2	NIPAM:AAc:1-aza-15-crown-5	3.3.7.	8 :1 :1
PNA3	NIPAM:AAc:1-aza-18-crown-6	3.3.7.	8 :1 :1

In general, the distributions of diameter of hydrogels prepared by suspension polymerization techniques are typically broad.[161] However, the distribution obtained by copolymerization of NIPAM and AAc (Figure 109) is not particularly broad: at 25 °C the average diameter is 116 μm with standard deviation of 35 μm. At 70 °C, above the LCST of the material, the distribution shifts to smaller diameters with an average of 93 μm and a standard deviation of 29 μm.

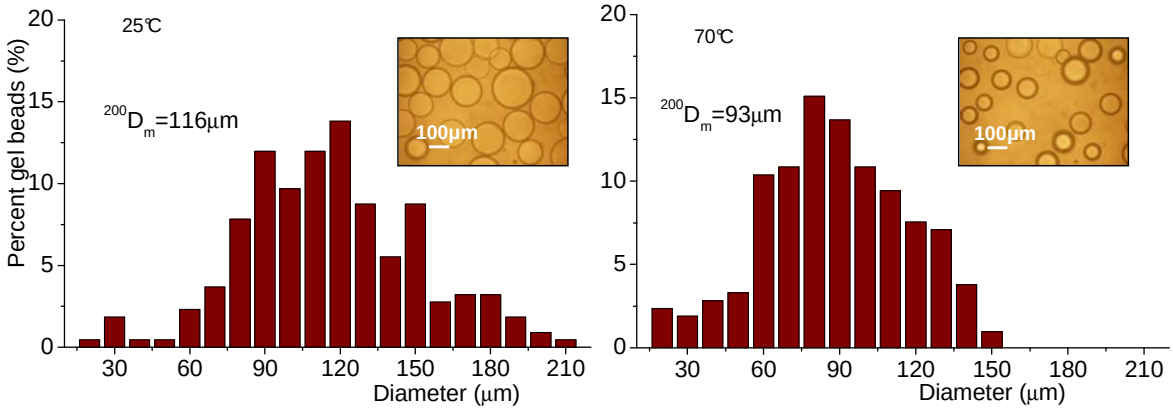

Figure 109: Diameters distribution of poly-(NIPAM-co-AAc) carrying 1-Aza-12-crown-4 (PNA1) in deionized water at 25 and 70°C.

Swelling degrees of PNA and PNA1 in aqueous solution and buffer pH 2 and 7.2 are plotted as function of temperature and in Figure 110.

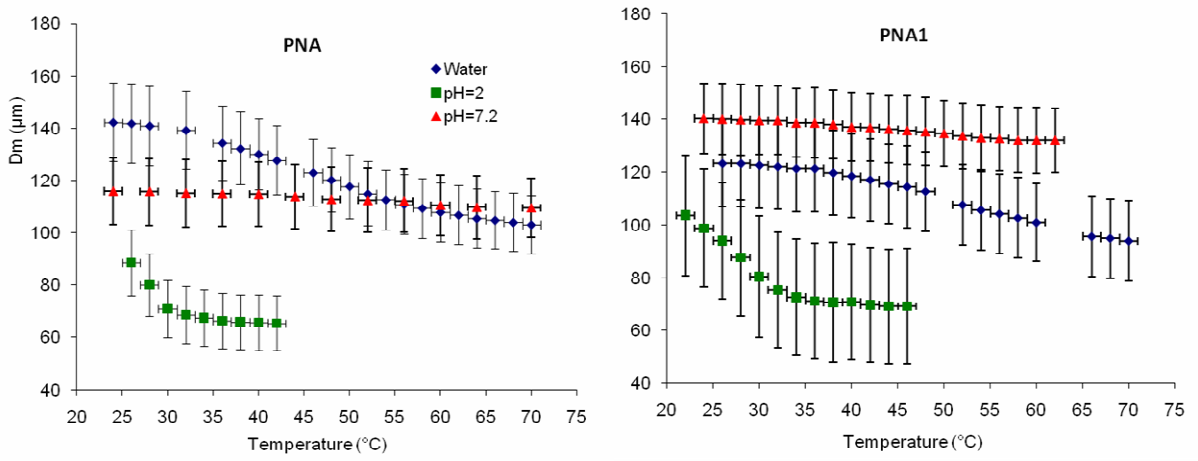

Figure 110: Temperature/pH dependence of $^{30}D_m$ of poly-(NIPAM-co-AAc) (PNA) and PNA1 in H_2O (●), pH 2 (■) and pH 7.2 (▲) buffer solution and the $^{30}D_m$ confidence intervals in the error bars.

These graphs were obtained by calculating the mean diameters of a population of about 30 beads and the error bar of each mean is reported in the graph as the confidence interval (α = 0.01) of the mean value. Figure 111 shows an example of the photographs taken for the PNA hydrogel ramp from 26 to 42 °C at pH 2.

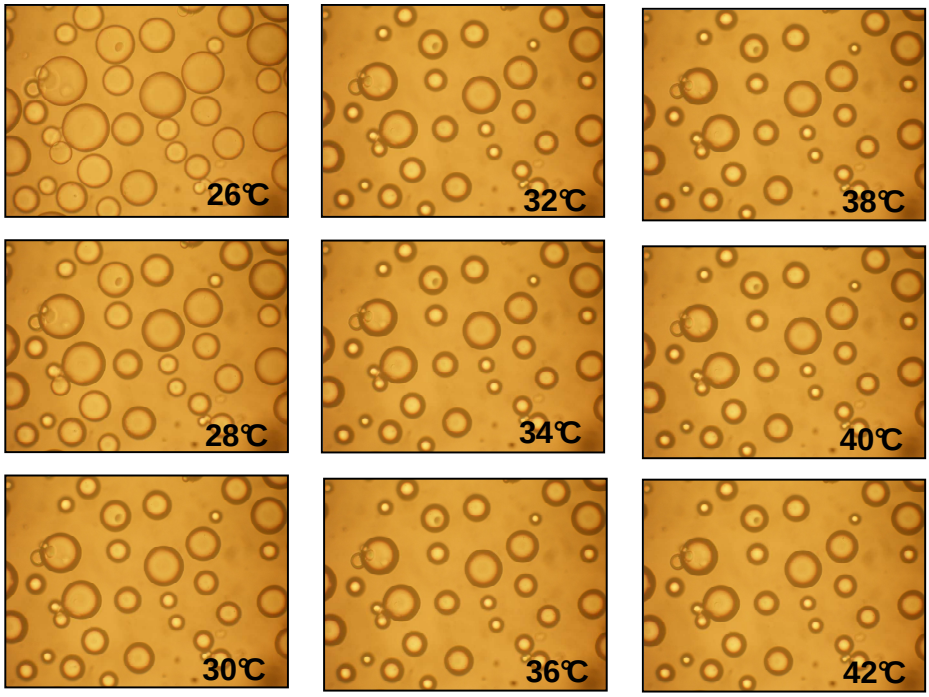

Figure 111: Photographs of the deswelling process of PNA hydrogel at pH 2.

The bead sizes are affected by different variables. In general, it should be mentioned that due to ionic strength effects, the degree of swelling of the hydrogels in pH buffer solution are usually smaller than in deionized water. In fact, the presence of salt breaks the clathrate structure of water molecules around the hydrophobic NIPAM hydrogel, leading the gel to collapse.[162] As expected, PNA hydrogel exhibits smaller diameters in buffer solutions with respect to those in water. It is also important to emphasise that the ionic strength depends upon concentrations and charges of the ions. Phosphate pH 7.2 buffer is composed of higher concentration of more charged ions than the pH 2 one and thus, it has higher ionic strength.

PNA displays pH-sensitivity exhibiting different swelling degrees at pH 2 and pH 7.2. At high pH, more PNA carboxylic groups (–COOH) are in their deprotonated anionic form ($–COO^-$) and this results in an increasing internal electrostatic repulsion. Thus, larger diameters and increase water absorption. Conversely, at low pH the PNA carboxylic groups are in their protonated form and additionally probable hydrogen-bonding between NIPAM and AAc units decreases further the hydrogel size.[163] Furthermore, the diameters

of PNA at pH 7.2 decrease less rapidly as function of temperature than those in deionized water and buffer pH 2. This suggests that also the temperature transitions are effected by ionic strength and the higher value of phosphate solution visibly reduces the thermo-responsive behaviour of the material. However, PNA at pH 2 displays a large change in size in response to temperature and thus excellent thermo-sensitivity.

The incorporation of new functional groups onto AAc should result in a reduction of pH-sensitivity; however, this is not observed and PNA1 exhibits larger diameters at both pH and an increased pH-response. Furthermore, the addition of *N*-Aza-crown ether does not affect the NIPAM thermo-sensitivity either in deionized water or in the buffers. The high PNA1 diameters in the buffers suggest that the introduction of *N*-Aza-crown ether adds a new contribution on the bead sizes that may be the result of the crown ether ability to scavenge the buffer metal ions. PNA1 at pH 7.2 exhibits a higher increase in diameters than that at pH 2. Phosphate buffer contains higher amounts of metals available for the *N*-Aza-crown and acrylic acid sites and at pH 7.2 the crown ether nitrogen lone pairs can freely interact with the cations (at pH 2 such activity is reduced by protonation of such lone pairs). The same increase is not observed in water which supports the assumption that *N*-Aza-crown incorporation affects the bead sizes only in presence of metal ions in solution. Indeed, in deionized water the PNA1 swelling degrees results slightly smaller than those of PNA. The introduction of *N*-Aza-crown ether decreases the quantity of hydrophilic acrylic acid groups and the hydrophilicity of the material results, therefore, decreased.

In order to confirm the ionic and the scavenging effect discussed, PNA1 was allowed to swell in aqueous solutions containing increasing amounts of KCl and the result obtained is illustrated in Figure 112.

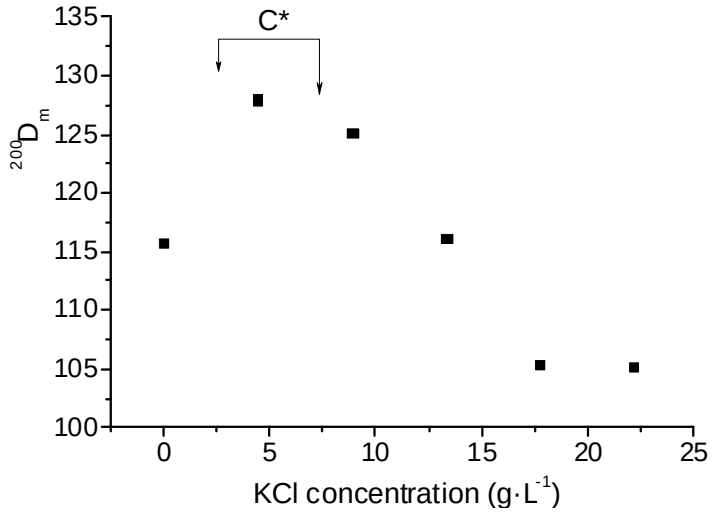

Figure 112: Swelling degrees of PNA1 in aqueous solutions containing increasing amounts of KCl, C* is a critical concentration.

At KCl concentration below a particular critical concentration (C*), the beads are in a swollen state and their $^{200}D_m$ is larger than that in deionized water. However, when the KCl concentration exceeds C*, the hydrogel beads begin to shrink reaching $^{200}D_m$ values below the deionized water one for high concentration of salt. At the low KCl concentration, the scavenging effect has the major contribution, as the ionic strength is still low resulting in the beads to swell. When the concentration of KCl reaches C*, the ionic strength is sufficiently high to play the major rule over the scavenging effect and this results in the beads shrinking.

For practical reasons the swelling degree test reported in Figure 110 was based on the observation of about 20-30 hydrogel beads. Due to small sample population observed these results are not statistically significant as indicated by the error bars of the different pH conditions overlapping in most of the measurements. However, $^{200}D_m$ (Table 26) have much lower confidence intervals (Table 26) and $^{30}D_m$ values of both PNA and PNA1 in the different solutions differ by less than 5 %, which suggest that 30 beads per population is representative for the system.

Table 26: Temperature/pH dependence and confidence interval (CI) of $^{200}D_m$ in H_2O, pH 2 and pH 7.2 buffer solutions for PNA and PNA1.

	PNA		PNA1	
	$^{200}D_m$ (μm) 25°C	$^{200}D_m$ (μm) 70°C	$^{200}D_m$ (μm) 25°C	$^{200}D_m$ (μm) 70°C
	CI	CI	CI	CI
H_2O	138	98	116	93
	6	6	6	5
pH=2	96	66	91	79
	6	5	4	4
pH=7.2	123	110	138	129
	6	6	6	5

5.5. Autoradiography experiments.

Preliminary autoradiography tests were carried out in order to estimate the sequestering activities of the selected materials (see Table 25) in different environmental conditions of pH and temperature.

Figure 113 shows the autoradiography testes obtained for PN (poly-NIPAM hydrogel), PNA (poly(NIPAM-co-AAc)), PNA1 (poly-(NIPAM-co-AAc) hydrogel incorporating 1-Aza-12-crown-4), PNA2 (poly-(NIPAM-co-AAc) hydrogel incorporating 1-Aza-15-crown-5) and PNA3 (poly-(NIPAM-co-AAc) hydrogel incorporating 1-Aza-18-crown-6) in sequestration of Sr 90.

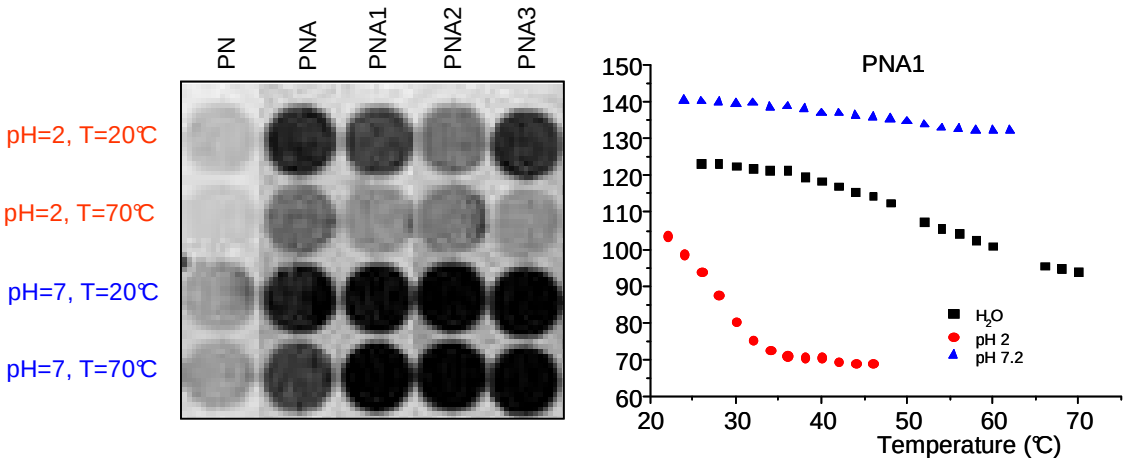

Figure 113: Autoradiography tests for PN, PNA, PNA1, PNA2 and PNA3 towards Sr-90 and the swelling experiments reported in Figure 110.

In general, in autoradiography a material able to retain a large quantity of radionuclide displays a dark spot whereas one unable displays a lighter one. The darkness of the spot can be translated in an average intensity background and the values related to the Figure 113 are listed in Table 27.

Table 27: Average intensity backgrounds for NIPAM hydrogels in sequestering experiments of Sr-90.

Conditions	Average Intensity Background				
	PN	PNA	PNA1	PNA2	PNA3
pH=2 T=20°C	446	1602	1390	1028	1568
pH=2 T=70°C	332	1071	984	793	806
pH=7 T=20°C	756	1788	1983	2072	1858
pH=7 T=70°C	689	1460	2038	1957	2034

Hydrogel beads based on only NIPAM (PN) exhibits the lowest activity in sequestration of Strontium 90 displaying light spots and low average intensity backgrounds. As expected, the introduction of acrylic acid (PNA) improves the activity of the material as acrylic acid can, when de-protonated, electrostatically attract cations (unexpectedly, PNA

also registered a good decontamination activity for pH 2). However, the highest activities were registered for the hydrogels incorporating *N*-Aza-crown ethers.

In general, all materials display enhanced activity at pH 7 that is likely because at such pH the nitrogen lone pairs of NIPAM and Aza-crown ethers are in their free form and the AAc groups are deprotonated. Thus, all the moieties which enable the hydrogel to scavenge cations are in their active form and the materials retain more Sr-90.

The swelling experiment reported in Figure 110 and added in Figure 113 perfectly matches with the autoradiography results: at pH 7, PNA1 exhibits high sequestering activity with a small effect given by temperature when the swelling test shows large diameters and small temperature transition; on the other hand, at pH 2, autoradiography displays much less activity and higher thermo-sensitivity when similarly the swelling experiment shows a greater temperature transition and smaller diameters. All this seems to suggest that the scavenging activity of PNA1 is proportional to the size of the material. The possibility that the beads just physically adsorb the metals in the structure along with water can be excluded as the swelling experiments (Figure 110) showed that PNA1 in deionized water exhibited smaller diameters than PNA in deionized water which imply that the introduction of *N*-Aza-crown ether decreases the hydrophilicity of the hydrogel. Decreasing hydrophilicity should lead the material to adsorb smaller quantity of water and this does not explain the increasing Strontium 90 removal. In addition, the crown ethers are functionalized onto the AAc groups and this reaction should decrease the pH response of the entire material as the amount of AAc moieties decrease. However, PNA1 exhibits larger diameters and higher Sr 90 decontamination at pH 7 which strongly imply that that is caused by the introduction of Aza-crown ether in the gel beads.

Although this experiment is only a preliminary evaluation of the hydrogel scavenging properties, the results seem to suggest that these materials may exhibit better selectivity at low pH. In fact, PNA1, PNA2 and PNA3 displayed high and similar average intensity backgrounds at pH 7 at 20 and 70 °C whereas at pH 2 PNA3 displays the highest intensity followed by PNA1 and last PNA2. The loss of selectivity can be, in general, explained by the crown ethers, being able to trap metal ions through 1:1 centro-

symmetrical conformations and/or 2 : 1 sandwich structures (discussed in section 1.2.) allowing Sr 90 retention also by the hydrogels carrying smaller crown ether rings.

In conclusion, the removal of Sr 90 by the poly-(NIPAM-co-AAc) hydrogels incorporating Aza-crown ethers is clearly influenced by environmental changes of pH and temperature. At pH 2 the activity is to some extent smaller than at pH 7 and dependent upon temperature and for example PNA3 displays twice higher Sr 90 removal activity at 20 °C respect to that at 70 °C. The removal is also dependent upon pH and for example both PNA2 and PNA3 display an increase of removal activity of about 2.5 times from pH 2 to pH 7 at 70 °C.

Autoradiography tests on the removal of Co 60 were also carried out and the results obtained are reported in Figure 114.

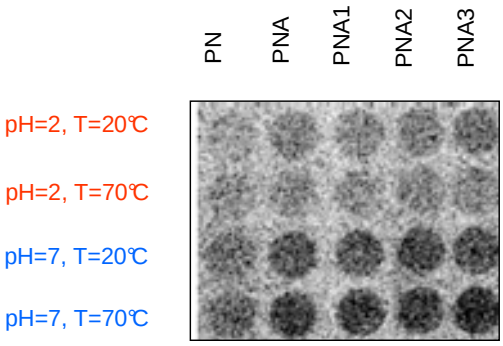

Figure 114: Autoradiography tests for PN, PNA, PNA1, PNA2 and PNA3 in removal of Co 60.

The related average intensity backgrounds are listed in Table 28.

Table 28: Average intensity backgrounds for the materials showed in Figure 114 for the removal of Co 60.

Conditions	Average Intensity Background				
	PN	PNA	PNA1	PNA2	PNA3
pH=2 T=20°C	32	50	55	49	60
pH=2 T=70°C	43	43	39	48	46
pH=7 T=20°C	55	85	79	93	88
pH=7 T=70°C	78	98	97	101	113

Differently from the previous Strontium autoradiography tests, the removal of Co 60 is not significantly enhanced by the introduction of Aza-crown ethers a part for a little increase displayed by PNA2. On the other hand, in accordance with the earlier results, the materials have enhanced activity at pH 7 and some extent of thermo-sensitivity at both pH.

5.6. Scintillation counting experiments.

A confirmation of the autoradiography tests and a quantitative estimation of the sequestering properties of the materials were obtained by scintillation counting experiments. These new tests were also carried out in different environmental conditions of pH and temperature. In the course of these experiments the selectivity of the materials was also estimated; each hydrogel was tested in parallel under two different conditions: first, with the targeted radionuclide on its own and then with the target radionuclide in competition with a common non-hazardous metal ion of size comparable to the radionuclide. Thus, Caesium (1.67 Å) was tested in competition with Potassium (1.33 Å), Strontium (1.18 Å) in competition with Calcium (1.00 Å) and Cobalt (0.65 Å) with tap water which contains many cations such as Potassium, Calcium and Sodium (0.97 Å).

The Caesium results are showed in the following Table 29.

Table 29: Scintillation results for PNA hydrogels towards Cs on its own and in competition with K.

	Caesium-Removal					Cs+K-Removal				
Conditions	PN	PNA	PNA1	PNA2	PNA3	PN	PNA	PNA1	PNA2	PNA3
pH=2, T=20°C	0	0	0	0	0	1	0	1	0	1
pH=2, T=70°C	0	0	0	0	0	0	1	1	1	0
pH=7, T=20°C	0	30	39	34	40	0	30	27	29	27
pH=7, T=70°C	1	30	37	35	40	0	29	25	30	26

Autoradiography experiments showed that the removal of the materials was tuneable by environmental changes of pH and temperature whereas this latter experiments show that only pH is affecting it. This suggests that there is a kinetic factor that needs to be considered in the thermo-responsive behaviour. The contact times used in autoradiography were in the order of minutes whereas in the scintillation counting extractions the materials were left to interact with the contaminated solution for 1 hours (some experiments were also carried out increasing the contact time to either 6 and 24 hours but no difference in retention was observed). This shows that the thermo-responsivity of the radiological retention is in terms of different contaminants absorption speeds at different temperatures. At low temperature the materials are more hydrophilic and rapidly incorporate the contaminants along with water into the network; on the other hand, at high temperature they become more hydrophobic and incorporate those relatively more slowly. When the material has sufficient time to interact with the solution it reaches an equilibrium retention value which is independent upon temperature.

At pH 2, all materials display a Caesium removal near or equal to 0 %. In this condition the AAc acid groups, the Aza-crown ether and the NIPAM nitrogens are protonated and therefore inactive towards cations. On the other hand, at pH 7 such groups can freely interact with Caesium ions. Although at pH 7, Caesium removal is not exhibited by the hydrogel based on only NIPAM (PN); this confirms the low results generally obtained in autoradiography for such material. The introduction of AAc (PNA) improves the removal to 30 % but the highest results are obtained for the materials incorporating *N*-Aza-crown

ethers - the improvements given by this addition are in the range of 4-10 %. As similarly observed in autoradiography, different size of the crown ether have a relatively small effect on the activity of the materials, yet this is probably due to a cooperation of the entire polymer structure in the metal sequestration.

In the experiments in competition with Potassium, PNA displays the same activity equal to 30 %; this means that although the materials do not display an excellent removal, it is highly selective. However, materials incorporating *N*-Aza-crown ethers (PNA1, PNA2 and PNA3) displays a decreased Caesium decontamination in presence of Potassium which indicates that these materials are not selective.

The Strontium results are showed in the following Table 30.

Table 30: Scintillation results for PNA hydrogels towards Sr on its own and in competition with Ca.

	Sr-Removal					Sr+Ca-Removal				
Conditions	PN	PNA	PNA1	PNA2	PNA3	PN	PNA	PNA1	PNA2	PNA3
pH=2, T=20°C	0	0	0	0	0	0	1	0	0	0
pH=2, T=70°C	0	0	0	0	0	0	1	0	1	0
pH=7, T=20°C	22	91	94	95	97	11	47	46	47	46
pH=7, T=70°C	29	91	95	95	94	17	48	45	44	44

As previously observed, all materials display a metal ion removal to some extent only at pH 7. Furthermore, this is not affected by either temperature or the different crown ether introduced. Conversely to the earlier results, in the case of Strontium removal, PN displays some retention activity of around 20-30 %. Such activity increases then to around 90 % as AAc is incorporated and reaches the highest value at 95 % as crown ether is added. Thus, similarly to the previous results, the introduction of crown ether increases further on the ability of the material to incorporate cations.

In the experiments carried out in competition with Calcium, all materials display lower retention which indicates that these materials are poorly selectivity in Strontium removal.

Results for Cobalt are showed in the Table 31.

Table 31: Scintillation results for PNA hydrogels towards Co on its own and in competition with Tap water.

	Co-Removal					Co+Tap-Removal				
Conditions	PN	PNA	PNA1	PNA2	PNA3	PN	PNA	PNA1	PNA2	PNA3
pH=2, T=20°C	0	0	0	0	0	0	1	1	0	0
pH=2, T=70°C	0	0	0	0	0	0	0	0	0	1
pH=7, T=20°C	1	85	96	96	94	9	85	93	90	92
pH=7, T=70°C	2	92	96	94	96	1	80	86	93	92

The best results were obtained for the Cobalt removal experiments. PN exhibits Cobalt decontamination near 0 % at all conditions whether tap water was used or not in the solution. The introduction of AAc raises the activity to 85-90 % but the highest values around 95-96 % were obtained for the hydrogels carrying crown ethers. These hydrogels, as the others, do not show much thermo-sensitivity and are only active at pH 7. More importantly, the removal does not substantially decrease in the presence of the salts contained in tap water which indicate that the materials are highly selective for Co over the presence of various non-hazardous ions.

In order to ensure reproducibility of the experiments, some extractions for PNA1 were repeated 3 times in exactly same conditions and with double amount of material. The results obtained are listed in Table 32.

Table 32: Reproducibility experiments for PNA1 and error bar.

Isotope	Temperature (ºC)	pH	% absorption	Mass of beads (mg)	Error
Caesium	20	7	37.64	10	0.51
			39.26	10	
			39.05	10	
			51.64	20	
	70		36.95	10	0.39
			38.23	10	
			37.98	10	
			50.88	20	
Strontium	20	7	94.26	10	0.08
			94.13	10	
			94.39	10	
			95.43	20	
	70		91.58	10	1.03
			91.78	10	
			94.78	10	
			93.22	20	

The method shows good reproducibility and double quantities of hydrogel beads give higher decontamination percentage (in range of 13-14 %) in a solution containing the same quantity of radionuclide. Based on these experiments it is also possible to calculate the error associated to the measurement using the formula: $error = \sigma / \sqrt{n}$, where σ is the standard deviation and *n* is the number of observations; the calculated values are reported in Table 32.

In conclusion, the decontamination activity of the selected materials (PN, PNA, PNA1, 2, 3) was studied for removal of Sr Co and Cs. The materials based on only NIPAM generally resulted in decontaminations near 0 %. As AAc is added, the PNA hydrogel generally displays an increase decontamination which is further increased by incorporation of the crown ethers (PNA1, 2 and 3). Different crown ethers did not show a defined difference in decontamination as probably the whole polymer network cooperates in the metal incorporation. However, scintillation counting tests showed that PNA1, 2

and 3 have good selectivity towards at least Cobalt in presence of non hazardous metals such as Na, K and Ca.

Furthermore, PNA, PNA1, 2 and 3 are pH and thermo-responsive also in terms of decontamination if in contact with radionuclide solutions for short times. Such pH and thermo-sensitivity was not generally observed during the scintillation counting experiments where the hydrogels and the contaminant solution were left in contact from 1 to 24 hours.

Chapter 6

Thermo-Responsive Copolymers based on non-linear PEG incorporating *N*-Aza-crown ethers

6.1. Preparation of *N*-Aza-crown ether incorporated, dual-stimuli responsive poly-(MEO_2MA-co-$POEGMA_{475}$-co-HEMA) hydrogel beads (PEGMAf1, 2 and 3, section 3.4).

Poly-(MEO_2MA-co-$POEGMA_{475}$-co-HEMA) hydrogel beads incorporating *N*-Aza-crown ethers were prepared following the route schematically shown in Figure 115.

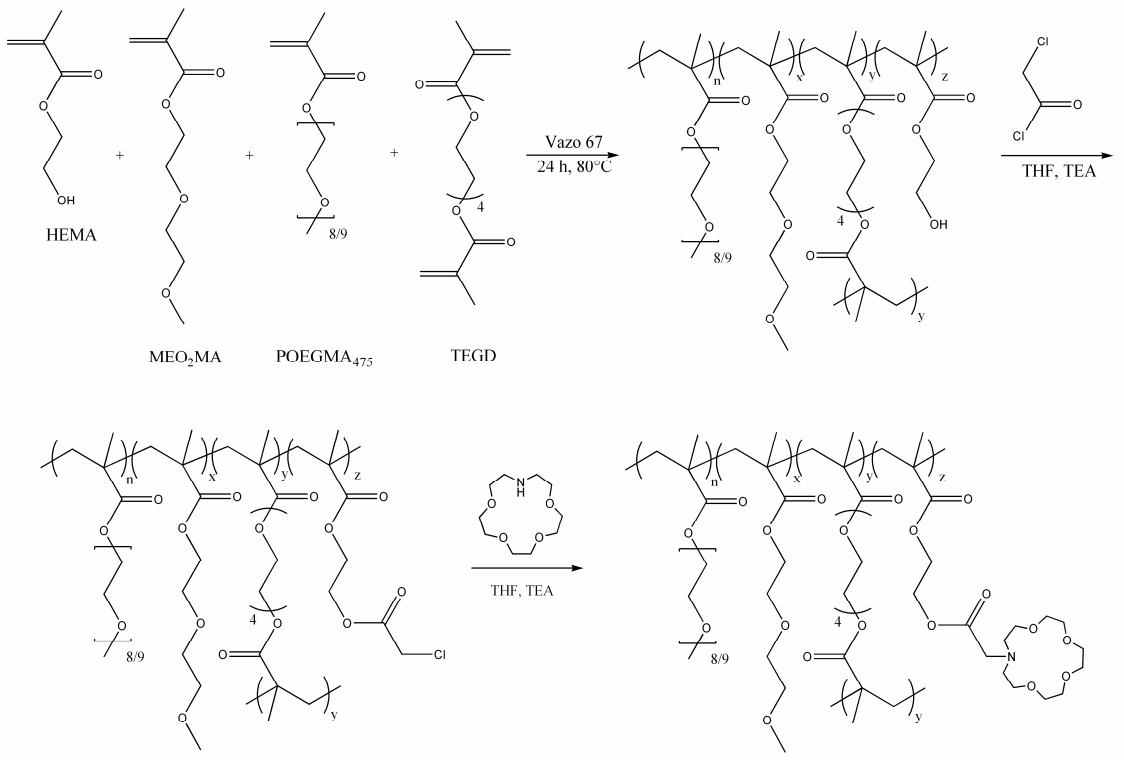

Figure 115: The synthetic scheme of incorporated N-Aza-crown ether poly-(MEO_2MA-co-$POEGMA_{475}$-co-HEMA), PEGMAf2.

6.1.1. Synthesis of the beads (PEGN, PEG, PEGCE, PEGNH, PEGNHfCE, PEGNHf, PEGNHf2, PEGA, section 3.4.1, 2, 3, 4, 5, 6, 7, 8, 9.).

The backbone network was made of MEO_2MA and $OEGMA_{475}$ (85 : 15 mole ratio) in order to obtain a swellable thermo-responsive hydrogel with LCST comparable to that of poly-NIPAM hydrogels;[13] in addition such hydrogel support is relatively insensitive to metal ions due to the absence of strong electron donors. HEMA was introduced into the polymer network as substrate for post-functionalization reactions.

Poly-(MEO_2MA-co-$OEGMA_{475}$-co-HEMA), designated as PEGMA, was first synthesized by free radical suspension copolymerization technique. The suspending agent is, in general, a key factor in suspension polymerization reactions as it decreases the interfacial tension between the monomer droplet and water to promote the dispersion of droplets and produce a thin layer around the droplet which prevents coalescence when a collision occurs. H_2O was used as continuous phase as the non-linear PEG monomers and cross linker agent are insoluble in such solvent. Different water soluble surfactants were tested and all experiments carried out are listed in the experimental section (section 3.4).

SDS (sodium dodecyl benzene sulfonate) was the first surfactant used and MEO_2MA homopolymerization (PEGN) and $MEO_2MA/OEGMA_{475}$ copolymerization (PEG) were carried out obtaining beaded hydrogels without evident amorphous polymer. The completed characterizations of both materials are listed in the section 3.4.1, 2 and shown in the appendix section (Figure 14 and Figure 15 in the appendix). After a successful suspension polymerization of the oligo-(ethylene glycol) methacrylate monomers; a copolymerization of MEO_2MA, $OEGMA_{475}$ and 1-Aza-18-crown-6 methacrylate was attempted (PEGCE). However, the presence of Aza-crown ether was not observed either by solid-state ^{13}C-NMR (reported in the appendix in Figure 16) or elemental analyses (listed in section 3.4.3). In particular the latter showed 0 % presence of N which is consistent with the unsuccessful copolymerization of the Aza-crown ether monomer in the hydrogel beads.

SDS was, then, tested on MEO_2MA/HEMA copolymerization (PEGNH). An issue in suspension copolymerization of HEMA, MEO_2MA and $OEGMA_{475}$ is the fact that HEMA is a water soluble monomer whereas MEO_2MA and $POEGMA_{475}$ are soluble in

organic solvents. As HEMA was used in the minority with respect to the other monomers, water was selected as continuous phase and a salting out agent was employed in order to reduce the solubility of HEMA in the continuous phase and allow copolymerization in the organic layer. NaCl (20 % aqueous solution) has been previously used as salting out agent on suspension homopolymerization of HEMA.[164, 165] However, when trying to dissolve SDS in NaCl aqueous solution, NaCl was acting as salting out agent towards the surfactant preventing its solubilization in the continuous phase and vice-versa if NaCl was added to the aqueous solution containing the surfactant, the SDS was preventing the solubilization of NaCl acting as a salting out agent. Thus, SDS was tested as surfactant and salting out agent by increasing its concentration in the continuous phase. However, incorporation of HEMA into the polymer was not observed as FT-IR spectra did not show a new broad peak in the region around 3500 cm^{-1}. Hexanol, which is a very good solvent for HEMA, was added into the monomer mixture in order improve the solubility of HEMA in the monomer phase with respect to the continuous phase; but still HEMA was not incorporated. HEC (Hydroxyethyl Cellulose), another water soluble surfactant, was found to be soluble in NaCl aqueous solution and was, therefore, tested in conjunction with another water soluble stabilizer, PVA (Poly vinyl alcohol). The new surfactant system was successful on both MEO_2MA/HEMA (PEGNH) and MEO_2MA/$POEGMA_{475}$/HEMA copolymerizations (PEGH) and the hydrogel beads obtained contained HEMA monomer as shown by FT-IR spectra (Figure 116). A new peak in the region around 3500 cm^{-1} belonging to the –OH of the HEMA appeared confirming the successful incorporation.

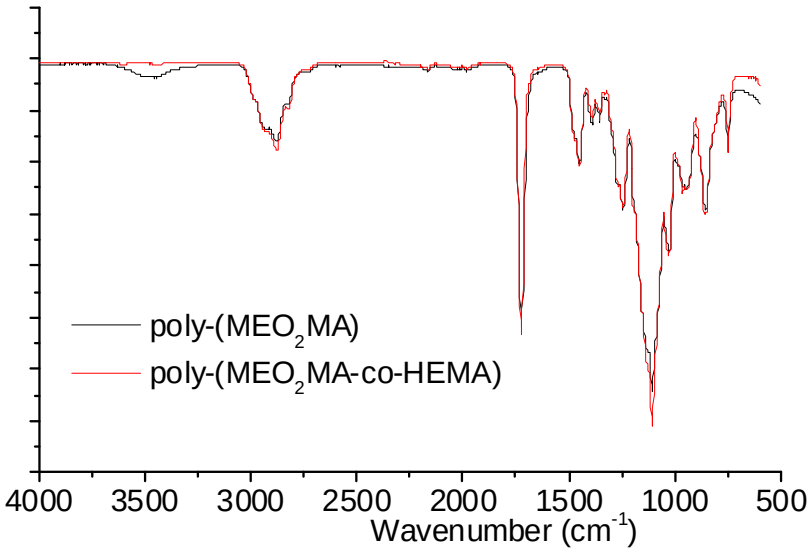

Figure 116: FT-IR spectra for poly-(MEO_2MA), PEGN, and poly-(MEO_2MA-co-HEMA), PEGNH.

Both MEO_2MA/HEMA and MEO_2MA/$POEGMA_{475}$/HEMA copolymers were, subsequently, successively post-functionalized by reaction with chloroacetyl chloride (PEGNHf) and N-Aza crown ethers (PEGNHf2) following the route reported in Figure 115. However, when the materials were re-dispersed in water, the hydrogel beads network slowly decomposed and after 24 hours only an amorphous powder was left in the aqueous solution. A reasonable explanation was given; organic polymer surfactants are often difficult to remove from the gel particles after suspension polymerization and so, they remain as a thin layer around the polymer droplets. HEC and PVA contain several hydroxyl groups and triethylamine traces may partially deprotonate this groups allowing their attack to the ester group of the cross linker with consequent breaking down of the hydrogel network. Inorganic powders can also be used as stabilizers in suspension polymerization reaction and such surfactants can be easily washed off using dilute acid.[120] The first inorganic powder system tested was $MgCl_2$ (magnesium chloride) as surfactant in conjunction with NaCl as salting out agent. Copolymerization of HEMA was successful; however, although the material was mostly beaded, it contained some coagulated polymer. MEO_2MA/HEMA copolymerization was then carried out using magnesium oxide (MgO) as stabilizing and salting out agent. The use of this inorganic powder in suspension homopolymerization of HEMA was reported in 1992.[166] Finally, a

suitable system was found and MgO (3 gr in 200 ml of H_2O) succeeded in both MEO_2MA/HEMA (PEGNH) and MEO_2MA/$POEGMA_{475}$/HEMA (PEGMA) copolymerizations. The hydrogels obtained in these conditions were, in fact, completely beaded without any coagulum and exhibited a new broad peak at 3500 cm^{-1} in their FT-IR spectrum which belongs to the HEMA hydroxyl groups.

6.1.2. Functionalization of the beads (PEGMAf, PEGMAf1, 2, 3, section 3.4.9, 10, 11.).

PEGMA was then post-functionalized following the route already reported in Figure 115. Chloroacetyl chloride was first incorporated to give a chloro acetylated PEGMA hydrogel (PEGMAf). PEGMAf was, then, reacted with a range of different ring size *N*-Aza-crown ethers and the resulting hydrogels are designated as PEGMAf1, PEGMAf2 and PEGMAf3 incorporating 1-aza-12-crown-4, 1-aza-15-crown-5 and 1-aza-18-crown-6, respectively. Successful incorporation was first confirmed by ^{13}C-NMR spectroscopy (Figure 117).

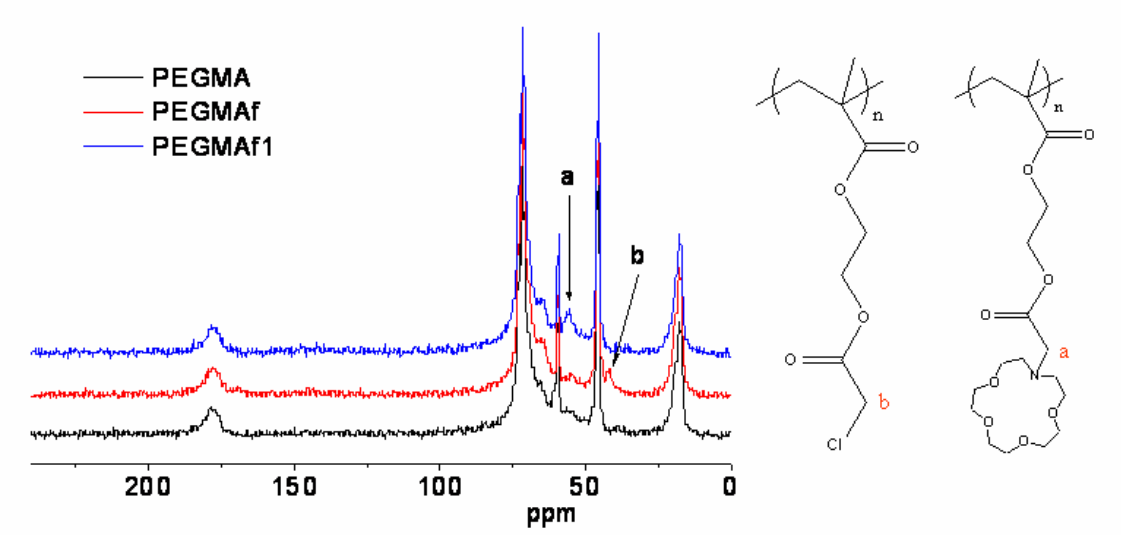

Figure 117: Solid-state ^{13}C-NMR spectra for PEGMA, PEGMAf and PEGMAf1 (a ~ 56 ppm, b ~ 42 ppm).

Solid-state ^{13}C-NMR spectrum of the PEGMA exhibited five broad peaks at 14-22 ppm (–CH_3 MEO_2MA and $PEOGMA_{475}$), 44-48 ppm (–CH– and –CH_2– backbone), 58-62

ppm (–O–CH_3 MEO_2MA and $PEOGMA_{475}$), 62-80 (–O–CH_2– MEO_2MA and $PEOGMA_{475}$) and 174-182 (–O–CO–) (black line in Figure 117).

Solid-state ^{13}C-NMR spectrum was also recorded after post-functionalization with chloroacetyl chloride and *N*-Aza-crown ether (PEGMAf and PEGMAf1, respectively, in Figure 117). The first spectrum showed the appearance of a new small signal at 42 ppm which belongs to the –CH_2–Cl of the chloroacetyl group. This signal disappeared in the PEGMAf1 spectrum, or actually, shifted towards higher yield (~ 56 ppm, –CH_2–N–) which is consistent with a successful post-functionalization with *N*-Aza-crown ether.

Elemental Analysis was carried out and the analysis for PEGMA, PEGMAf and PEGMAf1 are shown in the experimental section. This analysis was useful to clarify whether the crown ether was covalently bonded to the hydrogel or just physically absorbed. As expected, after functionalization with chloroacetyl chloride an increasing in chlorine content was observed as chloroacetyl groups were incorporated into the polymer matrix. After reaction of these groups with *N*-Aza-crown ether, the chlorine content decreases to 0 weight % whereas nitrogen content increases to 0.97 weight % which is consistent with the completed functionalization of the chloroacetyl groups by N-Aza-crown ethers. Although only the characterization for PEGMAf1 is discussed, similar evidences were observed with PEGMAf2 and PEGMAf3 and the fully characterization is reported in the experimental section.

In order to estimate the crown ether content, a controlling experiment was carried out. In this test PEGMAf was reacted in anhydrous THF and TEA in the same conditions of PEGMAf1, PEGMAf2 and PEGMAf3 but without the Aza-crown ether. Elemental analysis gave similar element contents as PEGMAf which suggest that in the functionalization reactions the crown ether completely replaced the chlorine into the beads as PEGMAf1/2/3 elemental analysis displayed approximately 0% chlorine. Thus, if we assume a 100% yield and a complete replacement of chlorine the Aza-crown ether contents are calculated as 14, 18 and 22 weight % for PEGMAf1, PEGMAf2 and PEGMAf3 respectively.

Figure 118 shows the TGA analysis of PEGMA, PEGMAf, PEGMAf1, PEGMAf2 and PEGMAf3.

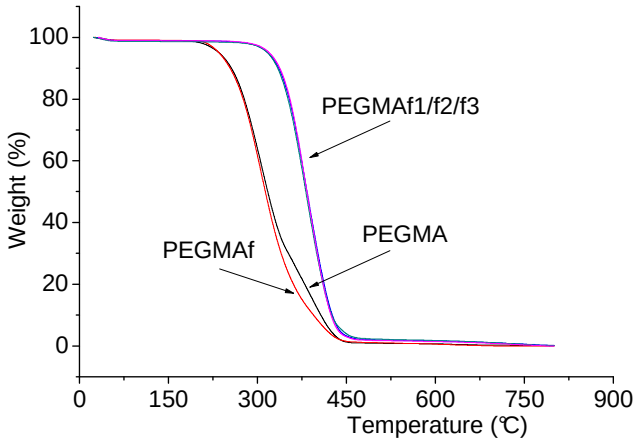

Figure 118: TGA analysis for PEGMA, PEGMAf, PEGMAf1, PEGMAf2 and PEGMAf3.

It can be clearly seen that the incorporation of N-Aza-crown ether has an effect on the thermal stability of the hydrogel. With the incorporation of *N*-Aza-crown ethers, new ethylene glycol groups are added into polymer network which result in an increase in stabilising "Van Der Waals" interactions. Thus, PEGMAf1, PEGMAf2 and PEGMAf3 exhibited 100 °C higher weight loss onsets with respect to PEGMA and PEGMAf hydrogels.

6.2. Swelling measurements as function of temperature and pH of thermo-responsive poly-(MEO_2MA-co-$OEGMA_{475}$-co-HEMA) hydrogel beads carrying *N*-Aza-crown ethers.

As found for the poly-(NIPAM-co-AAc) beads, the distribution diameters of the materials based on MEO_2MA, $POEGMA_{475}$ and HEMA (Figure 119) is not particularly broad: at 25°C the average diameter is 231 μm with standard deviation of 51 μm. At 70 °C, above the LCST of the material, the distribution shifts towards smaller diameters with an average diameter of 191 μm and a standard deviation of 39 μm.

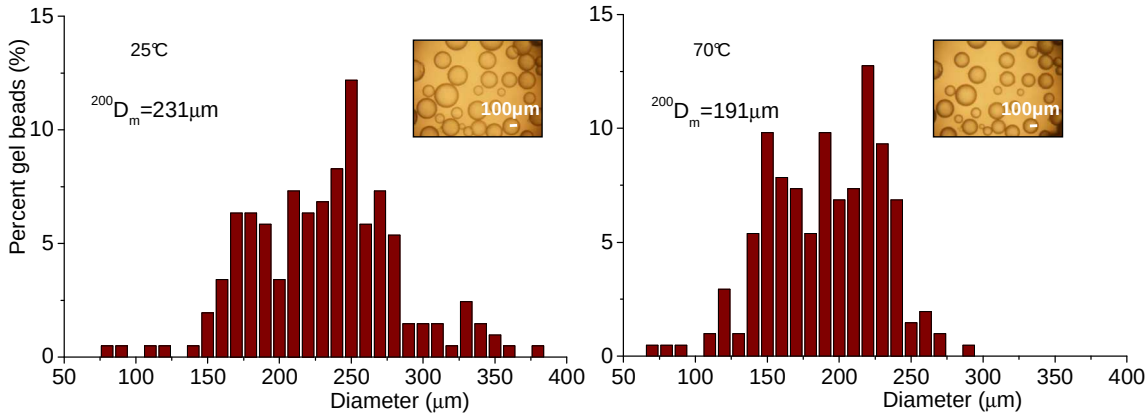

Figure 119: Diameters distribution for PEGMAf1 in pH 7.2 buffer solution at 25 and 70°C.

The swelling degrees of PEGMA and PEGMAf1 in aqueous solutions and in buffers are plotted as function of temperature and pH in Figure 120. In general, this second type of hydrogel displays broader temperature transitions which may be caused by the diameters being twofold larger than those obtained for PNA.

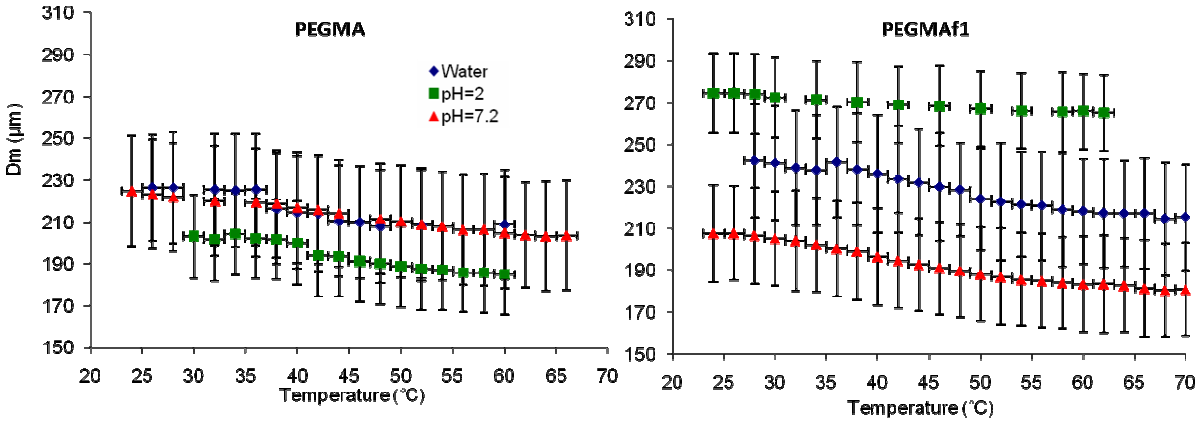

Figure 120: Temperature/pH dependence of $^{30}D_m$ of PEGMA and PEGMAf1 in H_2O (■), pH 2 (●) and pH 7.2 (▲) buffer solutions and $^{30}D_m$ confidence interval on the error bars.

These graphs were obtained by calculating the mean diameters of a population of 30 beads for each temperature and pH. The error bars expressed as confidence interval (α = 0.01) are also reported in the graph. Figure 121 shows an example of the photographs taken for the PEGMA hydrogel ramp from 24 to 70 °C at pH 7.2.

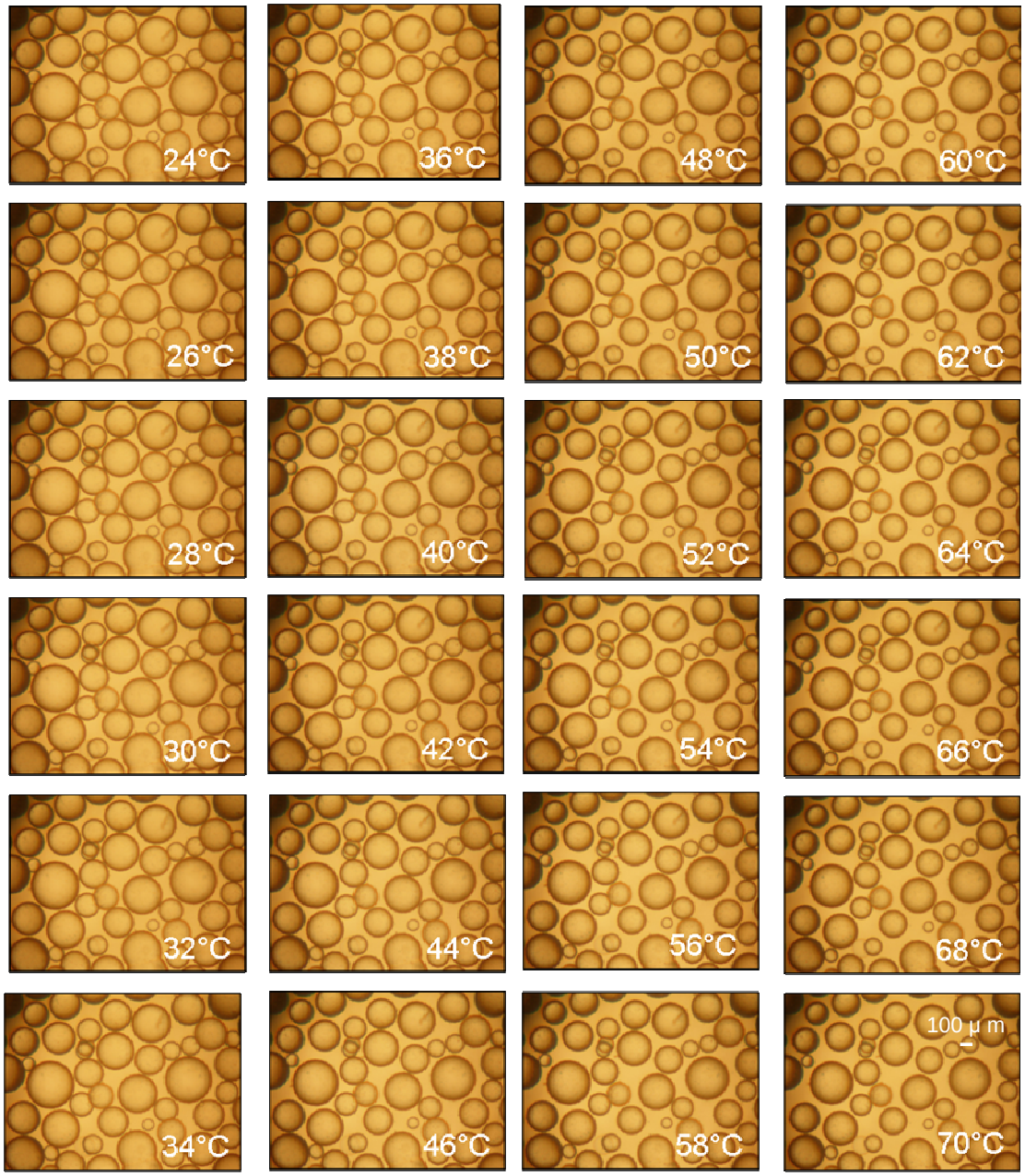

Figure 121: Photographs of the de-swelling process of PEGMA hydrogel at pH 7.2.

Although a full description of these data is very difficult due to the different variables involved in the swelling events considerations are listed below.

The thermo-responsive behaviour of poly-oligo-(ethylene glycol) macromonomers can be explained by the amphiphilicity nature of the macromolecule. In fact, while the ether oxygens form stabilising H-bonds with water, the apolar carbon-carbon backbone leads to

a competitive hydrophobic effect. Therefore, longer side chains can form more stabilising H-bonds with the same hydrophobic carbon-carbon backbone and thus the material result more soluble in water. Below the LCST the balance between the ether oxygen-water interaction (stabilising H-bonds) and the carbon-carbon backbone hydrophobic competitive effect is sufficient to allow solubilization. Above the LCST, the polymer-polymer interactions become more favourable and this causes the polymer to collapse.[149] The incorporation of *N*-Aza-crown ether into PEGMA results in an increase in the hydrogel hydrophilicity as new ether oxygens are added into the network. Thus, PEGMAf1 exhibits larger diameters in deionized water as a result of more stabilising H-bonds between ether oxygens and water.

PEGMA and PEGMAf1 exhibits a peculiar reversed behaviour at pH 2 and 7.2 that is likely caused in part by the pH and in part by the salts dissolved in the buffers. The presence of salts, similarly observed for NIPAM hydrogels, can lead to a partial dehydration of the hydrogel network with consequent decrease in hydrogel diameters. This effect was also observed by Lutz *et al.* for linear poly-oligo-(ethylene glycol) macromonomers,[13] and by Geckeler *et al.* for NIPAM hydrogels.[162] The ionic strength depends upon concentrations and charges of the ions; phosphate pH 7.2 buffer is composed of higher concentrations of more charged ions than pH 2 buffer and thus, it has higher ionic strength.

PEGMA exhibits similar diameters in water at pH 7.2 (225-210 μm) and smaller at pH 2 (200-180 μm). This seems to suggest that PEGMA is not as much affected as the NIPAM/AAc beads by ionic strength.

The presence of HEMA into PEGMA confers to the gel a relatively small pH sensitivity and this may be the cause of the smaller diameters displayed by PEGMA at pH 2. At pH 7.2 the HEMA (pK_a = 13.82) hydroxyl groups may be partially deprotonated resulting in a swelling of the bead caused by electrostatic repulsion. This implies that the contribution given by the pH affects more the PEGMA bead sizes than the ionic strength. However, at pH 2 the HEMA hydroxyl groups should be partially protonated ($-OH_2^+$) resulting also in a swollen state. However, such behaviour is not observed in the PEGMA plot.

The introduction of *N*-Aza-crown ether into the material should deactivate such pH sensitivity as the HEMA groups are fully functionalized with chloro acetyl chloride first and N-Aza-crown ether after. Instead, the functionalization increases and reverses the pH-response and PEGMAf1 exhibits an extraordinary large size at pH 2 (275-265 μm) and smaller one pH 7.2 (210-180 μm). This large size observed at pH 2 may be caused by partial protonation of the crown ether nitrogen lone pairs which lead to expansion of the material by electrostatic repulsion. In addition, the crown ether introduction does not decrease the thermo-response of the material and indeed PEGMAf1 displays an enhanced temperature transition at pH 7.2.

The ionic strength and scavenging effects clearly observed for PNA1 hydrogel in the previous paragraph are not as clear in the graphs reported in Figure 120. In order to confirm such effects also for this material, PEGMAf1 was allowed to swell in aqueous solutions containing increasing amounts of KCl and the result obtained is illustrated in Figure 122.

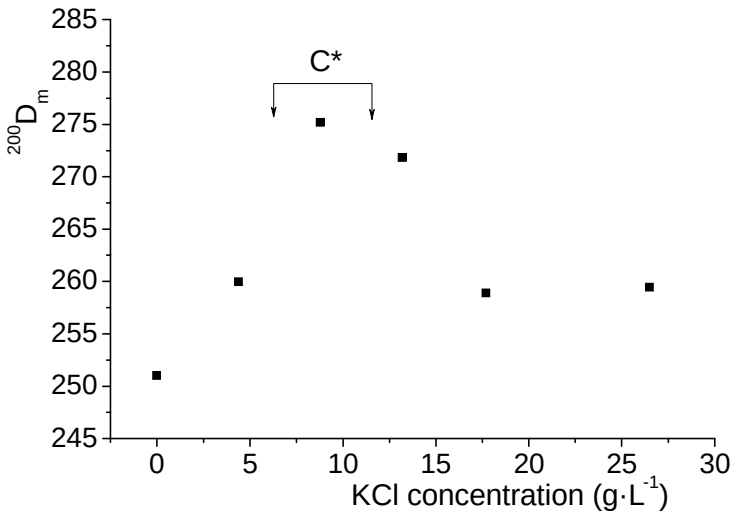

Figure 122: Swelling degrees of PEGMAf1 in aqueous solutions containing increasing amounts of KCl, C* is a critical concentration.

Similar results were obtained: at concentrations of KCl below a particular critical concentration (C*) the beads are in a swollen state and the $^{200}D_m$ is larger than that in deionized water. However, when the KCl concentration exceeds C*, the gel shrinks

reaching a constant $^{200}D_m$ at high concentration of KCl. At low concentration, the scavenging effect plays the major rule as the ionic strength is still low, resulting the beads to swell. When the concentration of KCl reaches C*, the ionic strength is sufficiently high to give the major contribution to the bead size resulting in the shrinkage of the gel beads.

This test also suggests that the ionic strength has a smaller contribution to these beads comparing with that observed in the previous NIPAM/AAc type. In fact, PEGMAf1 displays a C* in the range of 7.5 to 12.5 $g \cdot L^{-1}$ whereas PNA1 exhibited a lower C* in the range of 2.5 to 7.5 $g \cdot L^{-1}$. Moreover, the $^{200}D_m$ of PEGMAf1 reaches a minimum value at high KCl concentration which is higher than the one in deionized water whereas PNA1 exhibited mean diameter smaller than those obtained in deionized water at high KCl concentration.

These latter results combined with those obtained by the swelling experiments reported in Figure 120 suggest that the N-Aza-crown ethers incorporated have an influence in the swelling degrees of the PEGMAf1. This influence has at least three different contributions which are pH, ionic strength and *N*-Aza-crown scavenging effect. The size of the material is determined by the equilibrium of these contributions.

For practical reasons the swelling degree study reported in Figure 120 was based on the observation of 30 hydrogel beads. Due to the small data set these results are not statistically significant as evidenced by the overlapping of error bars of the mean diameters at different conditions (Figure 120). However, it acts as good guide as $^{200}D_m$ (Table 33) which has much lower confidence intervals (Table 33) differ by less than 5 % respect to $^{30}D_m$ for both PEGMA and PEGMAf1 in the different solutions. This suggests that 30 beads per population is representative for the system.

Table 33: Temperature/pH dependence of $^{200}D_m$ in H_2O, pH 2 and pH 7.2 buffer solution for PEGMA and PEGMAf1 and relative confidence intervals (CI).

	PEGMA		PEGMAf1	
	$^{200}D_m$ (μm) 25°C CI (μm)	$^{200}D_m$ (μm) 70°C CI (μm)	$^{200}D_m$ (μm) 25°C CI (μm)	$^{200}D_m$ (μm) 70°C CI (μm)
H_2O	231 12	210 10	251 12	222 11
pH=2	209 12	176 11	289 10	265 9
pH=7.2	227 11	204 10	231 9	191 7

6.3. Autoradiography experiments.

The materials studied in the following paragraphs of this chapter are summarised in the following Table 34.

Table 34: Key materials discussed in this and in the following paragraphs of this chapter.

Sample	Composition	Section	Composition (~)
PEGMA	MEO_2MA-co-$OEGMA_{475}$-co-HEMA	3.4.9.	7.65 : 1.35 : 1
PEGMAf1	MEO_2MA-co-$OEGMA_{475}$-co-:1-aza-12-crown-4	3.4.11.	7.65 : 1.35 : 1
PEGMAf 2	MEO_2MA-co-$OEGMA_{475}$-co-:1-aza-15-crown-5	3.4.11.	7.65 : 1.35 : 1
PEGMAf 3	MEO_2MA-co-$OEGMA_{475}$-co-:1-aza-18-crown-6	3.4.11.	7.65 : 1.35 : 1

The same autoradiography tests regarding Sr-90 removal were also carried out for the oligo-ethylene glycol hydrogels (Figure 123).

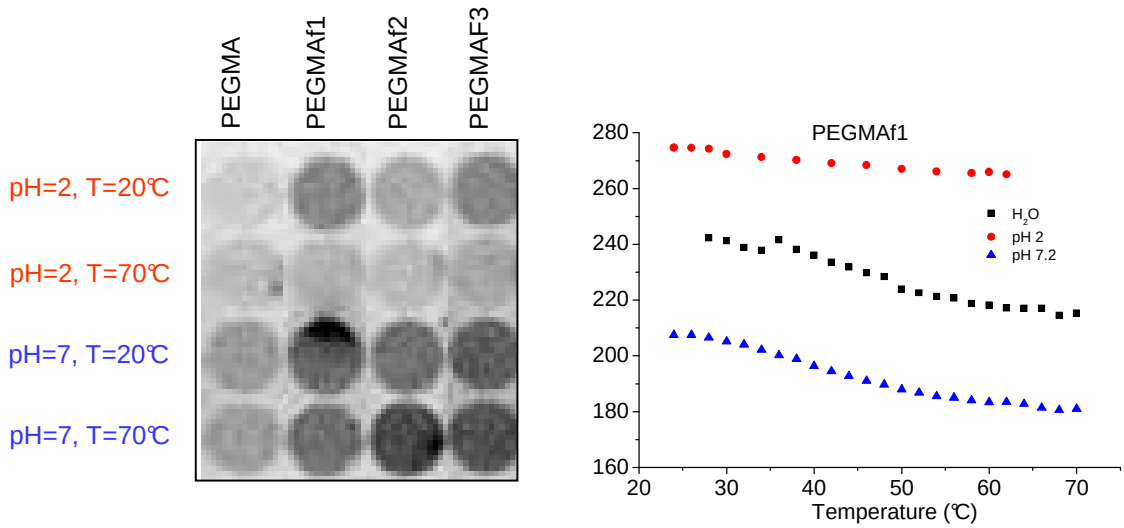

Figure 123: Autoradiography tests for PEGMA, PEGMAf1, PEGMAf2 and PEGMAf3 towards Sr-90 and swelling experiments reported in Figure 120.

The related average intensity backgrounds registered are listed in Table 35.

Table 35: Average intensity backgrounds for Oligo-ethylene glycol methacrylate hydrogels in sequestering experiments of Sr-90.

Conditions	Average Intensity Background			
	PEGMA	PEGMAf1	PEGMAf2	PEGMAf3
pH=2 T=20°C	308	855	575	846
pH=2 T=70°C	428	507	445	618
pH=7 T=20°C	700	1240	1031	1171
pH=7 T=70°C	671	1049	1377	1286

As observed for the materials based on NIPAM/AAc, the introduction of the Aza-crown ethers enhances the removal activity of the hydrogels and some materials display a two-fold increase in activity after the crown ether is added. However, in this second case the size of the beads is inversely proportional to the sequestering property. Thus, at pH 2 the beads are in a more swollen state and retain small quantities of Sr 90 whereas at pH 7 the

beads are shrunk and retain more radionuclide. At pH 2, the Aza-crown ether nitrogen lone pairs are protonated and the electrostatic repulsion of these positive charges likely cause the swelling of the beads with large adsorption of water. However, this electrostatic repulsion also considerably reduces the retention of the cations as the nitrogen lone pairs are the substrates that mainly bind the metals. Conversely, at pH 7 the nitrogen lone pairs are totally available and this allows the crown ether rings to trap more metals in their cavities.

In accord to the swelling experiments also the autoradiography tests shows that the Sr 90 removal is strongly affected by pH and much less by temperature even though the scavenging activity changes to some extent with temperature. So, PEGMAf1 PEGMAf2 and PEGMAf3 display different average intensity backgrounds at pH 2 and 7 under different temperatures. This also suggests that the material may display enhanced selectivity respect to the NIPAM/AAc materials at both pH. However, this difference in intensities backgrounds is relatively small and this lack of selectivity is likely caused by the crown ethers being able to form 1 : 1 and 2 : 1 complexes with Sr 90.

Autoradiography tests in removal of Co 60 were also carried out and the results obtained are reported in Figure 124.

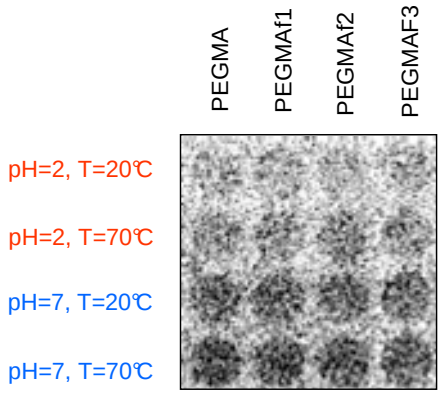

Figure 124: Autoradiography tests for PEGMA, PEGMAf1, PEGMAf2 and PEGMAf3 in removal of Co 60.

The related average intensity backgrounds are listed in Table 36.

Table 36: Average intensity backgrounds for the materials showed in Figure 124.

Conditions	Average Intensity Background			
	PEGMA	PEGMAf1	PEGMAf2	PEGMAf3
pH=2 T=20°C	29	31	27	29
pH=2 T=70°C	41	41	45	39
pH=7 T=20°C	61	62	60	57
pH=7 T=70°C	74	73	69	64

Differently from the previous Strontium autoradiography tests, the removal of Co 60 is not significantly enhanced by the introduction of Aza-crown ethers. On the other hand, in accordance with other results the materials have enhanced activity at pH 7 and some extent of thermo-response at both pH's.

6.4. Scintillation counting experiments.

A confirmation of the autoradiography tests and a quantitative estimation of the sequestering properties of the materials were obtained by scintillation counting experiments. These new tests were also carried out in different environmental conditions of Ph and temperature. In the course of these experiments the selectivity of the materials was also estimated; each hydrogel was, in fact, tested in parallel in two different conditions: first, with the targeted radionuclide on its own and then with the target radionuclide in competition with a common non-hazardous metal ion of size comparable to the radionuclide. Thus, Caesium (1.67 Å) was tested in competition with Potassium (1.33 Å), Strontium (1.18 Å) in competition with Calcium (1.00 Å) and Cobalt (0.65 Å) with Tap Water which contains many cations such as Potassium, Calcium and Sodium (0.97 Å). In general, differently from the NIPAM materials, the scintillation experiments for these materials were not always consistent and in most of the cases they were difficult to interpret.

The results obtained for Cs 137 decontamination are reported in Table 37.

Table 37: Scintillation results for PEG hydrogels towards Cs 137 on its own and in competition with K.

	Caesium-Removal					Cs+K-Removal				
Conditions	PEG	PEGMA	PEGMAf1	PEGMAf2	PEGMAf3	PEG	PEGMA	PEGMAf1	PEGMAf2	PEGMAf3
pH=2, T=20℃	0	0	36	40	38	1	1	0	0	0
pH=2, T=70℃	0	0	0	0	0	1	0	0	0	0
pH=7, T=20℃	8	1	0	0	0	1	1	0	0	0
pH=7, T=70℃	8	2	0	0	0	1	0	0	0	0

Beads based on oligo-ethylene glycol methacrylates (PEG) and oligo-ethylene glycol methacrylates and HEMA (PEGMA) exhibits small decontamination values near zero whether potassium was present or not and at different conditions of pH and temperature. The introduction of crown ethers increases the decontamination activity of PEGMAf1, PEGMAf2 and PEGMAf3 only at pH 2 and 20 °C. Similarly observed for the PNA materials, different crown ethers incorporated do not have an effect in the selectivity of the hydrogel and PEGMAf1, PEGMAf2 and PEGMAf3 display similar Cs decontamination around 35-40%. Furthermore, such removal seems to be dependent upon temperature as the same materials display removal around zero at 70 °C. At pH 7, decontamination equal to zero is observed for all PEGMA hydrogels. Swelling degrees showed that PEGMAf1 displays larger diameters at pH 2 which fits with the higher decontamination showed in this test as a result of large incorporation of water. On the other hand in these conditions the Aza-crown ether nitrogen should be in its inactive protonated form which suggests that the incorporation is mainly given by absorption of the solution by the material. This is also confirmed by the very low selectivity displayed by the same materials which show Cs 137 decontamination equal to zero in competition with Potassium ions.

The results obtained for Sr 90 decontamination are reported in Table 38.

Table 38: Scintillation results for PEG hydrogels towards Sr 90 on its own and in competition with Ca.

	Sr-Removal					Sr+Ca-Removal				
Conditions	PEG	PEGMA	PEGMAf1	PEGMAf2	PEGMAf3	PEG	PEGMA	PEGMAf1	PEGMAf2	PEGMAf3
pH=2, T=20℃	4	0	0	0	0	0	0	0	0	0
pH=2, T=70℃	4	0	0	0	0	1	0	0	0	0
pH=7, T=20℃	45	33	42	30	20	10	30	32	27	11
pH=7, T=70℃	38	19	40	20	8	12	28	28	17	12

Conversely from the previous results, in Sr 90 decontamination these materials display removal near or equal to 0 % at pH 2 and enhanced decontamination at pH 7. In this case some PEGMA gels seem to display some temperature effect given to the sequestration, exhibiting a smaller percentage at 70 °C. This same result was never observed for the NIPAM hydrogels in the scintillation counting extractions. The introduction of crown ether increases the percentage removal for only PEGMAf1 (42 %) but in general the addition does not significantly improve the removal ability of the hydrogels; PEGMAf2 shows similar activity and indeed PEGMAf3 shows decreased removal.

In the competition experiments with Ca, both PEGMAf1 and PEGMAf3 display a lower removal and therefore show non-selectivity for Sr. PEGMAf2 shows the same sequestration whether Ca is present or not but such activity is not to some extent superior to the one of PEGMA. Therefore, although PEGMA was expected to show no interference with the ions it demonstrated to be the better material in Sr selective removal. An interesting aspect of the PEGMA hydrogel incorporating crown ethers is that they were able to retain Cs at low pH and to be completely inactive towards it at high pH. On the other hand, they are able to retain Sr at high pH and are completely inactive toward this ion at lower pH.

The results obtained for Co 60 decontamination are reported in Table 39.

Table 39: Scintillation results for PEG hydrogels towards Co 60 on its own and in competition with Tap water.

	Co-Removal					Co+Tap-Removal				
Conditions	PEG	PEGMA	PEGMAf1	PEGMAf2	PEGMAf3	PEG	PEGMA	PEGMAf1	PEGMAf2	PEGMAf3
pH=2, T=20℃	0	0	0	0	0	0	0	0	0	0
pH=2, T=70℃	0	0	0	0	0	0	0	0	0	0
pH=7, T=20℃	9	23	26	12	0	19	19	13	10	0
pH=7, T=70℃	8	17	19	1	0	19	19	8	7	1

Similarly to the Strontium decontamination results, also in decontamination of Co 60 all materials display some percentage of decontamination at pH 7 and values near 0 % at pH 2. In general, however, all values obtained are small and the introduction of the crown ether seems to decrease such activity and the decrease seems to be proportional to the increase of the crown ether ring size.

In order to ensure reproducibility of the experiments, some extractions were repeated 3 times in exactly same conditions and with double amount of material. The results obtained are listed in Table 40 and Table 41.

Table 40: Reproducibility experiments for PEGMA and error bar.

Sample	Isotope	Temperature (ºC)	pH	% absorption	Mass of beads (mg)	Error
PEGMA	Cs	20	2	0.87	10	0.28
				0.04	10	
				0	10	
				0	20	
		70		0.54	10	0.18
				0	10	
				0	10	
				0	20	
PEGMA	Co+Tap	20	7	30.88	10	0.24
				31.37	10	
				30.53	10	
				40.88	20	
		70		26.19	10	1.88
				27.03	10	
				32.21	10	
				39.24	20	
PEGMA	Co	20	7	20.14	10	0.94
				23.32	10	
				21.07	10	
				30.53	20	
		70		15.28	10	0.66
				16.81	10	
				17.53	10	
				27.55	20	

Table 41: Reproducibility experiments for PEG and PEGMAf3 and error bar.

Sample	Isotope	Temperature (ºC)	pH	% absorption	Mass of beads (mg)	Error
PEG	Sr	20	7	45.57	10	1.16
				41.81	10	
				42.46	10	
				54.50	20	
		70		37.04	10	0.30
				38.06	10	
				37.42	10	
				47.00	20	
PEGMAf3	Co+Tap	20	7	1.63	10	0.43
				1.88	10	
				0.49	10	
				0.27	20	
		70		0	10	0
				0	10	
				0	10	
				0	20	

The method shows good reproducibility and increasing quantities of hydrogel beads give higher decontamination percentage (in range of 7-12 %) in a solution containing the same quantity of radionuclide. Based on these experiments it is also possible to calculate the error associated to the measurement using the formula: $error = \sigma / \sqrt{n}$, where σ is the standard deviation and *n* is the number of observations; the calculated values are reported in Table 40 and Table 41.

In conclusion autoradiography showed that, similarly observed for the NIPAM materials (PNA, PNA1, 2, 3), also the PEGMA hydrogels display pH and thermo-sensitivity in terms of decontamination at least in the removal of Co 60 and Sr 90. Autoradiography also shows that the introduction of crown ethers improves the removal but different crown ethers do not have an effect in the decontamination. Such improvement is not regularly observed from the same materials in the scintillation counting experiments carried out with longer contact times (from 1 to 24 hours). These experiments show that

PEGMA hydrogels are able to decontaminate Sr 90, Co 60 and Cs 137 much less than the NIPAM-AAc beads (PNA, PNA1, 2, 3) and that the introduction of crown ether in some cases improves the removal but in some others it results in a decrease. Furthermore, in general all the hydrogel beads studied display a reduced removal activity in presence of other non hazardous ions therefore the polymer beads are not selective for the studied radionuclides (Sr 90, Co 60 and Cs 137).

Chapter 7

Conclusions & Further Work

7.1. Conclusions.

7.1.1. Aza-crown ether statistical polymers.

Aza-crown ether statistical polymers were successively synthesised by grafting preformed poly-MMA-co-HEMA with chloroacetyl chloride and consequently with 1-aza-15-crown-5. O-(N-hydroxyethyl-1-aza-15-crwon-5)-methyl methacrylate (Aza-crown ether monomer with long arm) was successfully synthesised; however, both homo- and copolymerizations were not successfully achieved. The steric hindrance of the large ring structure likely slows down the reaction while the long polar arm may favour structures where the double bond is partially trapped into the Aza-crown ether ring. The complexation property of the copolymers of MMA and Aza-crown ether was investigated by potential measurements but the materials did not show any ability to extract K^+, Na^+ and Ca^{++} from aqueous solution to an organic phase.

7.1.2. Dual stimuli-responsive (temperature, pH) poly-(NIPAM-co-AAc) hydrogel beads incorporating different Aza-crown ether.

Aza-crown ether methacrylates with shorter arms and carrying different Aza-crown ethers (1-aza-12-crown-4, 1-aza-15-crown-5, and 1-aza-16-crown-6) were successfully synthesised and their copolymerization with NIPAM monomer was successful; however, in presence of a chain transfer agent the incorporation of crown ether monomer present limitations. On the other hand, a poly-NIPAM-co-Aza-crown ether methacrylate macromonomer containing 12 mol % of crown ether was successfully prepared. Such macromonomer was used to prepare a dual stimuli-responsive (temperature, pH) graft-type poly-(NIPAM-co-AAc-co-1-aza-15-crown-5 methacrylate) hydrogel which was successfully synthesised by random inverse suspension copolymerization of AAc, NIPAM and the poly-(NIPAM-co-1-aza-15-crown-5 methacrylate) macromonomer

previously synthesised. However, the amount of crown ether incorporated was too small and was not clearly detected by solid state NMR.

Thermo-responsive poly-(NIPAM-co-1-aza-15-crown-5 methacrylate) hydrogel beads were successfully synthesised by direct random inverse suspension polymerization copolymerization of 1-aza-15-crown-5 methacrylate and NIPAM.

Dual stimuli-responsive (temperature, pH) poly-(NIPAM-co-AAc) hydrogel beads incorporating different Aza-crown ether (1-aza-12-crown-4, 1-aza-15-crown-5, and 1-aza-16-crown-6) were successful synthesised by post-functionalization of preformed NIPAM/AAc hydrogel beads prepared by inverse suspension polymerization. The degree of swelling of these hydrogels was investigated by optical microscopy and the beads were able to swell and shrink in response of environmental changes of pH and temperature: the size of the beads can be fine-tuned by pH and temperature adjusts. The radionuclide removal towards Co 60 and Sr 90 was first studied by autoradiography with contact time in the range of 1-2 minutes. These tests showed that also the decontamination ability of the beads is tuneable with temperature and pH. These measurements also showed that the incorporation of crown ether increases the radionuclide removal although different crown ethers did not cause any difference in the decontamination. Scintillation counting experiments were also carried out in order to obtain a percentage of removal with and without other non- hazardous metals and therefore the selectivity of the beads. These new tests, conducted with contact time in the range of 1-24 hours, confirmed that the incorporation of crown ethers improves their ability to trap radionuclides but did not confirm the dual sensitivity of the decontamination. These experiments also showed that these polymers are highly selective towards Co 60 displaying 95 % removal whether the radionuclide was in deionised or tap water (containing Na, K, Ca etc.).

7.1.3. Thermo-responsive hydrogel beads based on non-linear poly ethylene glycol methacrylates and HEMA.

Thermo-responsive hydrogel beads based on non-linear poly ethylene glycol methacrylates and HEMA were successfully prepared. These materials were then

successfully post-functionalised first with chloroacetyl chloride and then with different *N*-Aza-crown ethers (1-aza-12-crown-4, 1-aza-15-crown-5, and 1-aza-16-crown-6).

The degree of swelling degree of these polymer beads was investigated by optical microscopy. Such studies showed that these beads are able to shrink and swell in response of environmental changes of temperature and pH and therefore the size of the beads is fine-tuneable by pH and temperature adjusts. The decontamination activity was first investigated by autoradiography measurements at short contact times (1-2 minutes range). Such technique showed that the incorporation of crown ether increases the radionuclide (Sr 90, Co 60) retention of the hydrogels and that the decontamination activity can also be fine-tuned by environmental changes of pH and temperature. Consequently scintillation counting tests were carried out at longer contact times (1-24 hours range). These tests showed that the introduction of crown ethers increases the decontamination activity only for some materials whereas some others resulted in a lower ability to remove the selected radionuclides but most importantly these new tests showed that generally these new hydrogels remove much less than those based on NIPAM/AAc. As similarly observed for the NIPAM/AAc beads also these non-linear PEG beads have radionuclide removal ability which is not dependent upon pH and temperature in the conditions of the scintillation counting experiments. Moreover, the high selectivity found for the NIPAM/AAc beads towards Co 60 was not found for any of the non-linear PEG beads with either Co 60, Sr 90 or Cs 137. In fact, these beads displayed at all cases a reduced radionuclide removal in the presence of other non hazardous metals.

In conclusion, the NIPAM/AAc hydrogen beads definitely showed higher removal and enhanced selectivity in decontamination of Co 60, Sr 90 and Cs 137 than the non-linear PEG hydrogel beads.

7.2. Further Work.

- Beads of smaller size should display larger geometrical changes with environmental stimuli. Therefore, an interesting piece of work would be to decrease the size of the beads in the range of few microns and see if the increase in responsivity would affect the decontamination of the material incorporating Aza-crown ethers.

- Other different ligands could also be investigated. For example, Aza-crown ethers carrying only nitrogens (Figure 125) usually display stronger interactions with heavy metals (discussed in section 1.2.2.) and thus the resulting material may display better decontamination with Sr 90, Cs 137 and Co 60.

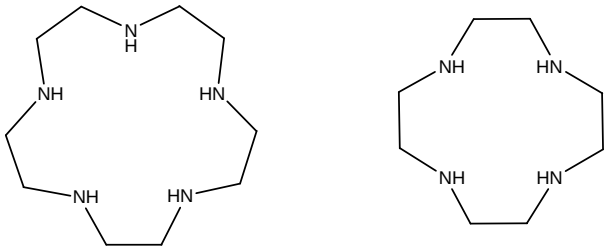

Figure 125: Aza-crown ethers containing only nitrogens.

- Another new ligand that could be incorporated in the beads with the crown ethers is the calyx pyrrole (Figure 126).

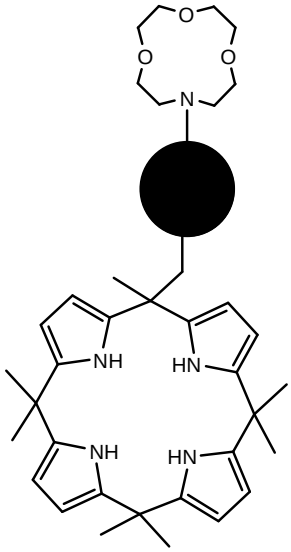

Figure 126: Beads incorporating crown ethers and calyx-pyrroles.

This ligand is known for its ability to bind anions [167] and it may therefore favour the decontamination of the radionuclides given by the crown ethers stabilising the counter ions into the hydrogel network.

- Beads of smaller size should display larger geometrical changes with environmental stimuli. Therefore, an interesting piece of work would be to decrease the size of the beads in the range of few microns and see if the increase in responsivity would affect the decontamination of the material incorporating Aza-crown ethers.

References

1. Wasikiewicz, J. M.; Mitomo, H.; Seko, N.; Tamada, M.; Yoshii, F. *J. Appl. Polym. Sci. FIELD Full Journal Title:Journal of Applied Polymer Science* **2007,** 104, (6), 4015-4023.

2. Wasikiewicz, J. M.; Nagasawa, N.; Tamada, M.; Mitomo, H.; Yoshii, F. *Nucl. Instrum. Methods Phys. Res., Sect. B FIELD Full Journal Title:Nuclear Instruments & Methods in Physics Research, Section B: Beam Interactions with Materials and Atoms* **2005,** 236, 617-623.

3. Yang, D. J.; Zheng, Z. F.; Zhu, H. Y.; Liu, H. W.; Gao, X. P. *Adv. Mater. (Weinheim, Ger.) FIELD Full Journal Title:Advanced Materials (Weinheim, Germany)* **2008,** 20, (14), 2777-2781.

4. Komarneni, S.; Kozai, N.; Paulus, W. J. *Nature (London, U. K.) FIELD Full Journal Title:Nature (London, United Kingdom)* **2001,** 410, (6830), 771.

5. Abusafa, A.; Yucel, H. *Sep. Purif. Technol. FIELD Full Journal Title:Separation and Purification Technology* **2002,** 28, (2), 103-116.

6. Bhaskarapillai, A.; Sevilimedu, N. V.; Sellergren, B. *Ind. Eng. Chem. Res. FIELD Full Journal Title:Industrial & Engineering Chemistry Research* **2009,** 48, (8), 3730-3737.

7. Bryce, D. L.; Adiga, S.; Elliott, E. K.; Gokel, G. W. *J. Phys. Chem. A FIELD Full Journal Title:Journal of Physical Chemistry A* **2006,** 110, (50), 13568-13577.

8. Tunca, U.; Yagci, Y. *Progress in Polymer Science* **1994,** 19, (2), 233-86.

9. Morris, G. E.; Vincent, B.; Snowden, M. J. *J. Colloid Interface Sci. FIELD Full Journal Title:Journal of Colloid and Interface Science* **1997,** 190, (1), 198-205.

10. Zhang, J.; Chu, L.-Y.; Cheng, C.-J.; Mi, D.-F.; Zhou, M.-Y.; Ju, X.-J. *Polymer FIELD Full Journal Title:Polymer* **2008,** 49, (10), 2595-2603.

11. Snowden, M. J.; Thomas, D.; Vincent, B. *Analyst (Cambridge, U. K.) FIELD Full Journal Title:Analyst (Cambridge, United Kingdom)* **1993,** 118, (11), 1367-9.

12. Beltran, S.; Baker, J. P.; Hooper, H. H.; Blanch, H. W.; Prausnitz, J. M. *Macromolecules FIELD Full Journal Title:Macromolecules* **1991,** 24, (2), 549-51.

13. Lutz, J.-F.; Akdemir, O.; Hoth, A. *J. Am. Chem. Soc. FIELD Full Journal Title:Journal of the American Chemical Society* **2006,** 128, (40), 13046-13047.

14. Amphlett, C. B.; McDonald, L. A. *J. Inorg. Nucl. Chem.* **1958,** 6, 145-52.

15. Mercer, B. W., Jr.; Ames, L. L.; Smith, P. W. *Nucl. Appl. Technol.* **1970,** 8, (1), 62-9.

16. Bhattacharyya, K. G.; Sen Gupta, S. *Adv. Colloid Interface Sci.* **2008,** 140, (2), 114-131.

17. Wang, S.; Peng, Y. *Chem. Eng. J. (Amsterdam, Neth.)* 156, (1), 11-24.

18. Braun, A.; Efremenkov, V. M.; Evans, D.; Gandhi, P. M.; Garamszeghy, M.; Geiser, H.; Hooper, E. W.; Kaufmann, F.; Luycx, P.; Martynov, B.; Mezga, L. J.; Neubauer, J.; Norden, M.; Pecha, M.; Piacek, P.; Potrok, M.; Sinha, P. K.; Stevens, T.; Tusa, E.; Zika, H. *Application of ion exchange processes for the treatment of radioactive waste and management of spent ion exchangers*; Wissenschaftlich Technische Ingenieurberatung,Germany.: 2002; pp i-viii, 1-115.

19. Komarneni, S.; Roy, R. *Nature (London)* **1982,** 299, (5885), 707-8.

20. Komarneni, S.; Roy, R. *Science (Washington, D. C., 1883-)* **1988,** 239, (4845), 1286-8.

21. Paulus, W. J.; Komarneni, S.; Roy, R. *Nature (London)* **1992,** 357, (6379), 571-3.

22. Nyman, M.; Tripathi, A.; Parise, J. B.; Maxwell, R. S.; Harrison, W. T. A.; Nenoff, T. M. *J. Am. Chem. Soc.* **2001,** 123, (7), 1529-1530.

23. Nyman, M.; Tripathi, A.; Parise, J. B.; Maxwell, R. S.; Nenoff, T. M. *J. Am. Chem. Soc.* **2002,** 124, (8), 1704-1713.

24. Pedersen, C. J. *Journal of the American Chemical Society* **1967,** 89, (10), 2495-6.

25. Pedersen, C. J. *Journal of the American Chemical Society* **1967,** 89, (26), 7017-36.

26. Pedersen, C. J. *Chemica Scripta* **1988,** 28, (3), 229-35.

27. Pedersen, C. J. Complexes of macrocyclic polyether with mercaptoimidazolines. 74-521025, 521025, 19741105., 1976.

28. Pedersen, C. J. *Journal of Organic Chemistry* **1971,** 36, (12), 1690-3.

29. Pedersen, C. J. *Journal of the American Chemical Society* **1970,** 92, 386-91.

30. Pedersen, C. J. *Federation Proceedings* **1968,** 27, (6), 1305-9.

31. Pedersen, C. J. Macrocyclic polyether compounds. 74-442909

3987061, 19740215., 1976.

32. Pedersen, C. J. *Journal of Organic Chemistry* **1971,** 36, (2), 254-57.

33. Pedersen, C. J. Macrocyclic polyethers. 1149229, 1969.

34. Pedersen, C. J.; Frensdorff, H. K. *Angewandte Chemie, International Edition in English* **1972,** 11, (1), 16-25.

35. Pedersen, C. J. *Organic Syntheses* **1972,** 52, 66-74.

36. Pedersen, C. J. *Journal of the American Chemical Society* **1970,** 92, 391-4.

37. J.J. Christensen, D. J. E., R.M. Izatt. *Chem. Rev.* **1974,** 74, 351.

38. Gokel, G. W.; Editor, *Crown Ethers and Cryptands*. 1991; p 190 pp.

39. Bradshaw, J. S.; Izatt, R. M. *Accounts of Chemical Research* **1997,** 30, (8), 338-345.

40. Izatt, R. M.; Pawlak, K.; Bradshaw, J. S.; Bruening, R. L. *Chemical Reviews (Washington, DC, United States)* **1991,** 91, (8), 1721-85.

41. Christensen, J. J.; Hill, J. O.; Izatt, R. M. *Science (Washington, DC, United States)* **1971,** 174, (4008), 459-67.

42. Steed, J. W. *Coordination Chemistry Reviews* **2001,** 215, 171-221.

43. Shinkai, S.; Ogawa, T.; Nakaji, T.; Kusano, Y.; Nanabe, O. *Tetrahedron Letters* **1979,** 19, (47), 4569-72.

44. Gokel, G. W.; Dishong, D. M.; Diamond, C. J. *Journal of the Chemical Society, Chemical Communications* **1980**, (22), 1053-4.

45. Stoddart, J. F.; Wheatley, C. M. *Journal of the Chemical Society, Chemical Communications* **1974**, (10), 390-1.

46. Hayward, R. C.; Overton, C. H.; Whitham, G. H. *Journal of the Chemical Society, Perkin Transactions 1: Organic and Bio-Organic Chemistry (1972-1999)* **1976**, (22), 2413-15.

47. Lehn, J. M. *Accounts of Chemical Research* **1978,** 11, (2), 49-57.

48. Lukyanenko, N. *Janssen Chimica Acta* **1992,** 10, (1), 12-18.

49. Lukyanenko, N. *Janssen Chimica Acta* **1992**, (Spec. Ed.), 5-12.

50. Ryba, O.; Petranek, J. *Journal of Electroanalytical Chemistry and Interfacial Electrochemistry* **1973,** 44, (3), 425-30.

51. Lehn, J. M. *Angewandte Chemie* **1988,** 100, (1), 91-116.

52. Cram, D. J. *Science (Washington, DC, United States)* **1988,** 240, (4853), 760-7.

53. Shehata, F. A. *Journal of Radioanalytical and Nuclear Chemistry* **1994,** 185, (2), 411-17.

54. Vanura, P. *Czechoslovak Journal of Physics* **1999,** 49, (Suppl. 1, Pt. 2, 13th Radiochemical Conference, 1998), 761-767.

55. Pearson, R. G. *Journal of the American Chemical Society* **1963,** 85, (22), 3533-9.

56. Pearson, R. G. *Science (Washington, DC, United States)* **1966,** 151, (3707), 1721-7.

57. Alexandratos, S. D. *Separation and Purification Methods* **1992,** 21, (1), 1-22.

58. Zong, Z.; Dong, S.; Hu, Y.; Xu, Y.; Liu, W. *European Polymer Journal* **1998,** 34, (5/6), 761-766.

59. Krakowiak, K. E.; Bradshaw, J. S.; Zamecka-Krakowiak, D. J. *Chemical Reviews (Washington, DC, United States)* **1989,** 89, (4), 929-72.

60. Sakamoto, H.; Kimura, K.; Koseki, Y.; Matsuo, M.; Shono, T. *Journal of Organic Chemistry* **1986,** 51, (25), 4974-9.

61. Arnold, K. A.; Hernandez, J. C.; Li, C.; Mallen, J. V.; Nakano, A.; Schall, O. F.; Trafton, J. E.; Tsesarskaja, M.; White, B. D.; Gokel, G. W. *Supramolecular Chemistry* **1995,** 5, (1), 45-60.

62. Bryce, D. L.; Adiga, S.; Elliott, E. K.; Gokel, G. W. *Journal of Physical Chemistry A* **2006,** 110, (50), 13568-13577.

63. Schultz, R. A.; White, B. D.; Dishong, D. M.; Arnold, K. A.; Gokel, G. W. *Journal of the American Chemical Society* **1985,** 107, (23), 6659-68.

64. Arnold, K. A.; Echegoyen, L.; Fronczek, F. R.; Gandour, R. D.; Gatto, V. J.; White, B. D.; Gokel, G. W. *Journal of the American Chemical Society* **1987,** 109, (12), 3716-21.

65. Kilic, Z.; Yildiz, M.; Hokelek, T.; Erdogan, B. *Journal of the Chemical Society, Dalton Transactions: Inorganic Chemistry* **1998**, (21), 3635-3640.

66. Walters, K. M.; Buntine, M. A.; Lincoln, S. F.; Wainwright, K. P. *Journal of the Chemical Society, Dalton Transactions* **2002**, (18), 3571-3577.

67. Suzuki, R.; Matsumoto, T.; Tanaka, K.; Takeuchi, Y.; Taketomi, T. *Journal of Organometallic Chemistry* **2001,** 636, (1-2), 108-123.

68. Kulygina, E. Y.; Vetrogon, V. I.; Basok, S. S.; Luk'yanenko, N. G. *Russian Journal of General Chemistry* **2005,** 75, (4), 628-631.

69. Newkome, G. R.; Marston, C. R. *Journal of Organic Chemistry* **1985,** 50, (22), 4238-45.

70. Sutherland, I. O. *Chemical Society Reviews* **1986,** 15, (1), 63-91.

71. Hosseini, M. W.; Lehn, J. M.; Duff, S. R.; Gu, K.; Mertes, M. P. *Journal of Organic Chemistry* **1987,** 52, (9), 1662-6.

72. Lehn, J. M. *Science (Washington, DC, United States)* **1985,** 227, (4689), 849-56.

73. Yohannes, P. G.; Mertes, M. P.; Mertes, K. B. *Journal of the American Chemical Society* **1985,** 107, (26), 8288-9.

74. Lehn, J. M.; Vierling, P. *Tetrahedron Letters* **1980,** 21, (14), 1323-6.

75. Izatt, R. M.; Bradshaw, J. S.; Nielsen, S. A.; Lamb, J. D.; Christensen, J. J.; Sen, D. *Chemical Reviews (Washington, DC, United States)* **1985,** 85, (4), 271-339.

76. Lamb, J. D.; Izatt, R. M.; Christensen, J. J.; Eatough, D. J. *Coord. Chem. Macrocyclic Compd.* **1979**, 145-217.

77. Dietrich, B.; Lehn, J. M.; Sauvage, J. P.; Blanzat, J. *Tetrahedron* **1973,** 29, (11), 1629-45.

78. White, B. D.; Arnold, K. A.; Gokel, G. W. *Tetrahedron Letters* **1987,** 28, (16), 1749-52.

79. Weber, E. *Kontakte (Darmstadt)* **1983**, (1), 38-52.

80. Weber, E. *Kontakte (Darmstadt)* **1984**, (1), 26-43.

81. Takagi, M.; Nakamura, H. *Journal of Coordination Chemistry* **1986,** 15, (1), 53-82.

82. Park, S. H.; Demberelnyamba, D.; Jang, S. H.; Byun, M. W. *Chemistry Letters* **2006,** 35, (9), 1024-1025.

83. Wen, Y. H.; Lahiri, S.; Qin, Z.; Wu, X. L.; Liu, W. S. *Journal of Radioanalytical and Nuclear Chemistry* **2002,** 253, (2), 263-265.

84. Kim, D. W.; Hong, C. P.; Kim, C. S.; Jeong, Y. K.; Jeon, Y. S.; Lee, J. K. *Journal of Radioanalytical and Nuclear Chemistry* **1997,** 220, (2), 229-231.

85. Kim, D. W.; Jeon, B. K.; Kang, B. M.; Lee, N.-S.; Ryu, H.-i.; Lee, Y.-i. *Journal of Colloid and Interface Science* **2003,** 263, (2), 528-532.

86. Christensen, J. J. E., D.J.; Izatt, R.M. *Chem. Rev.* **1974,** 74, 351.

87. Diaddario, L. L.; Zimmer, L. L.; Jones, T. E.; Sokol, L. S. W. L.; Cruz, R. B.; Yee, E. L.; Ochrymowycz, L. A.; Rorabacher, D. B. *Journal of the American Chemical Society* **1979,** 101, (13), 3511-20.

88. Frensdorff, H. K. *Journal of the American Chemical Society* **1971,** 93, (3), 600-6.

89. Arnold, K. A.; Gokel, G. W. *Journal of Organic Chemistry* **1986,** 51, (25), 5015-16.

90. Kimura, K.; Maeda, T.; Shono, T. *Talanta* **1979,** 26, (10), 945-9.

91. Smid, J.; Kopolow, S.; Hogen-Esch, T. E. *Macromolecules* **1971,** 4, (3), 359-60.

92. Thunhorst, K. L.; Noble, R. D.; Bowman, C. N. *Journal of Membrane Science* **1999,** 156, (2), 293-302.

93. Varma, A. J. *European Polymer Journal* **1986,** 22, (2), 111-13.

94. Kimura, K.; Sawada, M.; Shono, T. *Analytical Letters* **1979,** 12, (A10), 1095-102.

95. Baumann, T. F.; Reynolds, J. G.; Fox, G. A. *WM 99 Proceedings, Tucson, AZ, United States, Feb. 28-Mar. 4, 1999* **1999**, 2225-2230.

96. Collie, L.; Denness, J. E.; Parker, D.; O'Carroll, F.; Tachon, C. *Journal of the Chemical Society, Perkin Transactions 2: Physical Organic Chemistry (1972-1999)* **1993**, (10), 1747-58.

97. Peramunage, D.; Fernandez, J. E.; Garcia-Rubio, L. H. *Macromolecules* **1989,** 22, (6), 2845-9.

98. Shinkai, S.; Ishihara, M.; Manabe, O. *Polymer Journal (Tokyo, Japan)* **1985,** 17, (10), 1141-4.

99. Zhang, X.-Z.; Zhang, J.-T.; Zhuo, R.-X.; Chu, C.-C. *Polymer* **2002,** 43, (17), 4823-4827.

100. Nonokawa, R.; Yashima, E. *Journal of the American Chemical Society* **2003,** 125, (5), 1278-1283.

101. Kimura, K.; Yokota, G.; Yokoyama, M.; Uda, R. M. *Macromolecules* **2001,** 34, (7), 2262-2268.

102. Irie, M. *Journal of the American Chemical Society* **1983,** 105, (7), 2078-9.

103. Willner, I.; Rubin, S.; Wonner, J.; Effenberger, F.; Baeuerle, P. *Journal of the American Chemical Society* **1992,** 114, (8), 3150-1.

104. Kimura, K.; Kaneshige, M.; Yokoyama, M. *Chemistry of Materials* **1995,** 7, (5), 945-50.

105. Kimura, K.; Nakamura, M.; Sakamoto, H.; Uda, R. M.; Sumida, M.; Yokoyama, M. *Bulletin of the Chemical Society of Japan* **2003,** 76, (1), 209-215.

106. Nishizawa, K.; Nishida, T.; Miki, T.; Yamamoto, T.; Hosoe, M. *Separation Science and Technology* **1996,** 31, (5), 643-54.

107. Wichterle, O.; Bartl, P.; Rosenberg, M. *Nature (London, U. K.) FIELD Full Journal Title:Nature (London, United Kingdom)* **1960,** 186, (4723), 494-5.

108. Kopecek, J.; Bazilova, H. *Eur. Polym. J. FIELD Full Journal Title:European Polymer Journal* **1974,** 10, (6), 465-70.

109. Van Bos, M.; Schacht, E. *Acta Pharm. Technol. FIELD Full Journal Title:Acta Pharmaceutica Technologica* **1987,** 33, (3), 120-5.

110. Schacht, E. H. *J. Phys.: Conf. Ser. FIELD Full Journal Title:Journal of Physics: Conference Series* **2004,** 3, 22-28.

111. Braccini, I.; Perez, S. *Biomacromolecules FIELD Full Journal Title:Biomacromolecules* **2001,** 2, (4), 1089-1096.

112. Schacht, E.; Nobels, M.; Vansteenkiste, S.; Demeester, J.; Franssen, J.; Lemahieu, A. *Polym. Gels Networks FIELD Full Journal Title:Polymer Gels and Networks* **1993,** 1, (4), 213-24.

113. Schacht, E.; Vandichel, J. C.; Lemahieu, A.; De Rooze, N.; Vansteenkiste, S. *Spec. Publ. - R. Soc. Chem. FIELD Full Journal Title:Special Publication - Royal Society of Chemistry* **1993,** 138, (Encapsulation and Controlled Release), 18-34.

114. Gilbert, R. G. *Emulsion Polymerization: A Mechanistic Approach* **1955,** Academic, London.

115. P. A. Lovell , S. E.-A. *Emulsion Polymerization and Emulsion Polymers* **1977,** Wiley, Chichester.

116. F. Hoffman, K. D. *Farbenfabriken Bayer, Germany* **1909,** Patent (Ger.) No. 250 690.

117. W. Bauer, H. L. *Rohm and Haas, Darmstadt* **1931,** Patent. (Ger.) No. 656, 134.

118. M Mumzer, E. T., in: C.E. Schildknecht, I. Skeist. *Polymerization Processes* **1977,** Wiley, New York, p. 106.

119. Grulke, E. A. *"Suspension Polymerization" in Enciclopedia of Polymer Science and Technology, 2nd Edition* **1985,** Volume 16, (H. Mark Ed.) Wiley, New York, 443.

120. Yuan, H. G.; Kalfas, G.; Ray, W. H. *J. Macromol. Sci., Rev. Macromol. Chem. Phys. FIELD Full Journal Title:Journal of Macromolecular Science, Reviews in Macromolecular Chemistry and Physics* **1991,** C31, (2-3), 215-99.

121. Holtzscherer, C.; Candau, F. *Colloids Surf. FIELD Full Journal Title:Colloids and Surfaces* **1988,** 29, (4), 411-23.

122. Candau, F. O., R. H. . *Ed. An Introduction to Polymer Colloid* **1990,** Kulwer Academic Publishers; Dordrecht, p. 73.

123. Beerbower, A. H., M. W. McCutcheon's. *Detergents and Emulsifiers Annual; Allured Publishing Co.* **1971,** Ridgewood, NJ, 223.

124. Annaka, M.; Matsuura, T.; Kasai, M.; Nakahira, T.; Hara, Y.; Okano, T. *Biomacromolecules FIELD Full Journal Title:Biomacromolecules* **2003,** 4, (2), 395-403.

125. Trijasson, P.; Frere, Y.; Gramain, P. *Makromol. Chem., Rapid Commun. FIELD Full Journal Title:Makromolekulare Chemie, Rapid Communications* **1990,** 11, (5), 239-43.

126. Hernandez-Baraias, J.; Hunkeler, D. *Book of Abstracts, 210th ACS National Meeting, Chicago, IL, August 20-24 FIELD Full Journal Title:Book of Abstracts, 210th ACS National Meeting, Chicago, IL, August 20-24* **1995**, (Pt. 2), PMSE-176.

127. Omidian, H.; Hashemi, S. A.; Askari, F.; Nafisi, S. *J. Appl. Polym. Sci. FIELD Full Journal Title:Journal of Applied Polymer Science* **1994,** 54, (2), 241-9.

128. Hernandez-Barajas, J.; Hunkeler, D. J. *Polym. Adv. Technol. FIELD Full Journal Title:Polymers for Advanced Technologies* **1995,** 6, (7), 509-17.

129. Hunkeler, D.; Candau, F.; Pichot, C.; Hemielec, A. E.; Xie, T. Y.; Barton, J.; Vaskova, V.; Guillot, J.; Dimonie, M. V.; Reichert, K. H. *Adv. Polym. Sci. FIELD Full Journal Title:Advances in Polymer Science* **1994,** 112, (Theories and Mechanism of Phase Transitions, Heterophase Polymerizations, Homopolymerization, Addition Polymerization), 115-33.

130. Wang, G.; Li, M.; Chen, X. *J. Appl. Polym. Sci. FIELD Full Journal Title:Journal of Applied Polymer Science* **1997,** 65, (4), 789-794.

131. X. L. Xu, Z. C. Z., B. Fei, X. V. Ge, M. W. Zhang. *ActaPolym Sin.* **(1988)**, 134.

132. Crosato-Arnaldi, A.; Gasparini, P.; Talamini, G. *Makromol. Chem. FIELD Full Journal Title:Makromolekulare Chemie* **1968,** 117, 140-52.

133. Kurisawa, M.; Yui, N. *J. Controlled Release FIELD Full Journal Title:Journal of Controlled Release* **1998,** 54, (2), 191-200.

134. Philippova, O. E.; Hourdet, D.; Audebert, R.; Khokhlov, A. R. *Macromolecules FIELD Full Journal Title:Macromolecules* **1997,** 30, (26), 8278-8285.

135. Flory, P. J., *Principles of Polymer Chemistry*. 1953; p 672 pp.

136. Teraoka, I., *Polymer Solutions: An Introduction to Physical Properties*. 2002; p 400 pp.

137. Heskins, M.; Guillet, J. E. *J. Macromol. Sci., Chem. FIELD Full Journal Title:Journal of Macromolecular Science, Chemistry* **1968,** 2, (8), 1441-55.

138. Kumashiro, Y.; Ooya, T.; Yui, N. *Macromol. Rapid Commun. FIELD Full Journal Title:Macromolecular Rapid Communications* **2004,** 25, (8), 867-872.

139. Wang, L.-Q.; Tu, K.; Li, Y.; Zhang, J.; Jiang, L.; Zhang, Z. *React. Funct. Polym. FIELD Full Journal Title:Reactive & Functional Polymers* **2002,** 53, (1), 19-27.

140. Liu, F.; Tao, G.; Zhuo, R. *Polym. J. (Tokyo) FIELD Full Journal Title:Polymer Journal (Tokyo, Japan)* **1993,** 25, (6), 561-7.

141. Dong, L. C.; Hoffman, A. S. *J. Controlled Release FIELD Full Journal Title:Journal of Controlled Release* **1986,** 4, (3), 223-7.

142. Yoshida, R.; Uchida, K.; Kaneko, Y.; Sakai, K.; Kikuchi, A.; Sakurai, Y.; Okano, T. *Nature (London) FIELD Full Journal Title:Nature (London)* **1995,** 374, (6519), 240-2.

143. Kaneko, Y.; Sakai, K.; Kikuchi, A.; Yoshida, R.; Sakurai, Y.; Okano, T. *Macromolecules FIELD Full Journal Title:Macromolecules* **1995,** 28, (23), 7717-23.

144. Ni, C.; Wang, Z.; Zhu, X. X. *J. Appl. Polym. Sci. FIELD Full Journal Title:Journal of Applied Polymer Science* **2004,** 91, (3), 1792-1797.

145. Masson, P.; Beinert, G.; Franta, E.; Rempp, P. *Polym. Bull. (Berlin) FIELD Full Journal Title:Polymer Bulletin (Berlin, Germany)* **1982,** 7, (1), 17-22.

146. Hamaide, T.; Mariaggi, N.; Foureys, J. L.; Le Perchec, P.; Guyot, A. *J. Polym. Sci., Polym. Chem. Ed. FIELD Full Journal Title:Journal of Polymer Science, Polymer Chemistry Edition* **1984,** 22, (11, pt. 1), 3091-106.

147. Han, S.; Hagiwara, M.; Ishizone, T. *Macromolecules FIELD Full Journal Title:Macromolecules* **2003,** 36, (22), 8312-8319.

148. Zhao, B.; Li, D.; Hua, F.; Green, D. R. *Macromolecules FIELD Full Journal Title:Macromolecules* **2005,** 38, (23), 9509-9517.

149. Lutz, J.-F. *J. Polym. Sci., Part A: Polym. Chem. FIELD Full Journal Title:Journal of Polymer Science, Part A: Polymer Chemistry* **2008,** 46, (11), 3459-3470.

150. Gil, E. S.; Hudson, S. M. *Prog. Polym. Sci. FIELD Full Journal Title:Progress in Polymer Science* **2004,** 29, (12), 1173-1222.

151. Lutz, J.-F.; Weichenhan, K.; Akdemir, O.; Hoth, A. *Macromolecules (Washington, DC, U. S.) FIELD Full Journal Title:Macromolecules (Washington, DC, United States)* **2007,** 40, (7), 2503-2508.

152. Fechler, N.; Badi, N.; Schade, K.; Pfeifer, S.; Lutz, J.-F. *Macromolecules (Washington, DC, U. S.) FIELD Full Journal Title:Macromolecules (Washington, DC, United States)* **2009,** 42, (1), 33-36.

153. Cai, T.; Marquez, M.; Hu, Z. *Langmuir FIELD Full Journal Title:Langmuir* **2007,** 23, (17), 8663-8666.

154. Billington, D., Jayson, G.G., Maltby, P.J., *Radioisotopes*. Bios Scientific Publishers: 2002.

155. Sampson, C. B., *Textbook of Radiopharmacy: Factors Influencing the Choice and Use of Radionuclides in Diagnostic and Therapy*. NRCP Publications. Bethesda: 1990.

156. Becquerel, H. *Nobel Lectures, Physics 1901-1921* **1967**.

157. Backer, J. R. J., *Autoradiography: A Comprensive Overview*. Rotal Microscopical Society: 1989; Vol. 3 Microscopy Handbooks.

158. Amemiya, Y.; Miyahara, J. *Nature (London) FIELD Full Journal Title:Nature (London, United Kingdom)* **1988,** 336, (6194), 89-90.

159. Aydogan, A.; Coady, D. J.; Kim, S. K.; Akar, A.; Bielawski, C. W.; Marquez, M.; Sessler, J. L. *Angew. Chem., Int. Ed. FIELD Full Journal Title:Angewandte Chemie, International Edition* **2008,** 47, (50), 9648-9652.

160. Yagi, K.; Sanchez, M. C. *Polym. Sci. Technol. (Plenum) FIELD Full Journal Title:Polymer Science and Technology (Plenum)* **1984,** 24, (Crown Ethers Phase Transfer Catal. Polym. Sci.), 345-57.

161. Dowding, P. J.; Vincent, B. *Colloids Surf., A FIELD Full Journal Title:Colloids and Surfaces, A: Physicochemical and Engineering Aspects* **2000,** 161, (2), 259-269.

162. Jeria-Orell, M.; del C. Pizarro, G.; Marambio, O. G.; Huerta, M.; Geckeler, K. E. *J. Appl. Polym. Sci. FIELD Full Journal Title:Journal of Applied Polymer Science* **2006,** 100, (3), 1735-1741.

163. Bokias, G.; Staikos, G.; Iliopoulos, I. *Polymer FIELD Full Journal Title:Polymer* **2000,** 41, (20), 7399-7405.

164. Jayakrishnan, A.; Thanoo, B. C. *J. Biomed. Mater. Res. FIELD Full Journal Title:Journal of Biomedical Materials Research* **1990,** 24, (7), 913-27.

165. Scranton, A. B.; Mikos, A. G.; Scranton, L. C.; Peppas, N. A. *J. Appl. Polym. Sci. FIELD Full Journal Title:Journal of Applied Polymer Science* **1990,** 40, (5-6), 997-1004.

166. Kiremitci, M.; Cukurova, H. *Polymer FIELD Full Journal Title:Polymer* **1992,** 33, (15), 3257-61.

167. Aydogan, A.; Coady, D. J.; Lynch, V. M.; Akar, A.; Marquez, M.; Bielawski, C. W.; Sessler, J. L. *Chem. Commun. (Cambridge, U. K.)* **2008**, (12), 1455-1457.

Appendix

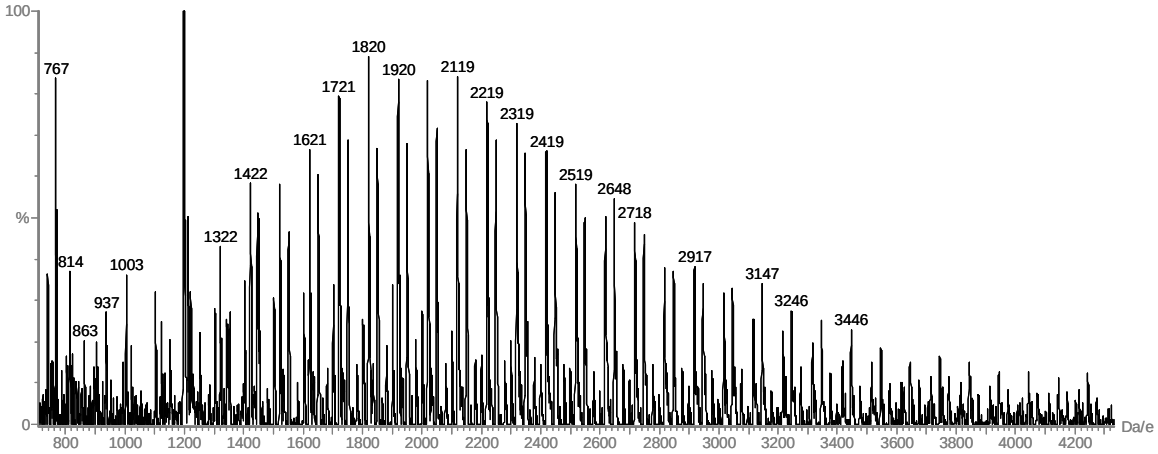

Figure 1: MALDI TOF of random-poly-$(MMA)_9$-co-$(HEMA)_1$ (sample DD7).

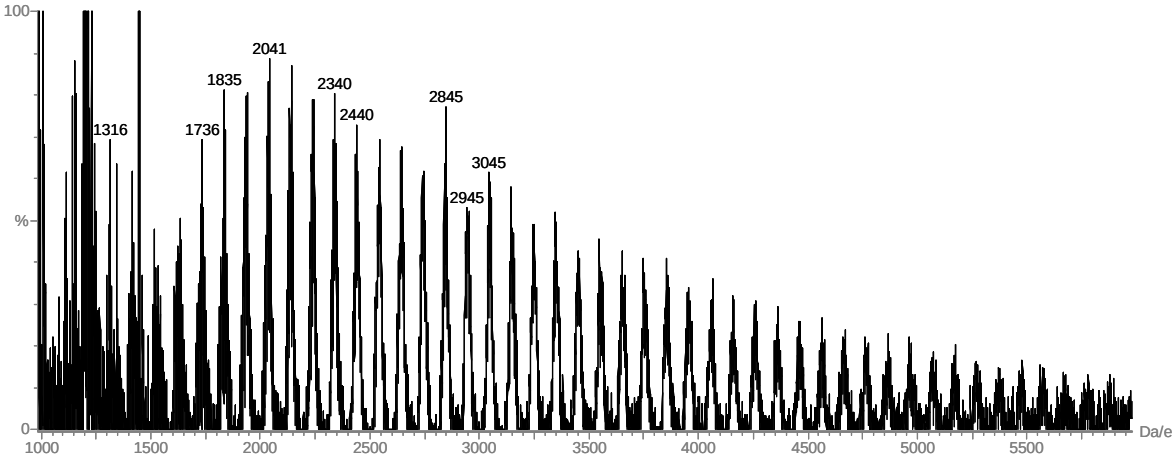

Figure 2: MALDI TOF of chloroacetyl random-poly-$(MMA)_{7.5}$-co-$(HEMA)_{2.5}$ (DD55).

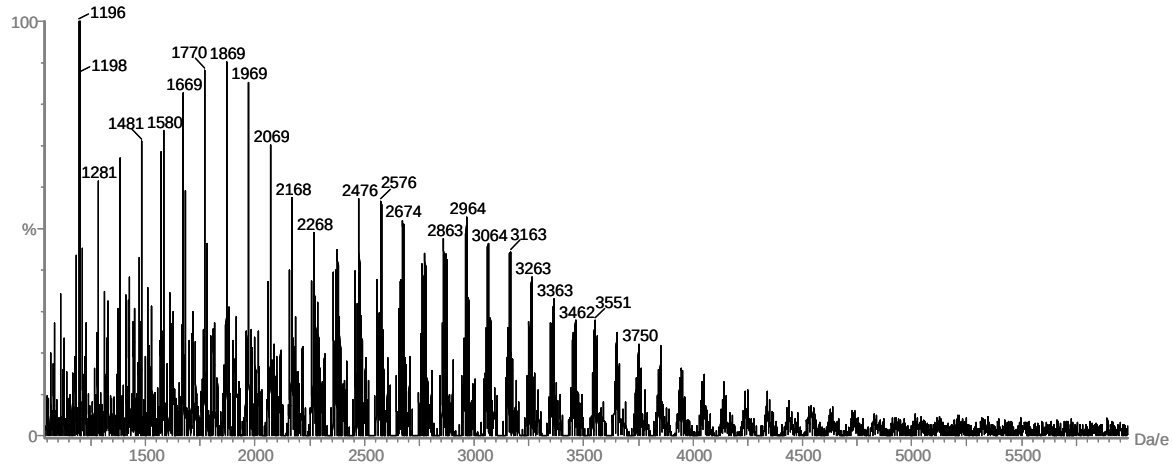

Figure 3: MALDI TOF of DD52 (MMA/Aza-crown ether: 50/50).

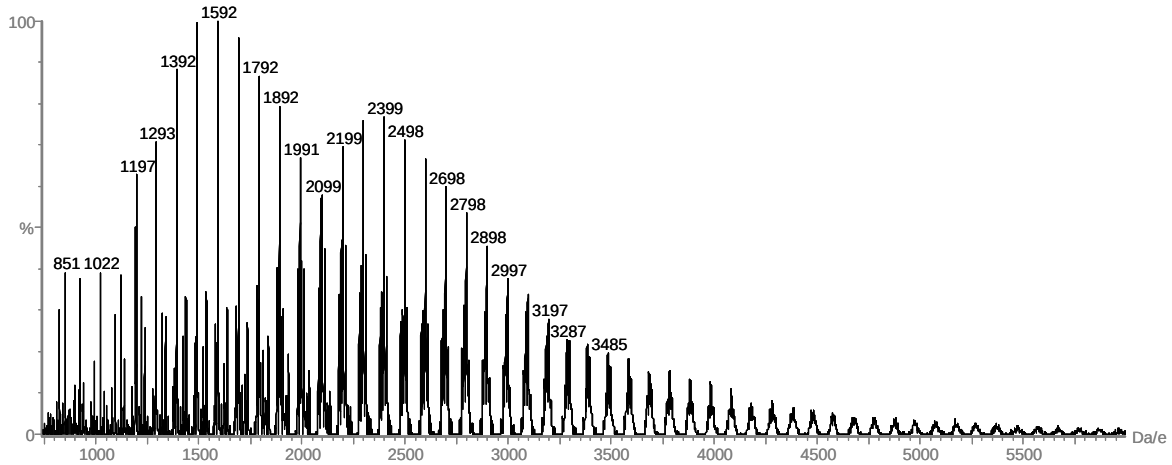

Figure 4: MALDI TOF of DD56 (MMA/Aza-crown ether: 75/25).

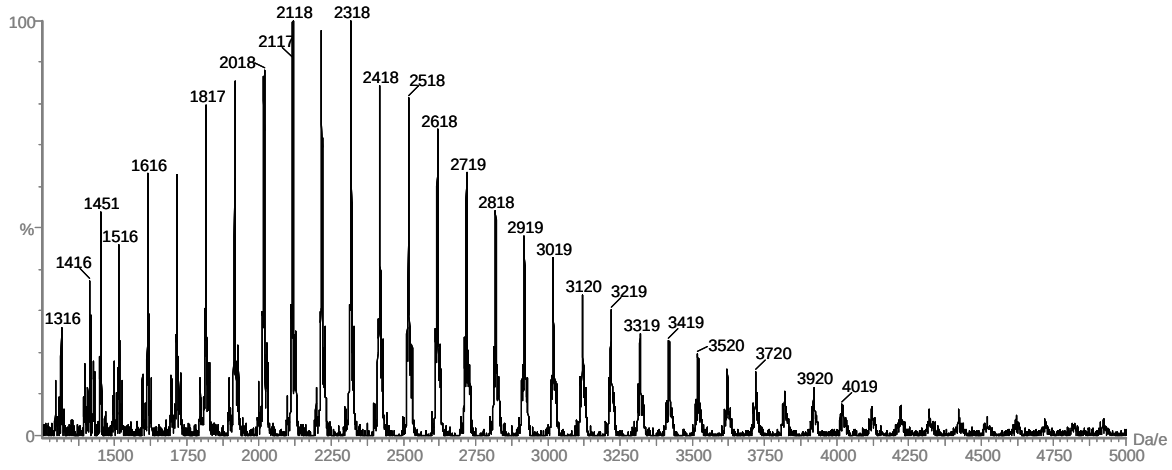

Figure 5: MALDI TOF of DD34 (MMA/Aza-crown ether: 90/10).

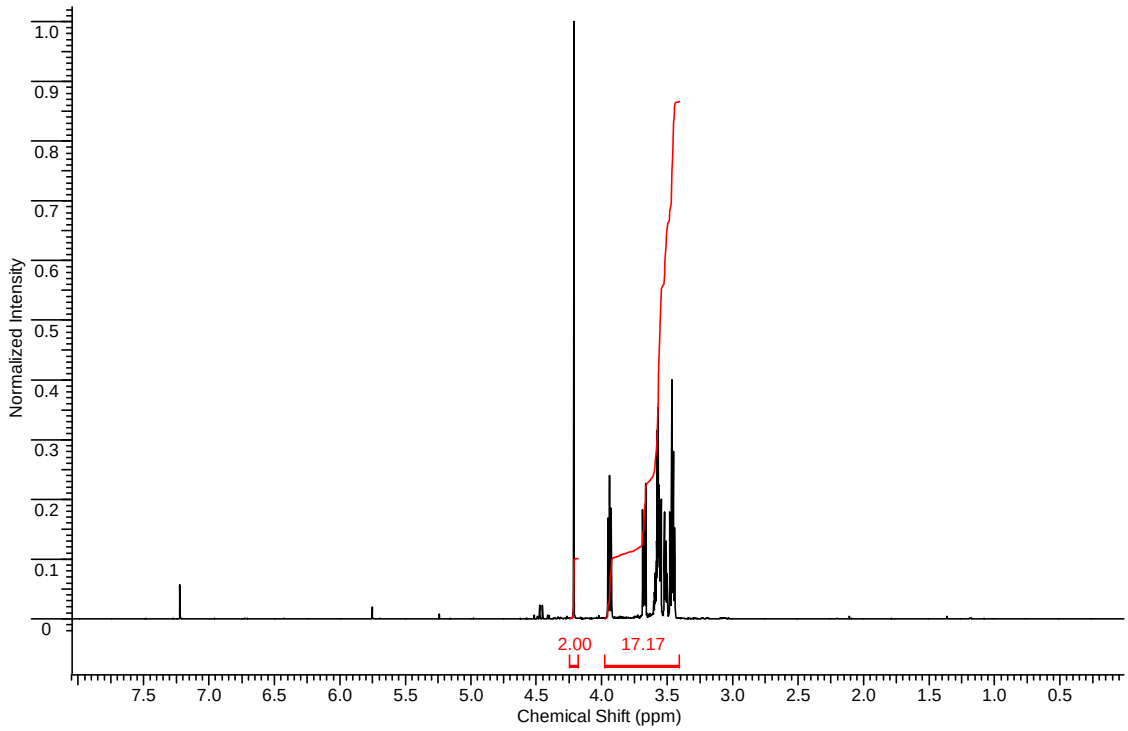

Figure 6: ^{1}H-NMR spectra of chloroacetyl 1-Aza-12-crown-4.

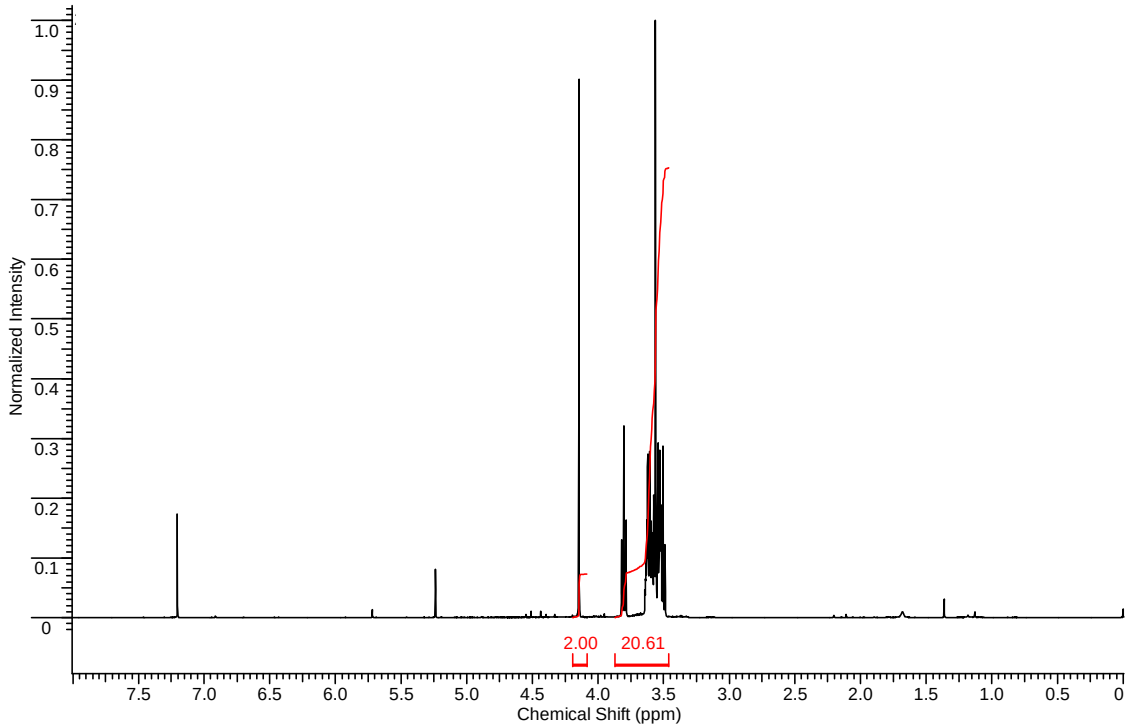

Figure 7: ^{1}H-NMR spectra of chloroacetyl 1-Aza-15-crown-5.

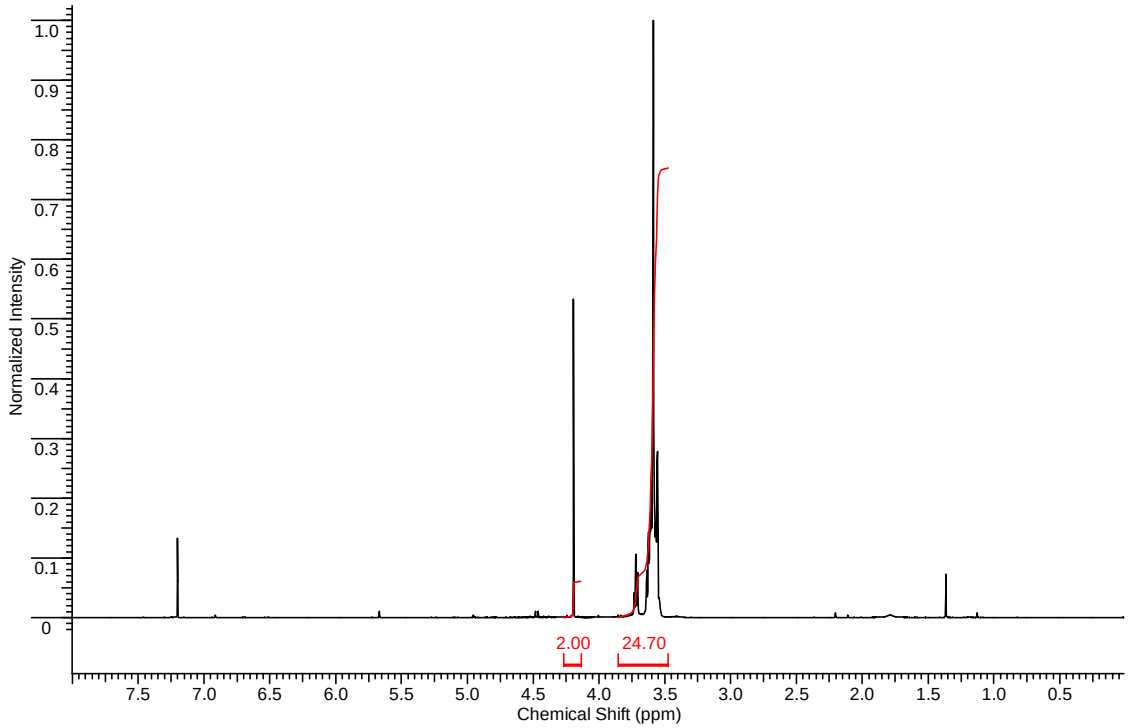

Figure 8: ^{1}H-NMR spectra of chloroacetyl 1-Aza-18-crown-6.

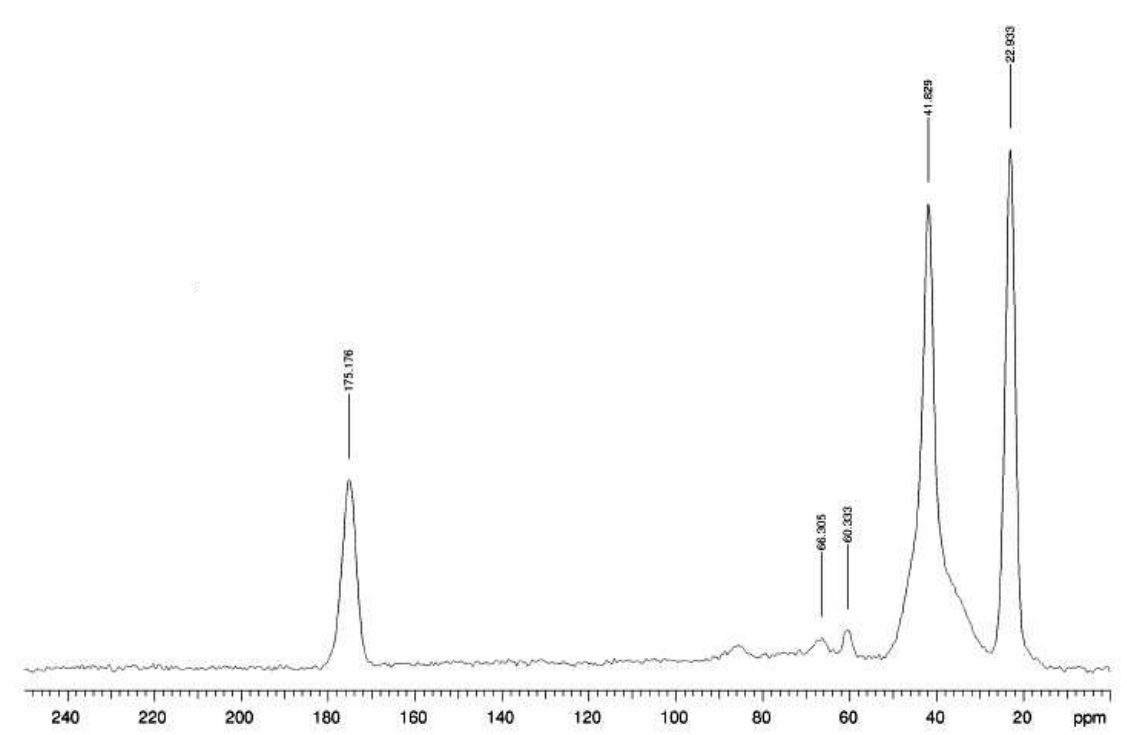

Figure 9: Solid State ^{13}C-NMR of poly-(NIPAM-co-HEMA) gel beads attempted to be functionalised by chloroacetyl 1-Aza-15-crown-5.

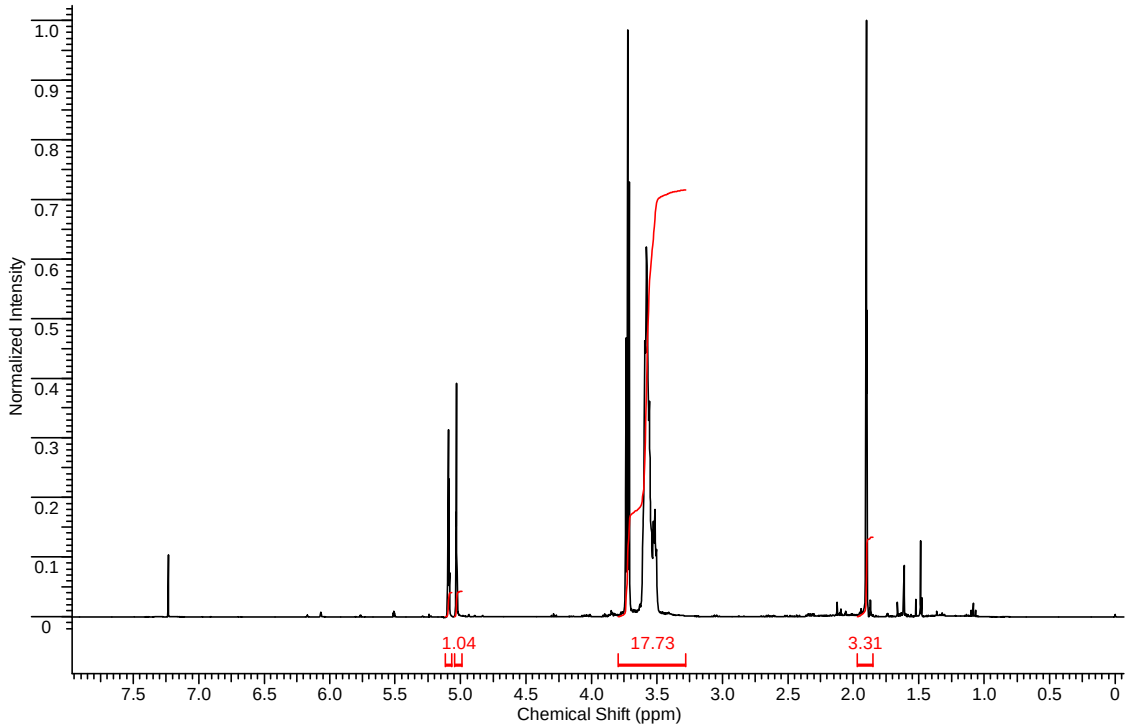

Figure 10: ^{1}H-NMR for 1-Aza-12-crown-4 methacrylate monomer.

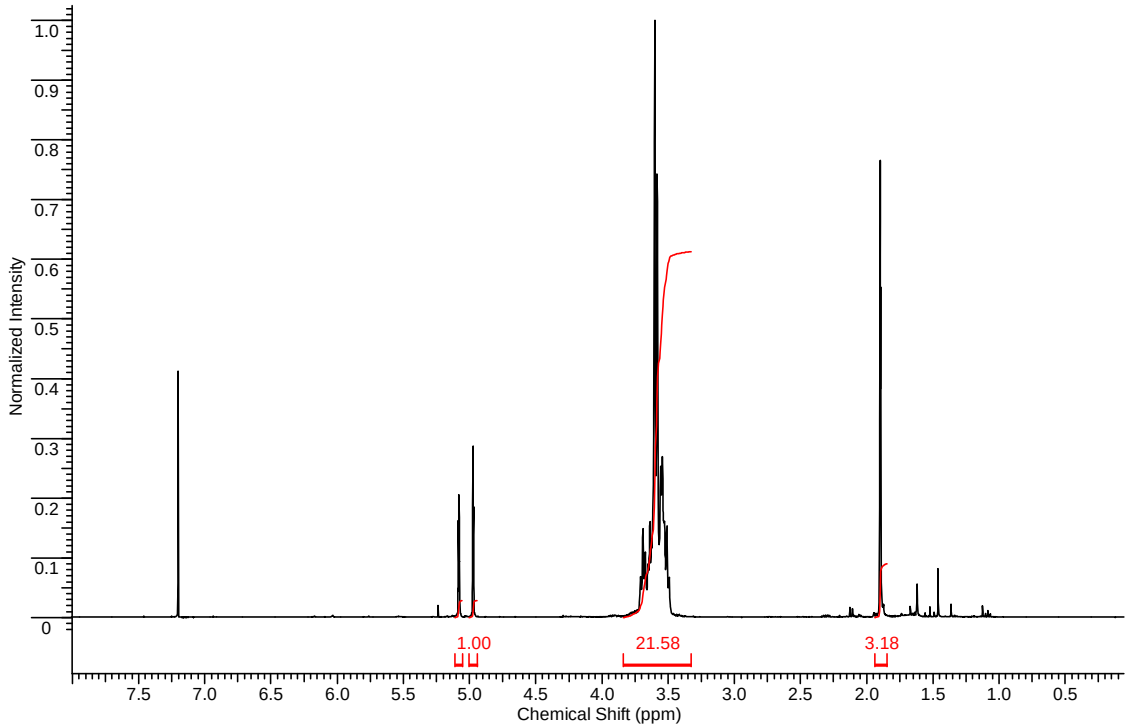

Figure 11: ^{1}H-NMR for 1-Aza-15-crown-5 methacrylate monomer.

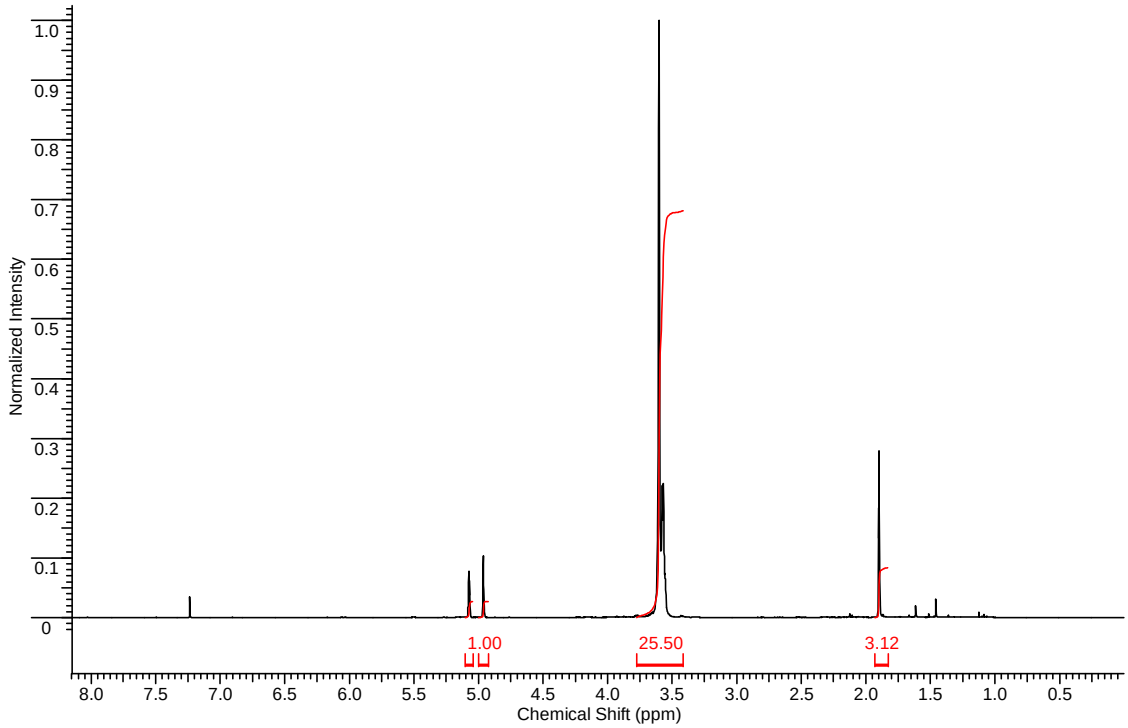

Figure 12: ^{1}H-NMR for 1-Aza-18-crown-6 methacrylate monomer.

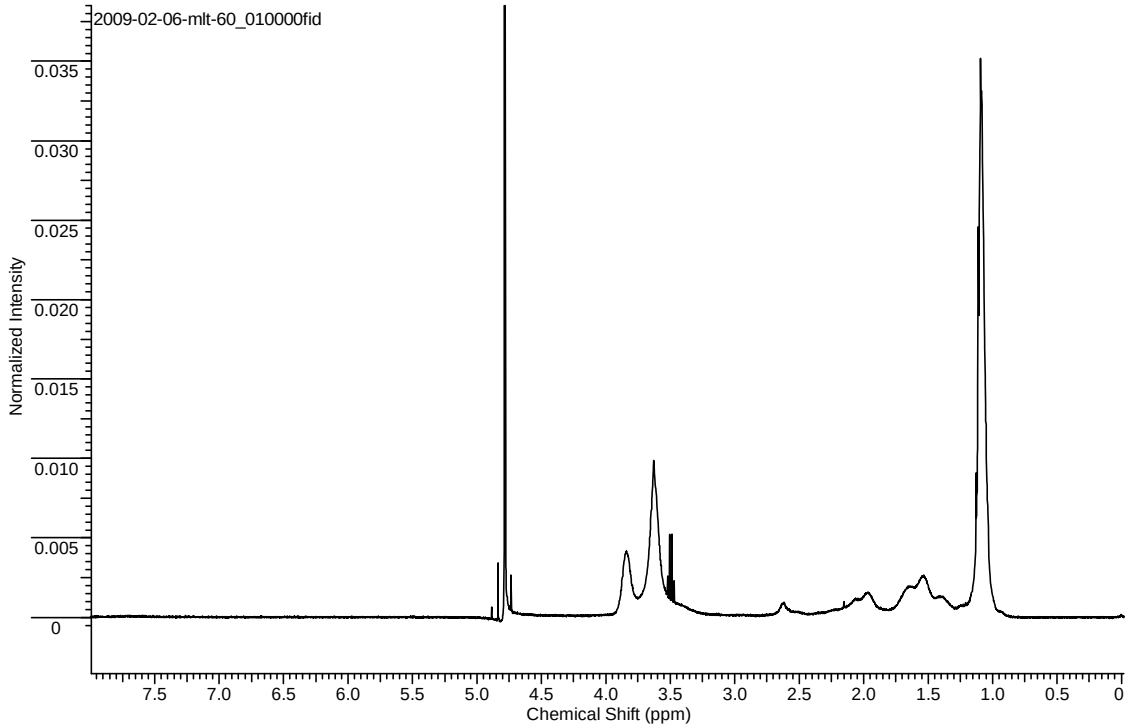

Figure 13: ^{1}H-NMR of copolymer poly-(NIPAM-co-1-aza-15-crown-5 methacrylate) prepared in the presence of HESH as chain transfer agent.

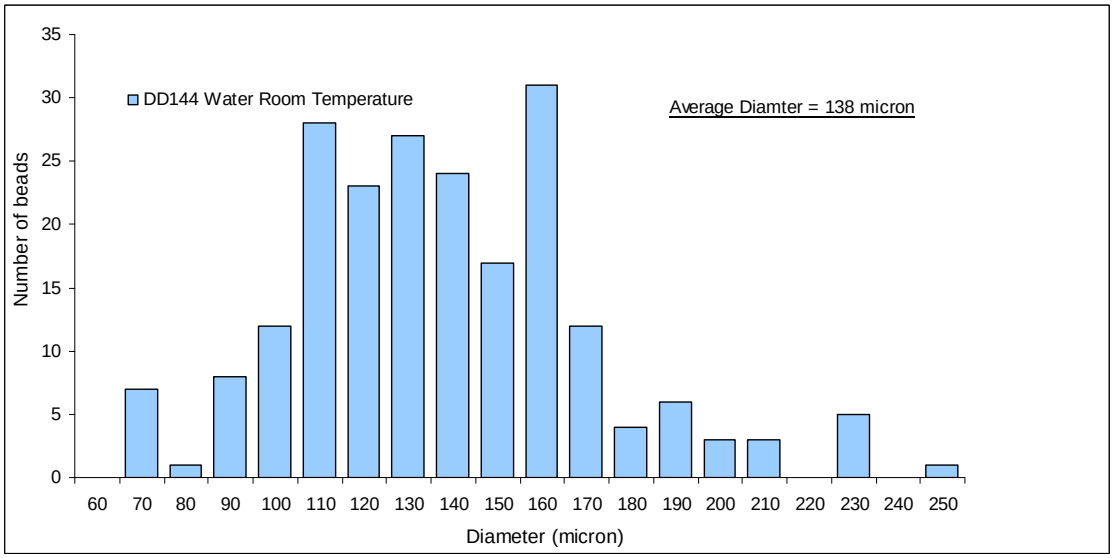

Figure 17: Distribution of diameters for poly-(NIPAM-co-AAc) hydrogel beads (DD144, PNA) in water at room temperature.

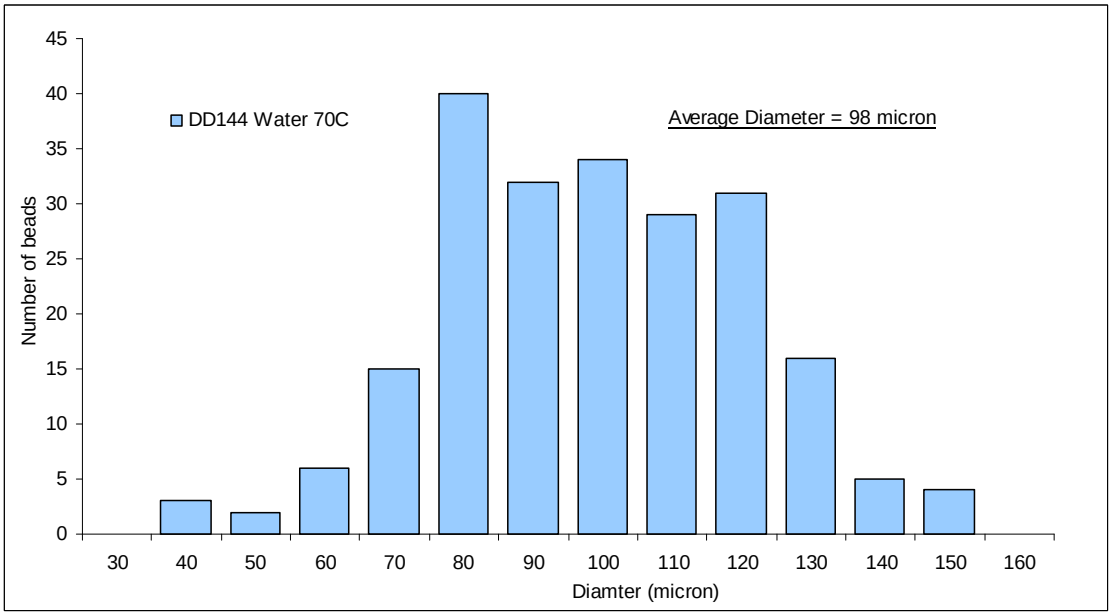

Figure 18: Distribution of diameters for poly-(NIPAM-co-AAc) hydrogel beads (DD144, PNA) in water at 70°C.

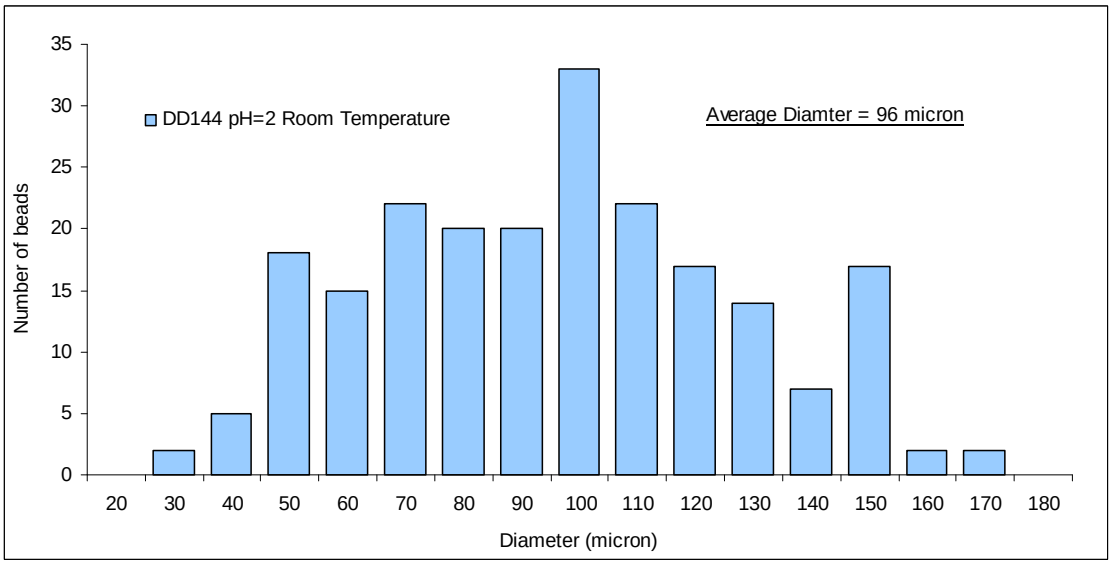

Figure 19: Distribution of diameters for poly-(NIPAM-co-AAc) hydrogel beads (DD144, PNA) in pH 2 buffer at room temperature.

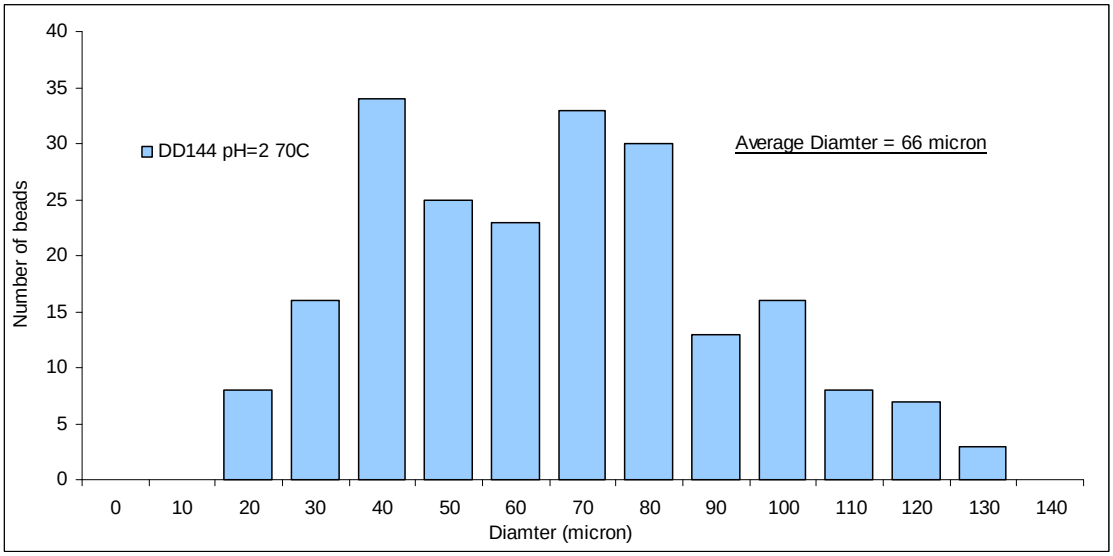

Figure 19: Distribution of diameters for poly-(NIPAM-co-AAc) hydrogel beads (DD144, PNA) in pH 2 buffer at 70°C.

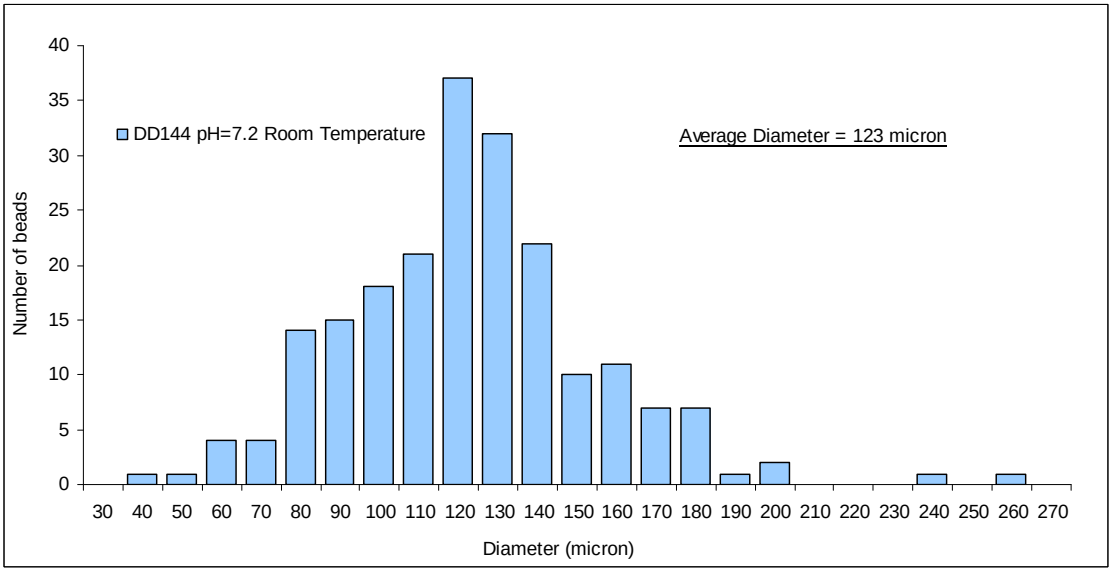

Figure 20: Distribution of diameters for poly-(NIPAM-co-AAc) hydrogel beads (DD144, PNA) in pH 7.2 buffer at room temperature.

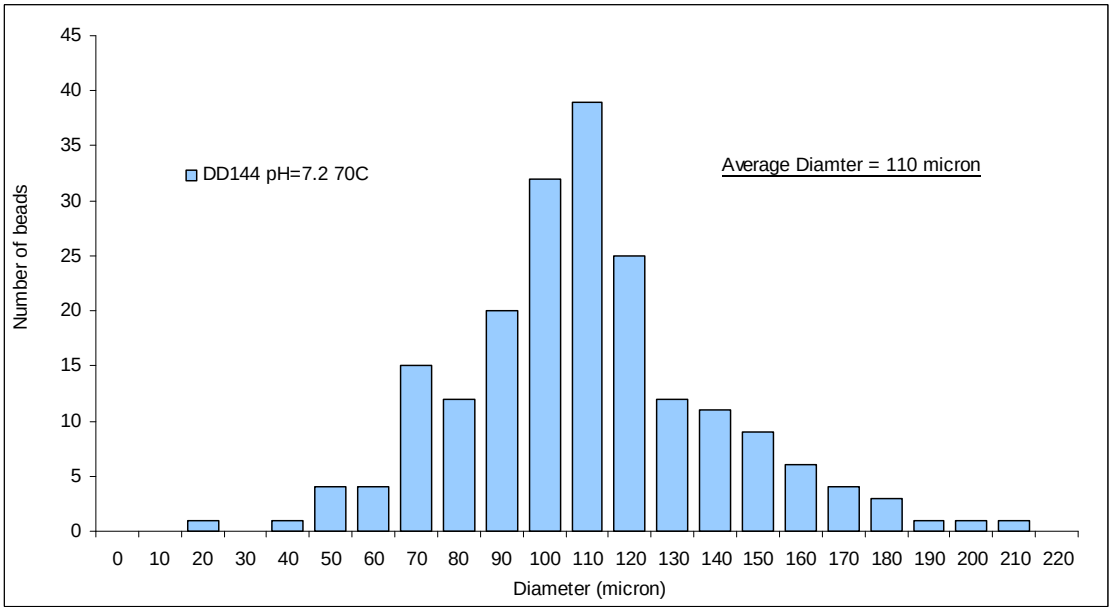

Figure 21: Distribution of diameters for poly-(NIPAM-co-AAc) hydrogel beads (DD144, PNA) in pH 7.2 buffer at 70°C.

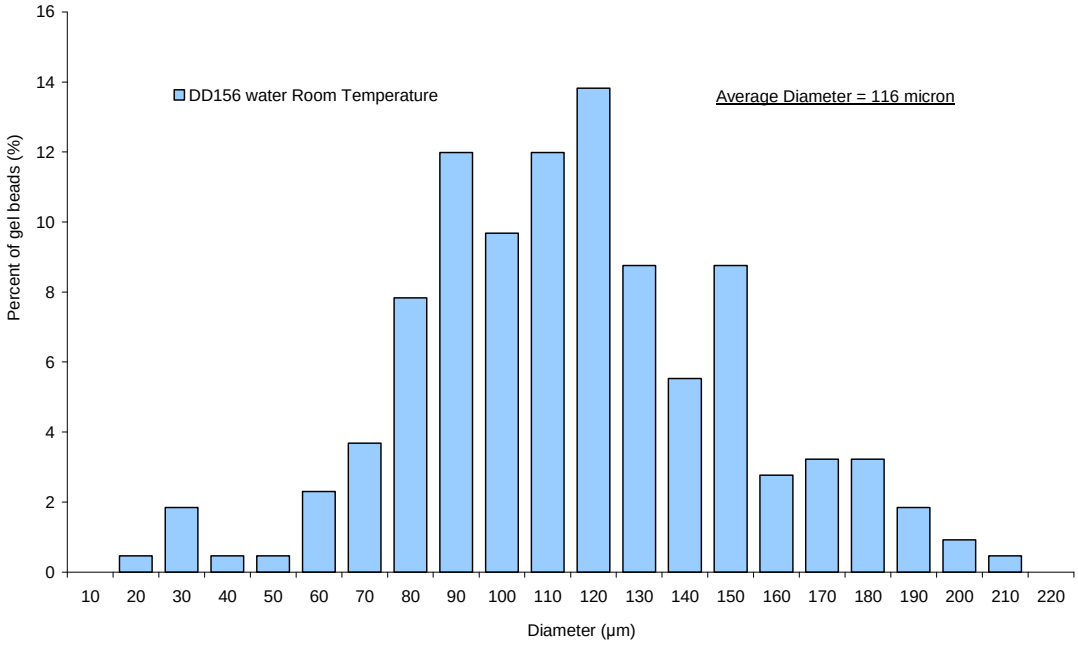

Figure 22: Distribution of diameters for poly-(NIPAM-co-AAc) hydrogel beads incorporating Aza-crown ethers (DD156, PNA1) in water at room temperature.

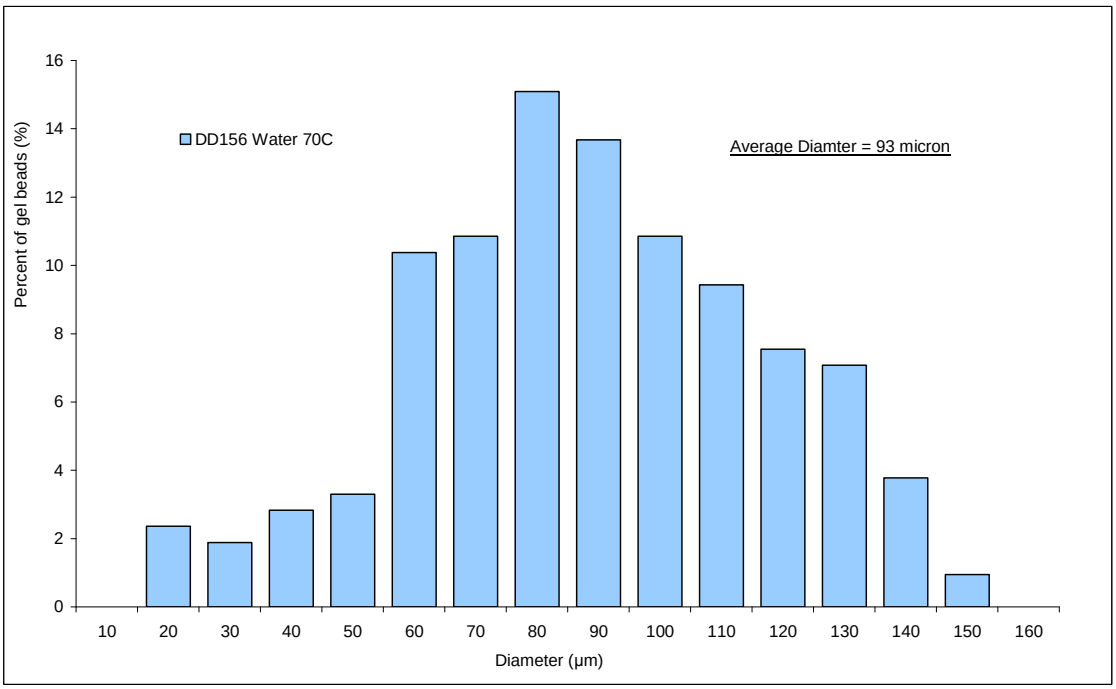

Figure 23: Distribution of diameters for poly-(NIPAM-co-AAc) hydrogel beads incorporating Aza-crown ethers (DD156, PNA1) in water at 70°C.

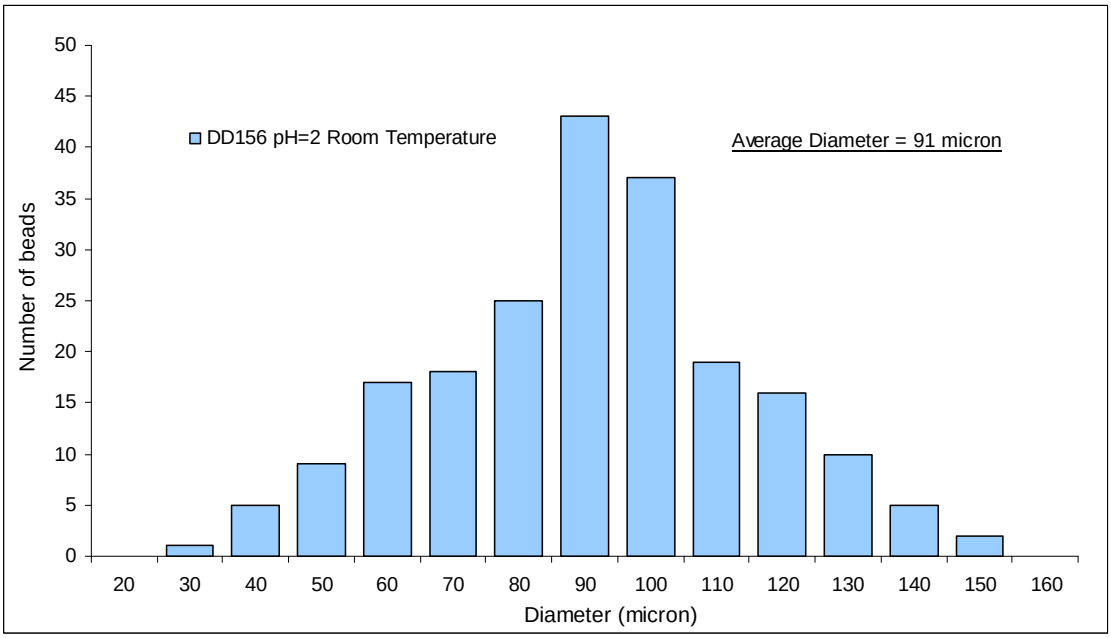

Figure 24: Distribution of diameters for poly-(NIPAM-co-AAc) hydrogel beads incorporating Aza-crown ethers (DD156, PNA1) in pH 2 buffer at room temperature.

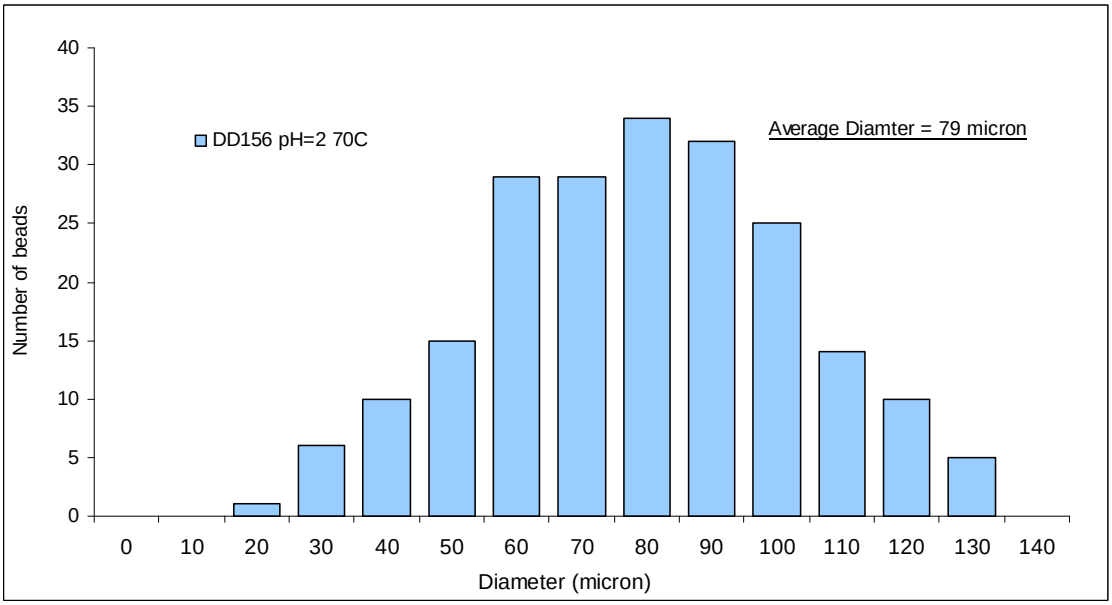

Figure 25: Distribution of diameters for poly-(NIPAM-co-AAc) hydrogel beads incorporating Aza-crown ethers (DD156, PNA1) in pH 2 buffer at 70°C.

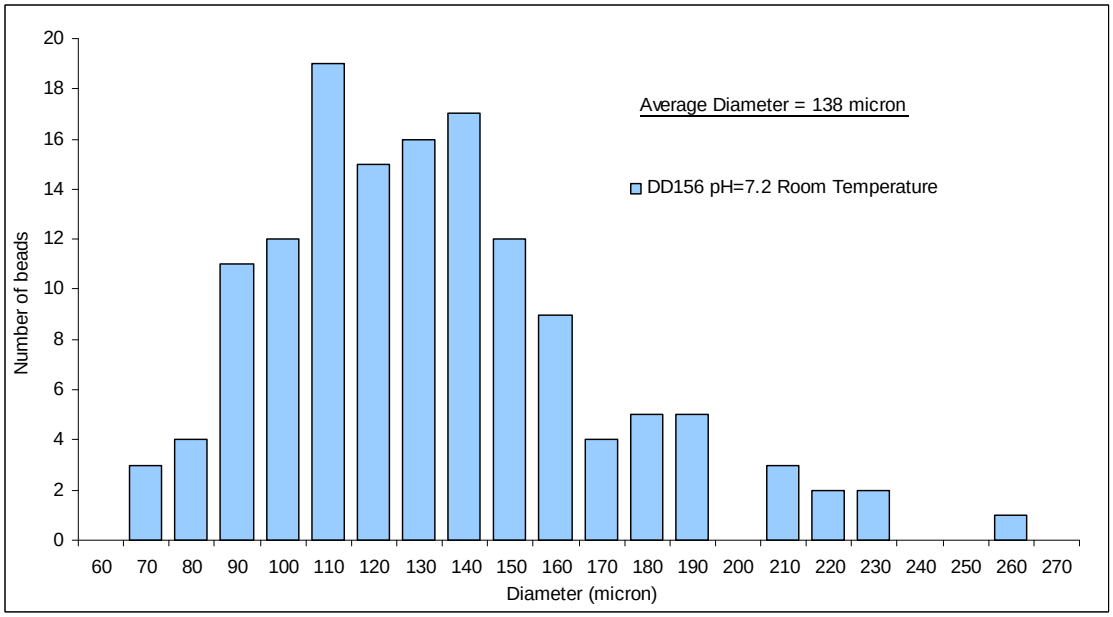

Figure 26: Distribution of diameters for poly-(NIPAM-co-AAc) hydrogel beads incorporating Aza-crown ethers (DD156, PNA1) in pH 7.2 buffer at room temperature.

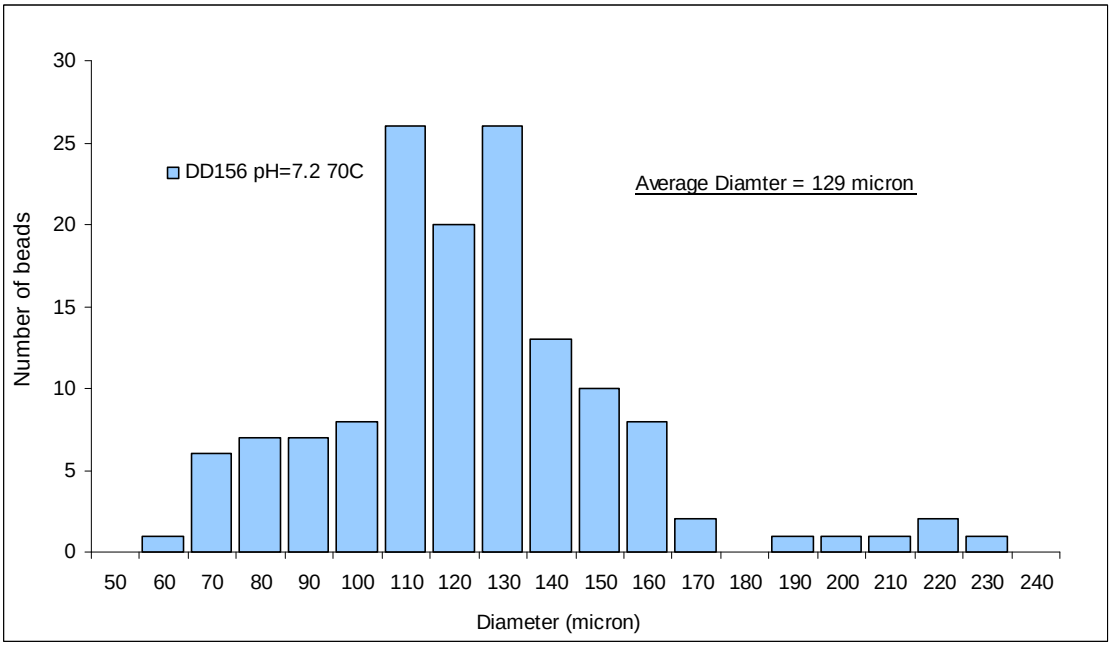

Figure 27: Distribution of diameters for poly-(NIPAM-co-AAc) hydrogel beads incorporating Aza-crown ethers (DD156, PNA1) in pH 7.2 buffer at 70°C.

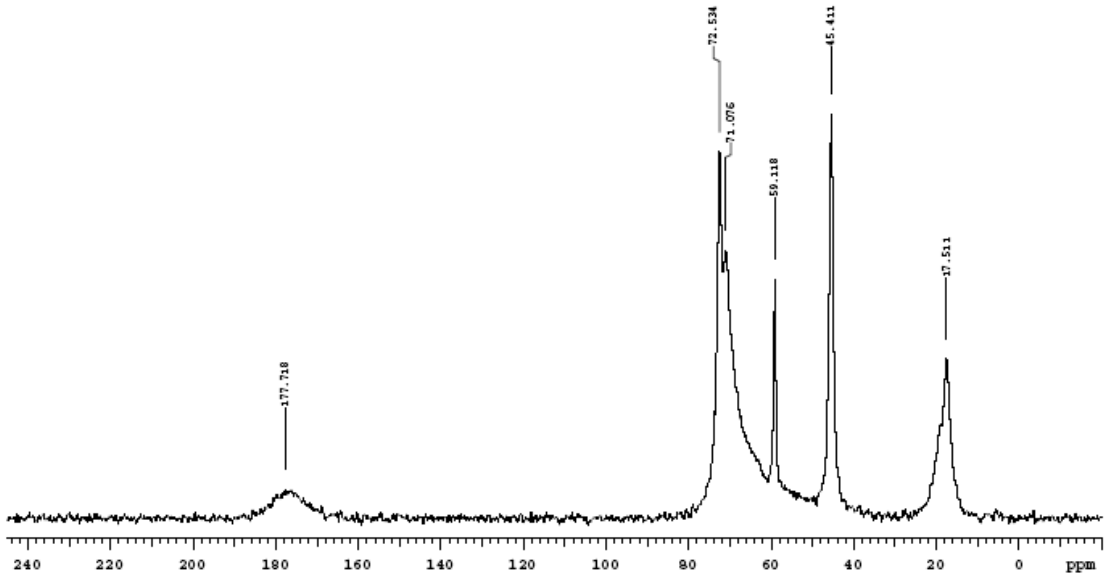

Figure 14: ^{13}C-NMR (solid state) of poly-(MEO_2MA) gel beads, PEGN.

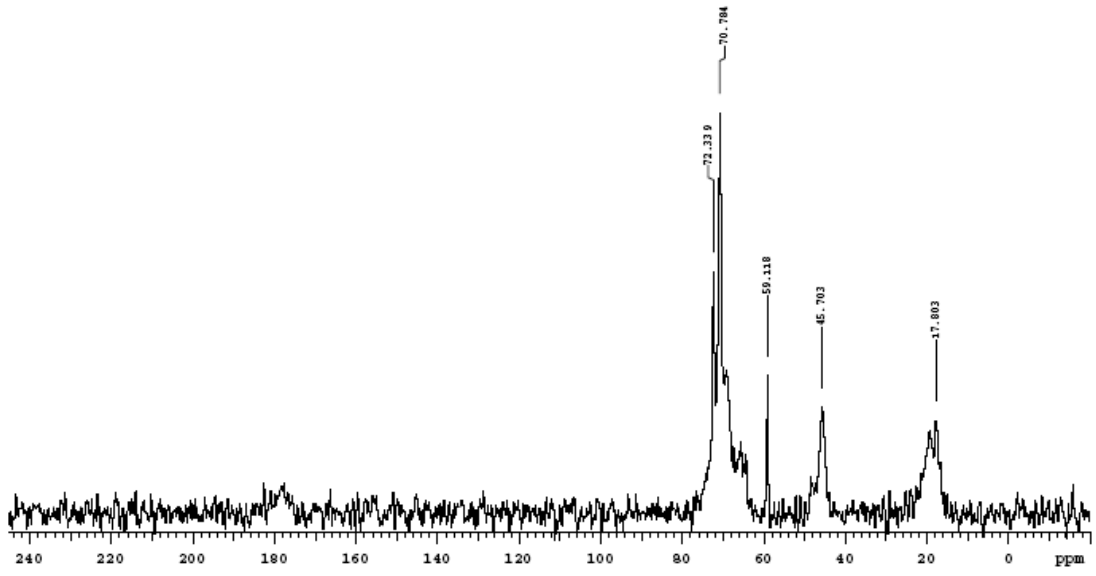

Figure 15: ^{13}C-NMR (solid state) of poly-(MEO_2MA-co-$OEGMA_{475}$) gel beads, PEG.

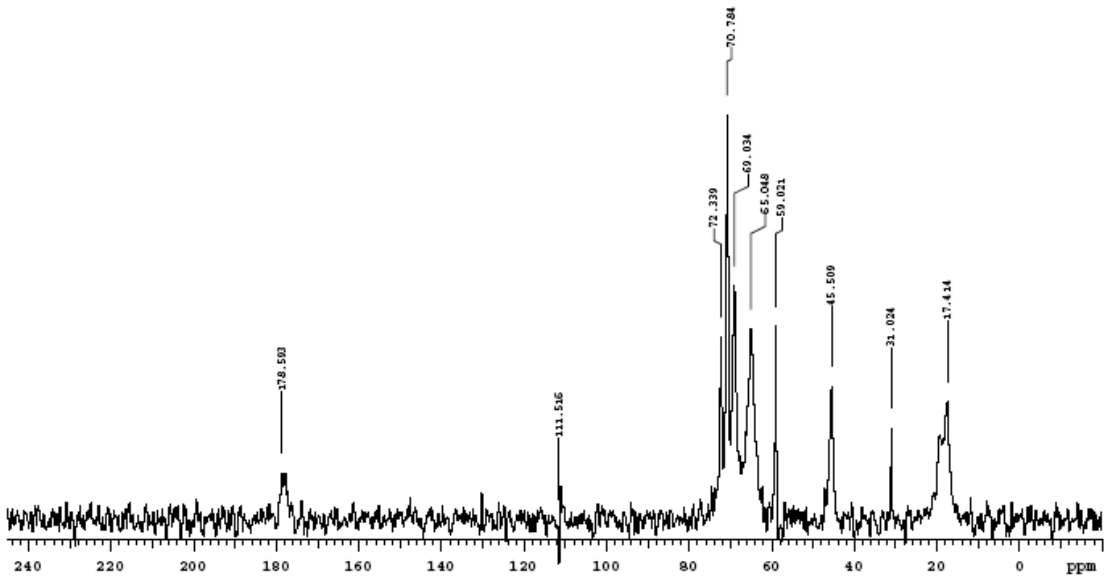

Figure 16: ^{13}C-NMR (solid state) of the attempted poly-(MEO_2MA-co-$OEGMA_{475}$-co-1-Aza-18-crown-6 methacrylate) gel beads, PEGCE.

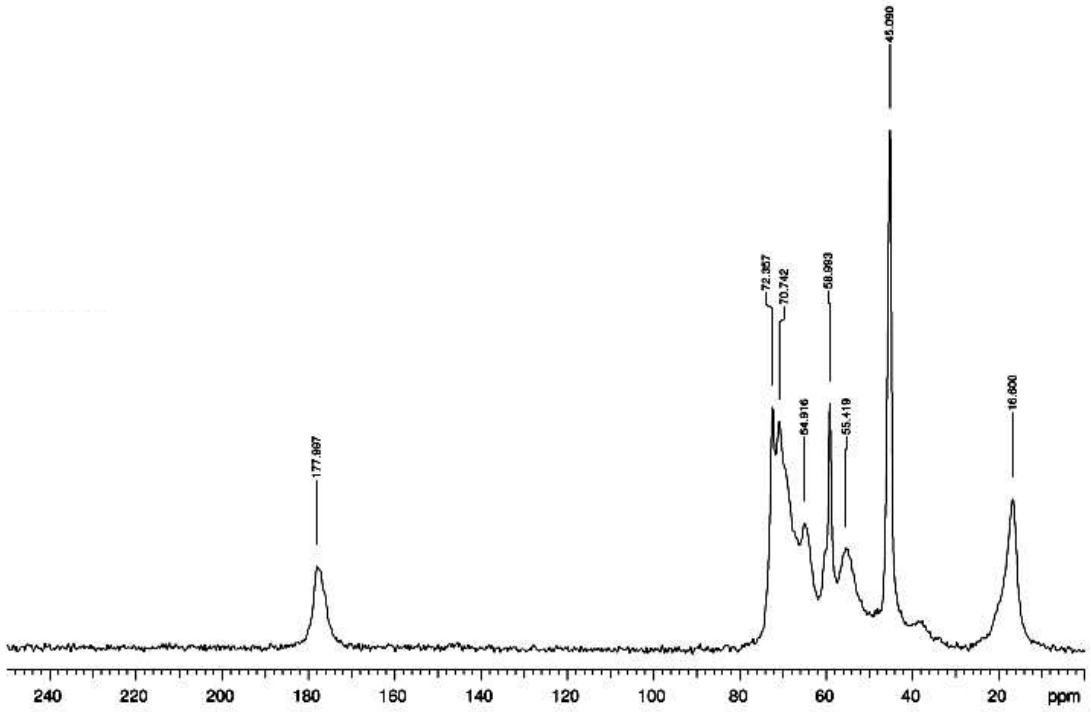

Figure 16: ^{13}C-NMR (solid state) of poly-(MEO_2MA-co-HEMA) gel beads, PEGNH.

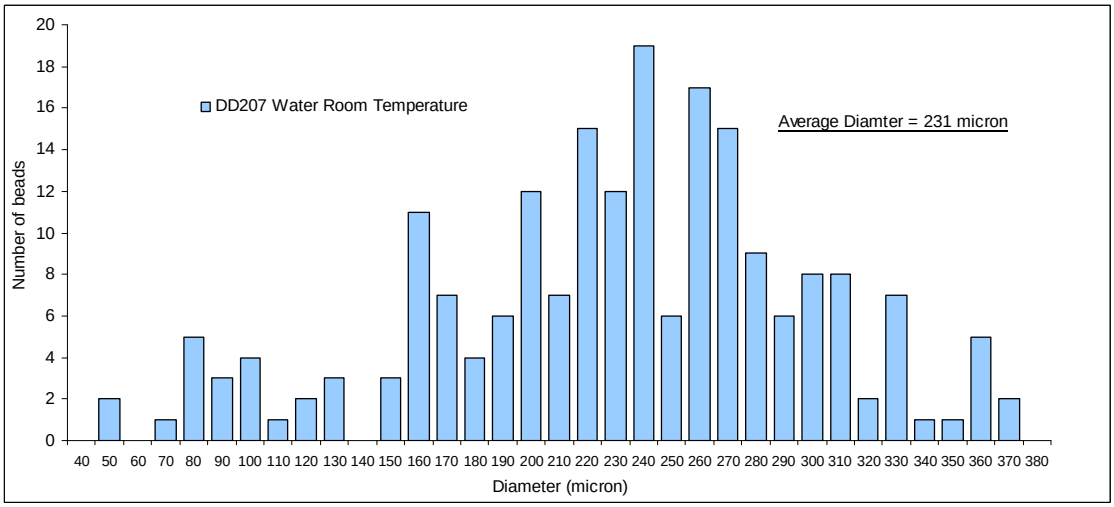

Figure 28: Distribution of diameters for poly-(MEO_2MA-co-$OEGMA_{475}$) hydrogel beads (DD207, PEGMA) in water at room temperature.

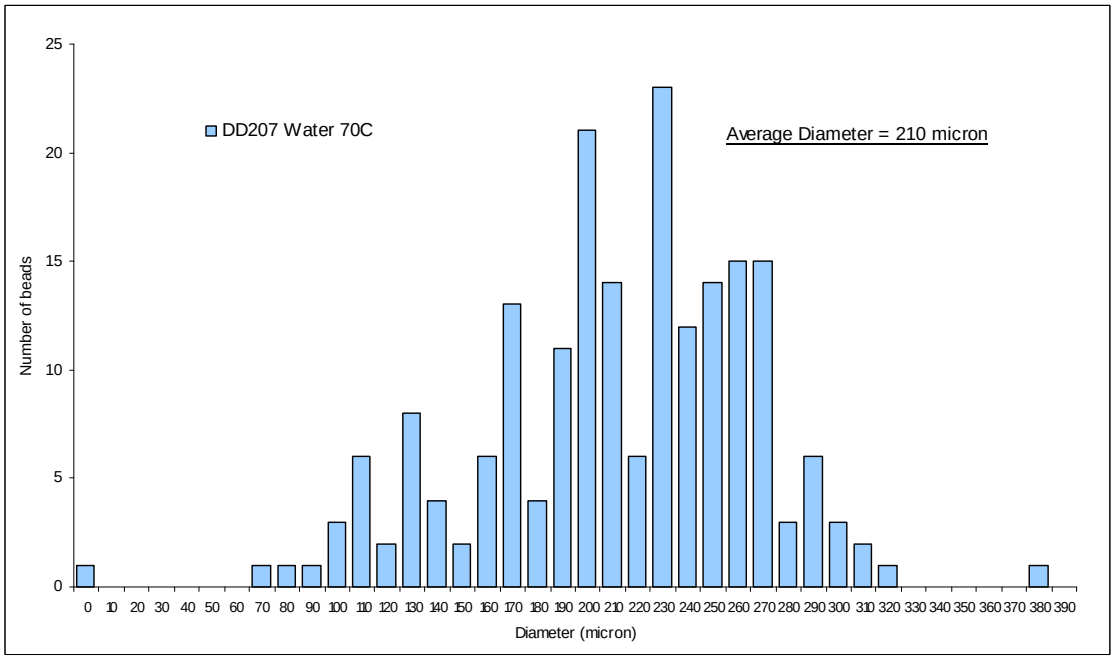

Figure 29: Distribution of diameters for poly-(MEO_2MA-co-$OEGMA_{475}$) hydrogel beads (DD207, PEGMA) in water at 70°C.

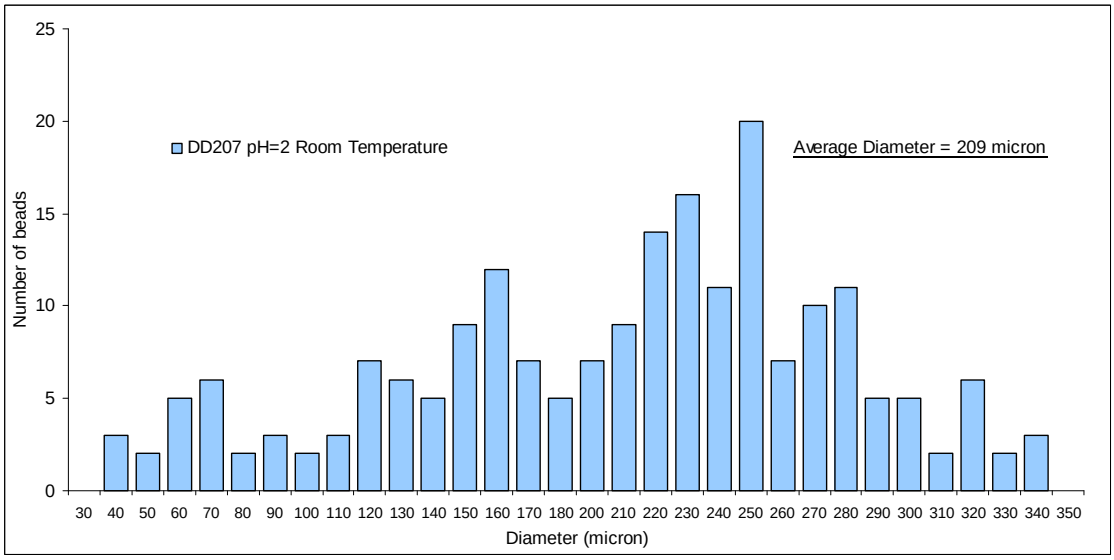

Figure 30: Distribution of diameters for poly-(MEO_2MA-co-$OEGMA_{475}$) hydrogel beads (DD207, PEGMA) in pH 2 buffer at room temperature.

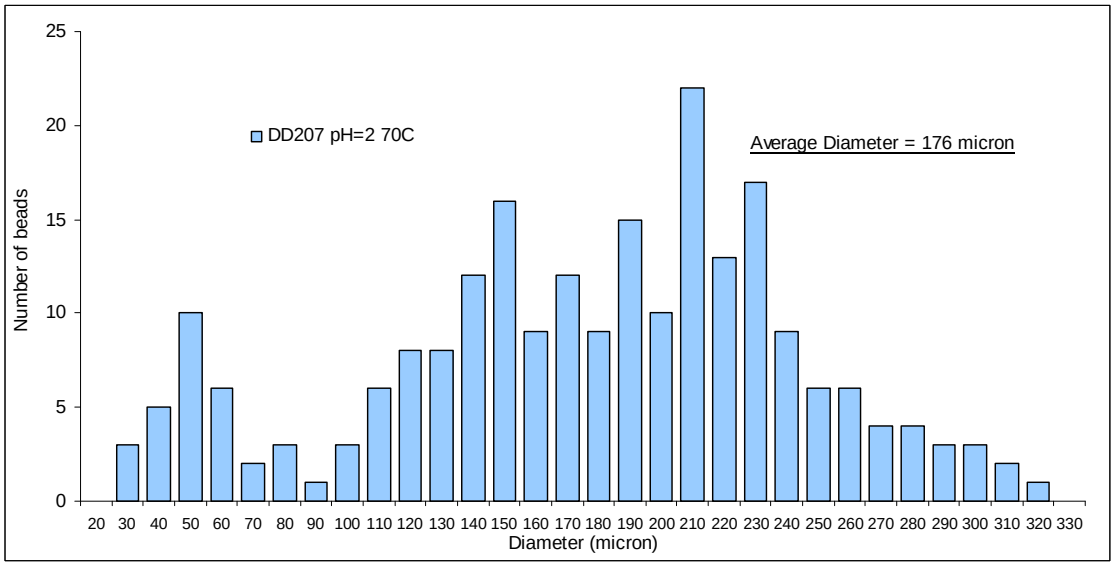

Figure 31: Distribution of diameters for poly-(MEO_2MA-co-$OEGMA_{475}$) hydrogel beads (DD207, PEGMA) in pH 2 buffer at 70°C.

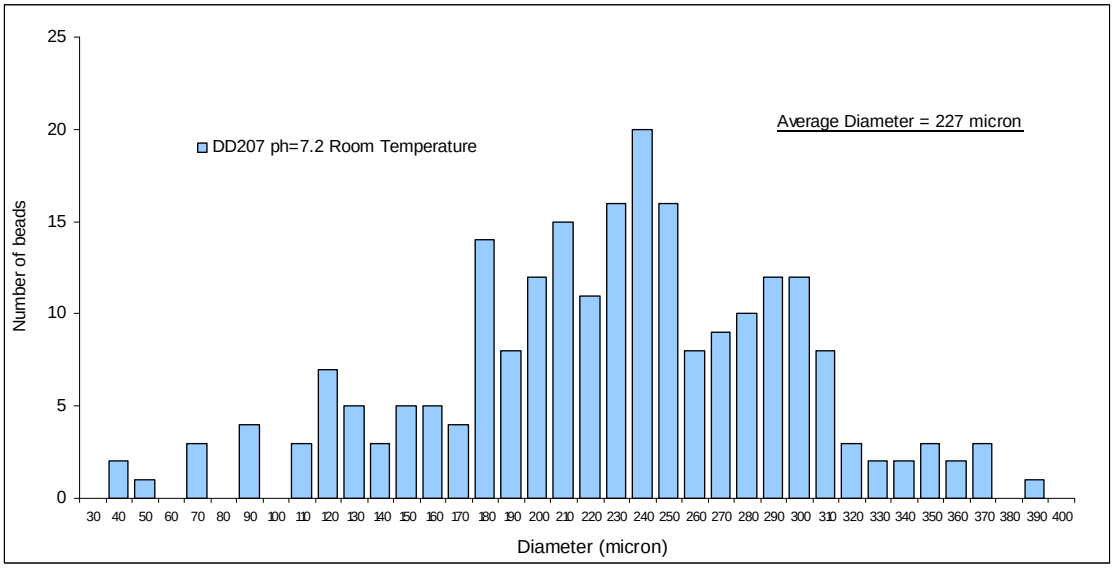

Figure 32: Distribution of diameters for poly-(MEO_2MA-co-$OEGMA_{475}$) hydrogel beads (DD207, PEGMA) in pH 7.2 buffer at room temperature.

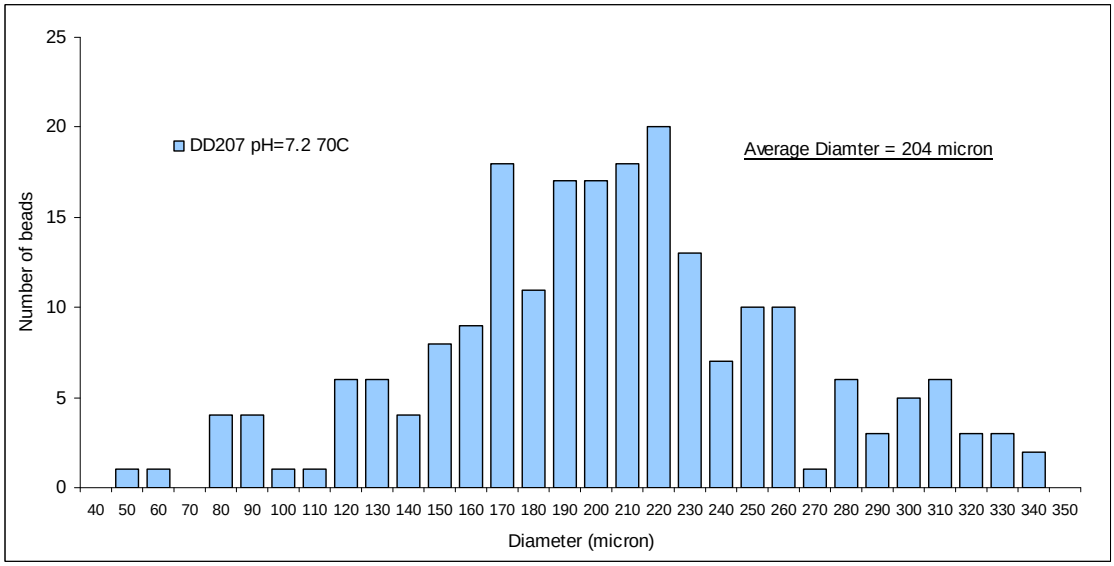

Figure 33: Distribution of diameters for poly-(MEO_2MA-co-$OEGMA_{475}$) hydrogel beads (DD207, PEGMA) in pH 7.2 buffer at 70°C.

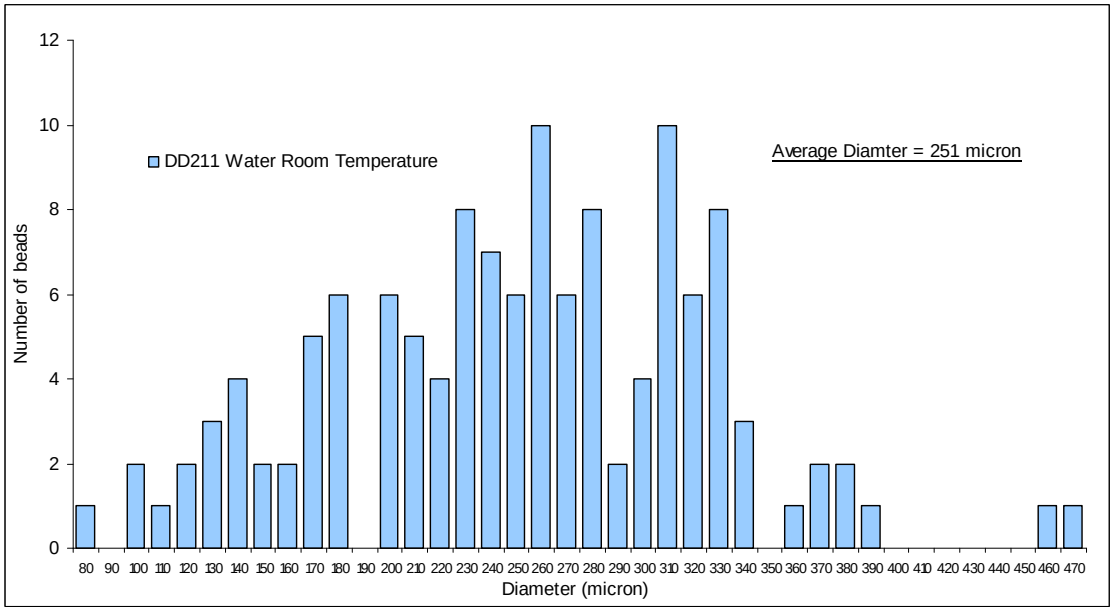

Figure 34: Distribution of diameters for poly-(MEO_2MA-co-$OEGMA_{475}$) hydrogel beads incorporating Aza-crown ethers (DD211, PEGMAf1) in water at room temperature.

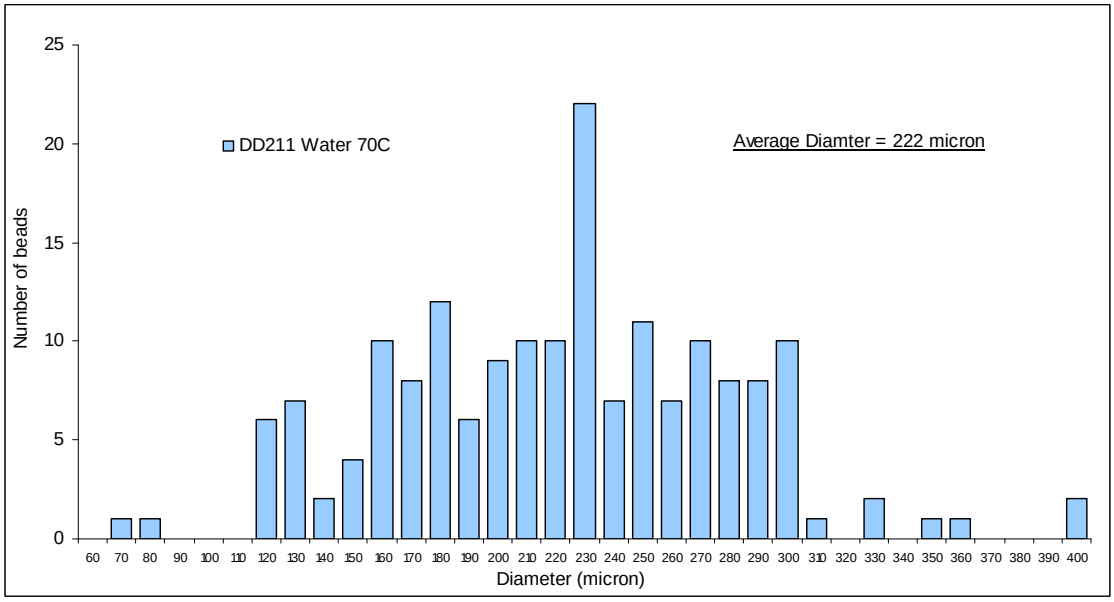

Figure 35: Distribution of diameters for poly-(MEO_2MA-co-$OEGMA_{475}$) hydrogel beads incorporating Aza-crown ethers (DD211, PEGMAf1) in water at 70°C.

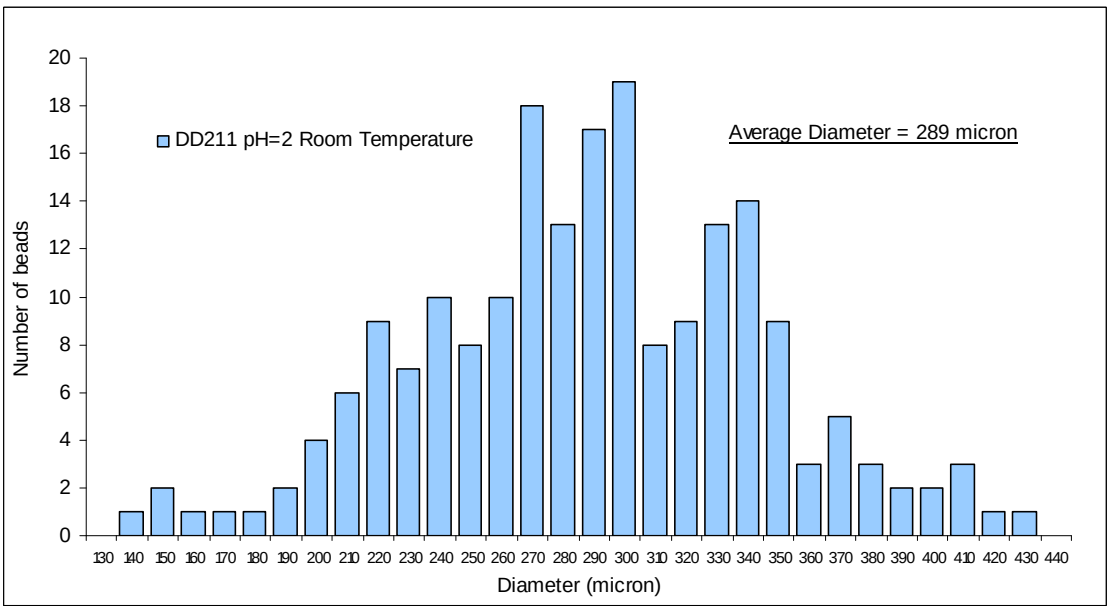

Figure 36: Distribution of diameters for poly-(MEO_2MA-co-$OEGMA_{475}$) hydrogel beads incorporating Aza-crown ethers (DD211, PEGMAf1) in ph 2 buffer at room temperature.

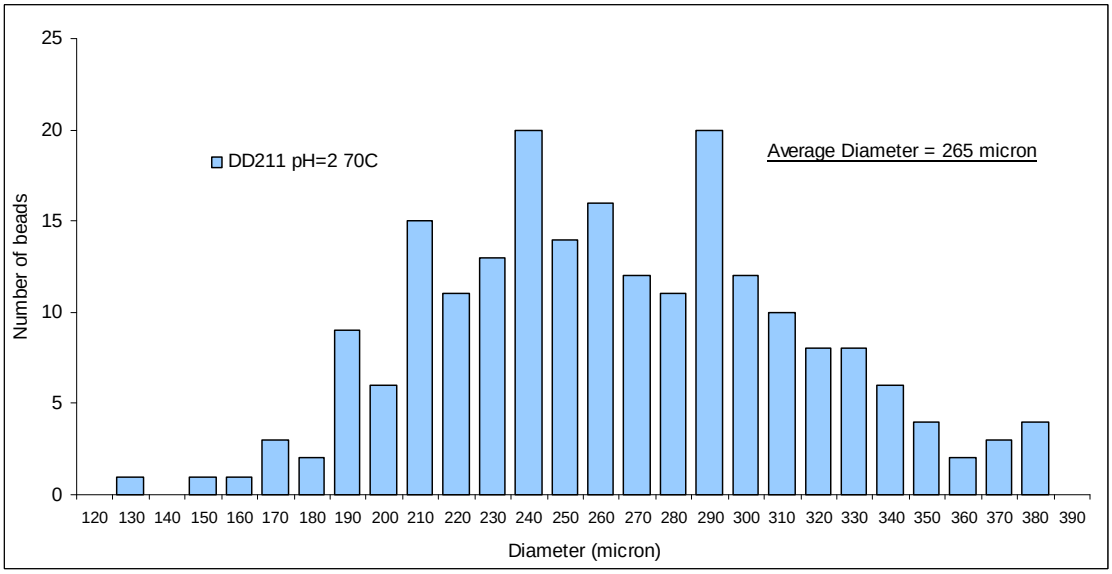

Figure 37: Distribution of diameters for poly-(MEO_2MA-co-$OEGMA_{475}$) hydrogel beads incorporating Aza-crown ethers (DD211, PEGMAf1) pH 2 buffer at 70°C.

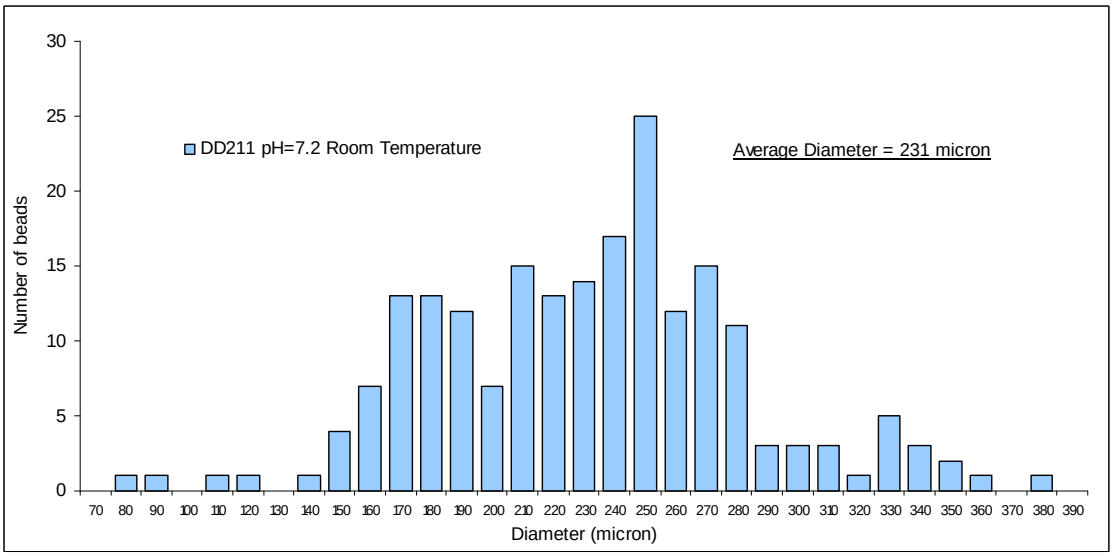

Figure 38: Distribution of diameters for poly-(MEO_2MA-co-$OEGMA_{475}$) hydrogel beads incorporating Aza-crown ethers (DD211, PEGMAf1) in ph 7.2 buffer at room temperature.

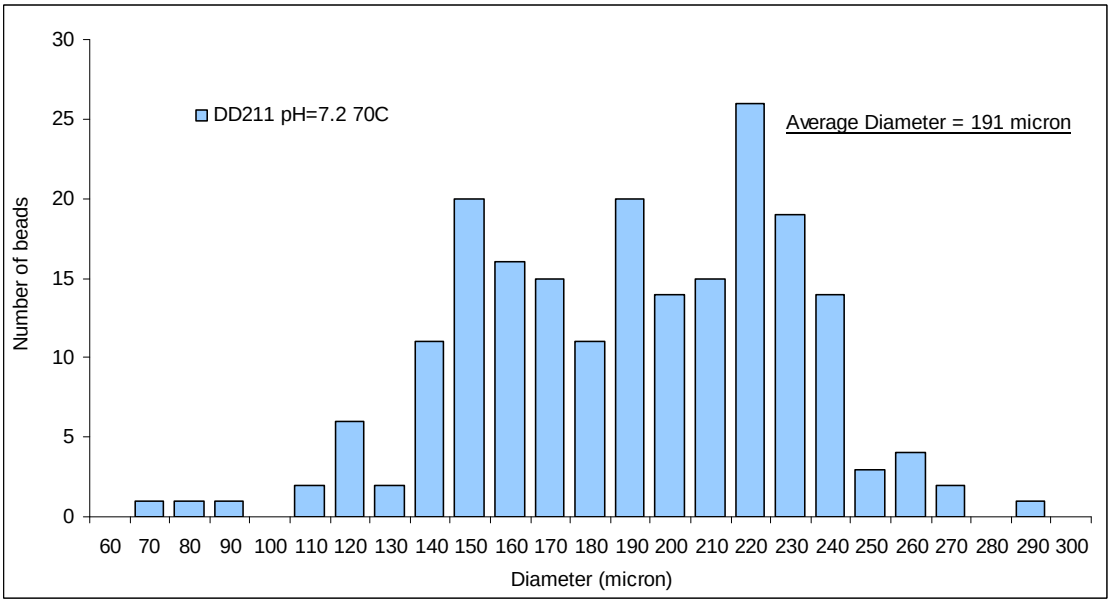

Figure 39: Distribution of diameters for poly-(MEO_2MA-co-$OEGMA_{475}$) hydrogel beads incorporating Aza-crown ethers (DD211, PEGMAf1) pH 7.2 buffer at 70°C.